

Pennsylvania State University

Annual Progress Report: 2007 Formula Grant

Reporting Period

July 1, 2009 – June 30, 2010

Formula Grant Overview

The Pennsylvania State University received \$7,538,293 in formula funds for the grant award period January 1, 2008 through December 31, 2011. Accomplishments for the reporting period are described below.

Research Project 1: Project Title and Purpose

High Field MRI - Limitations and Solutions - We are in the process of developing new techniques and technology that will make Magnetic Resonance Imaging (MRI) more accurate, more effective, more versatile, faster, and safer in the future. Because of the wide utility of MRI, this will have major benefits on many areas of medicine. We have recently ended a period of funding from the NIH regarding this work and have received very good scores with easily-addressable concerns in our first renewal application. We anticipate further NIH funding upon review of our revised renewal application. Pennsylvania Department of Health (PA DOH) funding will allow us to continue progress without major interruption during a gap in federal funding and allow for continued demonstrable progress should a second revised application for federal funds be necessary.

Duration of Project

9/1/2008 – 6/30/2010

Project Overview

To improve the accuracy, versatility, and safety of MRI we have recently developed the new technology of transmit radiofrequency (RF) arrays for spin excitation in MRI, which allows for unprecedented control over the RF electromagnetic fields used in MRI through space and time. The technology shows enormous potential for significantly reducing image nonuniformity due to RF field distortions in high-field MRI, potentially making many experimental, quantitative, and clinical MR techniques more accurate and safer. But methods for implementation, optimization, and safety-assurance of such systems will require further development. We will progress toward our goals during the year of PA DOH funding through the following Specific Aims:

Specific Aim 1: Determine specific array geometries and pulsing methods for the most effective implementation of transmit arrays. We will 1) begin to evaluate and optimize different competing transmit array geometries and pulsing methods with numerical calculation techniques,

and 2) begin to perform careful calculations to determine the best array geometries and pulsing methods in several different important configurations (imaging of head, body, etc. at different MRI field strengths).

Specific Aim 2: *Develop a reliable, real-time, computer-guided method of ensuring the safety of transmit arrays.* Unlike conventional RF coils in MRI, transmit arrays have the potential for an infinite number of different current and field distributions throughout time within a given human subject. We will use calculations of heating and temperature caused by RF fields in MRI and experiments in phantoms to begin the development and demonstration of a method to rapidly confirm the safety of specific MRI pulses and sequences with specific transmit arrays when loaded with human subjects. With this method it will be possible to ensure the RF safety of human subjects in real time during MRI involving transmit arrays.

Specific Aim 3: *Implement and demonstrate RF excitation systems with excellent excitation accuracy, uniformity, and speed, as well as ensured safety for several high field applications.* With the designs and methods resulting from the first two aims we will begin to implement and demonstrate RF transmit arrays, pulsing techniques, and safety monitoring methods far superior to existing designs and methods for several applications, including both body and head imaging. We will be able to begin this implementation near the end of the year of PA DOH funding.

Principal Investigator

Christopher M. Collins, PhD
Assistant Professor of Radiology
The PSU College of Medicine
NMR/MRI Bldg., H066
500 University Drive
Hershey, PA 17033

Other Participating Researchers

Chienping Kao, PhD, Sukhoon Oh, PhD, Yeunchul Ryu, PhD - employed by The PSU College of Medicine

Expected Research Outcomes and Benefits

The *long term* products of this research will include publicly-available data and tools, as well as demonstrated, published techniques and technology that will enable more accurate, more versatile, and safer MRI than possible today. We expect significant progress in several areas during the year of PA DOH funding.

Deliverables from Aim 1 will include:

- 1) Beginnings of a database reporting valuable information about both the potential capabilities and the safety information for many different array geometries when driven with different optimized pulse types.

Deliverables from Aim 2 are geared toward developing a fast, versatile, effective, and accurate method for safety monitoring during MRI of human subjects with transmit arrays:

- 1) An increasing library of numerical multi-tissue models of subjects with a variety of body types for accurate patient-specific MRI field calculations.
- 2) Beginnings of a validated method for using numerical calculations with these models and specific array geometries and pulse sequences for rapidly and accurately ensuring the safety of MRI with transmit arrays.

Deliverables for Aim 3 involve implementation and demonstration of transmit RF array systems including:

- 1) Novel transmit arrays and pulsing methods with superior performance to existing designs should begin in the second half of 2008.

Summary of Research Completed

Within PSU, this grant was funded as a “bridge” grant to help maintain continuity in research and personnel for meritorious grant projects that were experiencing a gap in funding. The funding from the PA DOH allowed for significant progress towards the goals of the aforementioned NIH grant that was not renewed on first application. The NIH grant was renewed on second application for a total of \$5,030,294 over 5 years, which is itself an indication of the success of the PA DOH bridge grant. Other progress from funds with the bridge grant includes a number of scientific publications at international meetings and in peer-reviewed journals, which are attached and summarized below. All of these works are aimed at developing new and improved methods for applying safe and effective radiofrequency (RF) electromagnetic energy to biological samples, including the human body as required during Magnetic Resonance Imaging (MRI), or Specific Aim 1 listed above. The Pennsylvania Department of Health is acknowledged for funding on each publication.

Peer-reviewed Journal Publications:

1. Park BS, Webb AG, Collins CM. “A method to separate conservative and magnetically-induced electric fields in calculations for MRI and MRS in electrically-small samples.” *J Magn Reson* 199(2):233-237, 2009. (August)

This work presented a method for separating two different mechanisms of heating by electrical fields in calculations of the RF fields in MRI. This is important because in principle one mechanism is not essential for MR imaging (and thus can hopefully be reduced with no effect on the MR signal), while the other is intrinsically tied to the MR experiment.

2. Park BS, Neuberger T, Webb AG, Bigler DC, Collins CM. *Faraday shields within a solenoidal coil to reduce sample heating: numerical comparison of designs and experimental verification.* *J Magn Reson* 2010;202:72-77. (January)

This work gave a comparison of arrangements of passive conductors used to significantly reduce the RF electrical fields that penetrate into a biological sample during MRI with solenoidal RF coils, and thus also significantly reduce the undesirable RF heating of these samples during MRI. Comparison was performed using 3D numerical field calculations and MRI experiments. Results include recommendations for best future designs.

Publications at Scientific Meetings:

3. Kao, Chien-Ping; Cao, Zhipeng; Oh, Sukhoon; Ryu, Yeun Chul; Collins, Christopher M. *Patch Antenna in Comparison to and in Combination with a Volume Coil for Excitation at 7T: Whole-Brain B1 Shimming and Consequent SAR. Proc. 2010 ISMRM, p. 1446*

The different approaches of “travelling wave MRI” in which waves are sent from one end of the magnet bore and more “conventional” MRI in which the object is placed in a volume array coil were compared and combined in high field MRI of the brain using numerical field calculations. The results showed that the two approaches, currently treated as competing approaches, can be quite complimentary such that their combination can result in safer, more effective MRI.

4. Collins, Christopher M.; Kao, Chien-Ping; Webb, Andrew G. *RF Wave and Energy Propagation in High Field MRI. Proc. 2010 ISMRM, p. 1479.*

This work presented a look at the nature of RF wave and energy propagation in high-field MRI using numerical field calculations. Specifically, the different approaches of “travelling wave MRI” in which waves are sent from one end of the magnet bore and more “conventional” MRI in which the object is placed in a volume array coil were compared and shown to be more similar than often thought.

5. Cao, Zhipeng; Dewal, Rahul; Sica, Christopher T.; Kao, Chien-Ping; Collins, Christopher M.; Yang, Qing X. *An Algorithm for Designing Passive Shim Sets Compensating for Anatomically Specific B0 Inhomogeneities. Proc. 2010 ISMRM, p.1544*

This work presented a novel algorithm for improving the homogeneity of the static magnetic fields in MRI of the human head using both active shim coils and passive magnetic materials.

6. Cao, Zhipeng; Sica, Christopher T.; Oh, Sukhoon; McGarrity, John; Horan, Timothy; Park, Bu Sik; Collins, Christopher M. *An MRI Simulator for Effects of Realistic Field Distributions and Pulse Sequences, Including SAR and Noise Correlation for Array Coils. Proc. 2010 ISMRM, p.1456*

7. Cao Z, Sica CT, Oh S, McGarrity J, Horan T, Park B, Collins CM. *Development of a Versatile MRI Simulator Considering Static, Gradient, and RF Field Distributions, Including SAR and Noise Correlation for Arrays. University of Minnesota Workshop on High Field Imaging and Spectroscopy, Minneapolis, MN, October 9-12, 2009. (Oral Presentation)*

8. Cao Z, Oh S, Sica CT, McGarrity J, Horan T, Park B, Collins CM. *Development of a Versatile MRI Simulator Including SAR and Noise Correlation for Multiple Transmit and Receive Coils in 3D. ISMRM Third International Workshop on Parallel MRI. Santa Cruz, October 23-26, 2009. (Oral Presentation)*

These last 3 works presented a newly-developed MRI system simulator capable of calculating image signal and noise, as well as sample RF heating with consideration of all pertinent electromagnetic fields throughout the sample in MRI. This simulator can be run on a desktop computer and should be a useful tool in design of safe and effective techniques and technology for MRI in the future. The 3 different presentations were given to different audiences with different specific interests, and each presentation was modified accordingly.

Summary of Progress towards Specific Aims

Toward Specific Aim 1, we have evaluated and compared several methods for improving efficacy and safety of RF fields in MRI in a variety of situations. As in the above works, this includes examination of effects of different RF array geometries and pulsing methods, as well as use of passive conductors to reduce electric fields and heating effects in the sample.

Toward Specific Aim 2, we have continued development of our computational methods for rapidly evaluating and reducing RF heating in MRI with transmit arrays. In October we finally received delivery of expensive (\$800,000) equipment needed to implement transmit array capability at our facility. We are now one of only a handful of sites in the world with transmit array capability on an MRI system used clinically at least part of the time, and are able to make much more rapid progress towards Aim 2. As is often the case in research with cutting-edge hardware, there have been a number of issues and technical difficulties, but progress continues.

Toward Specific Aim 3, we have successfully implemented and demonstrated the superiority of our array-optimized composite pulse to a conventional coil and pulsing method for improving efficacy and safety of the applied RF fields by using an MRI simulator currently under development at our laboratory. As with Specific Aim 2, progress toward Specific Aim 3 will increase now that the transmit array capability has been installed at our site.

Research Project 2: Project Title and Purpose

Interactions of the CA Protein in the Retrovirus Core - In retroviruses such as HIV, the human T-cell lymphotropic virus and the Rous sarcoma virus, a stage of the virus life cycle known as maturation involves very dramatic structural changes in the interior of the virus particle, leading to the activation of its infectious potential. The studies conducted as part of this project will use a combination of genetic and protein structural approaches to examine the molecular mechanisms that control this process in the formation of the functional core in the interior of the infectious particle. A detailed understanding of this essential step of virus infection will allow development of better inhibitors of capsid assembly for use as anti-retroviral drugs.

Duration of Project

1/1/2008 – 6/30/2009

Summary of Research Completed

This project ended during a prior state fiscal year. For additional information, please refer to the Commonwealth Universal Research Enhancement Annual C.U.R.E. Reports on the Department's Tobacco Settlement/Act 77 web page at <http://www.health.state.pa.us/cure>.

Research Project 3: Project Title and Purpose

Evaluation of Patient-Driven Playbook (A Patient Education Tool) - Diabetes has devastating consequences in terms of morbidity, mortality and health care costs. Between 2003 and 2004, two out of three Americans did not meet clearly identified evidence-based treatment goals. Yet the vast majority (84%) of patients believed that they were doing a good job managing their disease. A clear knowledge gap and educational opportunity thus emerged. By using a patient advocacy group, patient authors, and patient focus groups, a new tool, called the Penn State Diabetes Playbook, was developed to teach patients diabetes disease awareness and self-management skills. This project is designed to evaluate the Playbook alone or with nurse dialogue using motivational interviewing when it comes to educating, motivating and altering the behavior of patients with diabetes in a primary care setting.

Anticipated Duration of Project

1/1/2008 - 9/30/2010

Project Overview

The Playbook was created via a social marketing format which is a technique used to design programs that promote behavior change. Social marketing dictates that all program planning decisions must emanate from a consideration of the consumers' wants and needs which is divergent from more traditional, expert-driven approaches in which public health professionals determine what consumers need to know. This project will evaluate if providing patients with a patient-driven educational tool will decrease the emotional distress related to diabetes, increase medical knowledge of the disease, improve self-care behaviors and result in better clinical outcomes. The addition of a nurse educator using basic motivational interviewing techniques to explore use of this tool should increase success rates even further within these parameters. It is designed as a prospective, randomized-controlled trial. It has 3-arms with one group adhering to usual care, one group receiving the Playbook and one group receiving the Playbook with 15-30 minutes of nurse dialogue using motivational interviewing techniques. It will be important to determine what the incremental benefit of adding a nurse to the intervention is in order to help inform policy makers of the potential cost-benefit of such staff. Patients will be randomly assigned to one of the three arms. One hundred patients between the ages of 18-75 with type 2 diabetes seen by a primary care clinic will be identified and followed for six months. The four specific aims are (1) Determine the efficacy in decreasing emotional distress. (2) Demonstrate the ability in increasing medical knowledge. (3) Evaluate the capability to improve self-care behavior. (4) Examine the effect on clinical outcomes. The first three aims will be evaluated by use of surveys distributed at baseline, 4-weeks, 3-months and 6-months. These surveys include: (1) Problems Areas in Diabetes (PAID scale to assess emotional distress), which has been found

to be highly reliable (>.90) and responsive to changes during brief psychosocial and educational interventions, (2) the Summary of Diabetes Self Care Activities (SDSCA) survey, a reliable and valid measure of usual self-care behavior engaged in by persons with type 2 diabetes, which has been used to evaluate individuals' self-care behavior and adherence to diet, exercise, blood glucose testing, foot care, smoking, and self-care recommendations, (3) a Knowledge Questionnaire designed for this study to assess general disease knowledge, carbohydrate understanding and treatment of low blood glucoses, and (4) a Baseline demographics questionnaire. The fourth aim will be evaluated by Hemoglobin A1C checked at baseline, 3-months and 6-months.

Principal Investigator

Robert A. Gabbay, MD, PhD
Executive Director, Penn State Institute for Diabetes and Obesity
Penn State College of Medicine
500 University Drive
PO Box 850, H044
Hershey, PA 17033

Other Participating Researchers

David Mauger, PhD, Michelle S. Kavin, PA-C, CDE, Scott Mincemoyer RN, College of Nursing; Heather Stuckey, PhD, Shyam Sundar, PhD, Penn State College of Communications; Brian Smith, Penn State College of Information, Sciences and Technology - employed by Penn State

Expected Research Outcomes and Benefits

In the past decade studies such as the Diabetes Control and Complications Trial (DCCT) and the United Kingdom Prospective Diabetes Study (UKPDS) showed that intensively controlling glucose significantly reduces the risks of heart, eye and kidney disease. Yet patients throughout the country fail to achieve these goals. In order to reach treatment goals, patients with diabetes need to adhere to a healthy diet, obtain regular exercise, use medications appropriately, be consistent with glucose monitoring and possess the ability to make daily management decisions. These daily self-care behaviors, along with disease awareness and self-management skills, have proven critical to good diabetes outcomes. The current medical model with limited practitioner time, inadequate and at times poorly focused patient education material and lack of self-management training, has proven poor at teaching these skills. In addition, current patient education material fails to account for health literacy levels - the ability to read, understand, and act on health information. One out of five American adults reads at the 5th grade level or below, and the average American reads at the 8th to 9th grade level, yet most health care materials are written above the 10th grade level. Better tools are needed. Social marketing may be one avenue to create these tools. While successful in commercial aspects and many health care settings, social marketing has yet to be introduced into an approach for chronic disease care. If patient driven tools are successful at promoting behavior change and making information more accessible to those with low health literacy, it could improve the psychosocial and clinical

outcomes associated with diabetes that our current model of care has failed to achieve. This approach could be globally used to redesign patient materials for other chronic diseases such as Congestive Heart Failure, Coronary Artery Disease, and asthma where patient self-management is essential. And as more pay-for-performance programs disseminate across the country, cost effective tools such as this one and the incremental benefits of adding nurse education will play a large role in clinical care.

Summary of Research Completed

This report will include the expanded activities of the Interactive Web-Based Diabetes Self-Management Tool project. It was designed as an outgrowth from our work developing and testing a hard copy of the Playbook and is aimed to be an interactive, internet-based tool based upon the Penn State Diabetes Playbook that provides both educational and social networking opportunities to facilitate changes in diabetes self-management. The hypothesis is that by engaging patients in interactive behavior change technology using tailored messaging and directed message boards, the emotional distress related to diabetes will decrease, medical knowledge related to the disease will increase, and self-care management behaviors will improve. No study to date has used tailored messaging and social networking to impact diabetes self-management. Our goal is to see if we can expand the reach of the Diabetes Playbook, that has already received numerous awards for its usefulness (such as from the American Association of Diabetes Educators) through internet technology.

The web-based Diabetes Playbook content is based on the information from the hard-copy of the Playbook used in the initial evaluation. After recruitment and access to the internet program and informed consent, participants in the trial will be asked to complete four surveys (PAID, SDSCA, MDRTC and Demographics) for baseline. They will be led through a series of interactive, tailored modules based upon information from the Playbook. As participants answer the material correctly, they will receive encouragement and continue to the next multiple choice question. For incorrect responses, participants will be guided to the educational source in the Playbook where they can receive more information. After the educational component is completed, participants will then be linked to a social networking peer support system, where they can both read and submit their own suggestions of “what works well” for those with diabetes (collected prior to the trial). The peer support system will be moderated by one of the co-investigators for appropriate content. After 3 months, participants will be sent an automatic follow-up with the surveys. Both qualitative and quantitative (Likert) questions will be included to further expand upon the impact and usability of the tools. Upon successful completion of the initial educational tool and upon completion of the project, participants will receive compensation. The expected outcome is the successful creation of an interactive, internet based program based on tailored messaging in the Diabetes Playbook and social networking tool with initial data on the behavioral, emotional, educational and social impact of the modules.

- The creation of the web-based Penn State Diabetes Playbook has been completed with the collaboration of a multidisciplinary team, including input from the College of Information Science and Technology, College of Communications, College of Nursing and College of Medicine.

Technology

The “Interactive Web-Based Diabetes Self-Management Tool” was created using the Plone content management platform. The Survey Monkey online survey program was used for the creation of the online surveys and collection of data. The NING online platform was used for the creation of the social networking program. User analysis was directed through Google analytics.

Recruitment

When the creation of the two web-sites was completed and tested (the Diabetes Playbook and NING social networking site), advertisement for the study for subject recruitment was initiated in November, 2009 via paper announcements posted at various primary care clinic sites, and electronically via the Penn State Newswire, D-life (www.dlife.com), the Penn State Hershey Research Facebook account (www.facebook.com/PennStateHersheyResearch), and Craigslist (www.craigslist.com).

We currently have 48 people that have completed the consent forms, the baseline survey, the five learning modules and the follow-up survey. After the completion of this part of the study, the participants join the social networking program in NING for 90 days. At 90 days, the applicable participants are contacted to complete the final survey. There are currently 33 participants who have completed all aspects of the study with 15 pending completion of 90 days of participation on the social networking site and final survey. We are continuing to recruit in an attempt to reach a greater sample size with an initial goal of 50 patients (ages 18-75, English speaking) with diabetes.

Since the initiation of recruitment, applicable participants have been contacted via email to initiate compensation after the completion of the second survey. They were also contacted with email reminders to promote completion of the study when lags in participation were noted. Participants were again compensated after the conclusion of the study.

Table 1. Summary of Web-Based Intervention

Time	Task
Step 1: Baseline	Completion of Implied Consent; Baseline PAID, SDSCA, MDRTC, and Demographics
Step 2: 30-45 Min.	Completion of Web-Based Interactive Modules with Customized Tailored Messaging
Step 3:	Completion of PAID, SDSCA, MDRTC and Qualitative Questions
Step 4:	Linked to Peer Support Networking Forum
Step 5: 3 Months	Follow-Up to Assess PAID, SDSCA, MDRTC and Qualitative Questions (PAID compared to Step 1 Baseline)
Step 6:	Completion of Research with Incentive

Research Project 4: Project Title and Purpose

DeltaFosB and Reward Comparison in Mice - Drug addiction often leads to decreased motivation for things that were once pleasurable before drug use such as friends, family, work, hobbies, and even personal hygiene. This devaluation of naturally rewarding stimuli in the environment, in favor of the drug of abuse, leads to personal and public costs as the addict is no longer able to beneficially function in society. The present project combines the only animal

model of this phenomenon (i.e., drug-induced devaluation of natural rewards) with a rich mouse model to elucidate a possible molecular mediator of the neural plasticity that leads to this potentially devastating behavioral change.

Anticipated Duration of Project

7/1/2009 - 6/30/2011

Project Overview

Rats and mice avoid intake of a saccharin conditioned stimulus (CS) when it is paired with a drug of abuse such as morphine or cocaine. Apparently the rats avoid intake of the natural reward cue because the value of the gustatory stimulus pales in comparison to the subsequent reward produced by the drug. In fact, the rats that reduce their intake of the drug-associated taste cue the most; self-administer the most of a drug of abuse. Moreover, avoidance of the saccharin cue is exaggerated in Lewis rats and in Sprague-Dawley rats subjected to chronic morphine treatment, both models that are known to be drug sensitive. The augmented response to drug reward observed in these rats has been attributed to a range of neural adaptations, including elevated levels of the nuclear transcription factor Δ FosB. DeltaFosB levels increase and remain elevated after chronic drug exposure. Increases in Δ FosB sensitize a number of behavioral responses to drug rewards including conditioned place preference, acquisition and maintenance of drug self-administration, and performance for drug on a progressive ratio schedule of reinforcement. These data led us to hypothesize that transgenic mice with elevated Δ FosB in the striatum also would demonstrate exaggerated avoidance of a saccharin cue following saccharin-cocaine pairings. To our surprise, the opposite occurred. We concluded that the mice probably are more sensitive to all rewards, both drug induced and naturally occurring. The proposed studies will test this hypothesis in mice by selectively increasing Δ FosB in the nucleus accumbens using adeno-associated viral mediated gene transfer (AAV- Δ FosB mice). *Specific Aim I* tests whether elevation of Δ FosB will lead to an increase in preference for saccharin or a neutral salt stimulus, but not for an aversive (quinine) taste stimulus. *Specific Aim II* tests whether elevation of Δ FosB will augment (as initially predicted) cocaine-induced suppression of CS intake when a neutral or aversive tastant, rather than a rewarding tastant, serves as the gustatory CS. Finally, *Specific Aim III* tests whether ‘impulsivity’ is responsible for the failure to suppress intake of a natural reward cue following saccharin-cocaine pairings in mice with elevated Δ FosB.

Principal Investigator

Patricia Sue Grigson, PhD
Professor, Neural & Behavioral Science
Department of Neural and Behavioral Sciences
The Pennsylvania State University, College of Medicine
Milton S. Hershey Medical Center
500 University Drive, H181
Hershey, PA 17033

Other Participating Researchers

Christopher S. Freet, MS, PhD. student, Penn State College of Medicine

Jennifer E. Nyland – Graduate Student employed by Pennsylvania State University College of Medicine

Expected Research Outcomes and Benefits

According to DSM-IV, substance abuse and dependence involve a failure to fulfill major obligations at work, school, or home, the giving up of important social, occupational, or recreational activities, and continued drug use in spite of recurrent physical, legal, social, or psychological problems. Addiction, then, is a two-part problem involving chronic relapse and the concurrent devaluation of natural rewards. There are a number of critical animal models of craving and relapse. There are, however, no recognized animal models for the study of drug-induced devaluation of natural rewards. The present project describes our development of just such an animal model and the investigation of the underlying neural substrates.

Summary of Research Completed

This project combined the only animal model of this phenomenon (i.e., drug-induced devaluation of natural rewards) with a rich mouse model to elucidate a possible molecular mediator of the neural plasticity that leads to this, potentially, devastating behavioral change. In these studies we planned to use two different types of mice. The first are drug-sensitive mice that have an increase in the expression of DeltaFosB (Δ FosB) in the nucleus accumbens. The second are reward preferring inbred C57BL/6 mice vs. less preferring DBA/2J mice. *Specific Aim I* tested whether increased responsiveness to reward will lead to an increase in preference for saccharin or a neutral salt stimulus, but not for an aversive (quinine) taste stimulus. *Specific Aim II* tested whether increased responsiveness to reward will augment (as initially predicted) cocaine-induced suppression of CS intake when a neutral or aversive tastant, rather than a rewarding tastant, served as the gustatory CS. *Specific Aim III* tested whether ‘impulsivity’ is responsible for the failure to suppress intake of a natural reward cue following saccharin-cocaine pairings in mice with increased responsiveness to reward. Interestingly, in both cases, the results showed that the reward-preferring mice (the Δ FosB and the C57BL/6) exhibited not only greater sensitivity to the rewarding properties of drugs of abuse, as we expected, but also greater sensitivity to the rewarding properties of natural rewards such as sucrose or saccharin. As a consequence, these mice showed less, rather than more, cocaine-induced devaluation of the natural reward cue. Indeed, the preference for the natural reward appears to have protected the mice from the addictive properties of the drug. Papers related to this project are the following:

- 1) C57BL/6J mice demonstrate less impulsive choice compared with DBA/2J mice in a gustatory reward delay discounting task. Christopher S. Freet, Amanda Motter, & Patricia S. Grigson. Manuscript in preparation.
- 2) C57BL/6J mice demonstrate attenuated cocaine-induced suppression of saccharin intake compared with DBA/2J mice. Christopher S. Freet, Amanda Motter, Samantha Leeper, & Patricia S. Grigson. Manuscript in preparation.
- 3) Fischer rats are more sensitive than Lewis rats to the suppressive effects of morphine and the aversive opioid agonist, spiradoline. Christopher S. Freet, Robert A. Wheeler¹, Ellen

Leuenberger, Nicole A. Sublette, and Patricia S. Grigson, Manuscript in preparation.

Although these studies did not work out as hypothesized (i.e., we expected the high Δ FosB mice and the C57BL/6 mice to exhibit the greatest drug-induced devaluation of the natural reward taste cue), the findings were very important as they demonstrated that greater preference for natural rewards was very protective against drug-induced devaluation of a natural reward. This finding has clear implications for the treatment of human addicts.

That said, it also became evident that these mouse models were not going to further our understanding of the neural circuitry underlying drug-induced devaluation of natural rewards (the main objective of this project), because the unexpected preference for the natural reward blocked devaluation by drug. Thus, after Dr. Christopher Freet defended his thesis, Ms. Jen Nyland took over the project and began to use neurotoxic lesions to more directly assess the role of various nuclei in drug-induced suppression of intake of an otherwise palatable taste cue. In specific, she sought to test the hypothesis that an intact thalamic orosensory area is essential for drug-induced devaluation of natural rewards. The results of this study will address our main objective by furthering our understanding of addiction, drug-induced devaluation of natural rewards, and the neural underpinnings.

Experiment 1. An intact thalamic orosensory area is not required for the comparison of natural rewards.

Methods. The subjects were 33 male Sprague-Dawley rats housed individually in suspended, stainless steel cages in a temperature-controlled (21°C) animal care facility under a 12:12 hour light-dark cycle. Food and water were available ad libitum, except where noted otherwise. Subjects received bilateral electrophysiologically-guided ibotenic acid lesions of the thalamic trigeminal orosensory area (TOAx, n=17) or were injected similarly with vehicle and, thus, served as sham lesion controls (Sham, n=16). *Food Restriction.* Once having recovered from surgery (no less than 1 week), all rats were food-deprived to 90% of their free-feeding body weight, maintained by a once per day feeding. *Saccharin-Sucrose Pairings.* Subjects were habituated to the experimental chambers for 5 min a day for 3 days. During testing, all rats were given 3 min access to 0.15% saccharin, followed immediately by retraction of the first spout and 3 min access to a second spout containing either more 0.15% saccharin (Sac-Sac) or 1.0 M sucrose (Sac-Suc). There was one such pairing a day for 20 days and the latency to lick each bottle and the number of licks made on each was recorded.

Results. *CS Intake.* The licks emitted on bottle 1 (0.15% saccharin CS) were averaged into 2-day blocks (See Figure 1). Here and elsewhere, the data for the two lesion conditions were analyzed separately using repeated-measures analyses of variance (ANOVA) varying condition (Sac-Sac or Sac Suc) and 2 Day Block (1-10). When appropriate, post hoc comparisons were made using the Newman-Keuls test with α set at 0.05. Both the Sham Sac-Suc and TOAx Sac-Suc groups suppressed intake of the saccharin cue compared to intake of the saccharin cue by their respective Sac-Sac controls. Both the Sham and the TOAx groups had a significant Condition x Block interaction (Sham: $F=11.30$, $p<0.0001$; TOAx: $F=2.859$, $p<0.01$), significant main effects of condition (Sham: $F=547.0$, $p<0.0001$; TOAx: $F=14.32$, $p<0.001$), and Block (Sham: $F=15.42$, $p<0.0001$; TOAx: $F=4.148$, $p<0.0001$). This was further supported by post hoc tests showing significant sucrose-induced suppression of CS intake starting with block 3 for the Sham group

and block 6 for the TOAx group, $ps < .05$. An intact TOA, then, is not essential for the development of a sucrose-induced anticipatory contrast effect (i.e., sucrose-induced suppression of intake of a lesser valued saccharin cue).

Experiment 2. An intact thalamic orosensory area is essential for the comparison of a natural Polycose reward with morphine.

Methods. The subjects from the previous experiment were matched on the basis of their prior experience and assigned to a saline or a morphine treatment group. *Baseline Intake.* All subjects were placed on a water-deprivation regimen (5 min am/1 h pm) which continued for 7 days until 5 min morning intake stabilized. *Polycose-Morphine Pairings.* Subjects were given 5 min access to 0.03M Polycose (CS), followed 5 min later by an intraperitoneal injection of either 15 mg/kg morphine or an equal volume of saline. There was one such pairing a day with 48 hours in between pairings for a total of 6 pairings.

Results. *CS Intake.* Five min Polycose intake data from this experiment and those from a similar pilot study were pooled and analyzed using a 2 x 2 x 6 mixed factorial ANOVA varying lesion (Sham vs. TOAx), condition (saline vs. morphine), and trials (1-6). In the Sham lesioned morphine treated group, intake of the Polycose CS was suppressed compared with the saline treated Sham controls (see Figure 2). This conclusion is supported by post hoc tests of a significant Condition x Trial interaction ($F=28.56$, $p<0.0001$) showing significant morphine-induced suppression in the Sham lesioned controls beginning with trial 2, $ps < .05$. The TOAx group treated with morphine, however, failed to suppress intake of the Polycose CS compared to intake by the TOAx saline treated lesion controls, all $F_s < 1$. Thus, the same TOAx lesion that failed to disrupt the suppressive effects of a highly rewarding sucrose solution in Experiment 1, fully prevented morphine-induced suppression of Polycose intake in Experiment 2.

Experiment 3. An intact thalamic orosensory area is essential for the comparison of a natural saccharin reward with cocaine.

Methods. The subjects were naïve 32 male Sprague-Dawley rats housed individually in suspended, stainless steel cages in a temperature-controlled (21°C) animal care facility under a 12:12 hour light-dark cycle. Food and water were available ad libitum, except where noted otherwise. Subjects received bilateral lesions to the thalamic trigeminal orosensory area as described above (TOAx, $n=18$) or were injected similarly with vehicle and served as surgical controls (Sham, $n=14$). *Baseline Intake.* Following a week of recovery, all subjects were placed on a water-deprivation regimen (5 min am/1 h pm) which continued for 9 days until 5 min morning intake stabilized. *Saccharin-Cocaine Pairings.* Subjects were given 5 min access to 0.15% saccharin (CS), followed 5 min later by a subcutaneous injection of either saline or 10 mg/kg cocaine. There was one such pairing a day, at 48 h intervals, for a total of 5 pairings.

Results. *CS Intake.* As with the morphine study, the Sham lesioned cocaine treated group suppressed intake of the saccharin cue relative to the Sham lesioned saline injected controls (see Figure 3). In support, analysis of the data from the Sham lesioned group revealed a significant Condition x Trial interaction ($F=24.03$, $p<0.0001$), as well as significant main effects of condition ($F=459.8$, $p<0.0001$), and trial ($F=3.621$, $p<0.05$). Post hoc tests of the two-way interaction found a significant reduction in CS intake in the morphine-injected Sham rats following a single saccharin-cocaine pairing, $ps < .05$. The TOAx cocaine group, on the other

hand, appeared to have two distinct populations behaviorally. Thus, until histological analysis can identify missed lesions, the group was divided on the basis of the behavior into “Suppressors” (n=3) and “Non-Suppressors” (n=5) for analysis. The results indicate no significant difference in CS intake between the TOAx Saline group and the TOAx cocaine treated “Non-Suppressors”, while for the TOAx cocaine treated “Suppressors” a significant Condition x Trial interaction ($F=8.744$, $p<0.0001$), as well as significant main effects of Condition ($F=55.77$, $p<0.0001$), and Trial ($F=3.697$, $p<0.01$) were obtained. The “Non-Suppressors” also demonstrated an absence of neophobia to a hot trigeminal capsaicin solution, suggesting the TOA lesion appropriately targeted the trigeminal region of this nucleus in the “Non-Suppressors”. This was not the case for the rats that exhibited normal avoidance of the cocaine-associated saccharin cue (i.e., the “Suppressors”). Therefore, it appears that, when appropriately placed, the TOA lesion effectively eliminates both the suppressive effects of morphine and those of cocaine.

Experiment 4. An intact thalamic orosensory area is not required for lithium chloride-induced conditioned taste aversion.

Methods. The subjects from the first two experiments were reassigned to saline and LiCl conditions in a counterbalanced fashion regarding the assignment from the previous experiments. **Baseline Intake.** All subjects were placed on a water-deprivation regimen (5 min am/1 h pm) which continued for 8 days until 5 min morning intake stabilized. **NaCl-LiCl Pairings.** Subjects were given 5 min access to 0.1M NaCl (CS), followed 5 min later by an intraperitoneal injection of 1ml/kg LiCl (Trials 1-4, 0.009; Trials 5 and 6, 0.018 M; Trials 7 and 8, 0.0375 M; Trials 9-12, 0.15 M) or an equal volume of saline. There was one such pairing a day with 48 hours in between pairings for a total of 12 pairings.

Results. CS Intake. Both the Sham LiCl and TOAx LiCl groups avoided intake of the NaCl CS that was paired with LiCl-induced visceral malaise. Thus, a significant Condition x Trial interaction (Sham: $F=3.383$, $p<0.001$; TOAx: $F=2.083$, $p<0.05$), and significant main effects of condition (Sham: $F=23.89$, $p<0.0001$; TOAx: $F=12.04$, $p<0.001$), and Trial (Sham: $F=3.407$, $p<0.001$; TOAx: $F=2.453$, $p<0.01$) were obtained for both the Sham and the TOAx rats. Post hoc tests of the two-way interactions revealed that LiCl treatment significantly suppressed CS intake across the last two trials for the Sham lesioned rats and on the final trial for the TOAx rats.

Conclusion: Bilateral ibotenic acid lesions of the TOA prevent avoidance of a natural reward cue when paired with either morphine or cocaine, but not when paired with a putative rewarding stimulus (sucrose) or a putative aversive (LiCl) consequence. This is the first data set to dissociate the suppressive effects of a sweet with those of the drugs of abuse. As such, we must conclude that the comparison of drugs and sweets relies upon different neural circuitry than the comparison of disparate sweet rewards and/or that avoidance of a taste cue, in anticipation of the availability of a drug, is not mediated only by reward comparison (i.e., drug-induced devaluation), but also by cue-induced craving and/or relapse. The TOA, then, may be viewed as essential for the development of cue-induced craving and relapse as well. Given that addiction is a chronic relapsing disorder, this finding is of potential fundamental import.

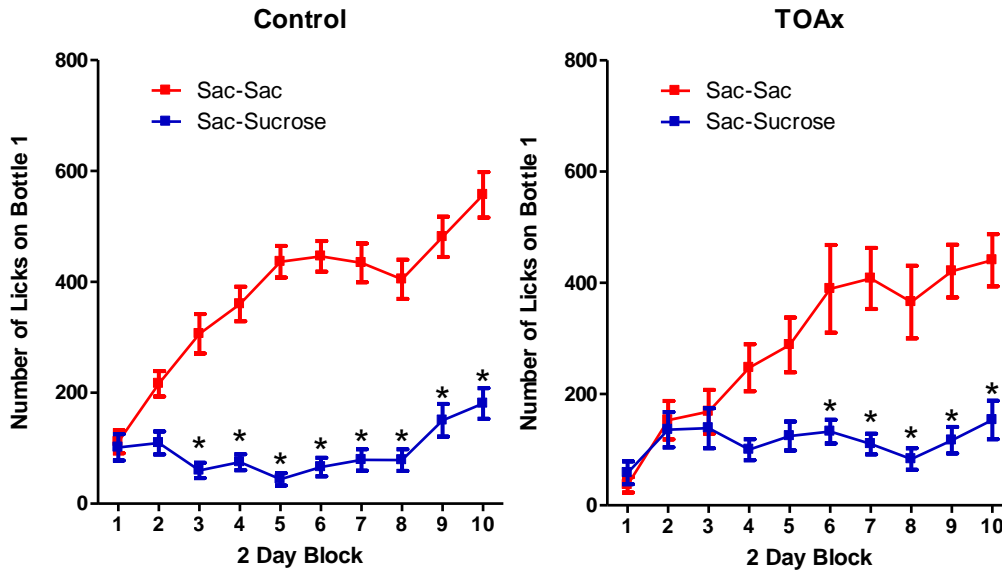


Figure 1. Saccharin-Sucrose Anticipatory Contrast

Mean (\pm SEM) number of licks for first bottle 0.15% saccharin for the Surgical Control (left) and TOAx (right) groups across 2-Day Blocks. Both the Sham lesioned Controls in the Sac-Suc condition (n=8) and the TOAx rats in the Sac-Suc condition (n=7) suppressed CS intake when paired with a preferred 1.0 M sucrose solution compared with Sham Sac-Sac (n=8) and TOAx Sac-Sac (n=6) groups, respectively. * = $p < 0.05$

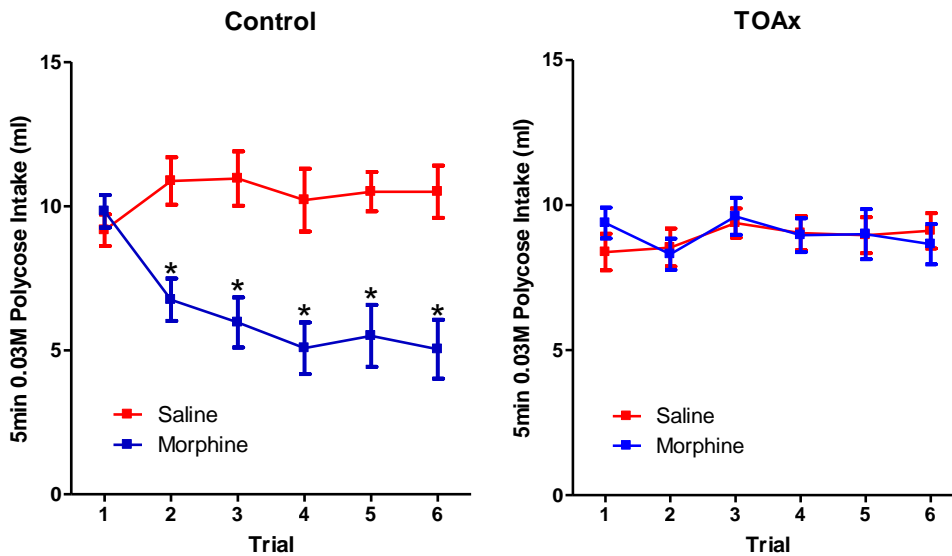


Figure 2. Polycose-Morphine

Mean (\pm SEM) intake of 0.03M Polycose for the Sham lesion controls (left) and for the TOAx (right) groups. The Sham lesioned morphine treated group (n=14) suppressed CS intake compared with the Sham lesioned saline controls (n=8), beginning with trial 2. The CS intake for the TOAx Morphine group (n=14) was not significantly different than the CS intake exhibited by the TOAx Saline treated group (n=13). * = $p < 0.05$

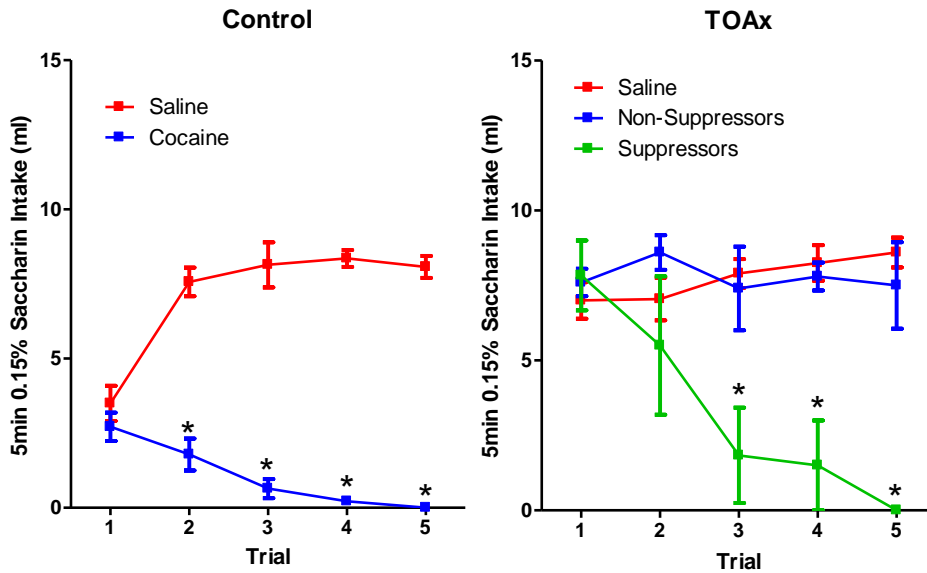


Figure 3. Saccharin-Cocaine

Mean (\pm SEM) 0.15% saccharin intake for Sham lesion controls (left) and TOAx rats (right). The Sham cocaine group (n=7) suppressed CS intake compared with Sham saline controls (n=7), beginning with trial 2. The TOAx Cocaine group was divided into Suppressors (n=3) and Non-Suppressors (n=5). The CS intake for the Non-Suppressors was not significantly different than the CS intake of the TOAx Saline group (n=10), however, the 3 subjects who did suppress were significantly different than the TOAx Saline group and the Non-Suppressors and the reduction in intake was significant beginning with trial 3. * = $p < 0.05$

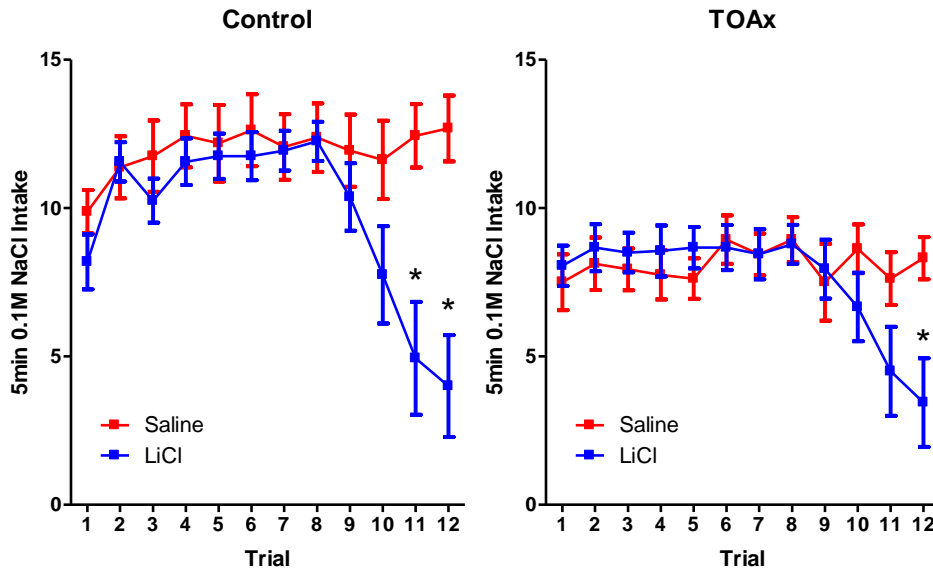


Figure 4. NaCl-LiCl Conditioned Taste Aversion

Mean (\pm SEM) intake of 0.1 M NaCl for Sham surgical controls (left) and TOAx (right) groups over trials 1 - 12. Subjects received 1 ml/kg LiCl with the following concentrations: Trials 1-4, 0.009; Trials 5 and 6, 0.018 M; Trials 7 and 8, 0.0375 M; Trials 9-12, 0.15 M; or an equal volume of saline. Although intake was slightly lower in the TOAx rats overall, ultimately, both the Sham LiCl-treated group (n=8) and the TOAx LiCl-treated group (n=8) suppressed CS intake relative to their saline treated counterparts. * = $p < 0.05$

Research Project 5: Project Title and Purpose

Iron-Induced Changes that Predispose to Malignancy - Hepatocellular carcinoma (HCC) is one of the most common cancers in the world and also one of the most deadly. It is clear that chronic excess iron deposition is implicated in the development of HCC. Understanding the cellular and molecular changes occurring in the liver exposed to chronic excess iron deposition may lead to the future identification of biomarkers for early detection of progression and may also provide improved strategies for early chemopreventive intervention.

Duration of Project

1/1/2008 – 6/30/2009

Summary of Research Completed

This project ended during a prior state fiscal year. For additional information, please refer to the Commonwealth Universal Research Enhancement Annual C.U.R.E. Reports on the Department's Tobacco Settlement/Act 77 web page at <http://www.health.state.pa.us/cure>.

Research Project 6: Project Title and Purpose

Nutrient Overload as a Causative Factor in Diabetic Retinopathy - The research project focuses on the novel view of nutrients as signaling molecules that act through signal transduction cascades to regulate various cellular functions. The nutrient sensing signaling pathways are not only interconnected at multiple levels but they are also coupled to the insulin receptor signaling pathway. Diabetes is a disease characterized not only by an impaired insulin receptor signaling pathway (due to lack of insulin and/or insulin resistance), but also by elevated blood concentrations of nutrients such as glucose, fatty acids and branched-chain amino acids. Therefore, the overall purpose of the project is to gain a better understanding of the relative contributions of the impaired insulin receptor and the nutrient-activated signaling cascades to the development of diabetic retinopathy.

Duration of Project

1/1/2008 - 6/30/2009

Summary of Research Completed

This project ended during a prior state fiscal year. For additional information, please refer to the Commonwealth Universal Research Enhancement Annual C.U.R.E. Reports on the Department's Tobacco Settlement/Act 77 web page at <http://www.health.state.pa.us/cure>.

Research Project 7: Project Title and Purpose

Co-Crystals of Novel Integrase Mutants and Retroviral DNA - The permanent integration of retroviral DNA into cellular DNA leads to immunodeficiency, neurological, and neoplastic diseases. The long-term goal of this project is to benefit human health by developing ways to interfere with retrovirus integration. The viral integrase enzyme causes integration by specifically nicking the ends of viral DNA at a precise location, and then inserting that viral DNA into any site in cellular DNA. However, our understanding of how this one enzyme interacts with, and acts on, two different kinds of DNA is limited. Analyzing the molecular structures of crystals that contain integrase bound to viral DNA could finally reveal how integrase distinguishes between viral and cellular DNA. Thus, this project is directed at making it possible to obtain these long-sought crystals.

Duration of Project

1/1/2008 – 6/30/2009

Summary of Research Completed

This project ended during a prior state fiscal year. For additional information, please refer to the Commonwealth Universal Research Enhancement Annual C.U.R.E. Reports on the Department's Tobacco Settlement/Act 77 web page at <http://www.health.state.pa.us/cure>.

Research Infrastructure Project 8: Project Title and Purpose

Research Infrastructure - Biological Research Laboratory Construction - The purpose of this project is to design and build an Animal Biosafety Level three (ABSL-3) research laboratory for the study of immunology and infectious diseases requiring high level biocontainment.

Anticipated Duration of Project

1/1/2008 – 12/31/2011

Project Overview

The scope of this project is to design and build an animal biosafety level three (ABSL-3) research laboratory for the study of immunology and infectious diseases requiring high level biocontainment. Even with the knowledge and biotechnology now available, we still face serious threats to human health and well-being from serious and highly transmissible infectious diseases and / or potential agents of bioterrorism such as avian influenza and anthrax. To respond, we must create a research environment and provide the infrastructure necessary to allow investigators to study these pathogens and discover new ways to detect, prevent or cure these diseases. The proposed Biological Research Laboratory will provide space, support, and biocontainment for basic, applied and diagnostic research; national, state and community outreach; and education on important human and / or zoonotic pathogens. It will include state of the art laboratories and animal resources, facilities and services that are recognized within and outside the University as being of the very highest quality consistent with our talents and resources. This facility will be composed of a number of ABSL-3 suites for *in vivo* research using small animal models of human disease (primarily rodents and poultry models). Each suite will have independent air locks to support multiple agent research as well as providing compartmentalization to mitigate cross-contamination concerns. Changing rooms and shower out facilities are included as required. Supporting the ABSL-3 suites will be BSL-3 laboratories for *in vitro* bacteriology, virology, and molecular biology procedures. Outside of the biocontainment area another support laboratory provides preparatory space for the activities within the barrier. The strategically located management office allows for oversight of the main entry way as well as the loading dock. A conference/classroom/break room allows for on-site training sessions and staff meetings. This \$5,000,000 building project will encompass 8,500 gross square foot, and will provide laboratories as well as animal holding space that will support the critical need for biocontainment research space at the Pennsylvania State University. This facility will be a unique and much needed resource for infectious disease research.

Principal Investigator

Mary J. Kennett, DVM, PhD, Diplomate ACLAM
Director, Animal Resource Program and Professor of Veterinary & Biomedical Sciences
101 CBL
The Pennsylvania State University
University Park, PA 16802

Other Participating Researchers

Biao He, PhD, Craig Cameron, PhD, Vivek Kapur, PhD - employed by Pennsylvania State University

Expected Research Outcomes and Benefits

The proposed Biological Research Laboratory, an Animal Biosafety Level 3 (ABSL-3) facility, presents excellent opportunities for infectious disease research and will greatly enhance the research capabilities on campus. It is not possible to do research with highly infectious agents such as anthrax and avian influenza without proper protection and biocontainment. This facility will provide special air handling capabilities to filter the exhausted air, liquid and solid waste decontamination, high security, and standard operating procedures within the facility to ensure the safe handling of such agents. The facility is organized into a central spine that connects all of the research spaces to the central decontamination and support areas of the project.

Summary of Research Completed

This project is progressing well, has increased in scope, and is moving into final design. The project was temporarily put on hold while the Penn State design team put together an expanded design and grant proposal for the National Center for Research Resources (NCRR) Recovery Act Construction Program. The goal of the grant proposal was to expand the ABSL-3 facility to include an insectary, and additional laboratory and animal holding space. In addition the expanded facility will have increased redundancies to meet National Institutes of Health (NIH) construction guidelines. The proposal was successful and an award of \$14.8 million was received to expand the facility. In accordance with the guidelines of the award, a phase 1 archeological review was performed and an environmental assessment is in progress. In addition, we have redesigned the facility to include additional features such as an insectary, a second BSL-3 laboratory and a second shower, as well as improved the redundancy of the building systems. The enhanced building project consists of a 20,000 GSF animal biosafety level three (ABSL-3) facility. The expanded facility will include microbiology and virology laboratories, cell sorting capabilities, animal biocontainment suites, and an insectary. This enhanced facility will support the study of emerging and zoonotic agents, vector borne diseases, the host pathogen interface, and vaccine development. As there is currently no ABSL-3 space on campus, the proposed building represents the fulfillment of a significant need for space to safely study highly infectious agents. Our immunology and infectious disease research program is growing rapidly, and to complement and enhance our current programs several new faculty members whose interests span the broad theme of pathogen evolution have been hired. In particular, we have recruited a new faculty member with ABSL-3 experience who will serve as the scientific director of the new facility. Two centers of excellence, the Center for Infectious Disease Dynamics and the Center for Molecular Immunology and Infectious Disease have formed around the core research groups in this area. Major thematic areas of research include the dynamic modeling of diseases, the evolution of viruses and bacteria in response to drugs and vaccines, the effects of climate change on pathogens, and the transmission dynamics of zoonotic infections.

We met with interested faculty groups to identify equipment needs, and designed the facility with respect to the identified and predicted need for each type of equipment and space with as much flexibility as possible within the constraints of BSL-3 design. The site for the building, near the current Animal Diagnostic Lab, was chosen as it is easily accessible from central campus and yet not near dense student populations. Now that the NIH proposal has been funded, we plan to submit a combined design document and schematic design document package to the NIH for their review prior to July 2, 2010.

The new containment zones are illustrated in Figure 1 and an artist's rendering of the BRL is shown in Figure 2.

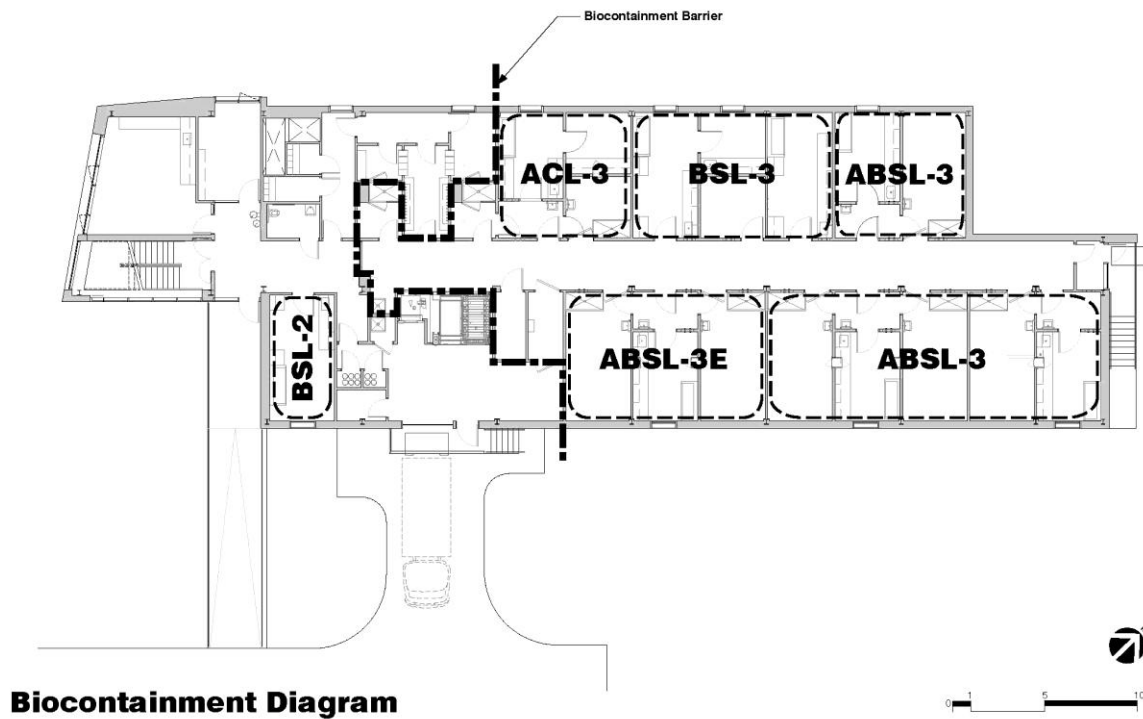


Figure 1. Containment zones for the ABSL-3 facility include the insectary (arthropod containment level-3 (ACL-3), Biosafety Level 2 and 3 (BSL-2 and BSL-3) laboratory space, and Animal biosafety level-3 (ABSL-3) and enhanced ABSL-3 (ABSL-3E) space.



Figure 2. An artist's rendering of the BRL, showing the main personnel entrance and loading dock.

Research Project 9: Project Title and Purpose

Translational Research in Polycystic Ovary Syndrome - The purpose of this project is to continue studies that will identify genetic contributions to Polycystic Ovary Syndrome (PCOS). PCOS is the most common cause of infrequent menses and excess male hormone in women and affects 5-10% of the female population. We intend to closely study families, where this disorder clusters, to better understand the heritability of its traits, as well as by studying the children of PCOS mothers to better understand how it develops. We will collect and study DNA and human thecal cells from ovarian follicles to better understand how a genetic variant in the Fibrillin 3 gene on chromosome 19 contributes to the etiology of the syndrome.

Anticipated Duration of Project

1/1/2008 – 12/31/2010

Project Overview

We will study families of women with PCOS (Aim 1) and thecal cells from ovarian follicles (Aim 2)

Specific Aim 1: To phenotype probands with PCOS and their parents and siblings, and to identify children of mothers with PCOS for future study.

Our goal is to phenotype 25 family units (consisting of a proband, her parents, and any sisters) and an estimated 75-100 human subjects. This phenotyping protocol has been in place since 1994, and involves for the proband with suspected PCOS: a questionnaire, blood tests for serum androgens and exclusions of other possible diagnoses (Congenital adrenal hyperplasia, hyperprolactinemia, etc.), blood for DNA extraction, a 2h oral glucose tolerance test, and a

transvaginal ultrasound. For the other family members, the oral glucose tolerance test and the transvaginal ultrasound (females only) is optional. Additionally we will identify mothers with PCOS and their young children (Ages 4-16) to participate in a protocol that if funded will study the children longitudinally for reproductive and metabolic abnormalities as they go through puberty.

Specific Aim 2: Find the determinants and identify effects associated with the genetic marker we have already identified (a microsatellite marker within the Fibrillin 3 gene- D19S884). What are the “downstream” effects of variation at D19S884 and neighboring sequences?

We will test the hypothesis that allele 8 of D19S884 “marks” a PCOS risk allele. Experiments will determine whether: (1) FBN3 is a PCOS susceptibility gene, (2) a gene located in the D19S884 region has alleles associated with PCOS, and (3) the D19S884 region regulates expression of a nearby gene that influences risk of PCOS. The goal of these experiments is to investigate the FBN3 locus and surrounding region to determine the underlying mechanism that explains the findings of linkage and association between D19S884 and PCOS. In normal and PCOS theca cells we will investigate: (1) whether allele 8 affects splicing of the FBN3 gene resulting in the formation of a novel transcript (which has unique biological activities that predispose to PCOS), (2) the possibility that D19S884 (and particularly allele 8) is a cis element that regulates expression of the FBN3 or other genes, and (3) if fibrillin 3 influences the function of theca cells.

Principal Investigator

Richard S. Legro, MD
Professor
M.S. Hershey Medical Center
H103, Dept. of Ob/Gyn
500 University Drive
Hershey, PA 17033

Other Participating Researchers

Jan McAllister, PhD - employed by Penn State College of Medicine

Expected Research Outcomes and Benefits

Specific Aim 1: Anticipated Results: We expect to continue to find a high prevalence of hyperandrogenism and glucose intolerance among first degree relatives of women with PCOS. Further we expect that most mothers with PCOS and their children will elect to participate in our protocol studying children when it is active.

Specific Aim 2: Anticipated Results: We expect to find alternatively spliced forms of the *FBN3* transcript involving exon 56 that have not been previously reported. We will take CCL25, a secreted chemokine, as an example of how we would approach documenting an association between D19S884 and expression of a candidate gene and the role that gene might play in

producing the PCOS phenotype. We expect to be able to utilize the approaches as outlined above for the study of CCL25 to confirm an association between the PCOS risk allele of D19S884 and altered CCL25 levels.

Summary of Research Completed

Since these monies were used as bridge monies for an ongoing phenotype and genotype project in familial polycystic ovary syndrome that was funded by the NIH before (beginning in 1994) and eventually after the bridge grant, the results below include data collected both during the NIH support period as well as from the current Tobacco Settlement Fund (TSF) period. Remaining Tobacco CURE Funds were devoted to salary support of the study coordinator, costs of assays, and patient costs for continuing the study during the unfunded period. Our enrollment data cites the subjects who were seen under the auspices of the TSF grant.

Enrollment data:

In 2009 we enrolled 41 women with PCOS, 27 family members, 29 male controls, and 14 female controls. In 2010 year to date we have recruited 22 women with PCOS, 27 male controls, 9 male controls, and 11 female controls.

Studies

We have examined the association of PCOS with several genes that have been associated with type 2 diabetes. We have found a lack of association between the sex hormone binding globulin (SHBG) gene and with multiple alleles associated with type 2 diabetes. Manuscripts are in preparation and should soon be submitted. Summaries follow:

SHBG gene

Context: Single nucleotide polymorphisms (SNPs) in the *sex hormone-binding globulin (SHBG)* gene are associated with type 2 diabetes mellitus (T2DM). *SHBG* has also been proposed as a candidate gene for the polycystic ovary syndrome (PCOS).

Objective: The study aims were: 1) to determine if any of four *SHBG* SNPs (rs1779941, rs6297, rs6259, and rs727428) are associated with PCOS; and 2) to determine if SNP genotype influences SHBG levels in women with PCOS.

Design: Using the transmission disequilibrium test (TDT), evidence of associations between *SHBG* SNPs and PCOS were analyzed. Additionally, correlations between SHBG levels and SNP genotype, body mass index (BMI), non-SHBG bound testosterone (uT), and insulin resistance estimated by the homeostasis model (HOMA-IR) were determined.

Setting: Academic medical centers.

Intervention(s): None

Patients or Other Participants: A total of 430 families having a proband with PCOS were included in the family-based study. Associations between SHBG and SNP genotypes were determined in 678 women with PCOS including probands from the family cohort.

Main Outcome Measure(s): Primary outcome measures included transmission frequency of SNP alleles and correlation coefficients between SHBG and allele frequency/metabolic parameters.

Results: No evidence of association between SNPs of interest and PCOS was found. However, in multivariate analyses, SHBG levels varied significantly with rs1799941 and rs727428 genotype after controlling for BMI, uT, and HOMA-IR.

Conclusions: Although *SHBG* SNPs previously associated with T2DM do not appear to be associated with PCOS status, rs1799941 and rs727428 genotypes are associated with SHBG levels independent of the effects of insulin resistance and obesity.

Other Alleles Associated with Obesity and Diabetes

Objective: Obesity and type 2 diabetes (T2DM) are frequently associated with polycystic ovary syndrome (PCOS). We designed this two-phase family-based and case-control genetic study to determine whether SNPs identified in genome-wide association studies (GWAS) as susceptibility loci for obesity or T2DM are also associated with PCOS.

Research design and methods: Members of 439 families having at least one offspring with PCOS were genotyped for SNPs previously associated with obesity or T2DM in GWAS analyses. Linkage and association with PCOS was assessed using the transmission/disequilibrium test (TDT). SNPs were also analyzed in an independent replication case-control study involving 395 women with PCOS and 176 healthy women with regular menstrual cycles.

Results: Only one of the 18 obesity-associated SNPs analyzed with the TDT was nominally significant for association with PCOS: rs2815752 in *NEGR1* ($c^2 = 6.11$, $P = 0.013$). Four SNPs in *FTO* and two in *MC4R* were associated with BMI as assessed with quantitative-TDT analysis; several of which replicated association with BMI in the case-control cohort. None of the SNPs associated with T2DM were associated with PCOS in either the family-based or case-control analysis.

Conclusions: PCOS is not associated with allelic variants in known T2DM loci. One SNP in *NEGR1* was nominally associated with PCOS in the family-based study but failed to replicate in the case-control analysis. SNPs in *FTO* and *MC4R* were found to be associated with BMI in PCOS women in both studies. These findings suggest that unique T2DM and obesity genes may be responsible for impaired glucose metabolism and elevated BMI in PCOS.

Publications:

Raja-Khan N, Kunselman AR, Demers LC, Ewens KG, Spielman RS, **Legro RS** A Variant in the Fibrillin-3 Gene is Associated with TGF- β and Aldosterone Levels in Women with Polycystic Ovary Syndrome. *Fertil Steril*, In Press PMID: *PMC Journal – In Process*

Research Project 10: Project Title and Purpose

Neural Systems of Ingestive Behavior - The purpose of this project is to investigate the pathways from the central gustatory system to brain structures that mediate reward, such as the nucleus accumbens. These experiments will elucidate where and how the hedonic effects of a taste, its pleasurable or aversive, are elaborated from the afferent sensory message.

Duration of Project

1/1/2008 - 6/30/2009

Summary of Research Completed

This project ended during a prior state fiscal year. For additional information, please refer to the Commonwealth Universal Research Enhancement Annual C.U.R.E. Reports on the Department's Tobacco Settlement/Act 77 web page at <http://www.health.state.pa.us/cure>.

Research Project 11: Project Title and Purpose

Nuclear Trafficking of the Retroviral Gag Protein - This project will support a graduate research assistant who is studying how retroviruses interact with the cells they infect. The project is designed to elucidate the mechanisms by which retroviral Gag proteins, the major viral structural proteins, utilize cellular transport machinery to travel throughout different subcellular compartments. The long-term goal of this work is to identify novel targets for anti-retroviral therapy.

Anticipated Duration of Project

10/1/2008 - 12/31/2010

Project Overview

Our research program focuses on understanding the molecular mechanisms used by retroviruses to commandeer cellular pathways for the assembly of new virus particles. We discovered that RSV Gag is actively transported into and out of the nucleus, which was unexpected, given that retroviral particles are released from the plasma membrane. We identified two independent nuclear localization sequences (NLSs) and a CRM1-dependent nuclear export signal (NES) in Gag. We hypothesize that RSV Gag enters the nucleus to bind to the viral genomic RNA (gRNA), forming a viral RNP complex within the nucleus. Our recent work has garnered substantial support for this hypothesis.

Aim 1. Examine Gag-Gag and Gag-viral RNA interactions in the nucleus and nucleolus. The earliest steps in virus assembly—those immediately following synthesis of Gag on cytosolic ribosomes—are poorly understood. We have preliminary evidence that RSV Gag transiently traffics through the nucleolus, and in this aim we will investigate the kinetics, interactions, and

purpose of intranuclear transit of Gag. Of critical importance to this aim are our well characterized RSV Gag trafficking mutants and our newly developed system for imaging Gag protein-protein and protein-RNA interactions in the nucleus. To study nuclear and nucleolar interactions of Gag, we propose to:

- a. Examine Gag-Gag interactions in nuclei of living cells.
- b. Define the mechanism underlying subnuclear and nucleolar trafficking of Gag.
- c. Examine viral RNP complex formation, mobility and kinetics in the nucleus.

Principal Investigators

Leslie J. Parent, MD
Staff Physician
Penn State College of Medicine
Hershey Medical Center
Infectious Diseases H036
500 University Drive
Hershey, PA 17033

Other Participating Researchers

Timothy Lochmann, Nicole Gudleski and Andrea Beyer – employed by Penn State College of Medicine.

Expected Research Outcomes and Benefits

This project focuses on defining the molecular mechanisms underlying RSV Gag nuclear trafficking and Gag-mediated gRNA encapsidation. The experimental plan is built on a firm foundation of novel published and preliminary data suggesting that Gag recruits nuclear and cytoplasmic factors to direct viral RNP transport from the nucleus to the site of virus assembly. Our integration of genetic, biochemical, proteomic, and dynamic microscopic imaging form a multi-pronged approach that has the potential to challenge the current dogma regarding how retroviruses select their genomes for incorporation into new virions. Our ultimate goal is to identify new targets for the development of antiretroviral therapy that could be used to treat retroviral diseases like AIDS.

Summary of Research Completed

We have broadened our studies to include other retroviral Gag proteins. For this project, we are studying the mouse mammary tumor virus (MMTV) Gag protein, which causes mammary adenocarcinomas in mice. Experiments performed by our collaborator Tatyana Golovkina, PhD (University of Chicago) identified the ribosomal L9 protein as a cellular factor that specifically interacts with MMTV Gag. Andrea Beyer, a senior graduate student in my laboratory, followed up on this observation to determine if there was any evidence in mouse mammary cells that Gag and RPL9 were indeed interacting. She found that overexpression of RPL9 induced nucleolar localization of MMTV Gag, indicating that it unexpectedly traffics through the nucleus. The role of this nucleolar localization is being actively pursued using support from this award.

Subaim1. Determine the mechanism underlying Rous sarcoma virus (RSV) Gag nuclear trafficking

RSV, like all retroviruses, contains the *gag* gene that encodes the Gag polyprotein, which coordinates assembly and release of virus particles at the plasma membrane. After translation in the cytoplasm on free ribosomes, it was originally thought that Gag was targeted directly to the plasma membrane via its membrane binding domain (M domain) (Subaim 1, Fig. 1.). However, we discovered that Gag transports transiently into the nucleus before going to the plasma membrane via two nuclear localization signals (NLSs) and a CRM1 dependent nuclear export signal (NES) (Fig. 1.). Based on viral mutants that bypass the nucleus and have reduced viral genomic RNA packaging, we hypothesized that Gag nuclear trafficking was required for viral RNA encapsidation. The present project focused on elucidating the molecular mechanisms underlying nuclear import, nuclear export, and the role of genome packaging in nucleocytoplasmic trafficking of Gag.

In earlier studies, we identified two NLSs in the Gag protein, a non-classical NLS in the MA domain and a canonical NLS in the NC domain. We also mapped the NES activity to a hydrophobic region in the p10 domain of Gag. To understand the mechanisms underlying Gag nucleocytoplasmic transport, we utilized an integrated approach encompassing *in vitro* biochemistry and *in vivo* cell biology techniques. In previous studies done in *Saccharomyces cerevisiae*, we found that the NC domain of Gag interacts with the classical α/β import (imp- α/β) factors while the nonclassical MA NLS interacts with the noncanonical importin-11 (imp-11). In the present studies, we confirmed these associations using co-immunoprecipitation in avian cells, the natural host for RSV (Fig. 2). In addition, we observed that overexpression of imp- β or imp-11 in RSV-infected cells enhanced the nuclear accumulation of Gag (Fig. 2, yellow arrows). Because of the rapid nuclear export of Gag, when only physiological levels of the import receptors were expressed (Fig. 2, white arrows), less Gag accumulated in the nucleus. These results suggest that Gag specifically utilizes imp- β and imp-11 for nuclear trafficking during infection and establishes a direct role of these import receptors in the viral life cycle.

To determine whether the importins bound directly to the Gag polyprotein, we constructed an expression vector for the production of recombinant RSV Gag made in bacteria (H6.Gag.3h; Fig. 1). To determine whether Gag interacted with imp- α directly or whether it used another protein as a bridge, we performed *in vitro* binding experiments. A small fraction of the total protein used in each pull-down was run on a gel to indicate the proteins were added to each assay (data not shown). A fraction of the unbound sample was analyzed to confirm the majority of the GST tagged protein pelleted with the beads (data not shown). Co-precipitation of Gag with GST-imp- α confirmed that Gag bound directly to imp- α (Fig. 3, top) but did not interact with GST-kap β 3, GST-kap β 2 (data not shown), imp- β , or GST alone. The RSV CA domain also did not interact with GST-imp- α , confirming the CA domain is not necessary or sufficient for Gag's interaction with imp- α . Imp- α did interact with a known binding partner, the SV40 NLS, showing this interaction is biologically relevant (Fig. 3). In addition, the RSV NC protein also bound directly to GST-imp- α , as predicted from genetic experiments performed in yeast. Together, these experiments confirm that RSV Gag binds directly to imp- α but not to imp- β for nuclear import.

The NLS within the NC domain overlaps the RNA binding domain/interaction domain (I) (Fig. 1). To determine whether Gag:imp- α interactions were inhibited by Gag:nucleic acid binding, we performed a competition experiment. Increasing amounts of a $\mu\psi$ RNA (an 82nt viral RNA containing the minimal packaging signal for the virus) or a random, nonviral 109mer DNA were added to equal concentrations of Gag and imp- α . GST-pulldown experiments were performed and the amount of Gag bound to imp- α was analyzed. Both the $\mu\psi$ RNA and the 109mer RNA acted as competitive inhibitors of imp- α :Gag interactions (data not shown). Increasing amounts of nucleic acids did not have an effect on imp- α :H6.NLS.GFP (SV40NLS) binding (data not shown), indicating that nucleic acids do not affect this interaction. Together, these results suggest Gag:imp- α interactions are competitively inhibited by nucleic acids, and the viral $\mu\psi$ vRNA is the most efficient competitor.

Based on these results, we hypothesize that the NLSs in MA and NC are recognized after synthesis of Gag in the cytoplasm. Once Gag is transported into the nucleus, the import factors dissociate. Our working model is that Gag then binds to the viral RNA in the nucleus, and the Gag-vRNA complex is then targeted to the plasma membrane for virus particle release. Based on this hypothesis, we proposed that Gag:CRM-1 interactions would be increased by nucleic acid binding. To test this idea, we incubated Gag with or without $\mu\psi$ RNA, and added GST-CRM-1 and RanGTP, which is required for CRM1 export activity. Viral $\mu\psi$ RNA was the most potent stimulator of Gag:CRM1 binding (Fig. 4A), suggesting that RNA binding induced a conformational change in Gag that increased its affinity for CRM1. Gag binding to CRM1 was dependent on Ran GTP (Fig. 4B). Together, these data support a model in which viral RNA serves as a signal for Gag nuclear export by promoting Gag association with the CRM1:RanGTP nuclear export complex. This result was recently published: Gudleski N, Flanagan JM, Ryan EP, Bewley MC, Parent LJ. Directionality of nucleocytoplasmic transport of the retroviral Gag protein depends on sequential binding of karyopherins and viral RNA. Proc Natl Acad Sci U S A. 2010 May 18;107(20):9358-63. Epub 2010 Apr 30. PubMed PMID: 20435918.

Subaim 2. Determinants of Gag nuclear trafficking: Mouse mammary tumor virus (MMTV) Gag interaction with ribosomal protein L9 (RPL9)

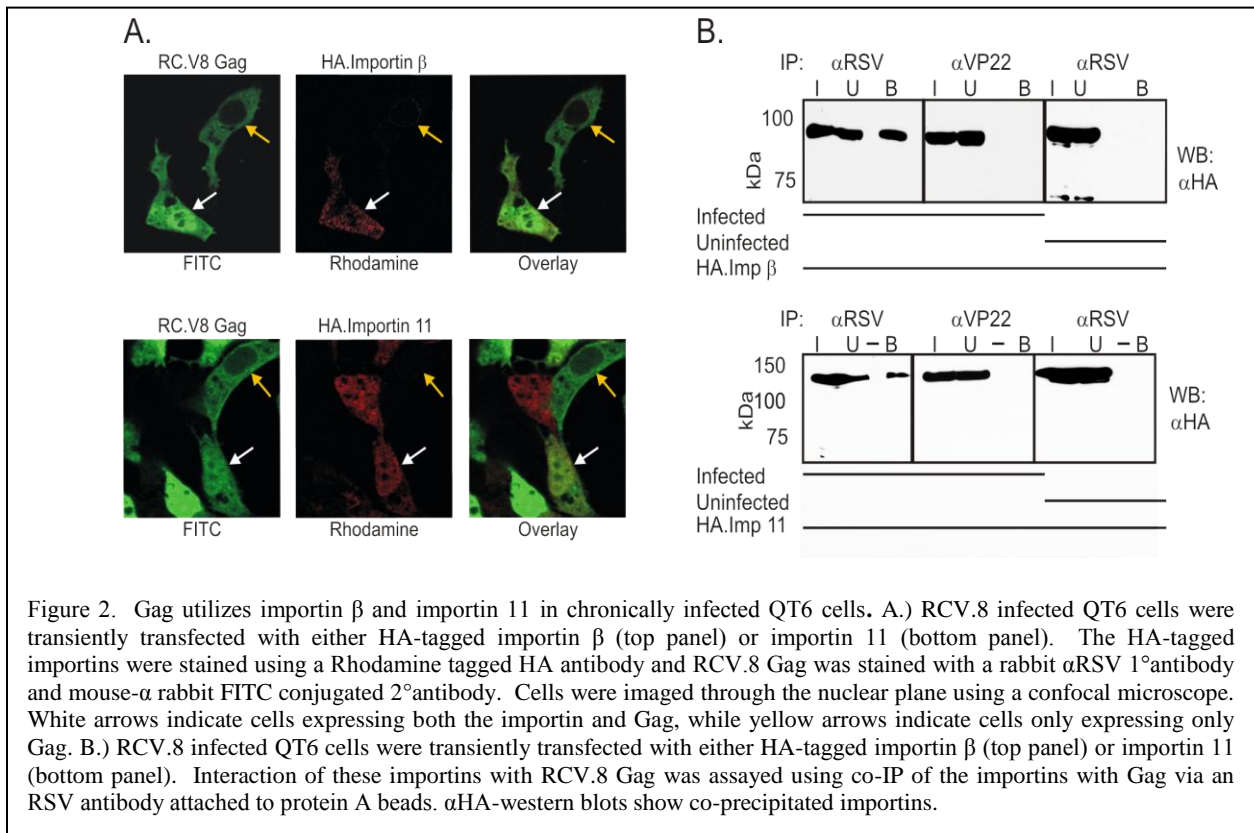
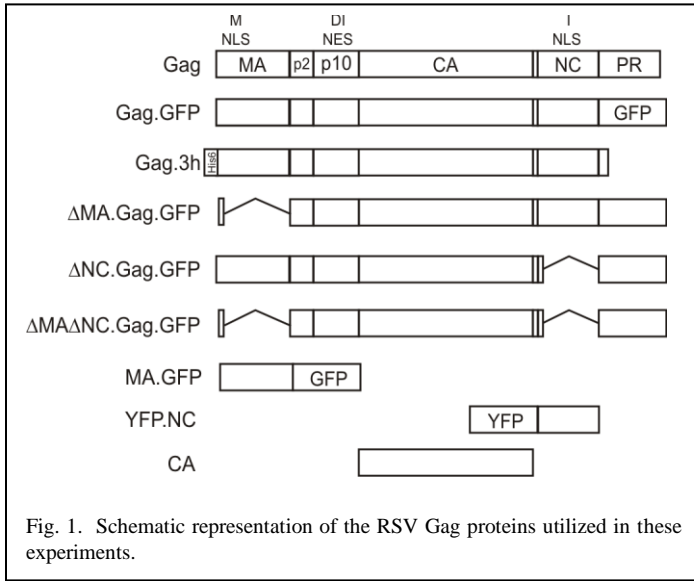
MMTV causes adenocarcinoma of the breast in mice, and an MMTV-like virus has been implicated in some cases of human breast cancer. MMTV Gag plays an important role in MMTV-mediated tumorigenesis. Our collaborator, Tatyana Golovkina (University of Chicago), performed yeast two hybrid studies using the Gag protein as bait and yielded an interesting result: ribosomal protein L9 (RPL9), a component of the 60S subunit of the ribosome, bound to C3H Gag, a highly tumorigenic strain of MMTV, but not with a less tumor-associated endogenous MMTV (Mtv-1). RPL9 has been implicated in tumor suppression, providing a possible mechanism explaining the C3H Gag-RPL9 interaction. The goal of this study was to validate the RPL9-Gag interaction in mouse mammary cells to provide insight on whether RPL9 plays a role in MMTV-mediated tumorigenesis and/or virus replication.

We reasoned that if MMTV Gag and Rib L9 were interacting, they would be present in the same location in cells. MMTV is a type B retrovirus, meaning that capsids are assembled in the cytoplasm before being transported to the plasma membrane for release (Subaim 2, Fig. 1). To determine whether MMTV Gag and RPL9 were co-localized in infected cells, we overexpressed

RPL9 in normal mouse mammary cells that were infected with MMTV and examined Gag and RPL9 localization. RPL9 was present primarily in the nucleolus, which was expected given that ribosomes are assembled in the nucleolus, but a portion of MMTV Gag had surprisingly relocated to the nucleolus along with RPL9 (Subaim 2, Fig. 2). To determine whether there was a direct interaction between Gag and RPL9, we performed FRAP (fluorescence recovery after photobleaching) and found a high level of FRAP efficiency, indicating a physical association between these proteins (data not shown). Thus, RPL9 causes accumulation of MMTV Gag in the nucleolus, providing evidence that another retroviral Gag protein undergoes a nuclear trafficking step.

More recently, we have mapped the interacting region of Gag to the p3-CA region. Detailed mapping of the residues involved in the interaction are ongoing. We also determined that the N-terminus of RPL9 contains two independent nucleolar retention signals that direct it to the nucleolus. These sequences are not required for Gag relocation to nucleoli. However, the C-terminal region of RPL9 does appear to contain the Gag-interaction domain (data not shown). Thus, we identified a cellular protein, RPL9, which interacts with MMTV Gag, causing it to redistribute to the nucleolus. This interaction may play an important role in the mechanism of tumor formation.

Figures for Subaim 1:



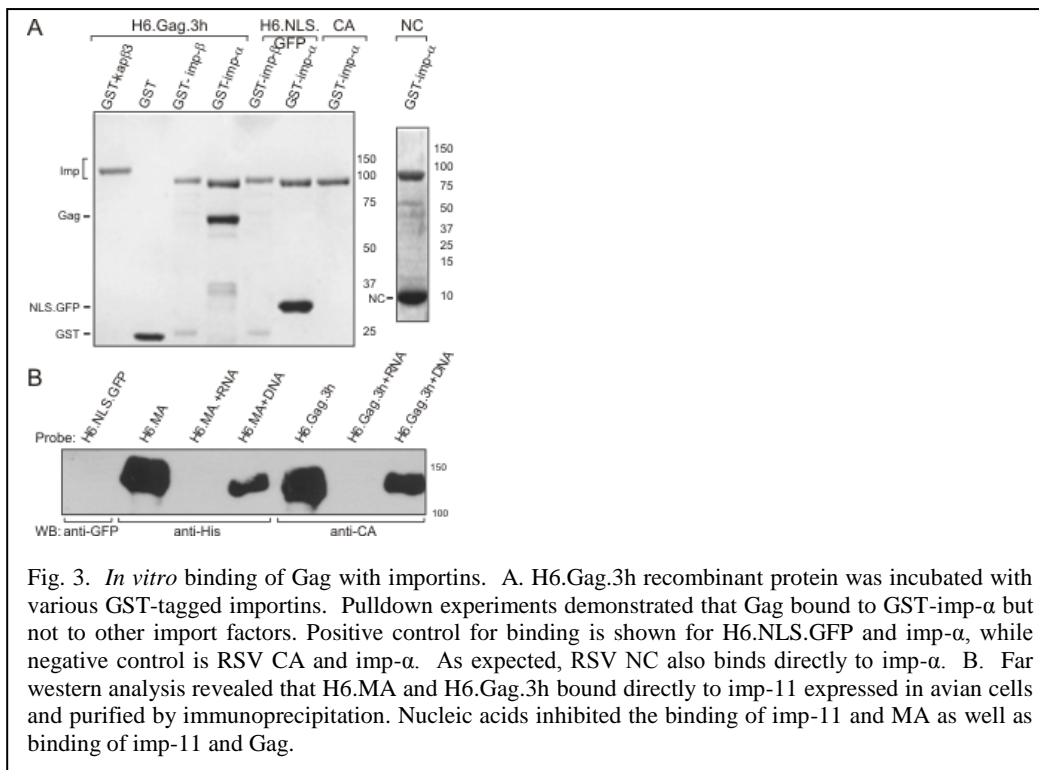


Fig. 3. *In vitro* binding of Gag with importins. A. H6.Gag.3h recombinant protein was incubated with various GST-tagged importins. Pull-down experiments demonstrated that Gag bound to GST-imp- α but not to other import factors. Positive control for binding is shown for H6.NLS.GFP and imp- α , while negative control is RSV CA and imp- α . As expected, RSV NC also binds directly to imp- α . B. Far western analysis revealed that H6.MA and H6.Gag.3h bound directly to imp-11 expressed in avian cells and purified by immunoprecipitation. Nucleic acids inhibited the binding of imp-11 and MA as well as binding of imp-11 and Gag.

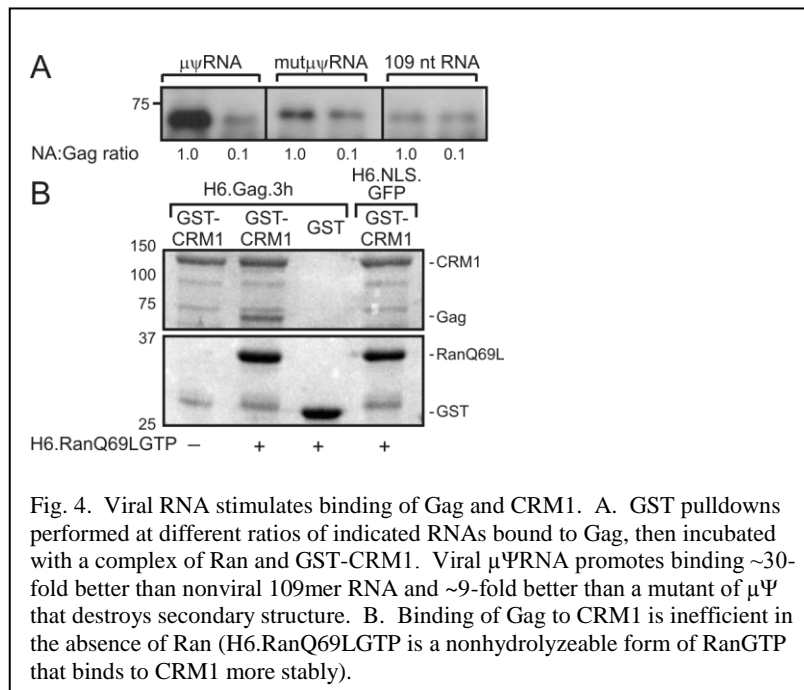


Fig. 4. Viral RNA stimulates binding of Gag and CRM1. A. GST pull-downs performed at different ratios of indicated RNAs bound to Gag, then incubated with a complex of Ran and GST-CRM1. Viral $\mu\psi$ RNA promotes binding ~ 30 -fold better than nonviral 109mer RNA and ~ 9 -fold better than a mutant of $\mu\psi$ that destroys secondary structure. B. Binding of Gag to CRM1 is inefficient in the absence of Ran (H6.RanQ69LGTP is a nonhydrolyzable form of RanGTP that binds to CRM1 more stably).

Figures for Subaim 2:

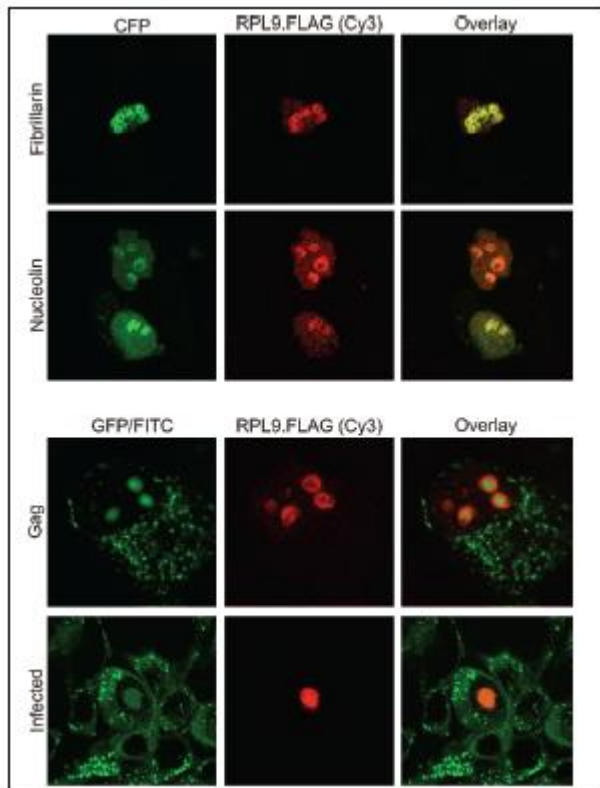
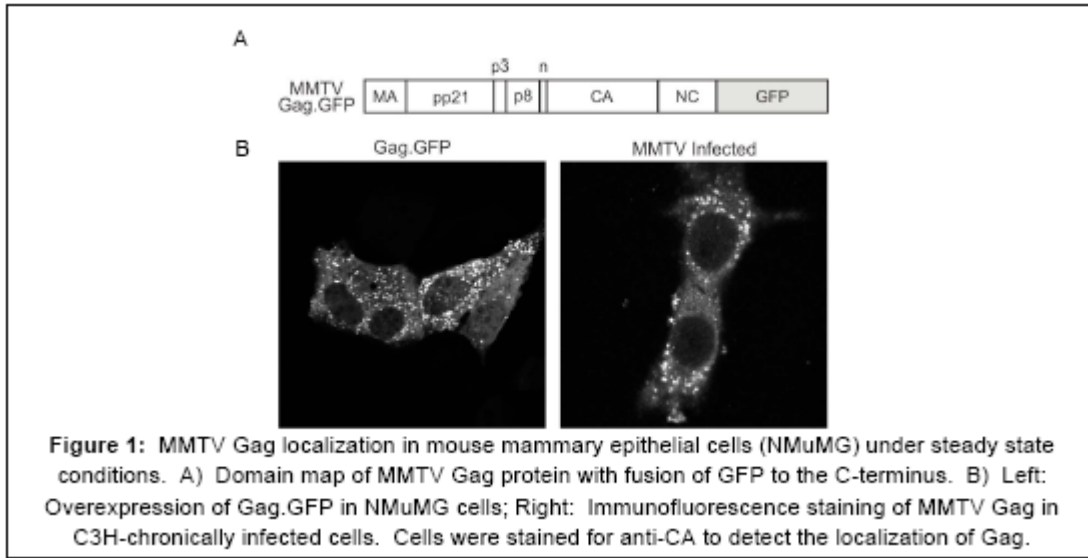


Fig. 2. Confocal microscopy showing localization of MMTV Gag in nucleoli with overexpression of RPL9. Upper panel: RPL9.FLAG overexpression in context of CFP-fused nucleolar markers fibrillarin and nucleolin. Lower panel: RPL9.FLAG overexpression in the presence of transfected Gag.GFP or Gag of chronically infected cells.

Research Project 12: Project Title and Purpose

Chronic Oxidative Stress and the Redox Proteome in Normal Breast Parenchyma - Breast cancer is a disease that is a long time in the making during decades of exposure of breast tissue to pro-carcinogenic conditions. In this project we will test the *hypothesis* that increased levels of reactive oxidants (molecules that disrupt protein function and may be related to carcinogenesis) in human breast tissue are associated with altered levels of specific regulatory molecules in these cells, thereby disrupting normal function. We will use newly developed proteomic techniques to obtain a global picture of the oxidized proteins present in human breast tissue. Demonstrating that these alterations occur would implicate the chronic and progressive exposure to oxidants as a pro-carcinogenic event and potentially provide endpoints that could be assessed during dietary and other therapeutic interventions designed to minimize or reverse these changes.

Anticipated Duration of Project

1/1/2008 – 12/31/2010

Project Overview

The overall hypothesis addressed in this project is that under conditions of chronic oxidative stress, oxidative modifications of proteins participating in signaling networks important for maintaining cellular homeostasis play an essential role in allowing breast cancer to develop within the stressed mammary epithelium. More specifically, failure to neutralize reactive oxidant species disrupts redox-responsive regulatory proteins and leads to cellular dysfunction, thus providing a milieu for cancer cells to evolve and ‘take over’. The “proof of principle” experiments proposed to test this hypothesis will focus on the cysteine/thiol moiety of proteins because of their known susceptibility to oxidation and evidence of the functional consequences of their state of oxidation. The two interrelated specific aims of the project are: *Aim 1*) to use proteomic methodology to establish the profile and amounts of thiol proteins in their reduced state and in a reversible state of oxidation in mammary epithelium and surrounding stroma of women without breast cancer who are representative of women living in our high breast cancer risk environment and; *Aim 2*) use cytochemical techniques to localize and assess the levels of markers of chronic oxidative stress in breast parenchyma of the same women.

Protein will be obtained for proteomic analysis from terminal ductal lobular units and interlobular stroma isolated by laser capture microdissection from sections from flash-frozen breast tissue obtained at reduction mammoplasty from cohorts of women of different age groups. Profile of reduced and reversibly oxidized cysteine/thiol proteins in the extracted proteins will be obtained using two-dimensional difference gel electrophoresis. Localization of markers of oxidative stress (including 4-hydroxynonenol, protein carbonyls and 3-nitrotyrosine) and their levels in tissues used for the proteomic studies will be determined using the method multiplex immunoblotting of tissue sections. This recently introduced method can yield data that are more quantitative and on a larger number of proteins from a tissue section than can be obtained using classical immunocytochemistry. Our hypothesis predicts that the levels of specific thiol proteins and their state of oxidation will vary as a function of the age of the tissue donors and the levels of markers of oxidative stress.

Principal Investigators

David S. Phelps, PhD
Professor of Pediatrics
Penn State College of Medicine
Department of Pediatrics, H085
M.S. Hershey Medical Center
500 University Drive
Hershey, PA 17033

Other Participating Researchers

Judith Weisz, MB BChir, Willard M. Freeman, PhD - employed by Penn State University

Expected Research Outcomes and Benefits

This project seeks to redefine the definition of what is normal. Our preliminary observations demonstrate that “normal” breast tissue obtained from young women in a population with a high breast cancer incidence is, in fact, already marked by signs of chronic oxidative stress, a potential precursor to carcinogenesis. This should, at a minimum, be considered as providing a permissive environment for the carcinogenic process. In this project we will use state-of-the-art protein analytical methods to identify the proteins that are modified in this tissue and to determine the nature of their modifications. This information will provide us with information about cellular processes and functions that may be altered by the modification of the proteins, potentially providing new insights into the mechanisms of carcinogenesis.

We expect the results we obtain in this project to offer two benefits in the future. One of these is a better understanding of the events that result from subjecting breast tissue to chronic oxidative stress. There are strong indications that this exposure disrupts normal biology and leads to carcinogenesis. We expect that the "discovery proteomics" approach that we will utilize will help us identify some of the specific proteins and biological processes that are involved in these disruptions, but were not previously linked to breast cancer carcinogenesis. The second benefit that will be derived from this study will be the identification of affected proteins that may serve as early markers of oxidative stress. These proteins may also prove useful in assessing levels of risk and for monitoring the effectiveness of efforts to reduce oxidative stress by dietary, pharmacologic, or other means, thereby contributing in the future to efforts to prevent breast cancer.

Summary of Research Completed

Some additional studies were conducted in support of Aim 1 where the focus is on proteomic studies of breast tissue. Our emphasis was on work involving formalin-fixed paraffin-embedded (FFPE) breast tissue. Several attempts were made to extract protein from FFPE breast tissue sections. Extraction protocols obtained from recent publications employing similar approaches in other cell and tissue types were successful in obtaining measurable protein extracts. However,

when two-dimensional gels were done using these extracts and then subjected to silver staining the resultant images did not have the desired resolution or quality.

We then performed similar procedures with FFPE tissue samples that were obtained by laser capture microdissection (LCM). Using LCM allows us to selectively extract the epithelium-rich terminal ductal lobular units (TDLU). We believed that working with sections that were enriched with epithelium could improve both the extraction and the resultant gels. To maximize our detection capabilities with these extracts, the protein was labeled with CyDye using a saturation labeling protocol. However, despite the changes in the samples this was not the case and despite the use of several different extraction protocols, the gels obtained were not markedly different from those described above that were obtained from whole breast tissue sections.

The main emphasis for this reporting period was on Aim 2 and the cytochemical localization and assessment of markers of chronic oxidative stress and other cellular proteins. This work was done with collaborators at General Electric (GE) Global Research using tissue sections provided by co-investigator, Dr. Weisz. GE has developed a novel and very powerful multiplex immunostaining method in which two specific antigens are immunostained with antibodies conjugated to different CyDyes, the localization recorded by microscopy, and sophisticated imaging systems used to digitize and evaluate the staining. The fluorescence is then quenched using their proprietary reagent and immunostaining done with two more antigens. This process can be repeated up to 100 times with multiple antibodies. Nuclei are stained with DAPI and used to superimpose successive images accurately.

Using this technology we are currently comparing sections from individuals with high amounts of immunostaining for 4-hydroxynonenal (4-HNE) with those from individuals with very low amounts of 4-HNE staining. In addition to staining with 4-HNE, a marker of chronic oxidative stress, they have been immunostained for: CD68, a macrophage marker; smooth muscle actin for myoepithelial cells; NF- κ B; Ki67, a replication marker; p53, a pro-apoptotic marker; cytokeratin; Glut 1, glucose transporter; MAPAPK2A, a protein kinase involved in the regulation of stress and inflammation. The localization and degree of immunostaining for these and other markers are currently being compared among individuals with different amounts of chronic oxidative stress, as well as in sections from the same individual from areas with varying degrees of chronic oxidative stress.

In conjunction with the immunostaining studies described above, a preliminary analysis of RNA isolated from tissue samples with high and low levels of 4-HNE has been done using a microarray from SA Bioscience Oxidative Stress and Antioxidant Defense. This microarray detects 84 mRNAs for proteins related to oxidative stress. Additional samples are being subjected to both the microarray analysis and the cytochemical analysis and will be compared to identify changes dependent on oxidative stress.

Research Infrastructure Project 13: Project Title and Purpose

Research Infrastructure for New Pesticide Technologies for Control of Insect-Borne Diseases like Malaria - This project is to provide the eight environmental chambers which will form the core of a state of the art Laboratory for the Experimental Analysis of Human Infectious Insects at

Penn State. Insects vector some of the globally most important human diseases, including malaria, and the control of mosquitoes continues to be one of the most potent weapons against these diseases. But existing chemical insecticides are failing. The new laboratory will develop novel strategies and technologies for sustainable control of vector-borne diseases. Fungal biopesticides offer considerable promise as a new, sustainable and environmentally friendly approach to protecting human health. In addition to globally significant research and extension outputs, this project has many potential Pennsylvania population based applications for other vector borne diseases, such as, West Nile, Lyme, erratically present diseases such as Eastern Equine Encephalitis and St Louis Encephalitis. All of these diseases have wildlife reservoirs and are carried to humans via insects. History shows that we can expect a variety of other vector-borne diseases which will emerge in future years.

Anticipated Duration of Project

1/1/2008 - 12/31/2011

Project Overview

The scope of this project is to design and build the environmental rooms which provide the light, humidity and temperature necessary to culture, maintain and experiment with the insect vectors which transmit diseases such as malaria, West Nile, dengue, sleeping sickness and elephantiasis. These chambers will form the key infrastructure to develop the Laboratory for the Experimental Analysis of Human Infectious Insects. This year, PSU recruited internationally the core personnel to found this laboratory. This laboratory will be a mosquito experimental facility in which large numbers of several species of the mosquitoes which transmit malaria can be reared. These mosquitoes will be used to assay the malaria transmission-blocking efficacy of natural and genetically engineered fungal isolates. Colonies of different species of mosquitoes will also be reared to investigate the potential of this technology for the control of other vector borne diseases, such as Dengue, West Nile Virus, Lyme Disease, Eastern Equine Encephalitis and St Louis Encephalitis. To this end, a laboratory building will shortly be renovated by PSU to provide a Laboratory for the Experimental Analysis of Human Infectious Insects.

The current grant application is for a key component of the research infrastructure: the eight environmental chambers required for mosquito colony maintenance and experimentation. These chambers will provide state of the art lighting, heat and humidity control required for large-scale production and maintenance of blood feeding mosquitoes which transmit human disease. The new facility will include a secure containment facility which will enable population and behavioral analysis of insects infected with malaria, as well as the facilities to culture human malaria for infecting mosquitoes.

A major use for this facility will be to develop fungal biopesticides against mosquitoes. These have the potential to provide cost-effective, green, evolution-proof control of malaria. Chemical insecticides like DDT have been – and continue to be – critical components of malaria control programs worldwide. However, their effectiveness is degrading in the face of environmental and health concerns and, most importantly, the evolution of resistance in mosquito populations. New strategies are needed. Fungal biopesticides offer considerable promise. Building on its existing

strengths in infectious disease dynamics, in agricultural pest control and in insect ecology, and with the recent strategic recruitments, Penn State seeks to be the leading world Center for developing and applying biopesticide technology to malaria, West Nile, Lyme, and other vector-borne diseases, which will emerge in future years.

Principal Investigators

Andrew F. Read, PhD
Professor of Biology and Entomology and Eberly College Distinguished Senior Scholar
Pennsylvania State University
Center for Infectious Disease Dynamics
Muller Laboratories
University Park, PA 16802

Other Participating Researchers

Matthew B. Thomas, PhD, Nina Jenkins, PhD, Simon Blanford, PhD - employed by Pennsylvania State University

Expected Research Outcomes and Benefits

The requested infrastructure will enable experimentation which will develop biopesticides for malaria control. There are in excess of a billion clinical cases of malaria annually, with over a million of these ending in death. This burden falls disproportionately on the poorest people on the planet, particularly their children. Increasingly concerns over human and environmental health are constraining the use of chemical insecticides, and the spread of mosquitoes resistant to chemicals like DDT is reducing the efficacy of traditional insecticides when they are deployed.

Fungal biopesticides would overcome these problems, thus generating substantial – and critically, sustainable – health gains. In addition, the technology has the potential to be applied to other vector borne diseases of global human and animal health importance, including West Nile, Lyme, Eastern Equine Encephalitis and St Louis Encephalitis, dengue and sleeping sickness.

The science required to generate these improvements in human health could also generate insights into host-pathogen interactions, pathogen-pathogen interactions, and resistance management, which will be applicable in other health contexts, including the development of new chemical insecticides and the identification of novel antimalarial compounds.

Summary of Research Completed

This was an infrastructure grant to support work with infectious insects. The Infectious Insect Facility is almost complete, after numerous delays beyond the control of the PI (finance, planning, project oversight, contract details). This is a state-of-the-art stand alone facility which will be available for use from September 2010 at a total project cost of \$2.85million. It is a 3,900 sq ft building, with the internal area completely rebuilt within the fully-gutted building shell, which was freshly re-roofed during the renovation. The entire facility runs at BSL2 with swipe

care access only. There are six environmental chambers (Conviron), three at 91 sq ft, and three at 116 sq ft. These have temperature control over 15-35 °C ±0.5°C, and relative humidity from ambient to 90% rh ±5%, all centrally controlled by computer. Three of the chambers have internal door access, and can be used with infectious insects. These environmental chambers form the expenditure of this grant.

The facility also includes two rooms (196 sq ft and 234 sq ft) which are fully insect-proofed and can each contain up to ten reach-incubators, backed up to an emergency power generator. There is a 345 sq ft laboratory fully equipped for up to four microscopy stations and conventional insect experimentation including CO₂ and reverse osmosis water. There is a 182 sq ft room for parasite culture, including two externally ventilated hoods for tissue culture and relevant incubators. The facility includes two bathrooms, administrative office and an unfinished area with the footprint for a small BSL3 laboratory. The HVAC for the building is fully backed up with duplicate systems, with the entire building have 8 air changes per hour, including sufficient heat evacuation capacity to deal with up to twenty reach-in incubators.

We expect the building and the environmental chambers will need considerable testing over the next few months with infectious insects. We expect to start experimental work in 2011. This work will be conducted as outlined in the research plan.

Research Project 14: Project Title and Purpose

Coupling Mechanisms of NOP Receptors and Calcium Channels - There are four opioid receptors that have been described and that are involved in transmitting pain signals within the nervous system. One of these receptors is known as the 'opioid receptor-like 1 receptor' or NOP receptor. When this receptor was discovered, it was found that activating the receptor would either cause pain or inhibit pain. Our laboratory has found that this receptor is expressed in stellate ganglion neurons and that it has the ability to be either silent or active in the absence of any agonist. The purpose of this research project is to study the pharmacology of constitutively active NOP receptors and study the mechanism by which these receptors obtain an 'active' state in the absence of agonists and how sodium ions affect this 'active' receptor.

Duration of Project

1/1/2008 - 6/30/2009

Summary of Research Completed

This project ended during a prior state fiscal year. For additional information, please refer to the Commonwealth Universal Research Enhancement Annual C.U.R.E. Reports on the Department's Tobacco Settlement/Act 77 web page at <http://www.health.state.pa.us/cure>.

Research Project 15: Project Title and Purpose

Dilatory and Constrictor Control of Coronary Blood Flow Velocity - The purpose of this study is to better understand mechanisms that control blood flow in the coronary arteries. This is important because the coronary arteries provide all of the oxygen to the heart muscle. The coronary circulation is highly unusual because the heart muscle cannot change the percentage of oxygen removed from blood as the amount of activity increases. Thus blood flow regulation becomes crucial in understanding how the heart works. In this project we will examine what substances make blood vessels enlarge and how and why the nervous system may make them become smaller.

Anticipated Duration of Project

1/1/2008 - 12/31/2011

Project Overview

Understanding how coronary blood vessels dilate and constrict can provide important clinical information. To date, most data have been published in animal models because human experiments have required invasive methods. Specifically, intracoronary Doppler guidewire techniques have been required to obtain direct coronary artery blood flow velocity data. In recent years reports demonstrate that advanced Transthoracic Duplex Ultrasound (TDU) technology may enable investigators to measure real time coronary blood flow velocity in humans. We propose a series of validation studies followed by a series of experiments to further characterize dilator and constrictor responses in humans.

In the first series of experiments, we will examine the dilatory effects of adenosine as coronary blood flow is measured using an invasive Doppler guidewire technique in patients during coronary angioplasty. These measurements will then be compared to coronary flow determinations obtained non-invasively with the Duplex Ultrasound technique. Studies will be performed in the same patients the morning after catheterization.

We will then begin a series of non-invasive experiments designed to determine how local factors dilate coronary arteries. We will then couple studies of coronary blood flow with non-invasive examination of left ventricular function using tissue Doppler techniques. We will examine the effect of static handgrip exercise on coronary blood flow and systolic and diastolic left ventricular function. Our initial hypothesis is that tissue Doppler indices of systolic ventricular function will increase in response to handgrip. We will also examine the effect of different levels of LDL cholesterol on the resistance responses to handgrip. We postulate that there will be a relationship between LDL levels and the coronary resistance response to handgrip.

Finally, we will compare the coronary blood flow responses during exercise and during hyperoxia in stable heart transplant patients and in normal control subjects. We hypothesize that responses to handgrip will be attenuated in transplant recipients whereas the responses to hyperoxia will not be attenuated.

Principal Investigators

Lawrence I. Sinoway, MD
Director, Penn State Heart & Vascular Institute
Penn State Milton S. Hershey Medical Center
Mail Code H047
500 University Drive
Hershey, PA 17033

Other Participating Researchers

Urs A. Leuenberger, MD, Afsana Momen, MBBS, Cheryl Blaha, RN, Mick Herr, PhD, Anandi Krishnan, PhD, Zhaohui Gao, PhD - employed by Penn State University

Expected Research Outcomes and Benefits

It is very important to understand the mechanisms by which the vessels that supply the heart muscle adjust their size as flow requirements change. Research in people on these issues has been dramatically hampered by the invasive nature of the methods needed to accomplish these goals. For this reason the overwhelming majority of science in this area has been performed in animal models. While this massive body of literature has greatly improved our care of patients with heart disease, many crucial questions remain. Indeed many of the most basic issues remain to be determined in humans. For example what substance(s) are responsible for the ability of human blood vessels to dilate as the work of the heart increases? Although many substances have been proposed the relative contribution of each of these substances remains unclear. In an analogous fashion, it is unclear what role the autonomic nervous system plays in regulating blood flow. Animal studies suggest that engagement of the sympathetic nervous system, a branch of the autonomic nervous system causes blood to be effectively redistributed from the outside of the heart to the inner portions of the heart. Studies to determine if such a system is operable in people have been lacking. In this application we will examine a new sound wave method to measure the speed of blood traveling in the large coronary arteries. We will validate this method and then we will examine a series of questions to examine the regulatory mechanisms described above in human subjects.

Summary of Research Completed

Validation of non-invasive transthoracic duplex ultrasound to measure coronary blood velocity in humans.

We completed analyzing data from six patients who underwent cardiac catheterization of the left anterior descending artery and compared coronary vasodilator responses to intravenous adenosine infusion using both intracoronary Doppler guidewire (invasive) and TTD (non-invasive) techniques. Adenosine had similar effects on HR, BP and peak diastolic CBV. Doppler tracings obtained using both techniques are shown in Figure 1. The relative increases in peak diastolic coronary flow velocity were similar and are shown in Figure 2.

These results were published in 2010.

Afsana Momen, Mark Kozak, Urs A. Leuenberger, Steven Ettinger, Cheryl Blaha, Vernon Mascarenhas, Vasili Lendel, Michael D. Herr, and Lawrence I. Sinoway. Transthoracic Doppler echocardiography to noninvasively assess coronary vasoconstrictor and dilator responses in humans. *Am J Physiol Heart Circ Physiol* 298: H524–H529, 2010.

The Effects of Sympathetic Activation and Hyperoxia on Coronary Blood Flow in Humans

Two physiologic stressors (100% oxygen and Lower Body Negative Pressure) were administered to healthy subjects. All subjects participated in the two hyperoxic challenges (Oxygen alone and oxygen with an infusion of Vitamin C) and two LBNP challenges (Lower Body Negative Pressure alone and after infusion of Phentolamine). In order to diminish the ordering bias, subjects participated in all three visits. Visit 1 included both a hyperoxia paradigm and incremental LBNP paradigm. Visit 2 included a phentolamine infusion prior to Lower Body Negative Pressure to block the α -adrenergic receptor. Visit 3 involved a Vitamin C infusion prior to breathing 100% oxygen to oppose NO-mediated local vasodilation. To lessen the effect of a sequence effect, Visits 1-3 were randomized. However, the phentolamine study was done after the incremental LBNP Visit to determine the appropriate level of Lower Body Negative Pressure needed for the drug study.

We studied 8 healthy volunteers (age 26.5 ± 1.1 yrs) and measured beat-by-beat changes in coronary blood velocity (CBV) and subendomyocardial systolic and diastolic function during lower body negative pressure before and after administration of an α -adrenoceptor blockade, phentolamine. During lower body negative pressure, coronary blood velocity significantly decreased (baseline 22.33 ± 1.75 cm/s, -5 mmHg 18.27 ± 1.19 cm/s, -10 mmHg 16.61 ± 1.20 cm/s and -15 mmHg 15.80 ± 1.27 cm/s, $P < 0.05$), whereas systolic and diastolic subendocardial myocardial function (S_m and E_m) did not change ($P = NS$) during lower body negative pressure at -5 and -10 mmHg. After administration of phentolamine, the coronary vasoconstriction during lower body negative pressure was attenuated (baseline 21.15 ± 1.37 cm/s, -5 mmHg 20.55 ± 1.33 cm/s, 10 mmHg 20.33 ± 1.22 cm/s and -15 mmHg 18.75 ± 1.04 cm/s. $P = NS$; Figure 3). This was associated with a significant decrease in diastolic function (E_m by Tissue Doppler Imaging) in the subendocardial myocardial layer (12.73 ± 0.36 cm/s at baseline vs. 11.46 ± 0.66 cm/s at -5 mmHg, $P < 0.05$) while myocardial systolic function (S_m) did not change at this level (S_m baseline 8.20 ± 0.30 cm/s vs. -5 mmHg 8.60 ± 0.54 cm/s, $P = NS$ Figure 4). These preliminary data provide the first evidence suggesting that sympathetic coronary vasoconstriction may play a beneficial role in human coronary regulation. These data are soon to be submitted as a manuscript.

Breathing 100% oxygen (hyperoxia) compared to room air promptly reduced coronary blood flow velocity by 28%, increased coronary resistance by 34% and decreased myocardial velocity by 11% (TDI) in the subendocardial layer (Figures 5 and 6). Vitamin C administration during hyperoxia significantly restored coronary blood flow velocity, resistance and myocardial function towards baseline measurements. Our findings, based on data from noninvasive techniques in healthy subjects, suggest significant circulatory effects of hyperoxia on coronary circulation and myocardial function. We speculate that these changes are mediated by Vitamin C-quenchable substances acting on the coronary microcirculation. These data were submitted for publication and the manuscript is under revision.

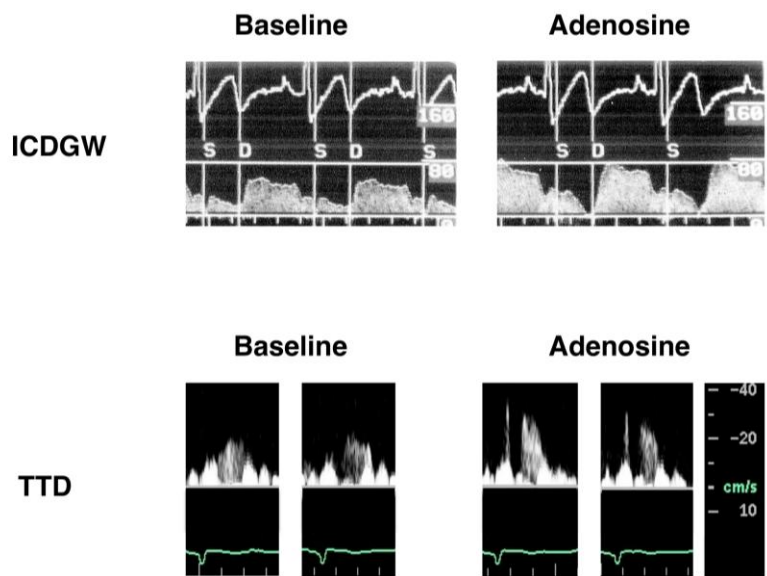


Figure 1. Representative Doppler coronary blood velocity signal tracings from a subject during baseline (left panel) and adenosine infusion (right panel) obtained by invasive intracoronary Doppler guidewire technique (ICDGW; top) and non-invasive transthoracic duplex ultrasound (TTD; bottom) technique. S and D represent the systolic and diastolic components of each velocity tracing. (Fig 2 from manuscript)

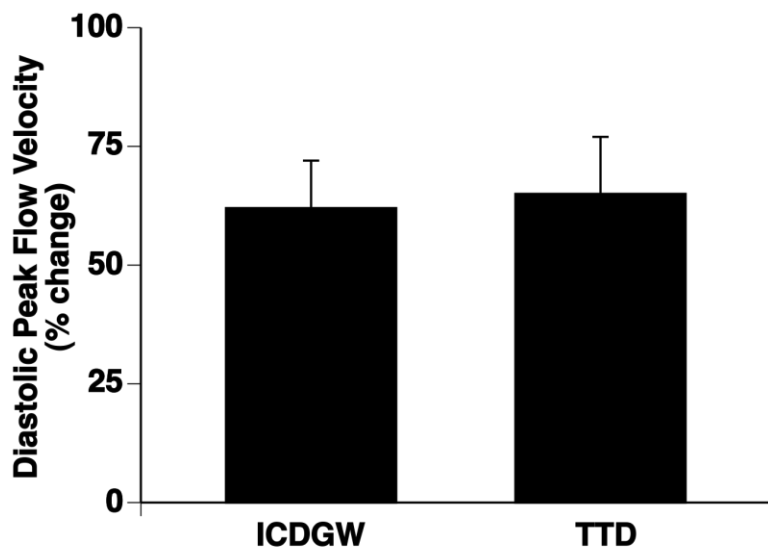


Figure 2. Data are presented as mean \pm SE and are shown as percent change from baseline in diastolic peak blood flow velocity measured by intracoronary Doppler guidewire (ICDGW) and

non-invasive transthoracic duplex ultrasound (TTD) technique during two study periods. Note the magnitude of increases in velocity is similar with two techniques. (Fig 3 from manuscript)

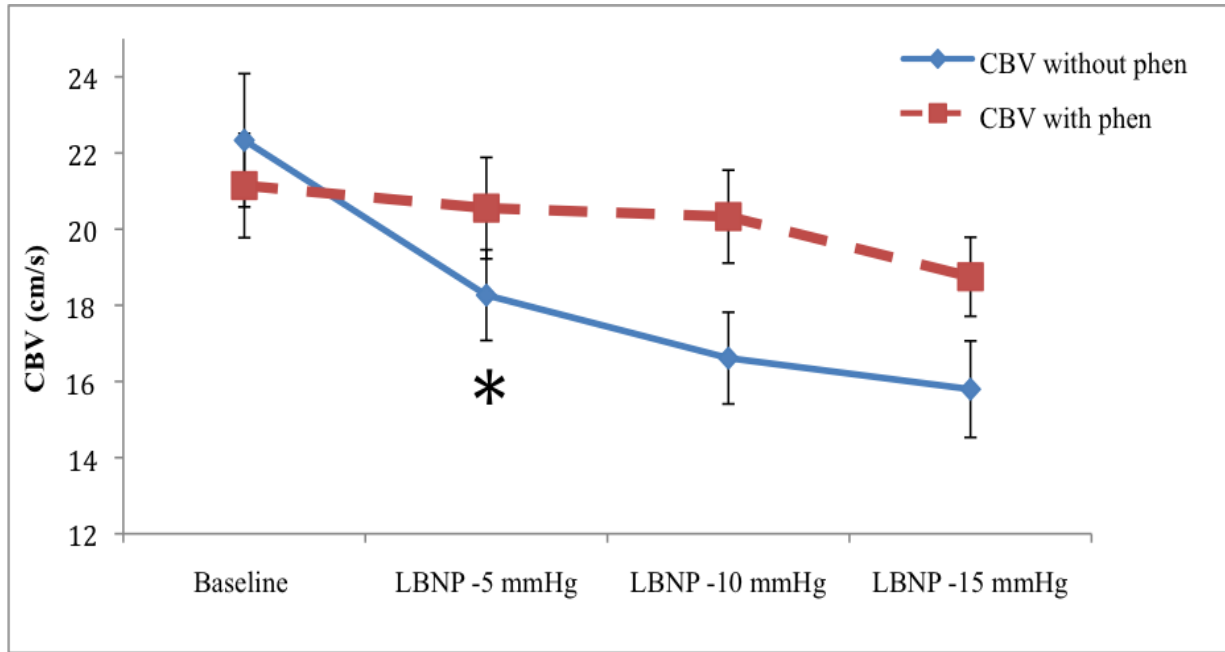


Figure 3. Coronary blood flow velocity (CBV) responses to LBNP with and without administration of Phentolamine (phen).

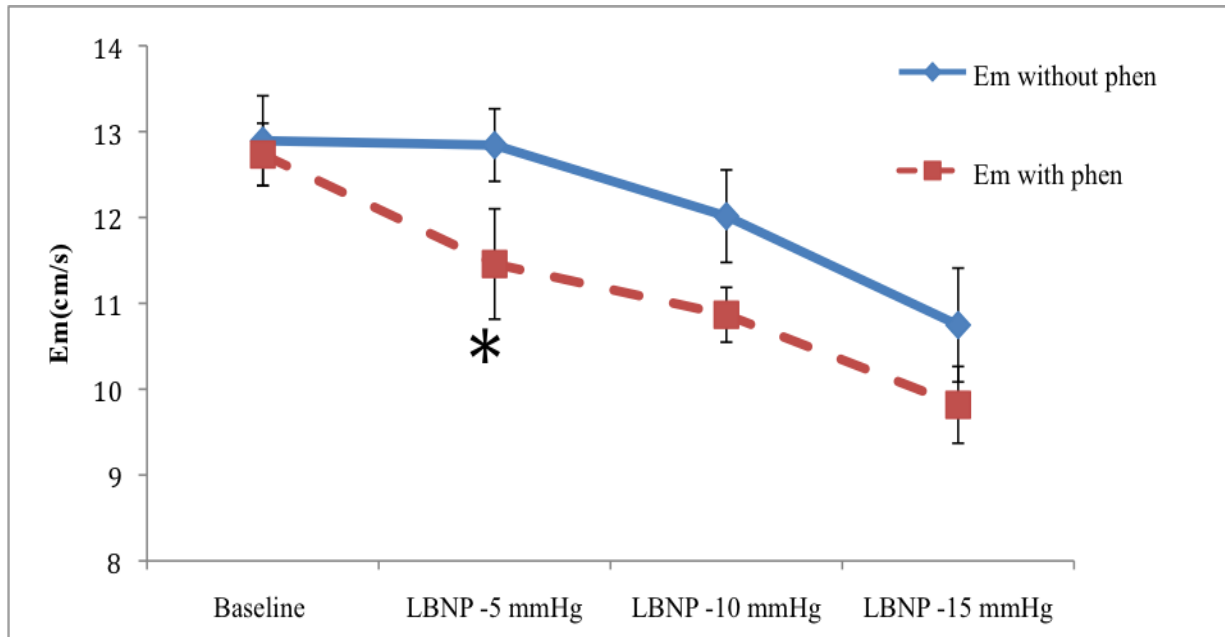


Figure 4. Left ventricular diastolic function (Em) response to LBNP with and without administration of Phentolamine (phen).

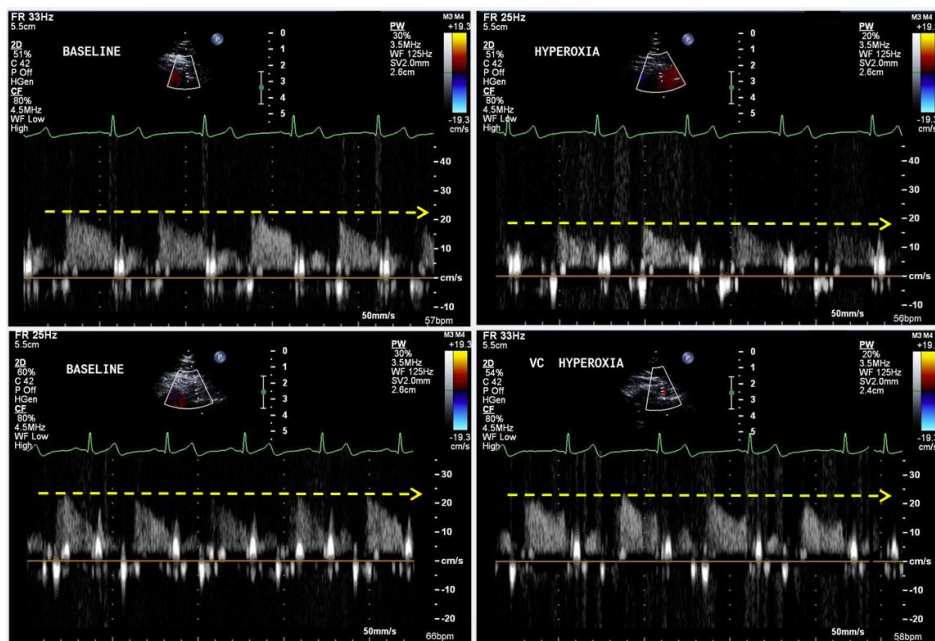


Figure 5. Effects of hyperoxia on coronary blood velocity with and without vitamin C. Representative recordings of coronary blood velocity at baseline and during hyperoxia. (Top) subject without administration of vitamin C, the wave signals are shown during room air (left) and during hyperoxia (right). Note, that during hyperoxia, the coronary blood velocity is lower than during baseline. (Bottom), after administration of vitamin C, the coronary blood velocity is preserved during hyperoxia.

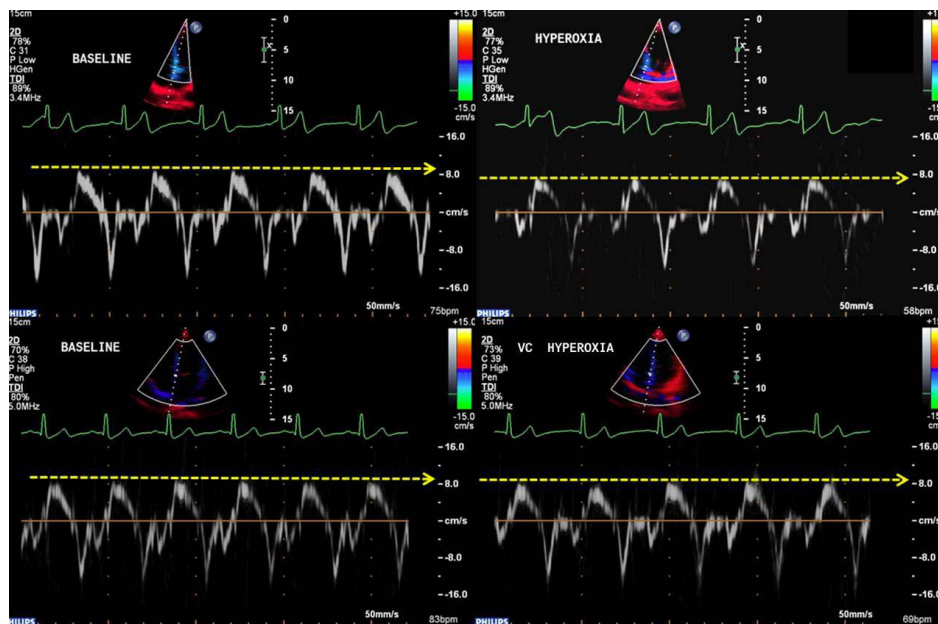


Figure 6. Effects of hyperoxia on myocardial function with and without vitamin C. Representative recordings of TDI tracings at baseline (left) and during hyperoxia (right). (Top) subject without administration of vitamin C. (Bottom) subject with vitamin C. Note, that the administration of vitamin C preserves myocardial function during hyperoxia

Research Project 16: Project Title and Purpose

Environmental Heavy Metals, Biomarkers of Susceptibility and Renal Cancer - This research will assist important efforts in cancer prevention by investigating cancer risk in a large population-based study among individuals at higher risk of renal cell cancer (RCC) (i.e., male smokers), by the use of established biomarkers of heavy metal exposure. The overall goal of the proposed study is to identify the risk of heavy metal exposure in the development of RCC at levels of exposure experienced by the general population and to determine whether there are other susceptibility factors (both genotypic and phenotypic) that can help predict cancer risk.

Duration of Project

1/1/2008 – 6/30/2008

Summary of Research Completed

This project ended during a prior state fiscal year. For additional information, please refer to the Commonwealth Universal Research Enhancement Annual C.U.R.E. Reports on the Department's Tobacco Settlement/Act 77 web page at <http://www.health.state.pa.us/cure>.

Research Project 17: Project Title and Purpose

Molecular Basis of Mechanotransduction in Bone Cells - The purpose of this project is to establish an animal model for studying mechanical loading-induced bone formation, and to identify important proteins involved in the loading-induced bone formation. Understanding of the loading-induced bone formation will lead to novel treatments for osteoporosis.

Duration of Project

1/1/2008 – 6/30/2009

Summary of Research Completed

This project ended during a prior state fiscal year. For additional information, please refer to the Commonwealth Universal Research Enhancement Annual C.U.R.E. Reports on the Department's Tobacco Settlement/Act 77 web page at <http://www.health.state.pa.us/cure>.

Research Project 18: Project Title and Purpose

Disseminating Effective Habits for Long-term Weight Loss - Most weight-loss interventions are not effective in producing long-term weight loss. The National Weight Control Registry (NWCR) has followed over 4000 individuals who achieved long-term weight loss to try to identify the characteristics of individuals who successfully maintained meaningful weight loss, including their dietary and exercise habits. We proposed to extend this study by developing a website www.achievetogether that will use information gathered from individuals who have successfully lost weight and kept it off to help guide those looking to lose weight. These data

will include identification of successful strategies, details of how these strategies were implemented, and how barriers were overcome. We will then determine whether use of the website is effective in producing weight loss, and how patterns of use predict successful weight loss.

Anticipated Duration of Project

1/1/2008 - 12/31/2011

Project Overview

The intent of this project is to test the utility of a website that contains data regarding weight-loss strategies that have been proven successful in producing sustained weight loss (www.achievetogether.com). Overall, the study will be conducted in three phases. In Phase 1, we will conduct in-depth interviews with 50 individuals who have lost weight and kept it off for at least one year. These individuals will be questioned regarding which strategies were used, how the strategies were implemented, and how barriers to using these strategies were overcome. The transcripts and quantitative data from their interviews will be entered into the www.achievetogether.com website. In Phase 2, we will recruit 100 overweight individuals and conduct a pilot randomized trial of the website, to understand whether use of the website will lead to better weight loss at 3 months. In Phase 3, we will make the website available to employees of the Milton S Hershey Medical Center, publicize its availability, track its use and analyze its use over time in order to better understand how to disseminate this and other web-based health interventions.

Principal Investigators

Christopher Sciamanna, MD, MPH
Chief, General Medicine Division
Penn State Milton S. Hershey Medical Center
500 University Drive
Hershey, PA 17033

Other Participating Researchers

Carla Miller, PhD, Kristen Kjerulff, PhD, Michele Shaffer, PhD, , Heather Stuckey, D.Ed., Jennifer Kraschnewski, MD, MPH – employed by Penn State University

Expected Research Outcomes and Benefits

The obesity epidemic is a growing concern in American health care. Thirty percent of the adult population is obese, and nearly two-thirds of the adult population is overweight. Obesity is associated with greater risk of serious diseases such as diabetes, heart disease, stroke, and some types of cancer. Being overweight can also result in social problems such as stigmatization and discrimination. In this project, we will gather detailed information from individuals who have been successful in both losing weight and keeping the weight off for at least a year. In particular,

we will focus on collecting diet and exercise information, as well as details on how these strategies were implemented, and how barriers were overcome. We will make this information available through a website, www.achievetogether.com, and test whether having this website available as a resource makes a difference in the ability of these individuals to lose weight.

Individuals accessing the website will be encouraged to enter information about their current exercise and eating habits, and the website will provide automated feedback about each habit. Habits will be categorized, into 3 categories: a) habits that are not working, b) habits that work, but that need to be used more consistently and c) habits that work and are used consistently. Users will be encouraged to change or delete habits that are being used but not helpful, more consistently use habits that are helpful but not being used, and continue to use habits that are helpful and being used consistently.

In the final phase of this project, we will make the website available to employees of the Milton S Hershey Medical Center and its insurance provider, Highmark. Given the interest of most adults in losing weight or maintaining a healthy weight and the fact that excessive weight is a risk factor for many common health conditions in the USA (e.g., diabetes, hypertension, high cholesterol), we believe that a web-based weight intervention may serve as a perfect offering for an employee health web-based portal.

Summary of Research Completed

Feasibility testing. We completed additional feasibility testing on the website to evaluate the ease of use of the site and to discuss which features work well and which features need improvement. The user-testing study consisted of 2 visits, spaced 2 weeks apart and frequent website use. We also held focus group sessions, where participants were asked to use our weight loss website for 2 weeks and then come in for an informal group discussion about each feature on the site. We were encouraged that individuals commented positively on the unique capabilities of the website. Illustrative comments included: "I watched some of the videos of the habits, and they were helpful - seeing people talk about it."; "I liked that it has a graph of your weight and your goal weight in your progress."; "After I submitted my goals, it has about if you want a table if you want to remember, and it has the days of the week and the reference....I like that because that way you can print it off and use it."

Randomized Controlled Trial (RCT). We then conducted a 3-month RCT of our Achieve Together weight loss website (www.achievetogether.com). The study included 100 overweight participants, who were randomized to either the intervention condition or a wait-list control condition. This study was approved by the Penn State Hershey Institutional Review Board and all participants provided written informed consent.

Participants: We recruited 100 participants with a BMI between 27 and 40 kg/m², aged 21-65. Additional inclusion criteria included Internet access either at home or at work, a valid email address, the ability to fluently speak and read English, and access to a scale to complete weekly weigh-ins. Participants were asked not to seek additional weight loss treatment. Participants were excluded for a positive response on the Physical Activity Readiness Questionnaire (PAR-Q), pregnancy (current, planned or previous within 12 months), planned or past weight loss surgery,

recent weight loss of ≥ 15 pounds in the past 6 months, inability to exercise, and a medical history of heart disease (myocardial infarction, congestive heart failure, unstable angina), stroke, diabetes, cancer, severe cognitive impairment or major psychiatric illness. Participants were recruited using multiple modalities (flyers, Internet) from an academic medical center. Research coordinators screened potential participants over the phone using a phone screening document to ensure they meet all eligibility criteria. Participants with questionable eligibility were referred to the Project Director or Principal Investigator for final review.

Baseline Measures: Participants who were eligible for the study completed a baseline visit to obtain consent and baseline assessment. This visit included measurement of height (Seca wall-mounted model 242), weight (Seca model 220), blood pressure (Allegiance Deluxe Sphygmomanometer, Cardinal Health), and multiple questionnaires, including the International Physical Activity Questionnaire (IPAQ), Block 2005 Food Frequency Questionnaire (FFQ), the Impact of Weight on Quality of Life questionnaire (IWQOL-Lite) and a baseline questionnaire assessing demographics, weight history and healthful habit use. Randomization took place at the baseline visit using concealed envelopes. Participants randomized into the treatment condition were additionally shown how to use the website.

Intervention: The Internet Website, AchieveTogether (www.achievetogether.com), was developed as a comprehensive weight loss program. AchieveTogether systematically incorporates 36 behavior change habits associated with weight loss, determined through our prior work with individuals who have successfully lost weight and kept it off.

Participants in the intervention condition first logged in to the website during the baseline assessment visit. At this time, they were encouraged to access the Achieve Together website at least once each week. If participants did not log-in during a given week, they received an e-mail reminder from the research coordinators. These email reminders included a motivational quote to inspire them to log back into the weight loss website. After 10 days of not using the website, the intervention participants received a phone call to better understand why they may not be using the website.

During each log-in session, a consistent set of activities occurred (see Figure 2). Participants were asked to enter their weight and height, how well their plan for a healthy weight has been going, and to clarify their goal weight. Participants were then asked to answer two questions about each habit they were using to lose weight: “Have you used this habit consistently?” (yes/maybe/no) and “Does this habit work well when you use it?” (yes/maybe/no). Participants received automated feedback about each habit they were currently using. Habits were categorized, according to the above questions, into 3 categories: a) habits that were not working, b) habits that worked, but that needed to be used more consistently and c) habits that worked and were used consistently. Participants were encouraged to change or delete habits that are being used but not helpful, more consistently use habits that are helpful but not used being used and to continue to use habits that are helpful and being used consistently (see Figure 3). Following this assessment, participants could search for habits that have helped people of similar age and gender to themselves. Additionally, participants were asked, at least each month, to rate one of the habits that are working particularly well or particularly poorly. Participants rated the habits

on a 5-point scale, similar to how products are rated on websites, and wrote some text about the habit.

Participants also had the opportunity to view photographs and video recordings of people talking about how they have successfully lost weight and kept it off. These photographs and videos were gathered from our prior work of individuals' success losing weight and keeping it off. An additional component of the website encouraged participants to communicate with a peer for advice. The website identified other individuals who were similar and who were using similar habits that the participants could then contact via email.

Participants in the control group had to wait 12 weeks before accessing the Achieve Together website.

Follow-up Assessment: After three months, all participants were directed to re-take the Block 2005 Food Frequency questionnaire online. Upon completion, they were asked to return for a follow-up visit. A research coordinator re-measured the participant's height, weight, and blood pressure. Participants were asked to complete the same questionnaires as during the baseline visit, including the International Physical Activity Questionnaire (IPAQ), the Impact of Weight on Quality of Life questionnaire (IWQOL-Lite) and a follow-up questionnaire of habit use. At this time, participants in the control group were given a log-in name and password to access the Achieve Together website. A research coordinator then showed control participants how to use the website and walked them through their first log-in.

Additional Measures: In addition to the measures described during the baseline and follow-up visits, we additionally examined adherence. Adherence measures included the total number of logins and the total numbers of weeks with at least one login.

Results:

Baseline Characteristics and Attrition

As shown in Figure 1, 176 participants were screened for eligibility to participate in the study. Of these, 76 were determined to be ineligible to participate with the top reasons due to having a BMI > 40, type 2 diabetes, or not being interested. The remaining 100 participants were randomized to either the intervention (n=50) or the control group (n=50).

Participant characteristics at baseline are described in Table 1. A majority of study participants were women (69.7%) and white (90.8%). The mean age of participants was 50.3 ± 11.0 years and baseline BMI was 33.2 ± 4.2 kg/m². A significant percentage of participants had comorbidities associated with being overweight as determined by self-report, including high blood pressure (68.0%), high cholesterol (40.0%), osteoarthritis (13.0%), and obstructive sleep apnea (10.0%). There were no statistically significant differences found between groups at baseline.

A total of 89 participants (89% of those enrolled at baseline) completed the 3-month follow-up assessments. Preliminary data analysis on the follow-up data is still being completed at this time (see Table 2).

Additional Qualitative Work. We have received additional funding under this award to collect more qualitative data for an R01 resubmission. We propose the following specific aims, to be completed over four months:

1. Recruit 40 adults identified through an electronic health record at Geisinger Medical Center, based on their success (or lack thereof) at either short-term or long-term weight control (10 successful/long-term, 10 unsuccessful/long-term, 10 successful/short-term, 10 unsuccessful/short-term).
2. Conduct qualitative research (in-depth interviews, journaling, and observation) with these participants to identify weight control practices.
3. Develop a protocol for analyzing the qualitative data collected above.

The goal of the overall R01 is to develop a self-reported measure of weight control practices that are the most strongly associated with future weight loss maintenance. The measure can be used to guide problem-solving interventions for weight loss maintenance, as generating a list of potential solutions is a key activity of the problem-solving approach. The list of practices can also serve as a menu of options for web-based weight control tools, such as that developed by our research team (www.achieve.together.com), which helps individuals select and adopt practices that are most likely to be helpful.

Figure 1. Study Participant Flowchart.

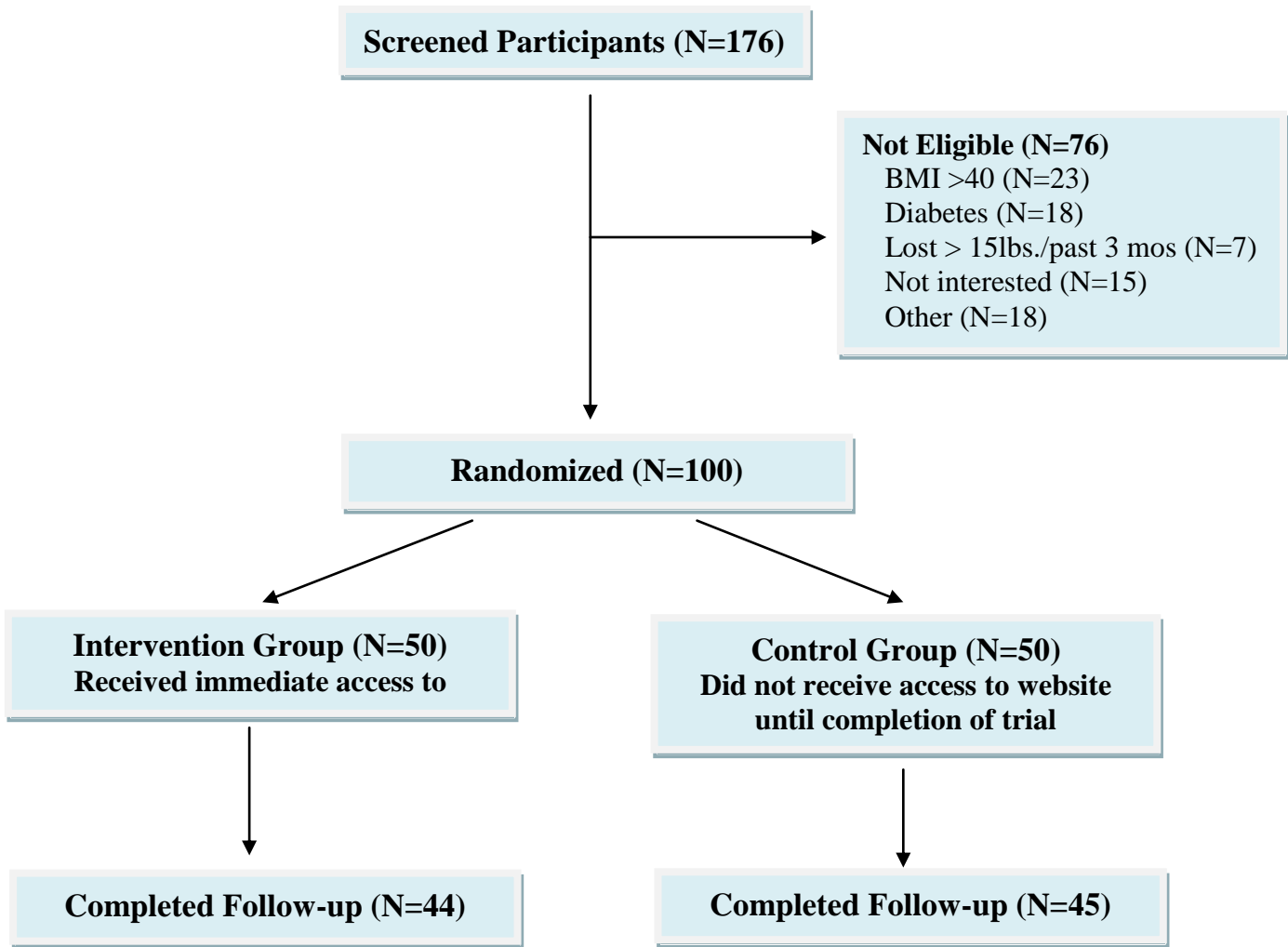


Figure 2. Outline of consistent activities taking place during each log-in session.

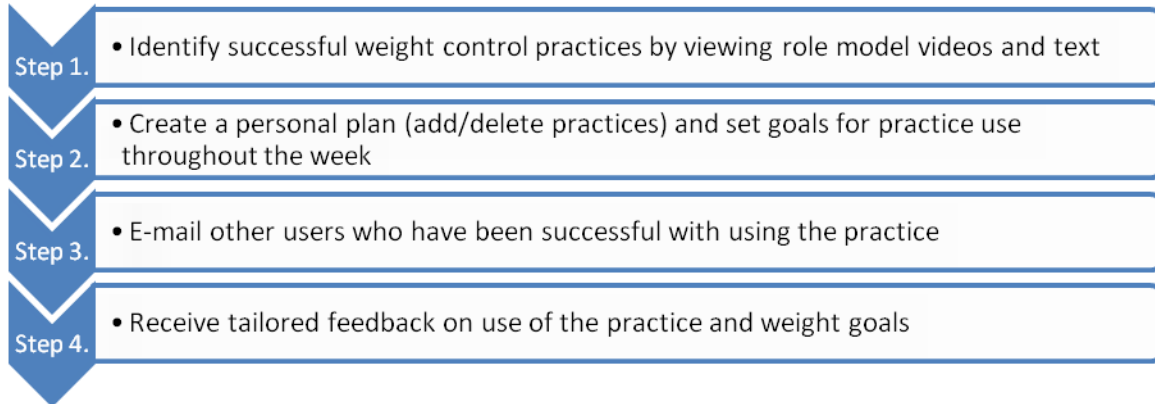


Figure 3. Screen Shot of Achieve Together Website (www.achievetogether.com).

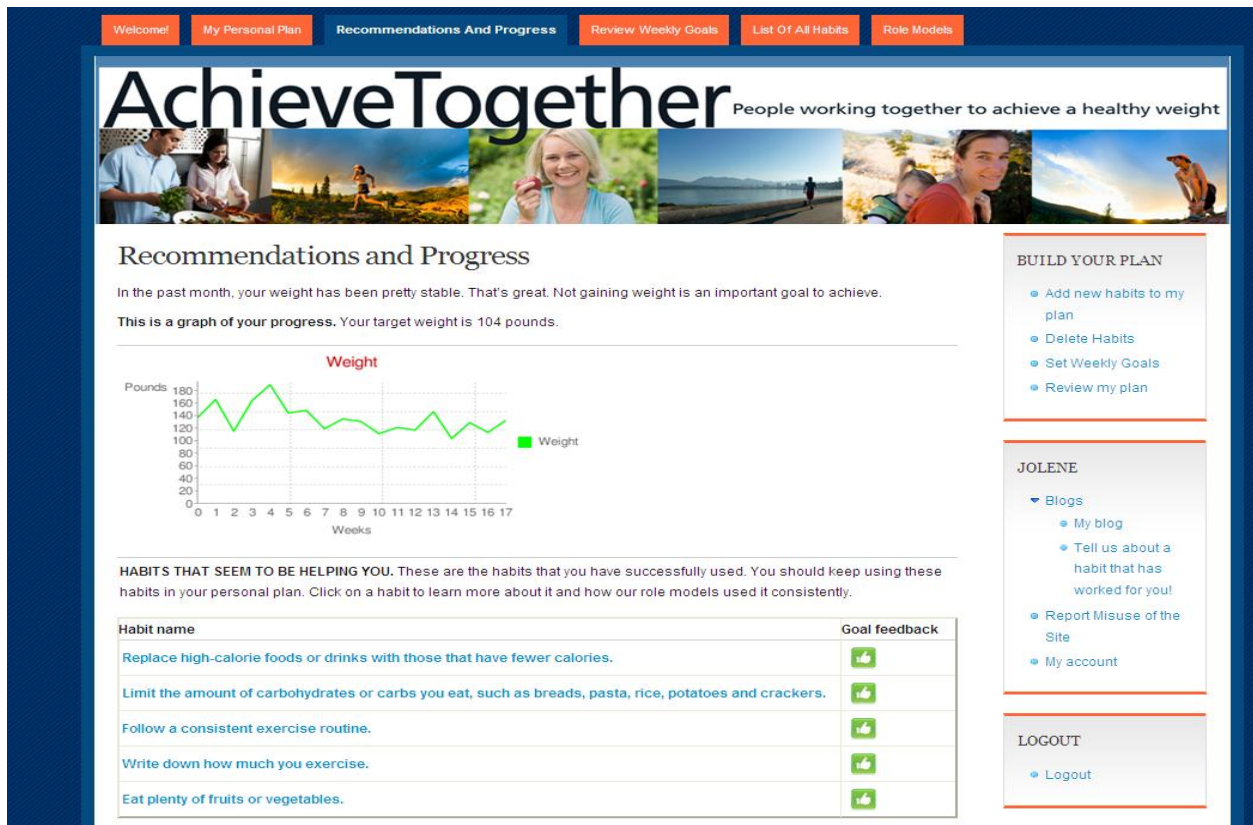


Table 1. Participant Characteristics of the Intervention Group vs. the Control Group (N=100).

Participant Characteristics ¹	Overall (N=100)	Control Group (N = 50)	Intervention Group (N = 50)	P value
Age in years, mean (SD)	50.3 (11.0)	49.9 (11.5)	50.7 (10.5)	0.72
Gender – Female (%)	69.7 (69)	77.6 (38)	62.0 (31)	0.09
Race – White (%)	90.8 (89)	86.0 (43)	95.8 (46)	0.32
High school education or less (%)	18.2 (18)	20.4 (10)	16.0 (8)	0.32
Marital status – Married (%)	75.0 (75)	74.0 (37)	76.0 (38)	0.06
Current weight (kg), mean (SD)	93.0 (14.4)	94.0 (15.1)	92.0 (13.6)	0.48
BMI, mean (kg/m ²)	33.2 (4.2)	33.7 (4.2)	32.7 (4.2)	0.26
Mean systolic blood pressure (mmHg)	125.7 (14.7)	124.3 (15.8)	127.1 (13.5)	0.34
Mean diastolic blood pressure (mmHg)	73.9 (9.3)	73.1 (9.4)	74.7 (9.1)	0.39
High Blood Pressure (%)	68.0 (68)	66.0 (33)	70.0 (35)	0.67
High cholesterol (%)	40.0 (40)	38.0 (19)	42.0 (21)	0.68
Osteoarthritis (%)	13.0 (13)	16.0 (8)	10.0 (5)	0.37
Obstructive sleep apnea (%)	10.0 (10)	12.0 (6)	8.0 (4)	0.51
Self-reported health status – Excellent/Very good (%)	40.0 (40)	32.0 (16)	48.0 (24)	0.30
Calorie Intake (kcal/day)				

¹ Characteristics reported as means (SD), unless otherwise stated.

Table 2. Changes in Outcomes during the 12-Week Intervention (N=89).

Outcome	Control Group (N = 50)	Intervention Group (N = 50)	Difference Between Groups
Body weight, kg	0.6 (-0.3, 1.4)	-1.4 (-2.2, -0.5)**	2.0**
BMI, kg/m ²	-0.4 (-1.2, 0.5)	- 1.1 (-1.9, -0.2)**	0.7
Systolic BP, mm Hg	-3.6 (-6.7, -0.5)*	-7.1 (-10.2, -3.9)**	3.5
Diastolic BP, mm Hg	2.2 (-0.2, 4.6)	-1.5 (-3.9, 1.0)	3.7*
IWQOL Total Score	0.6 (-2.2, 3.5)	2.6 (-0.2, 5.4)	2.0
IPAQ – Results			
Habit use	0.0 (-0.3, 0.3)	0.4 (0.2, 0.7)**	0.4*
Total daily caloric intake, kcal	-139.8 (-267.0, -12.5)*	-174.9 (-305.2, -44.6)**	35.8

¹ Changes reported as means (95% CI), unless otherwise stated.

* P-value < 0.05

** P-value ≤ 0.01

Research Project 19: Project Title and Purpose

Selective Autophagy in Yeast and in Mammalian Cells - The objective of this project is to examine whether a selective autophagy pathway that we originally identified in *Saccharomyces cerevisiae* is also present in mammalian systems. Vacuole Import and Degradation (*VID*) genes were isolated in regards to their role in the vacuole dependent degradation of gluconeogenic enzymes in yeast. Our preliminary results indicate an even broader role for *VID* genes in the survival of cells during chronological aging and during oxidative-stress in yeast. Cells lacking several of the *VID* genes are sensitive to oxidative stress and they have shorter life spans. Thus, *VID* genes protect cells from these stresses. Homologues of *VID* genes are found in mice and humans. It is the goal of this study to examine whether a similar Vid pathway exists in mammalian cells.

Duration of Project

7/1/2008 - 6/30/2009

Summary of Research Completed

This project ended during a prior state fiscal year. For additional information, please refer to the Commonwealth Universal Research Enhancement Annual C.U.R.E. Reports on the Department's Tobacco Settlement/Act 77 web page at <http://www.health.state.pa.us/cure>.

Research Project 20: Project Title and Purpose

Netrin-1 in Ischemia Reperfusion Injury of the Kidney - The purpose of this project is to gain a better understanding of how netrin-1 prevents ischemic renal injury. We will determine the receptors subtype which mediates netrin-1 protective effect against ischemic kidney injury and pathways through which netrin-1 mediates the protective effects.

Duration of Project

7/1/2009 - 6/30/2010

Project Overview

Acute renal failure is a common disorder which affects about 5% of all hospitalized patients. The overall mortality rate for acute renal failure, over 50%, has changed little since the 1960's. The financial burden of acute renal failure is estimated to be \$8 billion per year, or about \$130,000 per life-year saved. It is unlikely that this high mortality and associated cost will be reduced until we develop new mechanistically based therapeutic tools. Netrins are the prototypical axonal attractants and play an important role in guidance of axons during development. Although the kidney was found to have the highest netrin-1 expression among various tissues studied, the role of netrin-1 in kidney disease is unknown. My preliminary data indicate that netrin-1 may protect against renal ischemic injury. The objective of this study is to determine the role of Netrin-1 in ischemia reperfusion induced acute kidney injury. The purpose of this research is to generate

more preliminary data regarding the role of netrin-1 in ischemia reperfusion injury of the kidney. We will achieve our objectives using the following three specific aims: Specific Aim #1: Determine the expression of netrins and their receptors in normal mouse kidney and kidney derived cells; Specific Aim #2: Determine the role of netrin-1 and their receptors in ischemia reperfusion injury of the kidney, and Specific Aim#3: Determine the role of MAPK signaling in mediating netrin-1 biological effect in the kidney. We will use real-time RT-PCR, antibody infusion into mice, western blot analysis, and cell culture techniques to determine the role of netrin in ischemia reperfusion injury of the kidney. The proposed work is new and the role of netrin-1 in renal ischemia reperfusion injury has not been studied before. Understanding the mechanism through which netrin-1 protects the kidney from ischemic injury will direct us to new therapeutic strategies for ischemia reperfusion injury of the kidney and other organs as well.

Principal Investigator

Ganesan Ramesh, PhD
Assistant Professor
Penn State University College of Medicine
H040, Division of Nephrology
500 University Drive
Hershey, PA 17033
E-mail: gramesh@psu.edu
Phone: 717-531-5843
Fax: 717-531-6776

Other Participating Researchers

None

Expected Research Outcomes and Benefits

These studies will contribute to our long-term goal of understanding the mechanisms of acute renal injury with the purpose of designing preventive or therapeutic interventions. As a result of these studies, we expect that we will have an understanding of the role of netrin-1 in ischemia reperfusion induced kidney injury including site of expression, expression netrin receptors, role receptors in netrin-1 signaling and mediating protective effect and signaling pathways activated by netrin-1 in endothelial and epithelial cells. In future studies, we will be in position to: determine if these results are also applicable to other models of acute or chronic renal injury; characterize the function and regulation of newly identified downstream targets; determine the contribution of specific receptors to renal injury; and begin to manipulate the upstream and downstream targets of netrin-1.

Summary of Research Completed

Overwhelming evidence suggests that ischemia-reperfusion injury of the kidney is an inflammatory disease mediated by both innate and adoptive immune systems. The neuronal guidance molecule netrin-1 was shown to modulate inflammatory responses. Given that ischemic kidney is particularly prone to reperfusion elicited inflammation, we sought to determine the

function of netrin-1 and its receptor UNC5B in ischemia-reperfusion-induced inflammation. Renal ischemia-reperfusion caused rapid decrease in serum netrin-1 levels. Administration of recombinant netrin-1 either before or after renal ischemia-reperfusion reduced kidney injury, apoptosis, monocyte and neutrophil infiltration, and cytokine (IL-6, IL-1 β and TNF α) and chemokine (MCP-1, MDC, MIG, KC and 6Ckine) production. Analysis for different netrin-1 receptors on leukocytes showed very high expression of UNC5B, but not UNC5C, UNC5D, neogenin or DCC. Expression of UNC5A was low. Neutralization of UNC5B receptor reduced netrin-1-mediated protection against renal ischemia-reperfusion injury, and increased monocyte and neutrophil infiltration, serum and renal cytokine and chemokine production with increased kidney injury and renal tubular cell apoptosis. Finally, investigation into netrin-1 effect on CD4 T cell stimulation showed suppression of Th1/Th2/Th17 cytokine (IL-2, IL-6, IL-10, IL-13, IL-17, IFN γ , IL-4 and TNF α) production, *in vitro*. Our studies demonstrate that netrin-1 acting through UNC5B receptor reduces renal ischemia-reperfusion injury and its associated renal inflammation.

1. UNC5B neutralization antibody inhibits netrin-1-mediated attenuation of renal Ischemia Reperfusion Injury (IRI). To determine whether UNC5B mediates netrin-1 protective functions against renal IRI, *in vivo*, four groups of mice were subjected to bilateral renal pedicle clamping, and were followed for 72 h after reperfusion. UNC5B antibody or isotype matched antibody was administered, intraperitoneally, 18 h before clamping of renal pedicles. Netrin-1 or vehicle was administered, intravenously, 2 h before renal pedicle clamping. As shown in Fig. 1A, netrin-1 treated mice showed improved renal function compared with UNC5B antibody or isotype control antibody treated mice, as determined by measuring serum creatinine. Mice administered with both netrin-1 and UNC5B antibody showed increased renal injury suggesting that the netrin-1 protective effects are mediated through the UNC5B receptor.

Improved renal function with netrin-1 administration was associated with better preservation of renal morphology compared with vehicle treated kidneys (Fig. 1B, panel *I* and *II*). Administration of UNC5B antibody abolished netrin-1-mediated preservation of kidney morphology by increasing necrosis and cast formation in the renal tubules. In addition, administration of netrin-1 also inhibited ischemia-reperfusion-induced apoptosis of tubular epithelial cells (Fig. 1B, panel *III*), which was abolished in response to UNC5B antibody treatment.

2. Netrin-1 attenuates renal infiltration of leukocytes through UNC5B receptor, *in vivo*. Our earlier studies and present findings suggest that administration of netrin-1 reduces inflammation in renal IRI, but the receptor through which netrin-1 inhibits infiltration of leukocytes is not known. To determine whether UNC5B receptor mediates suppression of ischemia-reperfusion-induced renal leukocyte infiltration, kidneys (isolated from WT mice subjected to renal IRI and treated with netrin-1 and/or UNC5B antibody) were analyzed for different subsets of leukocytes at 6 h and 24 h after reperfusion. As shown in Fig. 2, renal IRI in vehicle treated mice showed a drastic increase in infiltration of monocytes and neutrophils into the kidneys (Fig. 2A and B) as compared with sham-operated mice. This increase in renal monocytes and neutrophils was significantly reduced in netrin-1-treated mice, suggesting that netrin-1 attenuates renal infiltration of leukocytes. However, administration of UNC5B antibody prevented netrin-1 suppression of monocyte and neutrophil infiltration into the kidneys,

suggesting that netrin-1 attenuates leukocyte infiltration through UNC5B receptor. UNC5B antibody inhibition of netrin-1 protective effects on kidneys was also observed at 24 h after reperfusion (not shown). UNC5B antibody alone treated mice which are subjected to IRI also showed increased infiltration of leukocytes as compared with sham operated mice (date not shown). However, except for a minimal increase in B cells, the number of renal CD4 and CD8 T lymphocytes, NK cells, plasmacytoid dendritic cells, macrophages (CD11c- F4/80+) and myeloid dendritic cells (CD11c+ F4/80+/-) in mice subjected to renal IRI was similar to sham-operated mice. These results suggest that netrin-1 inhibits infiltration of leukocytes into kidney by acting through the UNC5B receptor.

Studies had shown that IFN γ produced from neutrophils mediates IRI of the kidney. Having found that netrin-1 acting through UNC5B receptor inhibits infiltration of monocytes and neutrophils into kidney in renal IRI, we investigated IFN γ production in them in response to netrin-1 and/or UNC5B antibody administration. Renal cells obtained at 6 h after reperfusion were stained for IFN γ in monocytes and neutrophils, and analyzed by flow cytometry. We found more neutrophils positive for IFN γ in kidneys with ischemia-reperfusion injury compared with kidneys of sham-operated mice. However, the expression level of IFN γ in neutrophils was found to be almost similar between different groups of mice (not shown), consistent with an earlier report that infiltration of neutrophils, positive for IFN γ , is increased but not neutrophil IFN γ expression.

3. Netrin-1 reduction of cytokine and chemokine production is mediated through UNC5B receptor, *in vivo*. Cytokines and chemokines play an important role in the activation and migration of leukocytes into injured organs where they exacerbate tissue injury. Having determined that netrin-1 attenuates renal leukocyte infiltration through the UNC5B receptor, we investigated the effect of UNC5B receptor neutralization on netrin-1-mediated reduction of chemokine and cytokine production both in serum and kidneys after renal IRI. Serum and kidneys obtained from mice treated with netrin-1 and/or UNC5B antibody and subjected to sham or bilateral renal pedicle clamping were analyzed for different cytokines and chemokines by ELISA and real time RT-PCR, respectively. Ischemia-reperfusion significantly increased the levels of cytokines (IL-6, IL-10) and chemokines (MCP-1, monokine induced interferon gamma (MIG), Eotaxin, macrophage-derived cytokine (MDC), KC and 6CKine) in circulation at 6 h (Fig. 3A) and 24 h (not shown) after reperfusion in vehicle treated mice compared with sham-operated mice. Netrin-1 administration significantly reduced serum levels of different chemokines and cytokines. Netrin-1 suppression of cytokine and chemokine production in renal IRI was significantly reduced in UNC5B antibody-treated mice. Similarly, the expression of different cytokines and chemokines (IL-1 β , TNF α , IL-6, IL-10, MCP-1 and ICAM-1) in kidneys was increased at 6 h (Fig. 3B) and 24 h (not shown) after reperfusion in mice subjected to IRI compared with sham operated mice. Administration of netrin-1 suppressed the expression of IL-6 and MCP-1 at 6 h and 24 h after reperfusion, and ICAM-1, IL-1 β and TNF α at 24 h after reperfusion (not shown). Mice treated with UNC5B antibody before netrin-1 administration significantly decreased netrin-1-mediated reduction of renal cytokine and chemokine expression in renal IRI, suggesting that netrin-1 attenuates cytokine and chemokine production through the UNC5B receptor in renal IRI. Administration of UNC5B antibody alone had no impact on reperfusion induced increase in serum and renal cytokine and chemokine production. These

results suggest that netrin-1 attenuation of cytokine and chemokine production is mediated through the UNC5B receptor.

4. Netrin-1 regulates production of Th1/Th2/Th17 cytokines from CD4⁺ CD25⁻ T cells. The mechanism by which netrin-1 inhibits infiltration of leukocytes into kidneys is unknown. It is possible that netrin-1, acting directly on leukocytes, suppress cytokine and chemokine production. Given that CD4 T cells produce cytokines and chemokines and regulate neutrophil infiltration in renal IRI, we investigated the effect of netrin-1 on CD4 T cell cytokine production. CD4 T cells depleted of T reg cells were stimulated with CD3 antibody in the presence or absence of netrin-1. The levels of different cytokines produced by CD4 T cells in the absence of CD3 antibody were very low and comparable to that of netrin-1 alone treated cells. However, in the presence of CD3 antibody, CD4 T cells showed a dramatic and significant increase in Th1/Th2/Th17 cytokines (IL-2, IL-4, IL-6, IL-10, IL-13, IL-17, IFN γ and TNF α) as compared with non-treated CD4 T cells ($P < 0.0001$). The production of IL-5, IL-12, IL-23 and TGF- β cytokines was low and comparable between different groups. Addition of netrin-1 to CD3 antibody-treated CD4 T cells significantly reduced the production of different cytokines (IL-2, IL-4, IL-6, IL-10, IL-13, IL-17, IFN γ and TNF α) as compared with vehicle treated CD4 T cells ($p < 0.0001$). The inhibition of cytokine production by netrin-1 was dose dependent. Minimal effect was noticed with 100 ng/ml of netrin-1 and maximal inhibition was observed at 500 ng/ml of netrin-1 concentration. It is possible that the observed netrin-1 suppression of cytokine production resulted from induction of cell death in CD4 T cells. Therefore, we investigated the CD4 T cell viability in response to netrin-1 treatment by MTT assay. Rather than cell death, we noticed a moderate increase in CD4 T cell proliferation in response to netrin-1 and CD3 antibody treatment as compared with non- treated CD4 T cells ($p < 0.001$). These findings suggest that netrin-1, by acting directly on leukocytes, can suppress cytokine production, and thereby can attenuate renal IRI.

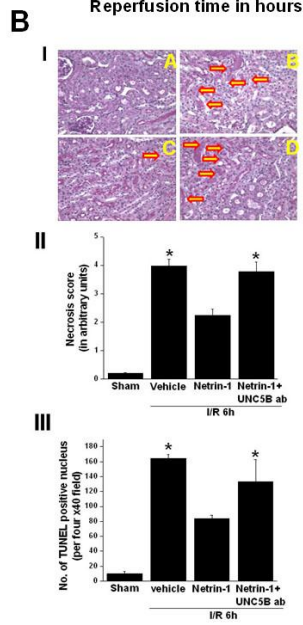
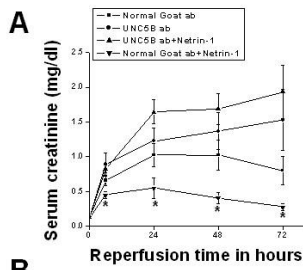


Figure 1. Neutralization of UNC5B receptor attenuates netrin-1 protection of kidney injury.

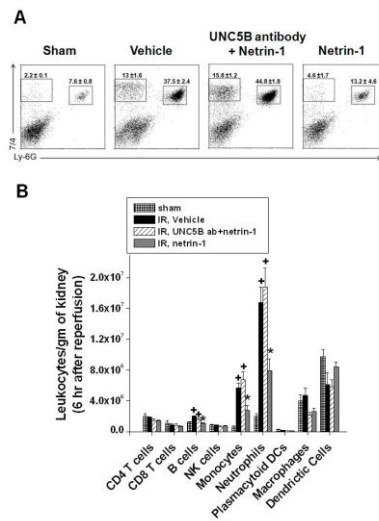
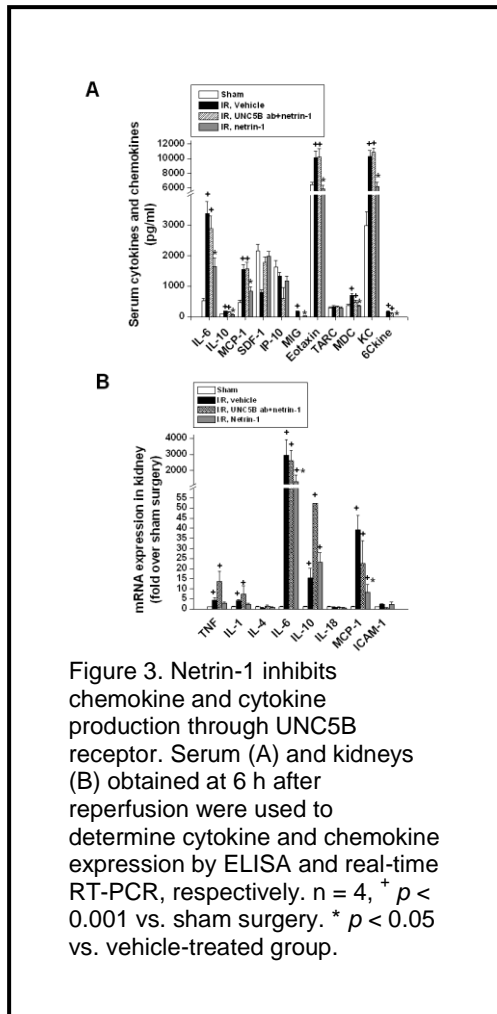


Figure 2. Netrin-1 injection reduces infiltration of monocytes and neutrophils into kidneys. $n = 4$. $+ p < 0.001$ vs. sham surgery, $* p < 0.05$ vs. vehicle-treated group.



Research Project 21: Project Title and Purpose

Structures in the Unfolded State Initiate Protein Folding - The central dogma of molecular biology states that DNA is transcribed into a messenger RNA which is translated into the amino acid sequence of a protein. However, we do not understand the means by which that linear sequence of amino acids is transformed into a unique three dimensional structure that is capable of function. This project examines the mechanism by which protein folding is initiated, identifying individual residues and structures that direct the folding of the protein to the correct final structure.

Duration of Project

7/1/2008 - 6/30/2010

Project Overview

The means by which the linear sequence of a protein assembles into a three dimensional structure that is capable of function is poorly understood. Of particular interest is how folding is initiated, and how incorrect folding is avoided before the correct structure is achieved. This project addresses the mechanism of folding initiation in β -sheet proteins by examining the structure of an initiation site for the folding of intestinal fatty acid binding protein (IFABP). We have identified a few residues in this 131 amino acid protein that appear to form tertiary contacts at concentrations of denaturant where the protein lacks secondary structure. These residues also interact with each other in the native state, suggesting that a scaffold of hydrophobic interactions similar to the native state is the first step in organizing the structure during folding. This mechanism for the folding of proteins is very attractive, because the presence of this template greatly reduces the number of conformations that need to be explored to find the native structure. The goal of this project is to understand the structure and behavior of this scaffold.

The specific aim of this project is to identify and characterize a subset of residues and structures that participate in the scaffold and measure the thermodynamic contributions of those residues to the stability of the site. Residues that participate in this site via sidechain contacts will be identified by combining site specific fluorine labeling and ^{19}F -NMR. Residues with backbone atoms that participate will be identified by comparing the intensity of the $^1\text{H}^{15}\text{N}$ -HSQC spectrum for the extended unfolded form of the protein at high concentrations of denaturant to the same spectrum at a more moderate concentration of denaturant where the initiating site is populated. Site directed mutagenesis will be used to modulate the thermodynamic stability of the initiating site and the roles of turns and hydrophobic interactions in this structure. Interatomic distances in the scaffold will be measured by site specific labeling of the protein with a paramagnetic relaxation agent. Finally, a series of mutations will be made that will destabilize the native state of the protein without affecting the stability of the initiating site, so that the state will be populated in the absence of denaturant. The proposed studies will lead to significant progress in understanding how the folding of IFABP is initiated, which has general implications for the initiation of folding in other β -sheet proteins.

Principal Investigator

Ira J. Ropson, PhD
Associate Professor
Penn State University
500 University Drive
Hershey, PA 17033

Other Participating Researchers

Paula M. Dalessio, PhD – employed by Pennsylvania State University

Expected Research Outcomes and Benefits

A number of diseases are caused by the misfolding of proteins, including conditions as diverse as Type II diabetes and Alzheimer's disease. In order to better treat these diseases, a better understanding of how proteins fold to the correct final structure is necessary. The hallmark of these diseases is the accumulation of misfolded proteins in intermolecular crossed β -sheet aggregates, which eventually form amyloid fibrils. The formation of these structures is a common feature of all the amyloid diseases, regardless of the protein that forms the aggregate. Many proteins not associated with any disease, including IFABP, form amyloid under defined solution conditions. The initiating sites for both correct protein folding and amyloid formation are found in structures that are populated in partially unfolded states. A better understanding of how the β -sheets of IFABP fold and avoid aggregation will enable us to understand how to prevent the formation of these aberrant structures.

Further, the various genome projects are producing a large number of DNA sequences, without knowledge of the structure or function of the protein products of many of those genes. Many of these newly discovered proteins have the potential to be therapeutic targets for a number of diseases. Without knowledge of the structure of these proteins, it will be difficult to understand their function. Understanding the mechanism by which proteins fold is important to predicting the structures of proteins solely from sequence information. The systematic study of the folding of a group of structurally related proteins will identify trends in folding mechanisms, and hypotheses on initiating sites and metastable intermediates can be checked by studies on other sequences. Deciphering the rules that govern hydrophobic core formation in this family will lead to a better understanding of the rules for core formation in other proteins.

Summary of Research Completed

Protein folding remains an enigma. We do not understand how the sequence of a protein dictates the final structure or the path by which that structure is obtained after synthesis on the ribosome. Previous efforts in our laboratory have shown that the folding of intestinal fatty acid binding protein (IFABP) and other members of the intracellular lipid binding protein family are completely reversible at neutral pH and fit well to a two-state model for the unfolding process at equilibrium. However, nuclear magnetic resonance (NMR) experiments showed the presence of an equilibrium intermediate for IFABP at concentrations of denaturant where the protein appeared to be completely unfolded by optical techniques. The purpose of this grant was to better understand the structure and role of this intermediate in the folding process. Our previous report described experiments performed with IFABP, including NMR backbone assignments for the unfolded state, and the prediction of the effects of site-directed mutagenesis on the stability and structure of the intermediate. We continued those studies for IFABP by examining the effects of another mutation on this intermediate, and extended those results to another member of this family, human bile acid binding protein (BABP). The structures of BABP and IFABP are nearly identical (most backbone atoms have a root mean square deviation of less than 1 Å). Thus, we wanted to determine if BABP showed similar behavior in its NMR spectra at high concentrations of denaturant. Our previous studies of the folding of BABP by stopped-flow fluorescence and circular dichroism showed that this intermediate appears to be present, although it is less stable and populated at lower levels compared to IFABP.

Standard 3-dimensional experiments (HNCO, HNCA, HNCOCA, HNCACB, HNCOCACB, HNN) were performed in 8M urea on a 600 Mhz spectrometer to determine the backbone assignments of BABP. NMRPipe (<http://spin.niddk.nih.gov/bax/software/NMRPipe/>) and NMRView (<http://www.onemoonscientific.com/nmrview/>) were used to process and analyze the resulting spectra. The assignment process is ongoing, and should be completed shortly. The chemical shift dispersion of resonances of unfolded proteins is much less than that of native proteins, and less than that of IFABP. As such, there is more spectral overlap for BABP than IFABP. About 75 of the resonances are well resolved in a 2D-¹⁵N,¹H-HSQC spectrum for ¹⁵N labeled protein (Figure 1). Preliminary studies of the spectra of BABP at lower concentrations of denaturant do not show the dramatic loss of intensity displayed by IFABP at similar denaturant concentrations. Rather, there appears to be a number of peaks that shift in frequency, suggesting that either the rate of exchange between the intermediate and unfolded states is faster, or that it is much less populated. Additional experiments are required to better understand this observation.

In our previous report, we described the effects of the V60N mutation on the relative stability of the intermediate and native state for IFABP. As predicted, the mutation lowered the stability of both the intermediate and native state due to the replacement of a hydrophobic residue with a polar residue. A second mutation was examined during this period, R106Q-IFABP. This charged residue is partially buried near the hydrophobic core of IFABP, and is important to the binding of the fatty acid ligand. This residue does not appear to participate in the intermediate state, but its replacement with glutamine stabilizes the native state to denaturation by fluorescence and circular dichroism. We have labeled this protein with 5FTrp using the same methods described in our previous report. We predict that the native state will be stabilized without changing the stability of the intermediate state. Thus, native state intensity would be observed at higher concentrations of denaturant, decreasing the relative population of the intermediate state. The spectra are shown in Figure 2 compared to wild type IFABP, and the fitted populations are shown in Figure 3. As was the case for V60N-IFABP, our predictions about the relative stabilities of the native and intermediate states for R106Q-IFABP were correct. Thus, we have shown the ability to make qualitative testable hypothesis about the effects of mutations on the relative stability of the native, intermediate and unfolded states. In collaboration with Dr. Osman Bilsel at the University of Massachusetts Medical School, we have been attempting to make quantitative estimates of the changes in stability for these states at equilibrium using the program Savuka that he has developed. The main difficulty in determining these stabilities appears to be in the fitting of the raw spectral data to an $N \rightleftharpoons I \rightleftharpoons U$ transition. The fits work well at the midpoint of the titration, but perform poorly with large errors whenever the population of any state is less than 5%. We are trying to address this problem so that these qualitative results can have quantitative statistics associated with them. A poster describing the measurements of the relative stability of these proteins was presented at the Protein Folding Gordon Conference in Ventura, CA in January 2010.

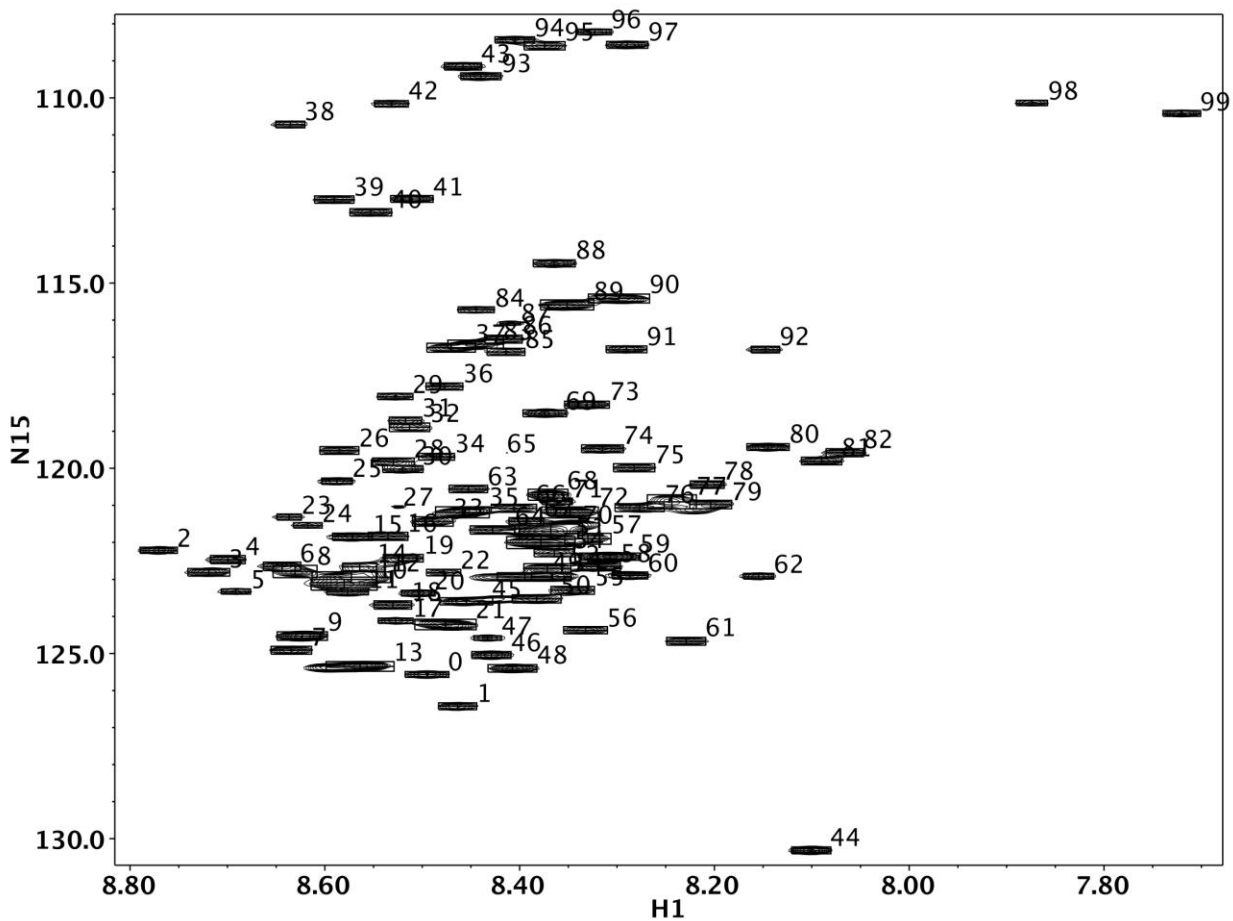


Figure 1. $^1\text{H}^{15}\text{N}$ -HSQC spectrum of uniformly labeled ^{15}N BABP at 8 M urea.

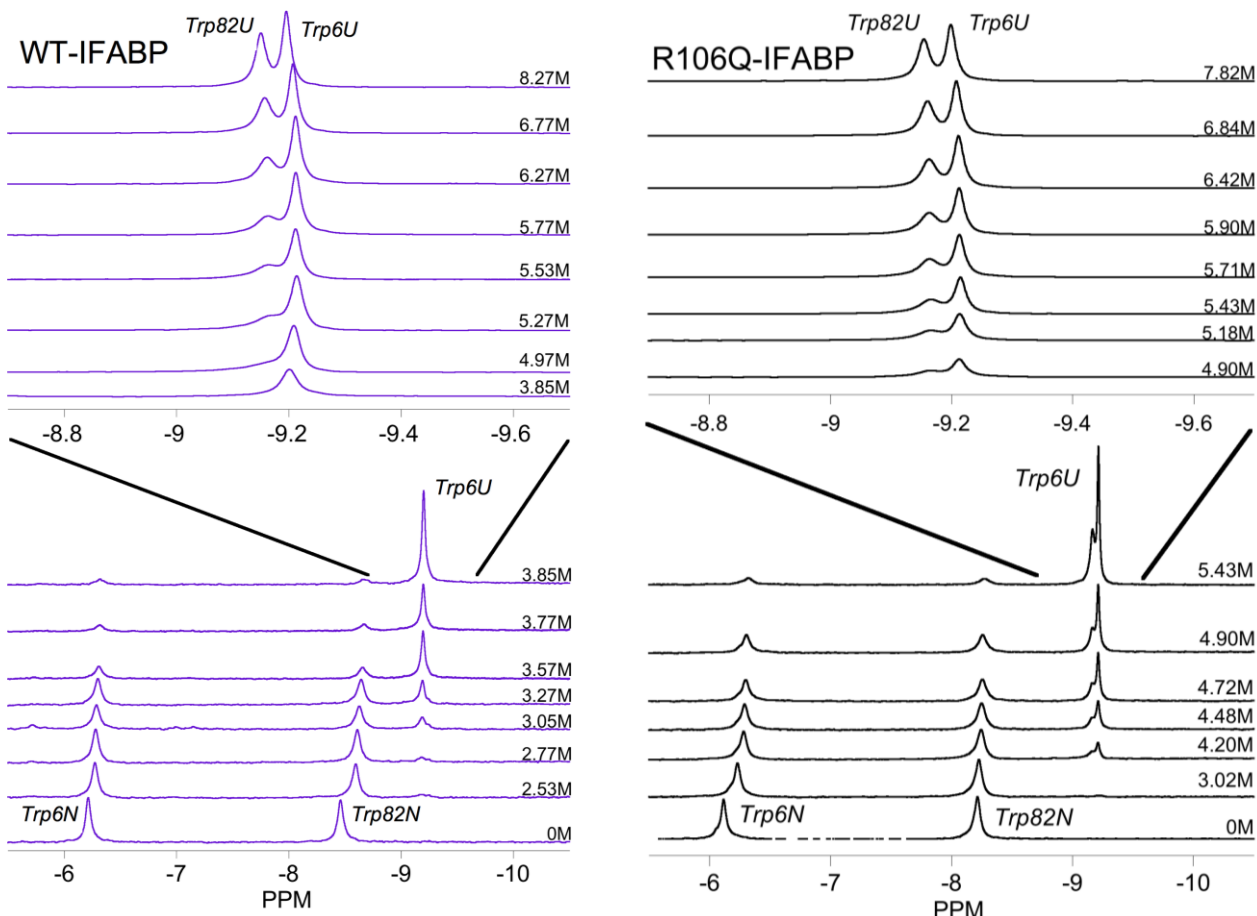


Figure 2: ^{19}F -NMR spectra for 5FTrp-WT-IFABP (left) and 5FTrp-R106Q-IFABP (right). The upper part of both panels display an expanded view of the spectra at concentrations of urea greater than 3.85M and 4.9M, respectively. The native (*Trp6N* and *Trp82N*) and unfolded (*Trp6U* and *Trp82U*) resonances are labeled in each panel.

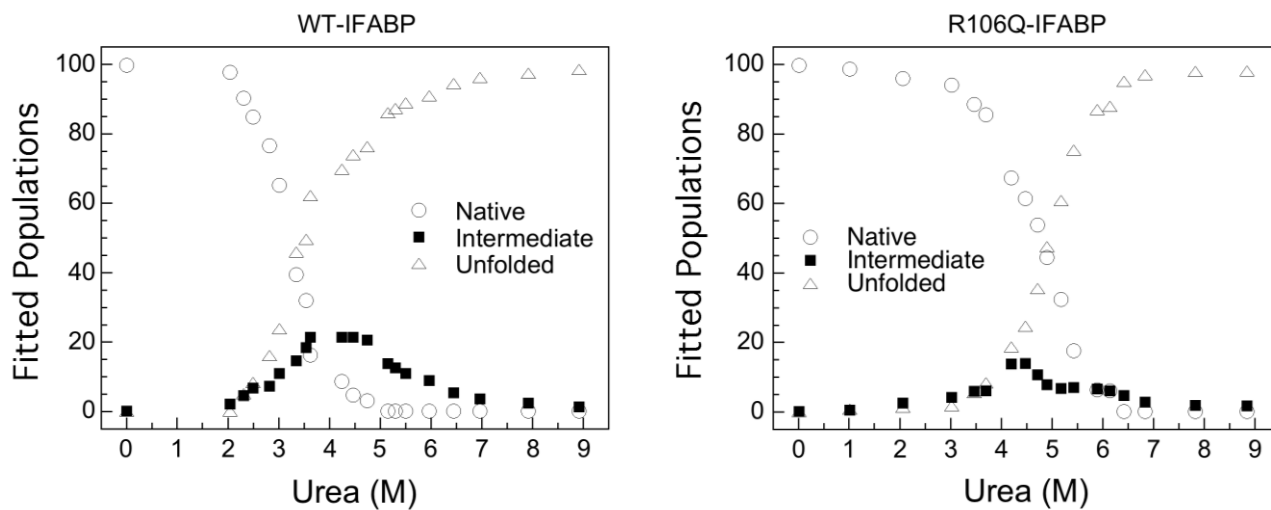


Figure 3. Fitted populations of native, intermediate and unfolded states of WT-5Ftrp-IFABP (left) and V60N-5Ftrp-IFABP (right).

Research Project 22: Project Title and Purpose

Mechanisms of Gene Regulation by EBV EBNA-1 Protein - The potential of Epstein-Barr virus (EBV) to cause cancer is dependent on establishment of a life-long latent infection within its human host's B lymphocytes. We have discovered a novel autoregulatory mechanism through which EBV can control expression of its EBNA-1 protein, whose function is critical to EBV persistence in B cells. We hypothesize that this enables the virus to maintain EBNA-1 levels below a threshold to prevent detection and removal of infected cells by the host's immune surveillance. The purpose of this research is to evaluate autoregulation of EBNA-1 expression in the context of infected B cells to permit us to test whether it is capable of allowing infected cells to evade the immune response. Ultimately, this may lead to therapeutic approaches to disrupt autoregulation of EBNA-1 to enhance the anti-EBV immune response.

Anticipated Duration of Project

7/1/2008 - 12/31/2010

Project Overview

Epstein-Barr virus (EBV) is able to persist lifelong as a latent infection within B lymphocytes with little overt disease. However, a breakdown in immune surveillance remains a significant risk factor for development of EBV-associated lymphoma, underscoring the highly evolved equilibrium that exists between this potentially oncogenic herpesvirus and the host immune system. This equilibrium is dependent on a selective down-regulation of EBV latency-associated gene expression during establishment of persistent infection in B lymphocytes that ultimately restricts expression to viral genes critical for maintenance of persistence, while precluding those with acute transforming properties and/or which encode dominant epitopes recognized by the EBV-specific T-cell surveillance. A pivotal process in this transition to restricted latency is a promoter switching event that enables exclusive expression of the essential EBV genome-maintenance protein, EBNA-1, from the promoter Q_p, which in reporter assays can be negatively regulated by EBNA-1 through its two binding sites immediately downstream of the transcription start site. We hypothesize that this apparent autoregulation is crucial to EBV persistence and its associated pathogenic potential by ensuring sufficient EBNA-1 for genome maintenance, while limiting EBNA-1 synthesis below a critical level that, if exceeded, would subject infected B cells to elimination by EBNA-1-specific cytotoxic T cells. Our broad, long-term objectives are to: 1) Define the mechanism through which EBNA-1 autoregulates its expression; 2) Determine its contribution to the control of EBNA-1 levels during EBV latent infection in B cells; and 3) Ultimately determine whether it does indeed contribute to immune evasion. The later two objectives will require us to address the specific aim of this research: To demonstrate that EBNA-1 expression from Q_p is autoregulated in the context of B cells latently infected with EBV, and that EBNA-1 levels in these cells can be manipulated by targeting Q_p. We will take two approaches. First, we will mutate the EBNA-1 binding sites in Q_p within the EBV genome, and then infect B cells with this mutant virus and wild-type EBV to assess the consequence of the mutations in Q_p on EBNA-1 levels. Second, in the B cells infected with these mutant and wild-type EBVs, we will introduce an inducible EBNA-1 expression gene, to demonstrate that

increasing EBNA-1 levels from an exogenous gene decreases its expression from the endogenous viral genome, as we would expect if the apparent autoregulatory function we have defined in reporter assays is active in these cells.

Principal Investigator

Jeffery T. Sample, PhD
Professor
Department of Microbiology and Immunology – H107
Penn State University College of Medicine
500 University Dr.
P.O. Box 850
Hershey, PA 17033

Other Participating Researchers

Carol A. Dickerson, MS – employed by Pennsylvania State University

Expected Research Outcomes and Benefits

Expected Outcomes

Overall, we expect to learn the extent to which the EBV protein EBNA-1 controls its levels in B cells that it infects. Specifically, we expect to learn: 1) Whether during restricted latency, i.e., that which enables EBV to persist within B lymphocytes, the level of EBNA-1 protein in these cells is determined primarily by EBNA-1 itself ; and 2) Whether EBNA-1 levels expressed from the promoters Cp and Wp during the growth or Latency III program (needed for the rapid expansion of EBV-infected cells early after infection) are higher than EBNA-1 expressed during restricted latency, and are capable of precluding the expression of EBNA-1 from Qp, thereby circumventing the autoregulatory mechanism of EBNA-1.

Expected Benefits

We expect our research to demonstrate that EBNA-1 does indeed autoregulate its expression from the promoter Qp in actual EBV infection. The primary benefit of this outcome is that it will satisfy a major requisite of our hypothesis, namely that EBNA-1 limits its expression below a certain threshold during EBV infection that may prevent infected cells from elimination by the host's anti-EBNA-1 immune surveillance. Further, from the experimental systems developed in this research to regulate EBNA-1 expression, we would be able to test whether disruption of the autoregulatory function of EBNA-1 would indeed result in higher levels of EBNA-1 and consequently significantly greater susceptibility to killing by anti-EBNA-1 cytotoxic T cells, and that by contrast, the level of EBNA-1 normally maintained during restricted latency (i.e., by autoregulation) would be insufficient for detection and elimination of infected cells.

Summary of Research Completed

For reasons outlined in the previous report, we needed to generate a new bacterial artificial chromosome (BAC) clone of the EBV genome contained in the latently infected Burkitt lymphoma (BL) cell lines Akata. Our progress for this year is outlined below.

Generation of a new EBV-BAC

At the beginning of the reporting period we had: 1) Completed construction of a targeting construct (plasmid p9495-BAC) containing the BAC DNA backbone, flanked on either side by EBV DNA that would allow for insertion of the BAC into the EBV genome within the *BDLF3* gene locus; and 2) Confirmed that the gene for dsRed (a fluorescent marker protein) within this targeting construct was functional upon transfecting it into HEK293 cells. Our next step was to recombine the BAC into the *BDLF3* locus within the genome of the Akata isolate of EBV, which to this point has been problematic:

Insertion of BAC via homologous recombination - Our first attempts to insert the BAC into the EBV genome relied on homologous between our targeting construct and the EBV genome within the latently infected BL cell line Akata. Briefly, p9495-BAC was digested with *Bam*HI to yield a linear DNA fragment consisting of the BAC flanked by EBV DNA on either side of the intended site of insertion within *BDLF3* (structure reported in Fig. 1 of 2009 report). This was then transfected into Akata cells by nucleofection; approximately two days post transfection the cells were placed under hygromycin B selection (HygB; resistance to this drug is encoded by the BAC) to permit outgrowth of cells that had incorporated the targeting construct. DNA was then isolated from clones of cells that were HygB^r, dsRed⁺ and analyzed by PCR to determine whether the targeting construct had correctly recombined within the *BDLF3* locus of the EBV genome in these cells. Unfortunately, very few HygB^r dsRed⁺ clones were obtained, and those we did generate did not contain the BAC within the *BDLF3* locus of the viral genome (presumably it had recombined non-specifically within the host cell genome).

Insertion of BAC via recombineering in E. coli - The most likely reason that we were unable to achieve appropriate insertion of the BAC within the EBV genome by simple homologous recombination within Akata cells was that the targeting arms, i.e., the EBV DNA on either side of the BAC, were not long enough to permit efficient recombination in these cells. Therefore, before generating a new targeting construct, we next attempted to insert the BAC into the EBV genome by “recombineering” in *E. coli*. Basically, this approach takes advantage of specific recombination systems that have been developed for this purpose in bacteria that require much smaller lengths of homology in the targeting arms (as little as 50-100 bp, though 0.5-1.0 kbp is always better). To do this, however, we had to introduce the circular EBV genome into the appropriate *E. coli* strain, along with our targeting construct. As a source of intact EBV genomes, we isolated the low-molecular-weight DNA fraction from Akata BL cells by Hirt extraction (this should be enriched for EBV DNA over the higher molecular weight DNA of the host chromosomes). This DNA was then used, along with the targeting construct, to transform the recombineering strain of *E. coli* SW105 (kindly provided by Dr. Neal Copeland, Mouse Cancer Genetics Program, NCI-Frederick). Although we tried several modifications, e.g., varying the amount of DNA used, and inducing expression of recombination proteins before or after

transformation, we were unsuccessful in achieving bacteria in which the BAC had appropriately recombined with the EBV DNA.

Generation of a new targeting construct - At this point we had no alternative but to generate a new targeting construct with which to select for homologous recombination with the endogenous EBV genome in Akata cells. The major modification is an increase in the length of each EBV targeting arm (on either side of the BAC DNA segment), from approximately 1.5-2.0 kbp to approximately 10 kbp. This should vastly increase the efficiency of homologous recombination. We are currently working on the generation of this targeting construct.

In a further attempt to increase recombination efficiency, besides introducing our new targeting construct into latently infected Akata cells, we will also employ Akata cells in which the EBV replication cycle has been induced. This may further increase the efficiency of recombination by virtue of the fact that the EBV genome is amplified approximately 1,000-fold during the replicative cycle of infection. The fact that the viral genome is more actively undergoing replication within “induced” cells may also contribute to a higher rate of recombination. This may have contributed to the excellent recombination efficiency observed in development of the EBV-BAC containing the B95-8 isolate genome of EBV by Hammerschmidt and colleagues (*Proc. Natl. Acad. Sci., USA*, 95:8245-8250, 1998). Specifically, the marmoset-derived lymphoblastoid cell line that carries the B95-8 isolate of EBV (and used in their work) is unusually permissive of EBV replication, unlike virtually all other EBV-infected B-cell lines, which tightly maintain latent infection. Even though the B95-8 cells used in the generation of the B95-8 BAC had not been treated to induce virus replication, the amount of linear EBV genomes (indicative of virus replication) present in the cells (as a consequence of spontaneous reactivation of EBV) was extremely high relative to the circular genomes (the latent infection form). (Note that because of the large deletion in the B95-8 genome, we are unable to use this EBV BAC clone, for reasons discussed in the 2009 report). Although recombination would occur most frequently within linear genomes in these cells, this apparently did not prevent efficient recovery of BAC clones of unit-length EBV genomes upon transformation of *E. coli* with DNA from Hirt extracts of the transfected B95-8 cells. While most EBV-infected B-cell lines are very resistant to the induction of EBV replication by various methods, cross-linking of surface IgG (i.e., the B cell receptor) on Akata cells is a relatively efficient method of inducing replication in this cell line, though not all cells within a culture of Akata cells respond equivalently to cross-linking. Currently, we are screening subclonal lines of Akata cells for those that can be efficiently induced to activate the EBV replicative cycle.

Extension of Project

In addition to the technical issues we have had, lack of consistent personnel effort to dedicate to this project has interfered with our progress. Since the postdoctoral trainee working on this project left prior to funding (see 2009 report), I have had to make do with my technician (15% effort supported by this grant since 08/01/09), and help from rotating first-year graduate students (3) when they were available, and working at the bench myself at times. Consequently, we have not finished the project as proposed. Although research funds (personnel and supplies) have now been completely expended as of 06/30/10, we plan to continue this work until we have been successful, as it is critical to several projects in the laboratory.

Research Project 23: Project Title and Purpose

Regulation of Mitochondrial Dysfunction and Diet-induced Obesity by ALCAT1 - Cardiolipin is an important lipid required for health and diseases. Like cholesterol, there are “good” and “bad” cardiolipins which are determined by the structure of the lipid. Increased levels of bad cardiolipin play a causative role in diabetes, obesity, hyperthyroidism, and aging. ALCAT1 is a cardiolipin synthetic enzyme recently identified in our lab. We have shown that this enzyme catalyzes the synthesis of bad cardiolipin, and its enzyme activity is elevated in diabetes and obesity. The project will validate ALCAT1 as a drug target for the treatment of diabetes and obesity using sophisticated molecular, cellular, enzymatic, and transgenic approaches.

Duration of Project

7/1/2008 - 6/30/2010

Project Overview

The long term goal is to elucidate the molecular mechanisms by which defective cardiolipin (CL) metabolism contributes to the onset of mitochondrial dysfunction and metabolic diseases from oxidative stress. CL is a key mitochondrial phospholipid required for mitochondrial oxidative phosphorylation and ATP synthesis. Like cholesterol, there is “good” and “bad” CL, which is determined by the content of linoleic acid. The side chains of a good CL are dominated by linoleic acid, and a bad CL is enriched with long chain polyunsaturated fatty acids. The ratio of good vs. bad CL is modulated by a “remodeling” process that involves deacylation by phospholipases and reacylation by lysocardiolipin acyltransferases. Defective CL remodeling in response to reactive oxygen species (ROS) leads to accumulation of bad CL and mitochondrial dysfunction which have recently been identified as common defects in metabolic diseases including diabetes, obesity, cardiovascular diseases, and aging. We have recently cloned the first acyltransferase (ALCAT1) involved in defective CL remodeling. Our preliminary data demonstrate that ALCAT1 plays a causative role in mitochondrial dysfunction and insulin resistance in response to ROS. This project will test the hypothesis that defective CL remodeling by ALCAT1 in response to oxidative stress causes mitochondrial dysfunction and exacerbates metabolic complications in diet-induced obesity. The project will be accomplished by two Aims: 1) To identify molecular defects in mitochondrial dysfunction and insulin resistance caused by ALCAT1 overexpression in C2C12 or L6 stable cell lines; and 2) To assess the physiological effects of ALCAT1 deficiency in mice on metabolic complications associated with diet-induced obesity. The project will also help to validate ALCAT1 as a novel drug target for diabetes and obesity, and thereby stimulate pharmaceutical industry interests in development of a novel treatment for metabolic diseases.

Principal Investigator

Yuguang Shi, PhD
Associate Professor
Dept. of Cellular and Molecular Physiology
Penn State College of Medicine
500 University Drive
Hershey, PA 17033

Other Participating Researchers

Caroline Romestaing, PhD, Xin Guo – employed by Pennsylvania State University

Expected Research Outcomes and Benefits

The results from specific Aim 1 will determine the role of ALCAT1 enzyme in regulating mitochondrial function and insulin sensitivity in a cell-based assay. Mitochondrial dysfunction has recently been identified at the center of metabolic diseases, including obesity, diabetes, heart diseases, hyperthyroidism, and aging. The results from Aim 1 will identify the molecular mechanism by which ALCAT1 causes mitochondrial dysfunction, which will be complementary to the results in Aim 2. The specific Aim 2 is designed to investigate the physiological role of the ALCAT1 gene in regulating the onset of diet-induced obesity and the related metabolic complications, such as diabetes and insulin resistance. A transgenic mouse line with targeted deletion of the ALCAT1 gene was recently generated in our lab. These transgenic mice provide a very good rodent model to study the potential physiological consequences of the deletion of the ALCAT1 gene. The results from Aim 2 will provide key information on how ALCAT1 deficiency affects the onset of diet-induced obesity. The work is highly significant, since consumption of a Western diet enriched with animal fat has been identified as one of the major contributors to the ongoing obesity epidemic in the United States. Specifically, we will be measuring the impact of ALCAT1 gene deletion on food intake, energy expenditure, body fat composition, and insulin sensitivity. Taken together, the proposed work will validate ALCAT1 as a drug target for diabetes and obesity. The results will also provide guidance and proof of principle studies on whether pharmaceutical inhibition of ALCAT1 enzyme will provide a novel treatment for diabetes and obesity. The results also will guide future studies in identifying a causative role of ALCAT1 in heart diseases and aging.

Summary of Research Completed

Major progress with our unused funds has been made in the past twelve months toward achieving goals set in the research aims of our grant, “*Regulation of Mitochondrial Dysfunction and Diet-induced Obesity by ALCAT1.*” We have generated some very exciting data in delineating the cellular function of ALCAT1 enzyme and its physiological role in regulating the onset diet-induced obesity and its related metabolic complications in ALCAT1 knockout mice as summarized below. Our new data extended the scope of our preliminary data and provided strong support of our central hypothesis that cardiolipin remodeling by ALCAT1 plays a key in regulating mitochondrial dysfunction and metabolic complications associated with diet-induced

obesity. Part of the results was recently submitted to *Cell Metabolism* for consideration of publication.

The Specific Aim 1 *To identify molecular defects in mitochondrial dysfunction and insulin resistance caused by ALCAT1 overexpression in C2C12 or H9c2 stable cell lines.* To analyze the effect of ALCAT1 on mitochondrial activity in metabolically active cell lines, we have recently generated H9c2 cells stably transfected with plasmids that overexpress the ALCAT1 cDNA or an empty expression vector (negative control) by plasmid transfection. The H9c2 cells are derived from mouse cardiomyoblasts commonly used to investigate mitochondrial function and insulin receptor-mediated signal transduction pathway. Using the stable cell lines, we analyzed changes in mitochondrial function and insulin receptor mediated signal transduction pathway. Our results showed that overexpression of ALCAT1 caused mitochondrial dysfunction and insulin resistance in H9c2 cells stably transfected with ALCAT1 expression vector, similar to the defects we have previously shown in C2C12 cells, further confirming a causative role of ALCAT1 in mitochondrial dysfunction and insulin resistance.

Our preliminary data showed that overexpression of ALCAT1 caused a defect in complex I activity as demonstrated by a significant increase in oxygen consumption stimulated by glutamate/malate, but not succinate/malate. The results also demonstrated a significant leak in mitochondrial membrane of C2C12 cells overexpressing ALCAT1, as suggested by a higher level of oxygen consumption rate in the presence of oligomycin in C2C12 cells stably transfected with ALCAT1 relative to the vector control. To provide further evidence for a causative role of ALCAT1 in oxidative stress, we recently analyzed the expression of genes involved in ROS production and oxidative response by real-time RT-PCR analysis. Our results showed that ALCAT1 overexpression significantly increased expression of genes that cause oxidative stress, such as NAD(P)H quinone oxidoreductase 1 (Nqo1) and NADPH oxidase 4 (Nox4), and decreased expression of a whole spectrum of genes encoding antioxidative enzymes, including glutathione peroxidases (Gpx), peroxiredoxin (Prdx), thioredoxin reductases (Txnrd), and superoxide dismutases (Sod) in C2C12 cells. The Nqo1 enzyme is essential for oxidative stress in mice and humans, and Nqo1 deficiency suppresses ROS production induced by hypoxia. Nox4 is an NAD(P)H oxidase homolog that stimulates the production of ROS in insulin sensitive tissues, and its expression was up-regulated by more than 29 fold by ALCAT1 overexpression in C2C12 cells. Furthermore, the mRNA expression of Ucp3 was elevated by more than three folds, which is consistent with the increased state 4 respiration caused by ALCAT1 overexpression. As a compensatory response to the increased levels of uncoupling respiration and ROS production, ALCAT1 overexpression significantly increases glycolytic activity in C2C12 cells as evidenced by significantly higher acidification rate of the culture medium analyzed by the XF-24 analyzer. In the coming year, we plan to further dissect molecular mechanisms underlying a defect in mitochondrial complex I activity using the C2C12 stable cell lines.

The Specific Aim 2 *To assess the physiological effects of ALCAT1 deficiency in mice on metabolic complications associated with diet-induced obesity.* Using the ALCAT1 knockout mice in 98% C57/Bl6 genetic background, we continued our preliminary studies on phenotypic characterization of ALCAT1 knockout mice to identify metabolic changes caused by ALCAT1 deficiency. We repeated our preliminary studies on the effect of ALCAT1 deficiency on the onset of diet-induced obesity using a large cohort of ALCAT1 knockout mice, and demonstrated

that ALCAT1 knockout mice were resistant to the onset of diet-induced obesity. We also investigated changes in metabolic complications commonly associated with diet-induced obesity in ALCAT1 knockout mice after 10 weeks of high fat feeding. Our results showed that the ALCAT1 knockout mice were also resistant to metabolic complications associated with diet-induced obesity, as demonstrated by glucose and insulin tolerance test. In contrast to the wild type control mice, the ALCAT1 knockout mice exhibited an improvement in glucose tolerance as a result of improved insulin sensitivity, as evidenced by hypersensitivity to insulin-induced hypoglycemia during insulin tolerance test. To determine the mechanisms accounting for the resistance to diet-induced obesity in ALCAT1 knockout mice, we have recently analyzed changes in food intake, water intake, physical activity, and energy expenditure in the male ALCAT1 knockout mice relative to the wild type control mice during 72 hours by housing the mice in metabolic cages which can monitor water intake, food intake, oxygen consumption, CO₂ production, and physical activity. Our results showed ALCAT1 knockout mice exhibited hyperphagia, hyperactivity, and hypermetabolism. In contrast to wild type control mice, the ALCAT1^{-/-} mice consumed 62.00% more food and 73.38% more water, respectively, per kg of body weight than wild type controls during the 24 hour period. The ALCAT1 knockout mice were also hyperactive, as evidenced by enhanced physical activity relative to the wild type control mice. Consequently, the energy expenditure rate was significantly higher in ALCAT1 knockout mice. This is caused by higher metabolic rate, as evidenced by the increased oxygen consumption rate. Furthermore, the respiratory exchange ratio (RER) during the 24 hour period was significantly elevated in the ALCAT1 knockout mice as compared with the wild type control mice, suggesting that the null mice burned more carbohydrate as a fuel.

To identify molecular mechanisms underlying metabolic phenotype of the ALCAT1 knockout mice, we next analyzed the effects of ALCAT1 deficiency and overexpression on mitochondrial fatty acid oxidation. Impairment of fatty acid oxidation is a contributing factor to insulin resistance in human obesity and type 2 diabetes. Using C2C12 cells stably overexpressing ALCAT1, we demonstrated that ALCAT1 overexpression significantly decreased the fatty acid oxidation rate, which is consistent with mitochondrial dysfunction and insulin resistance observed in the cell lines. Consistent with improved insulin sensitivity in ALCAT1 knockout mice, isolated liver mitochondria from the ALCAT1 knockout mice oxidized fatty acids faster than mitochondria from the control mice on a high-fat diet. Furthermore, the expression of SCD-1, a major hepatic enzyme involved in the synthesis of triglyceride, was significantly down-regulated in the liver of ALCAT1 knockout mice and up-regulated in C2C12 cells overexpressing ALCAT1. In the coming year, with other funds we are going to analyze the effect of ALCAT1 deficiency insulin receptor mediated signal transduction pathways in liver, skeletal muscle, and adipose tissues as outlined in our grant application, including changes in phosphorylation of Akt, JNK, and IRS proteins in response to insulin stimulation in ALCAT1 knockout mice.

Research Project 24: Project Title and Purpose

Novel Pathway Mediating Peripheral Sensitization of Esophageal Vagal Sensory Afferent Nerves
Abnormal esophageal sensations, such as esophageal-related noncardiac chest pain and heartburn, are common complaints. They are generated from noxious stimuli on esophageal sensory afferent nerves and transmitted to the central nervous system via both spinal and vagal

pathways. Esophageal inflammation sensitizes sensory afferents and enhances these abnormal sensations to induce visceral hypersensitivity. This involves both peripheral and central sensitization. The mechanism of peripheral sensitization of esophageal sensory afferents is still unclear. The long-term goal of our research is to study the mechanism of peripheral sensitization in a validated esophageal hypersensitivity model. This project focuses on peripheral sensitization of vagal sensory afferents in our guinea-pig *ex vivo* esophageal-vagal preparation.

Duration of Project

7/1/2008 - 6/30/2009

Summary of Research Completed

This project ended during a prior state fiscal year. For additional information, please refer to the Commonwealth Universal Research Enhancement Annual C.U.R.E. Reports on the Department's Tobacco Settlement/Act 77 web page at <http://www.health.state.pa.us/cure>.

Research Project 25: Project Title and Purpose

The Role of Microglial Priming in Diabetic Retinopathy - The purpose of this project is to conduct preliminary experiments to test the hypothesis that a systemic inflammatory event will couple with diabetes to cause a pronounced increase in retinal inflammation. We will use animal models to determine if infection or inflammation in other parts of the body may cause excessive inflammation in the diabetic retina. If so, this response may explain why some diabetic patients suffer from extreme retinal damage, while others do not. We will also determine if microglial cells in the diabetic retina are the initiators of this hyper-response. If so, then treatments that control microglial behavior may be useful for preventing the progression of diabetic retinopathy.

Duration of Project

11/24/2008 - 12/31/2009

Project Overview

Previous studies have demonstrated morphological and antigenic signs of microglial cell activation in diabetic retinas. Drawing an analogy to other neurodegenerative diseases, we hypothesize that diabetes primes microglial cells in the retina to be hyper-responsive to systemic inflammation, predisposing them to a maladaptive, pro-inflammatory and destructive response. Thus, we predict that a mild systemic inflammatory event will cause exaggerated expression of inflammatory genes in the diabetic retina that greatly exceeds the response observed in normal retina, and that this will coincide with complete microglial activation to a pro-inflammatory phenotype.

Specific Aim 1: To examine the effect of diabetes on the activation state of rat retinal microglia. Hypothesis: Diabetes causes retinal microglia to become partially activated, exhibiting morphologic and antigenic changes in the absence of pro-inflammatory gene expression.

Experiments will determine if diabetes causes rat retinal microglia to adopt a phenotype consistent with a non-inflammatory, but primed activation state. This state will be characterized by decreased ramification, increased expression of a surface antigen characteristic of microglial activation, a lack of expression of pro-inflammatory genes, and increased expression of an anti-inflammatory cytokine.

Specific Aim 2: To examine the combined effects of diabetes and systemic inflammation on inflammatory gene expression in the whole retina and retinal microglia.

Hypothesis: Microglia within diabetic retinas are hyper-reactive, causing an exaggerated pro-inflammatory response to systemic inflammation.

Experiments will determine if a mild acute systemic inflammatory challenge, modeled by peripheral treatment with bacterial lipopolysaccharide (LPS), causes a synergistic increase in inflammatory gene expression in retinas of diabetic rats that exceeds the combined effects of diabetes and systemic inflammation alone. Further experiments will determine if this response coincides with pronounced expression of pro-inflammatory genes by retinal microglia. These novel studies, if successful, will identify an important paradigm in diabetes retinopathy (DR) suggesting future examinations of the impact of systemic inflammation on retinal neuronal apoptosis and vascular permeability, as well as novel epidemiological studies and new treatment modalities to prevent progression to severe DR and therefore avoid vision loss.

Principal Investigator

Steven F. Abcouwer, PhD
Associate Professor
Penn State University College of Medicine
Milton S. Hershey Medical Center
P.O. Box 850, Surgery/H051
Hershey, PA 17033-0850

Other Participating Researchers

Thomas W. Gardener, MD, Ann Benko, PhD, Christopher Norbury, PhD – employed by Penn State University College of Medicine

Expected Research Outcomes and Benefits

The ultimate goal of this research project is to better understand the mechanism leading to loss of sight in diabetic patients, so that this can be prevented. Numerous studies have demonstrated that within 20 years of diagnosis over 90% of diabetic patients will demonstrate some degree of diabetic retinopathy (DR), as evidenced by visible changes in their retinas. However, a lower fraction of these patients, 40% of Type 1 diabetic patients and 5-10% of Type 2 diabetic patients, develop severe DR characterized by appreciable vision loss. Little has been done to investigate why most diabetes patients exhibit signs of DR while only a fraction progress to severe sight-threatening DR. We hypothesize that systemic inflammatory events, occurring outside the retina, contribute to DR progression and that a process called microglial priming is key to this phenomenon. This project will use an animal model to test these hypotheses. If successful, these

studies will provide the first evidence that this mechanism can contribute to changes in the diabetic retina. This data will help provide a rationale for clinical examinations of the correlation between systemic inflammation and DR progression. Ultimately, this project may provide a means to preserve the sight of patients with initial signs of DR by providing aggressive treatment of infection and inflammation or by therapeutic targeting of retinal microglial cells to prevent their hyper-reaction to systemic inflammation.

Summary of Research Completed

Since the last report, we have completed the following tasks and preliminary experiments:

- Developed methods to examine the activation state of rat retinal microglia by flow cytometry
- Examined the retinal microglial response to ischemia and reperfusion injury (an acute model exploited to work our experimental procedures) and to diabetes

Flow cytometric analysis of microglial activation was utilized to quantitatively study microgliosis in a streptozotocin (STZ)-induced diabetic rat model of DR and a rat ischemia-reperfusion (IR) model of acute retinal damage. Retinas were enzymatically dissociated and analyzed for expression of the monocytic markers CD11b and CD45, MHC class II antigen, and granularity by flow cytometry. Retinal microglia were identified as CD11b positive and CD45 low ($CD11b^+/CD45^{low}$) expressing cells and invading macrophage cells were identified as $CD11b^+/CD45^{high}$ expressing cells. Granularity has been shown to be indicative of phagocytic activity and MHC class II is indicative of progression to an antigen-presenting phenotype. Ischemia Reperfusion (IR) injury produced a marked increase in CD45 expression of $CD11b^+/CD45^{low}$ microglia, indicative of their activation. IR also caused an increase in the number of $CD11b^+/CD45^{high}$ macrophage cells in the retina. MHC class II expression and granularity increased in microglia following IR, suggesting increased phagocytic activity. Retinal microglia in rats experiencing 6 weeks of diabetes exhibited qualitatively similar, but lesser, increases in CD45 expression, MHC class II expression and granularity.

Flow cytometric analysis allowed the direct quantitative measurement of retinal microgliosis and macrophage infiltration. DR caused less microgliosis and macrophage infiltration than did IR, in keeping with the diminished rate of neurodegeneration in the chronic diabetic condition compared to the pronounced acute neurodegeneration caused by ischemia.

Figures of Results:

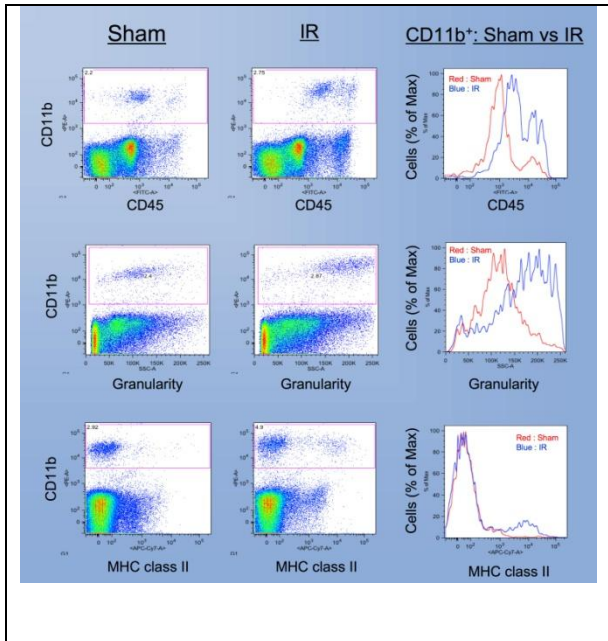


FIGURE 1: Retinal IR causes microgliosis with some infiltration of monocytic cells. Representative plots of flow cytometric analysis of retinal cells assayed for expression of the monocytic markers CD11b and CD45, side scatter of the excitation laser light (a measure of granularity) and MHC class II expression (a measure of activation to an antigen presenting phenotype). In the anesthetized animal, one eye was subjected to retinal ischemia for 45 min and reperfused for 48 h until termination of the animal. The contralateral eye was subjected to needle puncture and served as sham control. Histogram plots are a direct comparison of cells gated for positive expression of CD11b. Increased numbers of CD11b⁺/CD45^{high} cells suggest an infiltration of circulating macrophages into retinal tissue.

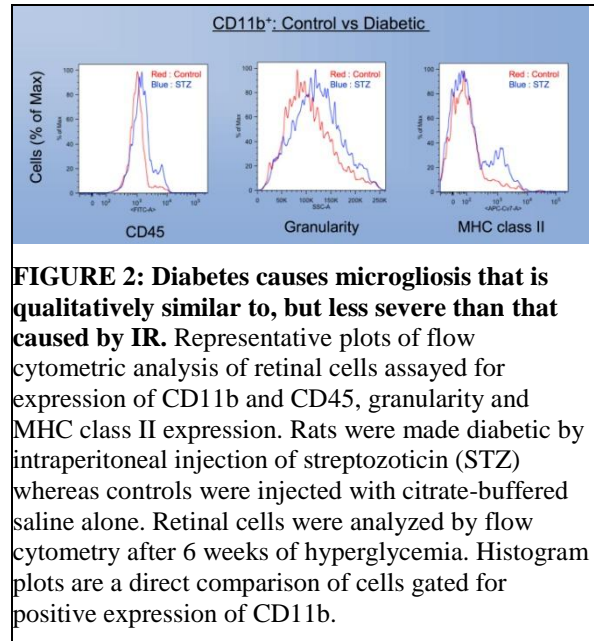


FIGURE 2: Diabetes causes microgliosis that is qualitatively similar to, but less severe than that caused by IR. Representative plots of flow cytometric analysis of retinal cells assayed for expression of CD11b and CD45, granularity and MHC class II expression. Rats were made diabetic by intraperitoneal injection of streptozotocin (STZ) whereas controls were injected with citrate-buffered saline alone. Retinal cells were analyzed by flow cytometry after 6 weeks of hyperglycemia. Histogram plots are a direct comparison of cells gated for positive expression of CD11b.

Research Project 26: Project Title and Purpose

Gag and CA Protein Interactions in Retroviral Capsid Maturation - This project examines the molecular mechanism by which the internal structure of infectious retrovirus particles, such as that of HIV, is formed during the process of virus release from the infected cells. Specifically, this work will test the novel hypothesis that a critical step in the virus assembly pathway is an interaction of the mature capsid protein CA with one or more molecules of its precursor protein Gag. This hypothesis will be tested with proteins derived from both the avian Rous sarcoma virus and HIV. By documenting the molecular mechanisms involved in detail, this project will provide critical insights that may be utilized for the development of new anti-retroviral drugs.

Duration of Project

11/24/2008 - 6/30/2010

Project Overview

Maturation inhibitors are a class of antiretroviral drugs that are showing great promise as a new approach to controlling HIV/AIDS. However, the development of such drugs is hampered by a lack of understanding of the underlying mechanisms of virus maturation. This project addresses the novel hypothesis that formation of the capsid structure in the core of a maturing retroviral particle is initiated by an interaction between the capsid protein CA and one or more molecules of either the viral Gag protein (precursor to CA) or cleavage intermediates of Gag. To test this hypothesis we will take the following approaches.

1. Characterize the interaction between the Rous sarcoma virus proteins CA and its immature form CA-SP in the assembly of capsid-like structures in vitro.
2. Determine the effects Gag and truncated Gag proteins of RSV and HIV on capsid assembly.
3. Initiate NMR studies that will assess the structural effects of SP on the CA protein

Principal Investigator

Rebecca C. Craven, PhD
Associate Professor
Penn State University College of Medicine
Room C6714
Dept. of Microbiology and Immunology
500 University Drive
Hershey, PA 17033

Other Participating Researchers

Leslie J. Parent, MD, John G. Purdy, Drs. Jyh Ming Lin, Ira Ropson, and Maria Bewley – employed by Penn State College of Medicine

Expected Research Outcomes and Benefits

In the human immunodeficiency virus (HIV), as well as the many other human and animal retroviruses, the core of the virus particle is the structure that carries out replication of the viral genome by the process known as reverse transcription. The successful conversion of the viral RNA genome into a DNA copy early in infection of a cell allows development of a persistent disease that will last for the lifetime of the individual. Antiviral drugs are available that interfere with this process and prevent the spread of infection within an individual and between individuals. However, drug side-effects and the development of viral resistance continue to limit their success in controlling the spread of HIV. The development of new approaches to antiviral therapy will give clinicians additional tools to better tailor the combination therapy for individual patients with the hope of improved success rates. For this reason, vigorous efforts to identify novel molecular targets for drug development are a priority in the virology research community.

The development of drugs that can target and block the function of the structural proteins in building the viral core is in the early stages but prospects look quite promising. Unfortunately,

our basic understanding of the molecular mechanisms of viral core formation is very limited. We will use a combination of genetic and biochemical methods to dissect the events of core assembly. It is expected that improvements in our understanding of these essential events in virus replication will stimulate the development of additional and better inhibitors of retrovirus replication for use in the treatment of AIDS and other human retroviral diseases.

Summary of Research Completed

The spacer peptide SP, located C-terminal to the capsid protein CA in the polyprotein precursor Gag, exists transiently in the maturing virus particle as a CA-SP cleavage intermediate. Previous research in the Craven laboratory has suggested that SP peptide exerts important regulatory activity on the formation of a functional capsid during maturation. The goal of this project is to characterize in vitro the influence of SP on the assembly of CA-SP, comparing it to the well-studied mature CA protein, and to test the hypothesis that SP sequence in the precursor Gag can interact with mature CA or the CA-SP cleavage intermediate to facilitate capsid formation. The experiments reported one year ago demonstrated that the purified CA-SP protein is capable of very robust assembly. Compared to the mature form of the capsid protein, the immature CA-SP is capable of assembling at lower protein concentrations and the reaction proceeds much more rapidly under standard conditions. Furthermore, the CA-SP intermediate is able to stimulate the assembly of mature CA in a mixed reaction. Progress that has been made on this project during the past year is outlined below.

Specific Aim 1. Analysis of the interaction between CA-SP and CA in capsid assembly.

1a. Co-assembly of CA and CA-SP.

The difference in assembly kinetics of CA and CA-SP in single protein reactions reported last year suggests that there is a significant difference in the rate limiting step (i.e., the nucleation) of assembly. We have now corroborated with two additional findings. Figure 1 demonstrates that the CA-SP protein, unlike CA, is capable of at least limited assembly in the presence of sodium chloride (rather than sodium phosphate) suggesting that presence of the SP partially relieves the dependence upon charge shielding provided by the multivalent anion phosphate as described for CA. In a separate experiment (1B), the ability of CA-SP to nucleate assembly of CA in a mixed reaction was tested. Purified CA or CA-SP protein were pre-incubated separately with sodium phosphate, then the pre-treated protein was used to spike a standard CA assembly reaction. The results in Figure 2 show that CA-SP, after a short preincubation with sodium phosphate, is able to accelerate the assembly of CA protein in a mixed reaction and that this ability is considerably greater than that caused by CA treated in the identical manner. As expected, both pre-treatments accelerated assembly over that seen in a reaction that was not pre-treated with salt (sodium phosphate). This finding is consistent with an action of the SP at the nucleation step.

During the past year we have begun to use biophysical approaches to compare the CA and CA-SP proteins to identify any structural differences that may explain the results above. To test the possibility that the SP peptide (at the end of CA-SP) alters the stability or protein folding behavior of the protein, circular dichroism spectroscopy was used to follow the equilibrium denaturation in guanidinium HCl (gdn-HCl). The CD spectra of untreated proteins were identical, indicating that there are no major differences in the alpha-helical content caused by the SP peptide (not shown). Likewise, the CD spectra for completely unfolded CA and CA-SP were

also indistinguishable (not shown). Figure 3 illustrates the denaturation response of the two proteins to increasing concentrations of gdn-HCl, monitored by ellipticity at 220 nm; CA and CA-SP are indistinguishable indicating no significant difference in protein stability. Preliminary nuclear magnetic resonance (NMR) experiments that will allow us to use NMR to assess influence of the SP on protein structure at a higher resolution are described below.

1b. Electron microscopy. EM analyses of assembled CA, CA-S and CA-SP proteins, as well as mixtures of proteins, have been repeated to obtain higher quality images and to test alternative methodologies for EM grid preparation. The improved images we are obtaining now (not shown) will allow better discrimination of the different classes of particles formed by CA-SP *in vitro*. This will in turn enable us to pursue reconstruction of the particles from negative-stained specimens. As a complementary approach, high resolution imaging of the CA-SP particles by cryo-electron microscopy is also being pursued, as of this writing, in collaboration with the laboratory of Dr. Alasdair Steven (National Institutes of Health, NIAMS, Bethesda MD).

1c. Effects of SP mutations on assembly ability of CA-SP. Cloning vectors for expression of various mutant forms of CA-SP were created during the first year of this project. Testing of the mutant proteins is underway. A D52A substitution in the N-terminal domain of the CA protein interferes with formation of normal intersubunit interactions needed for capsid maturation (previously published, Purdy et al. 2008). In the context of CA-SP, however, the D52A mutation had no effect on assembly that could be detected by turbidimetric analysis (Figure 4). The effects of an S241L substitution in the SP region is described in section 1d below. The evaluation of additional substitutions within SP has been delayed briefly, pending the results of cryo-EM analysis of CA-SP particles (mentioned above). The assessment of the cryoEM data, in consultation with Dr. Maria Bewley, will allow us to choose the most informative mutations to be tested for their effects on CA-SP, rather than the shotgun approach originally proposed.

1d. Can a nucleation defect in CA be rescued by a compensating mutation in CA-SP?

Two previously published studies from the Craven lab suggest that an S241L substitution in SP that was identified in a spontaneous revertant virus corrects the lethality of a F167Y mutation in the CA CTD by restoring normal capsid nucleation in the maturing virus (JB Bowzard et al. J. Virol. 75:6850, 2001; JG Purdy et al. 82:5951, 2008). We set up an *in vitro* assembly experiment to test the prediction that F167Y and S241L would exert opposing effect on behavior of purified CA protein. First, a virus growth experiment was performed to confirm the previous virus replication data and, more importantly, to assess the strength of suppression of the F167Y growth defect *in vivo* in a more quantitative fashion than we had used previously (Figure 5A). The spread of a GFP-expressing virus through a culture of transformed chicken cells (DF-1 cells) was followed by flow cytometry to measure the fraction of cells expressing GFP. The rate of spread was calculated over the period of exponential growth. The double mutant F167Y/S241L spread at a rate equal to 32.5% of that of the wild-type virus, compared to 4.8% for the F167Y single mutant, confirming a previous work. This effect is slight compared to other previously described compensatory mutations from this lab. Next, purified proteins bearing the single or double mutations were tested in the *in vitro* assembly reaction, monitored by turbidity at 450 nm (Figure 5B). As has been described for CA protein, the F167Y mutation crippled the assembly ability of CA-SP. Addition of the second mutation S241L further impaired the assembly reaction, in contrast to its stimulation of infectivity in the virus. This suggests the S241L

suppressor acts through a different mechanism than previously described suppressors of F167Y.

*Specific Aim 2. Effects of Gag and truncated Gag proteins on capsid assembly in vitro.
2a and 2b. Effects of Gag and RNA on the in vitro assembly of the CA and CA-SP proteins.*

The ability of Gag protein (with or without RNA) to nucleate the assembly of CA in vitro was tested. Gag was preincubated for 15 min with RNA (an RNA fragment containing the RNA packaging signal of the RSV genome) under conditions that would favor their association. Then the Gag protein (with or without RNA) was added to a capsid assembly reaction containing CA, CA-SP or a combination of the two in CA assembly buffer. Assembly of higher order structures was followed by turbidity at 450 nm. Neither Gag, nor RNA, nor the combination exerted any effect on CA assembly, either stimulatory or inhibitory (Figure 6A). Thus, the experiment failed to support our hypothesis that the Gag protein can nucleate assembly of the mature CA. In clear contrast, however, CA-SP assembly and CA/CA-SP co-assembly were both sensitive to the addition of Gag (with or without RNA) – generally showing greatly slowed kinetics together with reduced total light scattering (6B and C). These findings are consistent with a scenario in which Gag competes with CA-SP for self-assembly and suggests that the CA-SP intermediate maintains the protein interaction capabilities of the CA-SP region of Gag. Further characterization of any complexes of Gag + CA-SP forming under these conditions will require additional methodologies and is beyond the scope of this project.

Specific Aim 3. NMR studies of RSV C-SP.

The results above are consistent with a role of SP in regulating assembly ability. We would expect that the strong effect of SP on assembly will prove to be due to either effects of the peptide on structural features or dynamics of the protein or on its ability to form intermolecular interfaces. In an extension of the characterization of CA-SP and its assembly ability, in August 2009 we were awarded a supplement to support the initiation of nuclear magnetic resonance spectroscopy (NMR) studies of the CA-SP protein. During the past year, with the help of Drs. Jyh Ming Lin and Ira Ropson, Dept of Biochemistry and Molecular Biology, we have begun this work. NMR data sets for ¹³C-¹⁵N labeled full-length CA protein have been collected. Figure 7A presents the 2D analysis of proton and nitrogen chemical shifts in the amide fingerprint region for the full-length CA protein. Assignments of residues in the full-length CA protein are nearly complete (~95%). As a check on the quality of the data, we next compared the spectrum of the full-length protein with that of the isolated C-terminal domain which we have previously obtained. The composite chemical shift index is plotted in Figure 7B for each residue in the CTD (residues 155- 235) and the upstream interdomain linker region. Residues with a high relative chemical shift index (potentially indicative of structural differences between the two proteins) are clustered at the N-terminal end of the CTD suggesting that structure in this region is strongly influenced by the NTD in the full-length protein, consistent with established structural models. We are now ready to extend this work by comparing the spectra of full-length CA and CA-SP proteins to identify regions whose structural properties are influenced by the presence of the SP. These studies will provide preliminary data for a new NIH proposal to be submitted in October 2010 or February 2011.

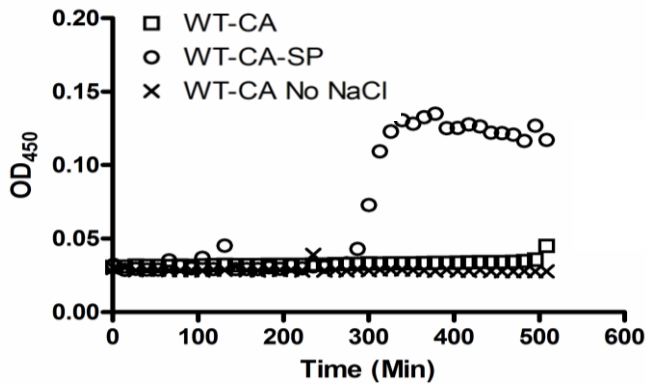


Figure 1. Turbidimetric assay shows greater ability of CA-SP to self-associate upon mixing with NaCl.

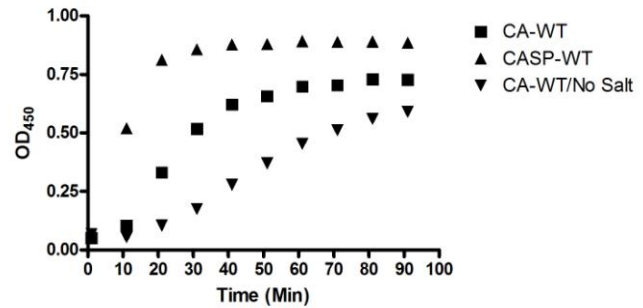


Figure 2. Pre-incubation of CA-SP stimulates of CA assembly consistent with enhanced nucleation. CA-WT/no salt = no pre-incubation.

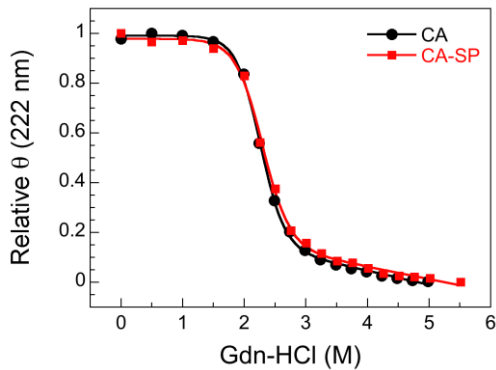


Figure 3. Analysis of protein unfolding in the presence of guanidinium hydrochloride under equilibrium conditions shows no difference in protein stability between CA and CA-SP.

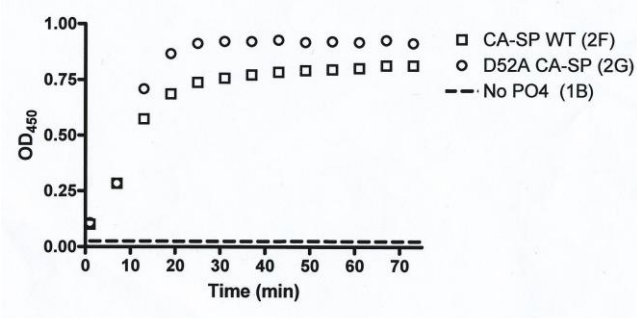


Figure 4. D52A mutation in CA-SP does not compromise assembly measured by turbidity.

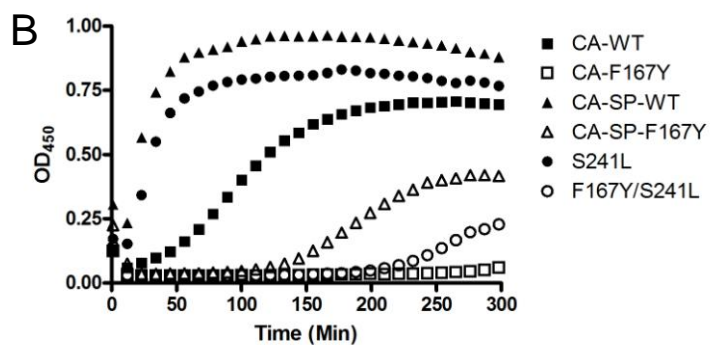
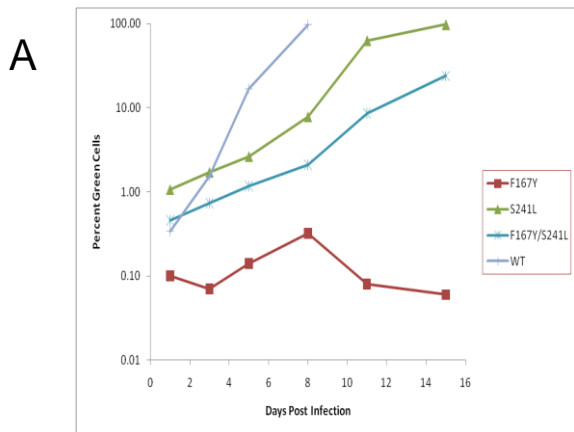


Figure 5. The S241L mutation in the SP region can partially correct a replication defect in virus bearing the lethal F167Y mutation (A) but does not correct the in vitro assembly defect (B).

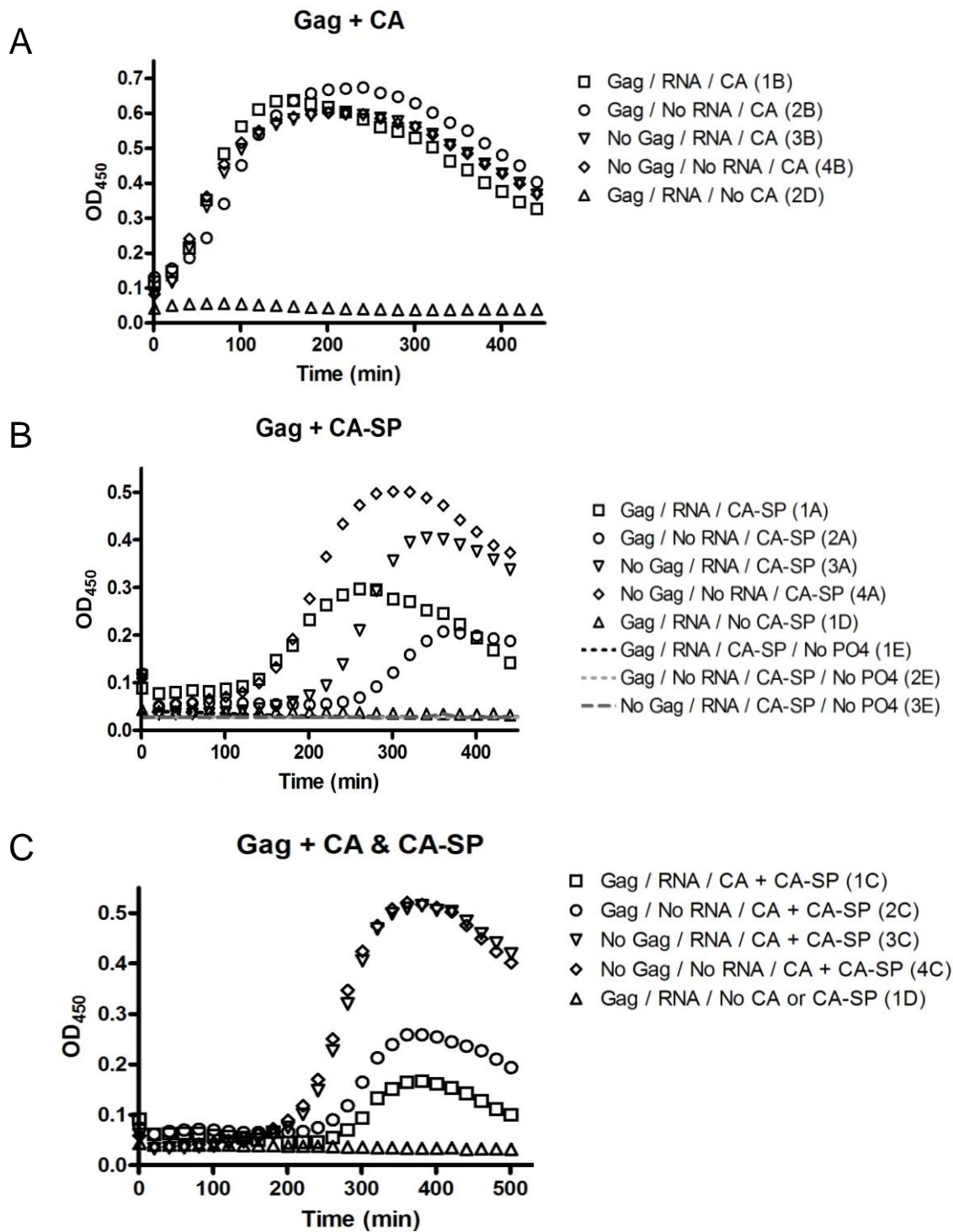


Figure 6. Influence of Gag protein on the assembly of CA and CA-SP measured by turbidity.

A. CA protein is assembled in the presence of Gag. B. CA-SP is assembled in the presence of Gag. C. The influence of Gag on the co-assembly of CA and CA-SP is monitored.

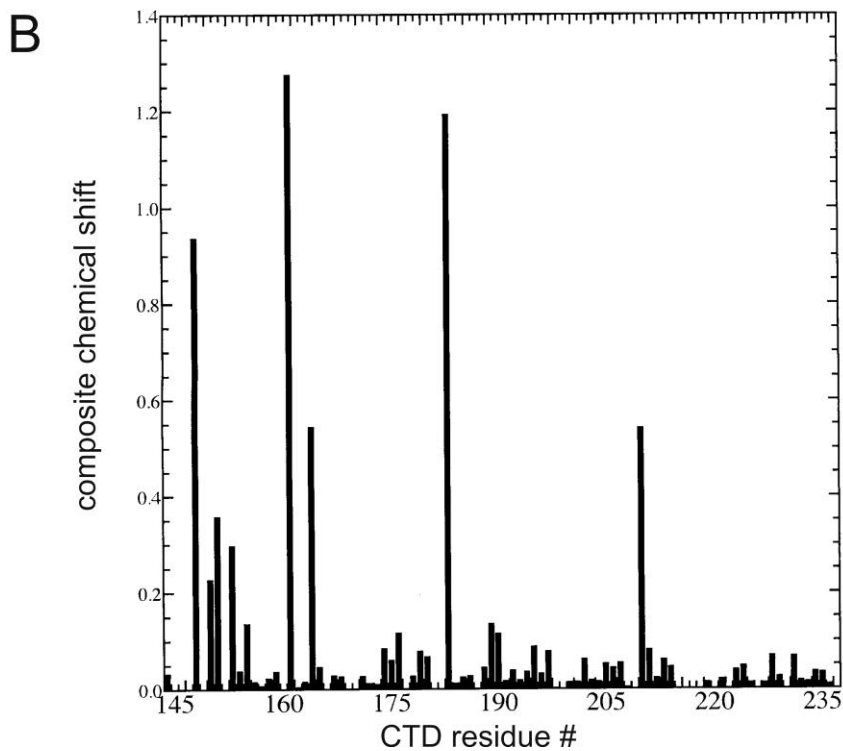
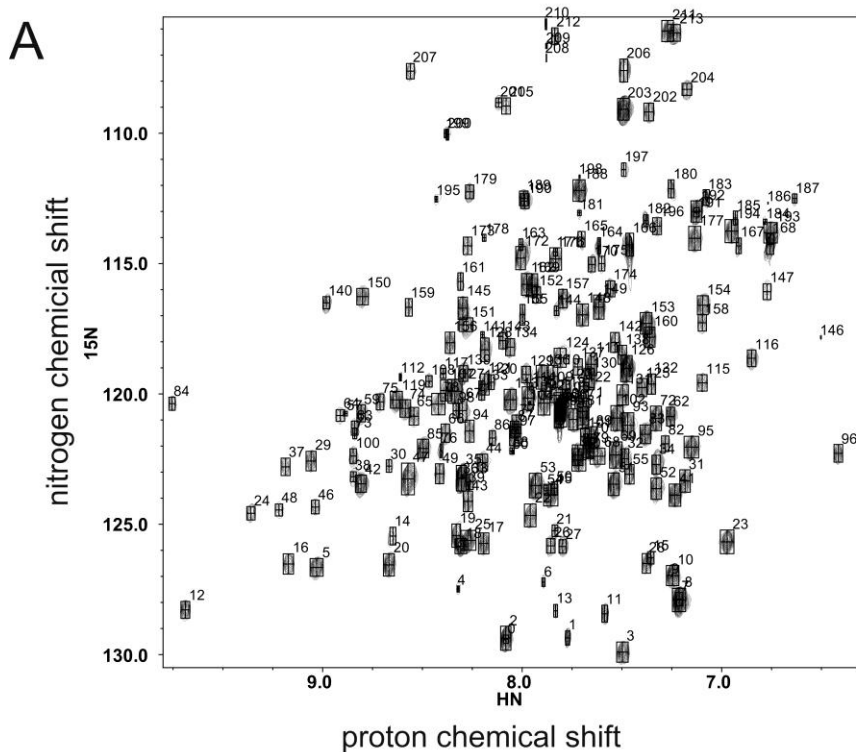


Figure 7. NMR analysis of full-length CA protein.
 A. The 2D spectrum of CA protein in the amide fingerprint region. Residue assignments are indicated. B. The composite chemical shift index for each residue in the CTD and upstream interdomain linker region is shown.

Research Project 27: Project Title and Purpose

The Effects of Air Quality on Human Reproduction - Air quality has been identified as a significant risk factor for respiratory and cardiovascular disease and for a variety of cancers. It is likely, based on preliminary data from this project that air quality also adversely affects human reproduction. We will use the model of assisted reproductive technology, i.e., in vitro fertilization (IVF) for our study. This paradigm allows us to determine exact dates of oocyte development, ovulation (i.e., the day of oocyte retrieval), fertilization, implantation, and duration of pregnancy, which allow for more accurate correlation of outcomes with ambient air quality. Our primary goal is to establish the relationship between air quality at the home zip code of the subject or in the IVF lab and fertility outcomes after IVF. Our long range objective of this study is to design a randomized trial to improve air quality both in the lab and in the IVF subject's external environment to improve reproductive outcomes.

Duration of Project

11/24/2008 - 6/30/2010

Project Overview

The specific aims of our project are to explore the effects of air quality on reproductive outcomes resulting from assisted reproductive technology (in vitro fertilization or IVF). This involves a unique collaboration between reproductive endocrinologists, an environmental epidemiologist, and a geographer. We will apply existing tools of air quality research (i.e., using measurements of ambient air pollution from the network of air quality monitors maintained by US Environmental Protection Agency (EPA), the Aerometric Information Retrieval Systems (AIRS), and interpolation using the Geographic Information System (GIS). These methods are increasingly popular for estimation of geocoded location-specific ambient air pollutant concentration, and were originally developed for the study of human diseases (cardiovascular and pulmonary), but we will now apply them for the first time to a population of subfertile couples. This vulnerable population is perhaps more likely to suffer the effects of poor air quality, and the IVF model allows us to precisely determine air quality exposure during key reproductive events (i.e., ovulation, fertilization, and implantation). We will initially examine archived data of reproductive outcomes from three IVF centers.

Specific Aim 1: To apply the currently established GIS-based methods and use the existing air pollutants data from EPA's network of air quality monitors to estimate air qualities that our study participants were most likely exposed to during the IVF-process. This objective will enable us to obtain the estimation of five criteria pollutants, including PM10, PM2.5, So2, No2, O3, and Co. for our current cohort of over 7,000 women who have undergone IVF procedures.

Specific Aim 2: To systematically investigate the associations between the above exposure matrix of each pollutant and the following IVF procedure outcomes.

Principal Investigator

Richard S. Legro, MD
Professor of Obstetrics and Gynecology
Penn State College of Medicine
Department of Obstetrics and Gynecology, H103, RM C3604
500 University Drive
Hershey, PA, 17033

Other Participating Researchers

Duanping Liao, PhD, William C. Dodson, MD – employed by Penn State College of Medicine

Expected Research Outcomes and Benefits

If air quality plays a role, however small, in assisted reproduction, as our preliminary data suggests, then there is tremendous opportunity to develop predictive models for success incorporating ambient air quality, and ultimately develop a clinical intervention such as improved air filtration in the IVF lab or a face mask worn by the participant during periods of decreased ambient air quality while undergoing IVF treatment and to test these interventions in well-designed prospective clinical trials. The findings from our study will also hold implications for unassisted spontaneous reproduction in the larger population especially in developing countries, but we have chosen the IVF model because it allows for more precise calculations of exposure to air quality during the key moments of the reproductive cycle.

Summary of Research Completed

Enrollment Data:

We have enrolled 7403 females who have undergone IVF for this study.

We have successfully achieved both aims listed below and a summary follows of each. The full details can be found in the published manuscript listed below.

Specific Aim 1: To apply the currently established GIS-based methods and use the existing air pollutants data from EPA's network of air quality monitors to estimate air qualities that our study participants were most likely exposed to during the IVF-process. This objective will enable us to obtain the estimation of five criteria pollutants, including PM10, PM2.5, So2, No2, O3, and Co. for our current cohort of over 7,000 women who have undergone IVF procedures.

Specific Aim 2: To systematically investigate the associations between the above exposure matrix of each pollutant and the following IVF procedure outcomes.

Specific Aim 1: Home and IVF Clinic Site Geocodes Patient home zip codes were obtained, and the coordinates (latitudes; longitudes) of the centroid of each zip code were assigned according to the U.S. Census 2000 Federal Information Processing Standards (U.S. Census Bureau, 2008). The coordinates of IVF clinical centers were geocoded using ArcView (Redlands, CA).

Air Pollutant Concentrations: All ambient criteria air pollutant concentration data recorded at monitors operating in the contiguous U.S. during the study period (2000-2007) were obtained from the U.S. Environmental Protection Agency Air Quality System (Air Quality System, 2007). The data included the longitude and latitude of each monitor. The data were cleaned and then used to fit national scale, log-normal kriging with a spherical model for spatial interpolations to produce geocoded location-specific daily mean concentrations of criteria pollutants (PM_{2.5}, PM₁₀, SO₂, NO₂, and O₃) at the patient's home locations and IVF clinic centers for the entire study period (Liao, et al., 2007, Liao, et al., 2006, Whitsel, et al., 2006). From these daily criteria pollutants concentration data, the daily concentrations of PM_{2.5}, PM₁₀, SO₂, NO₂, and O₃ were calculated for each patient during the entire IVF cycle and pregnancy (Table below) and used to estimate the exposure matrix. We did not perform spatial interpolations on carbon monoxide as it is considered a local pollutant, or on lead since our GIS models for this pollutant have not been validated in other studies (Whitsel et al, 2006).

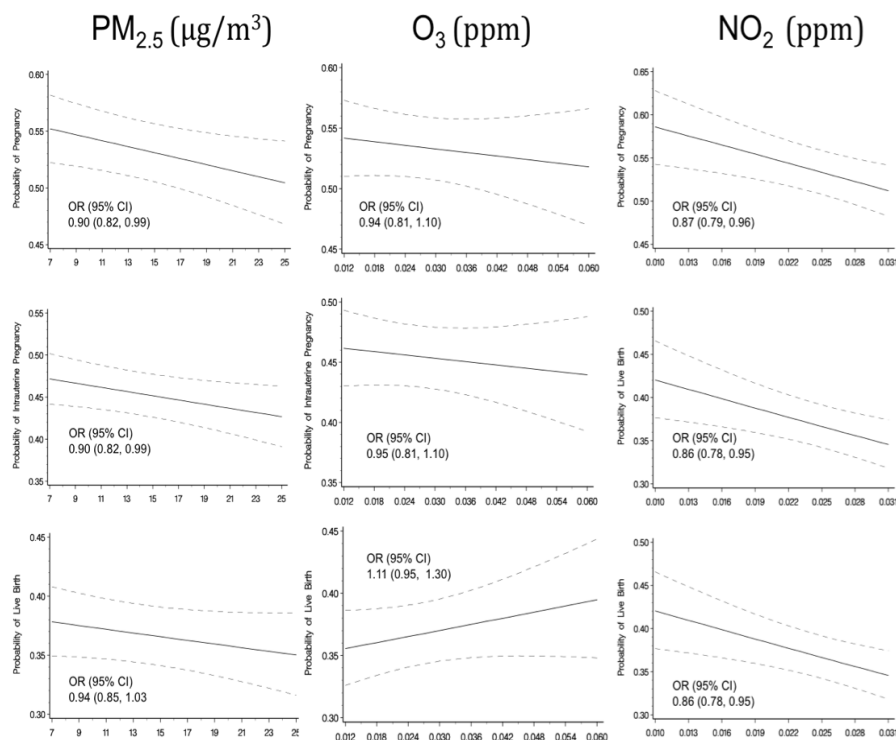
Specific Aim 2: We noted a consistent adverse effect of increasing concentrations of NO₂ on the odds of live birth at all time segments in an IVF cycle (Table below), at home and at the IVF lab (Figure below), with the largest effect size in the time period from embryo transfer to determination of pregnancy (Odds Ratio = 0.76, 95% CI 0.66-0.86), although the time period from embryo transfer to the date of live birth was marginally significant (p=0.07). No significant effects were identified for SO₂, although outcomes were consistently poorer with increasing SO₂ exposure, and this trend was nearly significant for intrauterine pregnancy rates according to SO₂ concentration at the IVF clinic during the period of embryo culture (data not shown). The effects of ozone were bidirectional. Increasing levels of ozone during the period of oocyte maturation were associated with increased chance for a live birth (P = 0.02), whereas after embryo transfer it was associated with a significantly decreased odds of live birth (P = 0.002). To place the effects of a one standard deviation of the air pollutants in context, we noted in our population that a one year increase in age was associated with decreased chance of pregnancy (OR 0.91, 95% CI 0.90 to 0.92).

Table: Distribution of Air Pollution Variables	PM _{2.5} Exposure (µg/m ³)	PM ₁₀ Exposure (µg/m ³)	SO ₂ Exposure (ppm)	NO ₂ Exposure (ppm)	O ₃ Exposure (ppm) 8-hour rolling average
A. Average daily concentration from medication start to oocyte retrieval (patient home)	14.08 [4.17]	23.80 [5.15]	0.059 [0.022]	0.019 [0.0058]	0.038 [0.014]

Table: Distribution of Air Pollution Variables	PM2.5 Exposure (µg/m3)	PM10 Exposure (µg/m3)	SO2 Exposure (ppm)	NO2 Exposure (ppm)	O3 Exposure (ppm) 8-hour rolling average
B. Daily concentration on the date of retrieval (IVF clinic)	14.45 [7.81]	23.93 [10.17]	0.063 [0.030]	0.019 [0.008]	0.038 [0.018]
C1. Average daily concentration from oocyte retrieval to embryo transfer (patient home)	14.12 [5.77]	24.10 [7.59]	0.059 [0.025]	0.019 [0.007]	0.038 [0.015]
C2. Average daily concentration from oocyte retrieval to embryo transfer (IVF clinic)	14.35 [5.77]	23.94 [7.56]	0.063 [0.025]	0.019 [0.007]	0.038 [0.015]
D. Average daily concentration from embryo transfer to pregnancy test (14 days) (patient home)	14.17 [4.08]	24.06 [4.95]	0.059 [0.022]	0.019 [0.006]	0.038 [0.014]
E. Average daily concentration from embryo transfer to pregnancy outcome date	14.01 1.96]	23.85 [2.52]	0.057 [0.012]	0.018 [0.004]	0.037 [0.009]

Table : Odds Ratio of Live Birth [with 95% Confidence Intervals] per unit change in particulate matter (PM 2.5 and 10), NO ₂ , SO ₂ , and O ₃ air concentration by IVF cycle interval at patient home.	Per 8 µg/m ³ increase PM _{2.5}	Per 10 µg/m ³ increase PM ₁₀	Per 0.03 ppm increase SO ₂	Per 0.01 ppm increase NO ₂	Per 0.02 ppm increase O ₃
A. Average daily concentration from medication start to oocyte retrieval	1.03 [0.91- 1.16]	1.08 [0.98- 1.18]	1.00 [0.91- 1.10]	0.80 [0.71- 0.91]	1.26 [1.10- 1.44]
C1. Average daily concentration from oocyte retrieval to embryo transfer	0.96 [0.89- 1.04]	1.00 [0.93- 1.07]	0.94 [0.87- 1.02]	0.87 [0.79- 0.96]	1.06 [0.96- 1.18]
D. Average daily concentration from embryo transfer to pregnancy test (14 days)	1.00 [0.89- 1.12]	1.05 [0.94- 1.16]	0.94 [0.86- 1.04]	0.76 [0.66- 0.86]	1.23 [1.07- 1.41]
E. Average daily concentration from embryo transfer to the date of livebirth	0.82 [0.55- 1.23]	0.76 [0.53- 1.09]	0.96 [0.73- 1.27]	0.76 [0.56- 1.02]	0.62 [0.48- 0.81]

Figure below: Pregnancy and Live Birth Regression lines and 95% CI lines with concentration of three pollutants (PM_{2.5}, O₃, and NO₂) at the IVF lab site from retrieval till transfer (x axis) with the probability of the three events (y axis), pregnancy as determined by serum pregnancy test, intrauterine pregnancy as determined by ultrasound, and live birth. This is a single pollutant model adjusted for confounders.



Publications:

Legro RS, Sauer MV, Richter KS, Mottla GL, Li X, Dodson WC, Liao D. Effect of Air Quality on Assisted Human Reproduction. *Hum Reprod* 2010 May;25(5):1317-24. Epub 2010 Mar 13. *PMCID: PMC Journal – In Process*

Research Project 28: Project Title and Purpose

New Methods for Studying Mitochondrial Mutations and Common Chromosome Fragile Sites in Cancer - Mutations are the cause of human genetic diseases. Thus, elucidating the mechanisms and risk factors of mutagenesis is of great significance. We intend to test the utility of new methods for studying mitochondrial mutations, the methods that rely on using the latest sequencing technologies. Additionally, we will investigate alterations in chromosome structure that are a hallmark of solid tumors. The mechanisms by which such alterations arise during cancer are not fully understood. We propose to use a combined computational-biochemical approach to discover DNA sequences in the human genome that are associated with sites of chromosome breakage.

Anticipated Duration of Project

11/24/2008 - 12/31/2011

Project Overview

The first part of this project is focused on mitochondrial mutations causing >200 human genetic diseases. Mitochondrion is an organelle of cellular energy synthesis and, as a result, possesses mutagenic metabolites in high quantities. Our First Specific Aim is: *To investigate the use of novel sequencing technology to the studies of mitochondrial mutations.* We will test how high throughput short-read sequencing can improve the detection of levels of mitochondrial disease-causing mutations. This is critical for precise estimation of mitochondrial DNA (mtDNA) mutation rates and for the prognosis and treatment of mitochondrial diseases as well as for preventing mitochondrial disease transmission. As part of this Specific Aim, we will collect blood and buccal cell samples from 500 mother-child pairs, isolate DNA from these samples, and will investigate mutations that occur in the maternal germline.

The objective of the second part of this project is to elucidate how the structure of an individual genome underlies the risk of developing chromosomal aberrations during cancer. We have discovered that microsatellites (short DNA repeats) pose a significant block to DNA synthesis in a sequence-dependent manner. Microsatellites are present within common fragile sites (CFS), regions of the genome prone to chromosomal instability in tumor cells. Our Second Specific Aim is: *To test a hypothesis that DNA replication inhibition within CFS is due to the density and/or arrangement of specific microsatellite sequences, relative to other areas of the genome.* We propose to use statistical classification and comparative genomics techniques to identify critical features of the human genome associated with chromosomal fragility. Genome elements identified computationally will be tested directly using biochemical analyses. The experiments outlined in this study will elucidate DNA replication dynamics through CFS and the mechanisms/factors responsible for DNA breakage. The identification of key sequence elements responsible for CFS can lead to elucidation of individual genetic risk factors and environmental exposures that act to increase chromosomal instability during cancer.

Principal Investigator

Kateryna Makova, PhD
Associate Professor
Penn State University
305 Wartik Lab
University Park, PA 16802

Other Participating Researchers

Francesca Chiaromonte, PhD, Laura Carrel, PhD, Kristin Eckert, PhD, Ian Paul, MD- employed by Penn State University

Expected Research Outcomes and Benefits

An improved identification of mutations in mtDNA will be of great clinical and scientific significance. *First*, this will allow for more accurate identification of disease-causing alleles and thus a better diagnosis and earlier treatment of diseases caused by mutations in mtDNA. This will have a major effect on and is expected to improve genetic counseling. *Second*, this project will provide important information on the mechanisms of mutations in mtDNA – the cause of genetic diseases.

This research is highly relevant to unraveling cancer etiology. Understanding DNA replication dynamics through CFS will help to elucidate the mechanisms and endogenous factors responsible for inducing DNA breakage at these chromosomal sites. In addition, current CFSs were identified using cytogenetic techniques, and likely represent only a subset of genomic regions that are prone to rearrangement. Our proposed bioinformatics approach will allow us to understand global mechanisms of chromosomal instability in human cells and can lead to a fine-scale mapping of chromosomal rearrangement sites within the human genome in future studies. The identification of key sequence elements underlying DNA replication inhibition and DNA breakage can lead to the identification of individual genetic risk factors or environmental exposures that increase chromosomal instability during neoplastic progression.

Summary of Research Completed

Below we outline our substantial preliminary results obtained in partial fulfillment of Aim 1. Here we describe the analysis of *three* mother-child pairs whose mtDNA we sequenced so far, as well as a further refined method for defining the sequencing/PCR error threshold.

Defining the error threshold. One of the challenges of this project is to determine what alterations in allele frequencies between two tissues of the same individual, or between a mother and her child, are significantly above the sequencing/PCR error inherent to our experiment – thus allowing us to identify somatic or germline mutations as well as heteroplasmy frequency shifts. To determine the “background” level of alterations in our sequencing reads due to sequencing instrument and/or PCR errors, each mtDNA sample (from each of the two tissues per individual), was amplified and sequenced twice. In total, we analyzed data for 2 replicates of each of 12 tissues samples, i.e. 3 mother-child pairs = 6 individuals x 2 tissues (blood and buccal) = 12 samples (Table 1).

Since our aim is to determine an error threshold for our experiment, we use the premise that if at a site all reads indicate the same (invariant) nucleotide in one replicate, then the presence of reads having different (deviant) nucleotide(s) at the same site in another replicate is very likely to indicate an error (of course this might also be due to an extremely low-frequency heteroplasmy not sampled in the first replicate, however, we disregarded this possibility for the time being). The frequency of deviant nucleotides at such a site was considered to be this site’s error frequency. For instance, at site X, all 700 reads indicated an “A” in replicate 1 of a sample, while at the same site 997 reads indicated an “A” and 3 reads indicated a “T” in replicate 2. The error frequency was therefore computed as $3/1000 = 0.003$. If different deviant nucleotides were present at a site (e.g. two “T”s and one “G”), their frequencies were summed up to obtain the

site's error frequency (still 0.003).

For each of the 12 individual tissue samples, we therefore compared the two sequenced replicates as follows. *First*, we identified all sites with a coverage of at least 200 reads. This eliminated very few sites (Table 1), and was required to minimize statistical fluctuations in error frequency associated with low coverage. *Second*, among these sites, we identified all sites with invariant nucleotides among reads in replicate 1 (Table 1) and calculated their error frequencies in replicate 2. Usually, thousands of such sites were found (Table 1). *Third*, we performed a reciprocal operation; namely, we found all sites with invariant nucleotides among reads in replicate 2 (Table 1) and calculated their error frequencies in replicate 1. This was repeated for each of the 12 individual tissue samples.

This resulted in a background error frequency distribution pulled across 12 samples (Fig. 1). Error frequencies tended to be very low -- indeed, below 1% for 99.9% of the sites invariant in (at least) one of the replicates. However, for a measurable number of sites, error frequencies ranged between 1-1.9%. Notably, these sites usually had high sequencing coverage (data not shown), allowing us to assume, conservatively, that sequencing/PCR error in our experiments would very seldom exceed 2% (used as threshold). Interestingly, repeating the above procedure by restricting attention to sites with coverage above 500x (instead of 200x) lowered the threshold somewhat (to 1.5%) -- however, the increased coverage requirement substantially reduced the number of sites considered (data not shown).

Identification of heteroplasmic sites. We next considered each individual tissue sample separately (here the reads from two replicates were pooled). Using the error threshold determined above, we defined heteroplasmic sites as sites with a minor allele with frequency $\geq 2\%$. We found 1-4 heteroplasmic sites in each sample (Table 2).

Identification of somatic shifts in heteroplasmic frequencies and somatic mutations. At each of these heteroplasmic sites identified in this manner, we compared minor allele frequencies between the two tissues representing the same individual (a mother, or a child). If the difference in minor allele frequency was $\geq 2\%$, the site was defined as undergoing a somatic shift in heteroplasmic frequency. If, in addition, this somatic shift occurred from absence (within an error threshold) in a tissue to presence in another tissue, we identified the site as a candidate somatic mutation site. We found no candidate somatic mutation sites in our present data.

Identification of germline shifts in heteroplasmic frequencies and germline mutations. Finally, we compared minor allele frequencies at heteroplasmic sites between a mother and her child in each of the three pairs. If the difference in minor allele frequency between any tissue of a mother and any tissue of her child was $\geq 2\%$, the site was defined as undergoing a germline shift in heteroplasmic frequency. Note that our definition allows for somatic and germline shifts in heteroplasmic frequency at the same site. We did find one site with germline heteroplasmic frequency shift in our present data: site 8992 had allele frequencies 31.5%, 30.8%, 46.5%, and 42.9% in mother 4 blood, mother 4 buccal, child 4 blood, and child 4 buccal, respectively. Thus, at this site we observed both a somatic heteroplasmic frequency shift in a child, and a *germline frequency shift* between a mother and a child.

Among germline heteroplasmic frequency shift sites, we identified candidate germline mutation sites as those in which the germline shift occurred from absence (within an error threshold) in the mother to presence in the child. Remarkably, we did find a candidate germline mutation site in our present data: site 710 in pair 10 had allele frequencies of 0.10%, 0.07%, 2.30%, and 3.20% in mother's blood, mother's buccal, child's blood, and child's buccal, respectively. Thus, at this site a $\geq 2\%$ -shift occurred from $\sim 0\%$ in maternal tissues to significantly higher values in her child, suggesting a *germline de novo mutation* leading to heteroplasmy at this site.

These preliminary results demonstrate our ability to generate and process data, from sample collection to completion of the statistical analyses required to identify somatic and germline heteroplasmic frequency shifts and de novo mutations.

Individual	Tissue	Repl.	Sites with $\geq 200x$	Median coverage	Number of invariant sites
Mother 4	blood	1	16490	1275	6812
Mother 4	blood	2	16537	2031	4667
Mother 4	buccal	1	16547	2357	3774
Mother 4	buccal	2	16519	1527	5508
Child 4	blood	1	16557	3808	1981
Child 4	blood	2	16563	6557	764
Child 4	buccal	1	16523	1292	6178
Child 4	buccal	2	16543	2314	3576
Mother 10	blood	1	16558	3188	3005
Mother 10	blood	2	16534	1813	5015
Mother 10	buccal	1	16564	3777	1963
Mother 10	buccal	2	16562	2776	3263
Child 10	blood	1	16502	1228	4262
Child 10	blood	2	16544	2133	6755
Child 10	buccal	1	16551	2349	3050
Child 10	buccal	2	16556	2362	3187
Mother 15	blood	1	16543	3487	2981
Mother 15	blood	2	16542	3707	2555
Mother 15	buccal	1	16530	1840	5048
Mother 15	buccal	2	16537	2453	3535
Child 15	blood	1	16541	2802	3643
Child 15	blood	2	16531	2298	4627
Child 15	buccal	1	16548	3860	2146
Child 15	buccal	2	16529	2395	4155

Table 1. The numbers of sites with coverage $\geq 200x$ (out of a total of 16571 sites sequenced for mtDNA per sample) and of invariant sites.

Individual	Tissue	All detected heteroplasmic sites	Sites with somatic freq shift	Sites with germline freq shift	Sites with germline mutation
Mother 4	blood	2 (+2*)	NO	1 (site 8992)	NO
Mother 4	cheek	2 (+1*)			
Child 4	blood	2	1 (site 8992)		
Child 4	cheek	2			
Mother 10	blood	1(+1*)	NO	NO	1 (site 710)
Mother 10	cheek	1			
Child 10	blood	2	NO		
Child 10	cheek	2			
Mother 15	blood	1	NO	NO	NO
Mother 15	cheek	1			
Child 15	blood	1	1 (site 310)		
Child 15	cheek	1			

Table 2. Detected heteroplasmic sites.

*Sites that had allele frequencies above threshold in one tissue, but below it in another tissue, however the allele frequency difference was not significant at such sites between the two tissues as well as between a mother and a child.

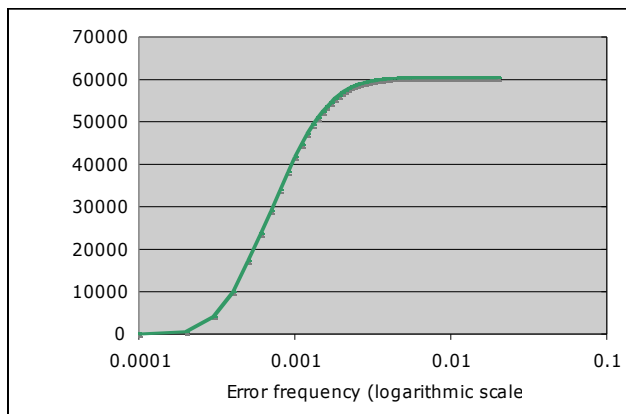


Figure 1. The distribution (cumulative distribution function) of error frequencies for sites invariant in at least one of the two replicates sequenced for each individual tissue sample. The total number of sites considered is 60445, the sum of sites in the last column of Table 1.

Research Project 29: Project Title and Purpose

Proteomic and Molecular Analysis of Formalin Fixed, Paraffin Embedded Tumors - Every day, benign and malignant tumor tissues are biopsied or removed surgically and evaluated by a pathologist to establish a diagnosis and prognosis (i.e., Is it cancerous? What type of cancer?). However, much information that might aid in making a diagnosis remains unstudied within these collected tissue samples. One difficulty has been that the tissues are preserved in such a way (formalin fixation and paraffin embedding) that makes standard methods of molecular biology difficult to use. Recently, emerging technologies have made it possible to obtain some of this untapped information. Our goal is to couple these techniques in a way that has not yet been done at Penn State University – College of Medicine (PSU-COM) to compare two different types of tumors. If successful, these methods will be important for basic science studies, and could be developed further as powerful clinical diagnostic tools.

Anticipated Duration of Project

11/24/2008 - 4/30/2011

Project Overview

The molecular diagnosis of cancers has been the subject of intensive research in recent years. The goal of this work is to perform a demonstration project that seeks to diagnose specific tumors using a series of techniques that have not been previously performed at the PSU-COM. Our objective is to perform laser capture microdissection of *formalin fixed, paraffin embedded* (FFPE) tissues followed by proteomic and molecular analyses. To accomplish this goal, we have assembled a matrix biologist, a proteomics expert, an orthopaedic oncologist and a practicing orthopaedic pathologist with long term experience in sarcoma. We believe that a successful outcome would be of great benefit to the research community at PSU-COM and elsewhere

because it would facilitate a wide variety of studies.

Specific Aim 1: Distinguish two sarcoma tumor types by their ECM protein composition.

Hypothesis: Tumors that arise from different source tissues can be distinguished based upon the extracellular matrix proteins they produce.

Rationale: Even closely related tissues such as cartilage and bone have distinct, non-overlapping extracellular matrix (ECM) protein expression. We believe these protein patterns remain after oncogenic transformation, and will allow the distinction of the two tumor types. Laser capture microdissection will allow the selective proteomic analysis of only the ECM proteins, and result in a simpler sample with greater relative protein content.

Specific Aim 2: Distinguish between similar tumors with clinically distinct behaviors.

Hypothesis: Benign and malignant tumors arising from the same tissue can be distinguished by the expression of key genes.

Rationale: Mesenchymal neoplasms that share a common tissue origin can have a similar histopathologic appearance, but radically different clinical behaviors. We will use laser capture microdissection to isolate cells from FFPE tissues, and extract RNA to compare benign and malignant mesenchymal tumors for expression of genes known to affect metastatic potential.

Specific Aim 3: Identify grade-specific extracellular matrix protein biomarkers for cartilage lesions.

Hypothesis: The histological range of benign to high-grade cartilage tumors will be reflected in the extracellular matrix (ECM) proteins produced locally within the tumors. These abundant, stable proteins can serve as definitive biomarkers to distinguish benign from malignant cartilaginous lesions.

Rationale: Tumor grade is the single most important prognostic factor in cartilaginous lesions (Giuffrida et al., 2009). It is also the greatest determinant in selecting a course of clinical treatment. Importantly, determination of cartilage lesion grade is particularly difficult and reliability is low even among experienced radiologists and pathologists. Thus, improvement in grading reliability will have an immediate and positive impact on clinical outcomes. The spectrum of benign to high-grade cartilage tumors is observable by subtle histological differences. These differences will be present at the molecular level in the extracellular matrix (ECM) proteins produced locally within the tumors. Mass spectrometry can be used to identify these differences between grades. Accordingly, these abundant ECM proteins can be used as grade-specific biomarkers for cartilaginous lesions.

Principal Investigator

Timothy M. Ritty, PhD
Assistant Professor
Penn State College of Medicine
Orthopaedics
Mailcode H089, Room 3804
500 University Drive
Hershey, PA 17033

Other Participating Researchers

Elizabeth Fraumeni, MD, Edward J. Fox, MD, Bruce Stanley, PhD – employed by Penn State

Expected Research Outcomes and Benefits

Specific Aim 1 Expected Outcomes: Because dozens of ECM proteins are produced exclusively by osteoblasts (e.g. osteocalcin) or chondrocytes (e.g. type II collagen), we anticipate the identification of 10-20 proteins that are uniquely produced by either osteosarcoma or chondrosarcoma. Upon successful completion of preliminary samples, work is to continue on patient samples of enchondroma and chondroma tumors. These samples will be de-identified, formalin fixed paraffin embedded archival tissues. Based on our early work, we anticipate the identification of 100-150 proteins per sample quantified by iTRAQ, and that approximately 5% of these will be statistically informative between tumor types.

Specific Aim 2 Expected Outcomes: Due to the hypoxic, anhydrous conditions of tissues in paraffin, we anticipate the successful extraction of RNA from LCM captured cells. Even if the mRNA is slightly degraded, TaqMan primer sets typically amplify only very short amplicons (100-150bp), and so detection may be only slightly affected and will be normalized by GAPDH and beta actin controls. Additionally, we expect to see increased expression of the integrin subunit alpha V, and MT1-MMP (MMP14) in the more metastatically aggressive cancers.

The major benefit of these two Specific Aims will be a new ability to distinguish these two tumor types from one another. This is especially critical. They respond differently to chemotherapy. Therefore, there may eventually be a direct clinical benefit to the patients with these tumors as they may be diagnosed with greater certainty, and treated with greater confidence. Further, these techniques can be applied to many other tumor types. The potential exists that these techniques could aid clinical treatment of cancer patients in several additional ways; for example, improved tumor staging or determination of metastatic potential.

Specific Aim 3 Expected Outcomes: Cartilaginous lesions have observable histopathological differences at the extremes of the cartilage lesion spectrum. These differences are manifested at the molecular level in the local ECM proteins produced within the tumor. *The disparities in ECM protein composition, if identified, could serve as abundant biomarkers that have the potential to diagnostically aid intermediate staging or have prognostic value.*

Summary of Research Completed

In our last progress report, we described how the work had evolved into an application on a second clinical problem – that of the distinction of benign enchondromas from malignant chondrosarcomas. Our preliminary work from the last period has produced an NIH R21 application to NCI. We have received additional CURE funds to generate preliminary data in support of this application.

1. Increased analysis power through relative quantitation and preliminary identification of a biomarker. Through the last year, we have focused upon the distinction of benign enchondroma

from malignant chondrosarcoma. In our previous reporting period, our protein identification data was binary, i.e., either present or not detectable. We have greatly increased the power of our analysis by the use of isobaric tags to label our peptides. This technique allows relative quantitation of proteins across multiple samples, and in our case – benign versus malignant samples. Quantitation has significantly increased our analysis power. With our statistician collaborator, Dr. Jason Liao, four differentially expressed proteins were identified at 10% false discovery rate despite the small sample size of three per group. Larger sample sizes will substantially increase the power and identify more differentially expressed proteins. The biomarker with the lowest p value is TGFBI (β ig h3), an extracellular matrix protein associated with a metastatic phenotype in a variety of carcinomas, but never before reported in sarcomas. We are currently validating with secondary methods.

We have improved our abilities to analyze our mass spectrometry data through the creation of proprietary software in-house.

2. More thorough and objective reporting of protein identification: When two or more proteins receive an equal identification score, Protein Pilot (ABI) randomly chooses a “representative winner” and the others are “equivalent winners” and assigned a score of “0”, as all identifying peptides are then considered to belong to the representative winner. However, all are equally likely to be the protein that is detected. Authors commonly report the “representative winner” as the identified protein, when in fact; others were identified with equal certainty. The problem with this is that some of these proteins might not just be isoforms, but are actually the products of different genes. This is a key limitation, even deficit, of the current state of the art analysis provided by Protein Pilot (ABI) that has not been addressed in the literature. To rectify this problem, we have authored software to use the genomic identifiers for each identified protein, and work backwards to the gene that encodes it. In this way, *we now can report all gene products equally associated with one identification event*.

3. Increased protein, peptide analysis and quality control capabilities: We have authored software to automate tasks that would have been unrealistic to perform manually, especially on large data sets. We are now capable of the following in automated or semi-automated ways: A. molecular weight determination and distributions for identified proteins, B. enumeration and distributions for peptide length, C. percent of protein coverage by peptides, D. grouping of gene ontology designations, and E. identification of missed tryptic cleavages. This greatly increases our ability to perform quality control on our runs, and to compare samples in ways that were not previously possible.

Research Project 30: Project Title and Purpose

Signaling Pathways in Epidermal Stem Cell Proliferation and Skin Carcinogenesis - Our research will attempt to determine what role the polyamine pathway plays in early skin cancer development. There is strong experimental evidence indicating the location of epidermal stem cells that are modified by carcinogen exposure is in a specific area of the hair follicle. By directing expression of transgenes to this region of the epidermis in mice, we can modify gene expression in stem cells and ask what effect these genetic alterations have on tumor development. Understanding the pathways that control epidermal stem cell proliferation is

important to the area of public health, because these cells are targets for gene therapy approaches in cancer prevention and treatment.

Duration of Project

11/24/2008 - 6/30/2009

Summary of Research Completed

This project ended during a prior state fiscal year. For additional information, please refer to the Commonwealth Universal Research Enhancement C.U.R.E. Annual Reports on the Department's Tobacco Settlement/Act 77 web page at <http://www.health.state.pa.us/cure>.

Research Project 31: Project Title and Purpose

Genetic and Proteomic Analysis of the UL84 Gene of Human Cytomegalovirus - In immunocompromised individuals, opportunistic human cytomegalovirus (HCMV) infections can produce life-threatening syndromes involving almost every organ, but more commonly pneumonia, hepatitis, diseases of the central nervous system, and secondary immune suppression. In addition, HCMV can cross the placenta and is the most common viral cause of congenital defects. The purpose of this research project is to identify the mechanisms of action of an essential viral protein. Elucidation of these mechanisms could lead to the identification of therapeutic targets for management of HCMV illnesses.

Anticipated Duration of Project

11/24/2008 - 12/31/2010

Project Overview

Human cytomegalovirus causes mostly sub-clinical or mild primary infections in immune competent hosts but persists in 60-90% of the human population. In immunocompromised individuals, opportunistic infections can produce life-threatening syndromes involving almost every organ, but more commonly pneumonia, hepatitis, CNS diseases, and secondary immune suppression. In addition, HCMV can cross the placenta and is the most common viral cause of congenital defects. Although several anti-virals limit morbidity and mortality, the drugs have significant toxicity and the development of resistance is common. None of these agents has been licensed for use in pregnant women. Accordingly, there remains widespread interest in the further elucidation of the virus-host interaction to reveal potential molecular targets for control. The UL84 gene is essential for viral DNA replication and also participates in the regulation of gene transcription in virus infected cells. Evidence suggests that this gene has other important functions as well. The goal of this project is to identify new UL84 binding partners and develop mutants that will provide a foundation for a more directed grant proposal. The working hypothesis is that multiple activities of UL84 are directed toward modification of the functions of cellular proteins. The first specific aim will employ recombinant DNA technology to develop mutant viruses with altered UL84 genes. These mutants will be useful reagents for analysis of

UL84 gene function. The second specific aim will evaluate cellular proteins that are candidates for participating in functional interactions with the UL84 protein. Candidate cellular proteins identified previously by a global proteomic investigation will be tested individually for their ability to bind to the UL84 protein by standard methods to analyze protein-protein interactions. Ultimately, elucidation of the roles of UL84 protein interactions with cellular proteins should reveal mechanisms used by the virus to reprogram the host cell and could lead to the identification of therapeutic targets for management of HCMV illnesses.

Principal Investigator

David J. Spector, PhD
Professor
Dept. of Microbiology and Immunology MC H107
Penn State College of Medicine
500 University Drive
Hershey, PA 17033

Other Participating Researchers

None

Expected Research Outcomes and Benefits

We expect to identify one or more cellular proteins that associate with the viral UL84 protein in infected cells and to have learned whether a candidate cellular protein's function is altered in infected cells and whether or not the protein is required for infection. Depending on the nature of the cellular protein, this information will be used to formulate one or more specific hypotheses regarding how UL84 alters host cell function. We also expect to have produced a series of viral mutants with UL84 gene alterations and to have determined which of the gene lesions interferes with viral replication and which ones produce proteins that retain the ability to promote replication. The mutants will be critical reagents for investigating the precise mechanism by which UL84 protein alters the function of a particular cellular protein. Detailed investigation of such mechanisms will be the focus of a future proposal to support the work. The health benefit of particular projects such as this one cannot be predicted. The combined efforts of many investigations of viral gene function are likely to generate information that suggests new therapeutic targets for control of HCMV disease.

Summary of Research Completed

Work has been accomplished in the following parts of the project:

Specific Aim 1a. to develop genetic reagents for analysis of UL84 gene function: to construct a set of structurally and functionally informed set of mutants.

Last year we reported the isolation of four viruses with UL84 mutations in the strain TB40/E clone 4 (c14) genome. Figure 1 is a representation of the UL84 amino acid sequence from three

different primate virus genomes, human, chimp and rhesus. The mutated residues are underlined in the figure. The viruses were designated m1 (del 87-95), m2 (L121A, L128A), m3 (del 241-253) and m4 (del 161-175). The rationale and expected phenotypes were described in last year's report.

All of these mutant viruses are viable. The production of mutant UL84 proteins in infected cells was assayed by immunofluorescence (Fig. 2) and immunoblotting (Fig. 3). For immunofluorescence, MRC5 human diploid fibroblast cells were grown on cover slips. At various times after infection, the infected cells were fixed and stained with a primary mouse monoclonal antibody against a viral protein and with a secondary anti-mouse antibody conjugated to the fluorophore Cy3. For immunoblotting, cell extracts were prepared at various times after infection. Proteins were separated on polyacrylamide gels, blotted to nitrocellulose and detected by chemiluminescence after incubation first with the same mouse monoclonal antibodies used for immunofluorescence and then with a secondary antibody conjugated to horseradish peroxidase.

The data show that all of the proteins were synthesized in infected cells. The m4 protein accumulated at much lower levels than the other mutant proteins. The immunofluorescent image of m4-infected cells and anti-UL84 antibody was obtained with an extended exposure to visualize the protein. As expected, all of the proteins, except m3, accumulated primarily in the nucleus. As expected, m3 accumulated primarily in the cytoplasm.

Four more mutant viruses (Fig. 1) were constructed by the same methods described in last year's report. The first has two point mutations (L228A, L230A; m5) in a sequence shown to function as a nuclear export signal. The second (del536-553, m6) deletes a sequence conserved in primate cytomegaloviruses. The third mutation (L359A, m7) alters a second nuclear export signal, and the fourth mutation (L228A, L330A, L359A); m5/7) affects both nuclear export signals and has been reported to produce a protein whose export cannot be detected. All of these mutants are viable but UL84 protein production has not yet been characterized.

Specific Aim 1b. to develop genetic reagents for analysis of UL84 gene function: to produce a UL84-null viral genome and develop a complementation system for its propagation.

Last year we reported construction of a UL84-null mutant in TB40GFPBAC by inserting the galK cassette in place of the UL84 coding region as described above. We also reported preliminary data that the BAC (TB40GFpBAC Δ 84galK) was non-viable. However, further investigation showed that this BAC produces virus in permissive MRC5 cells. Two other similar constructs isolated independently from TB40/E BACs that have either a different color marker or no color marker also produced virus. These results show that the UL84 gene, shown by others to be essential for the growth of strains ad169 and Towne, is not essential for growth of TB40/E cl4. This strain is highly endotheliotropic and also grows to high titer in fibroblasts. We also constructed similar galK gene replacements of UL84 in the ad169 and FIX BAC clones. FIX is an epitheliotropic strain with a genomic organization much more similar to TB40/E than to Ad169 or Towne. Both the ad169 and FIX versions of the UL84-deletion virus were non-viable. The TB40/E mutant grew in a variety of permissive cell lines besides MRC5 including human foreskin fibroblasts and human retinal pigmented epithelial cells (ARPE-19).

The UL84 deletion virus was characterized by a variety of methods. The UL84 deletion and galK gene replacement were confirmed by PCR (Fig. 4) and Southern blotting (Fig. 5). For the PCR, either BAC DNA or virus DNA was isolated and amplified with primers that distinguish between galK and UL84-containing genomes. For the Southern blot, BAC DNA was isolated and cut with restriction enzyme BamHI. The DNA fragments were separated by gel electrophoresis, transferred to nitrocellulose, and hybridized to labeled UL84 or galK probes. The lack of UL84 protein accumulation was observed in both immunofluorescence (Fig. 6) and immunoblotting (Fig. 7) experiments. Finally, the growth of the mutant was compared directly to wild type in an experiment in which cells were infected and then harvested at various days after infection (Fig. 8). The virus in the samples was assayed by plaque titration. The kinetics of growth were similar, although not identical, and the yields of mutant virus were slightly though reproducibly reduced.

This result is important for several reasons. First, it explains why all of the mutants were viable even though some were predicted to compromise essential UL84 functions. Second, it means that natural HCMV can have an activity that allows growth in the absence of the UL84 gene. Since the essential function of UL84 in laboratory strains is highly likely to be related to the initiation of viral DNA synthesis, TB40/E must have the capacity to bypass the UL84 requirement for this process, implying strongly that TB40/E contains either a UL84-independent origin of replication or encodes a gene product that can substitute for UL84. Either way, natural strains would have a more robust DNA replication capacity than laboratory strains, which presumably lose the capacity upon repeated passage.

Specific Aim 2a. to evaluate cellular binding partners of UL84 from a proteomic data set by determining whether the interactions can be confirmed in infected and/or transfected cells.

No further activity on this aim

P16727|UL84_HCMVA
gi|20026675|ref|NP_612717.1|
Q772N1|Q772N1_RHCM6

CKLTENTTEKTSPVTLAMVCGDL----- 586
EQQQTPATEKPSVTLAMICGDL----- 573
AQQQSPTNNKPVTIAMVCNQRQPQQQPQNSASFP 512
: .*:. .**:*:*.*.:

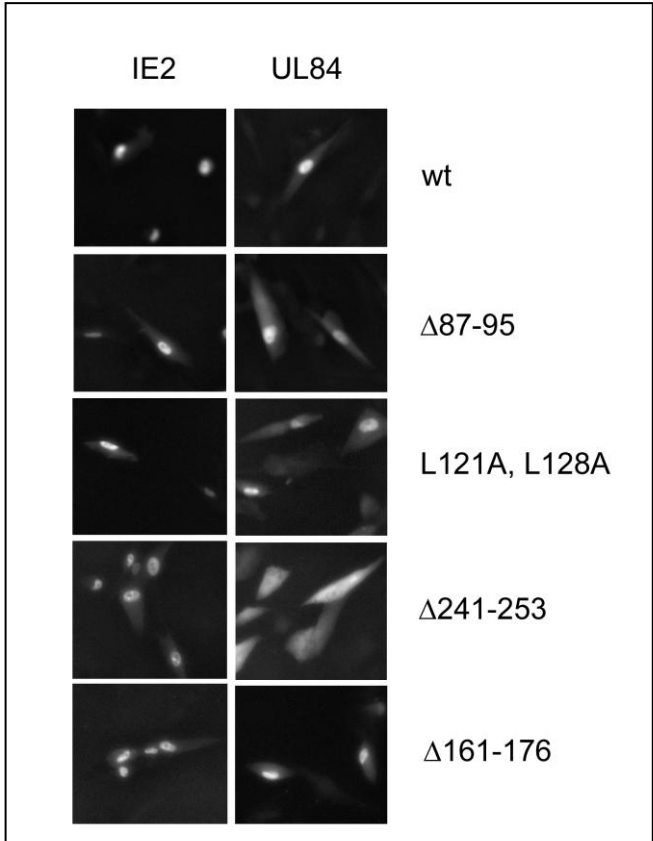


Fig. 2. Assay of UL84 expression in virus-infected cells by fluorescent antibody. MRC5 cells were infected with the mutant indicated at a MOI of 0.1 - 0.5 and fixed at 24 hours post infection. Cells were stained with mAb 9G3 (UL84) or 3A9 (IE2) and images were captured with a 20X objective.

Fig. 4. Amplification of DNA sequences in viral DNA and BAC clones. BAC or viral DNA was prepared and amplified with primers specific for UL84 or GalK as described in Methods. The diagram shows the bands predicted from the position of the primers. Lane designations:
 1) TB40GFPΔ84GalK viral DNA;
 2) TB40GFPΔ84GalK BAC DNA;
 3) TB40GFP BAC DNA;
 4) No DNA; M. DNA markers.

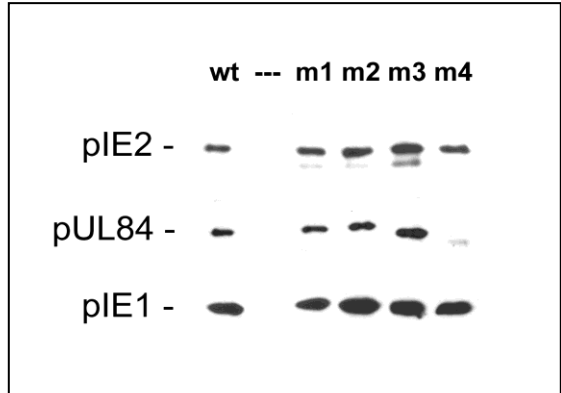
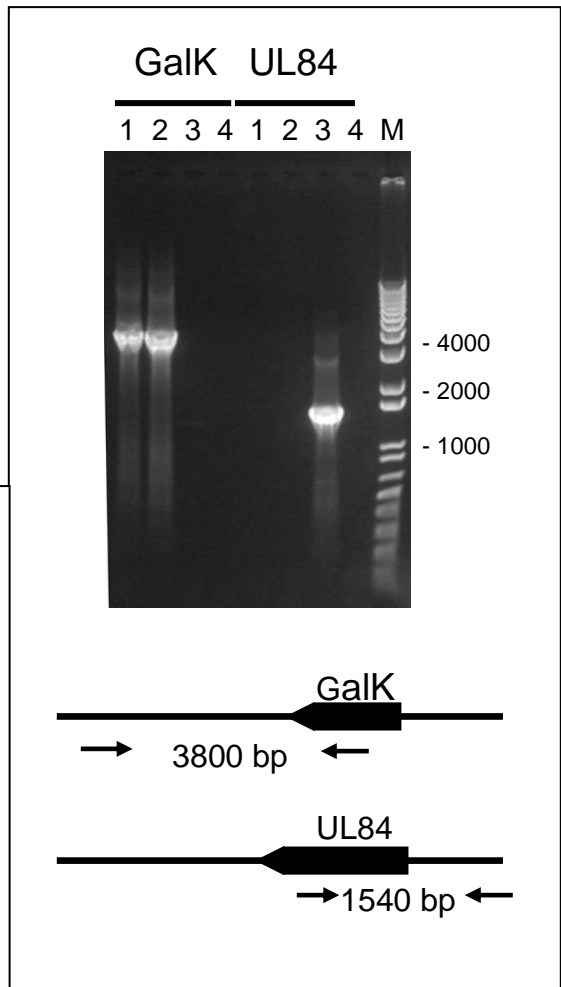


Fig. 3. Assay of protein expression in infected cells by immunoblotting. MRC5 cells were infected with the mutant indicated at a MOI of 0.5 - 1.0, and extracts were prepared at 48 hours post infection. Blots were probed with mAb 9G3 (UL84), 3A9 (IE2), or 1D12 (IE1).



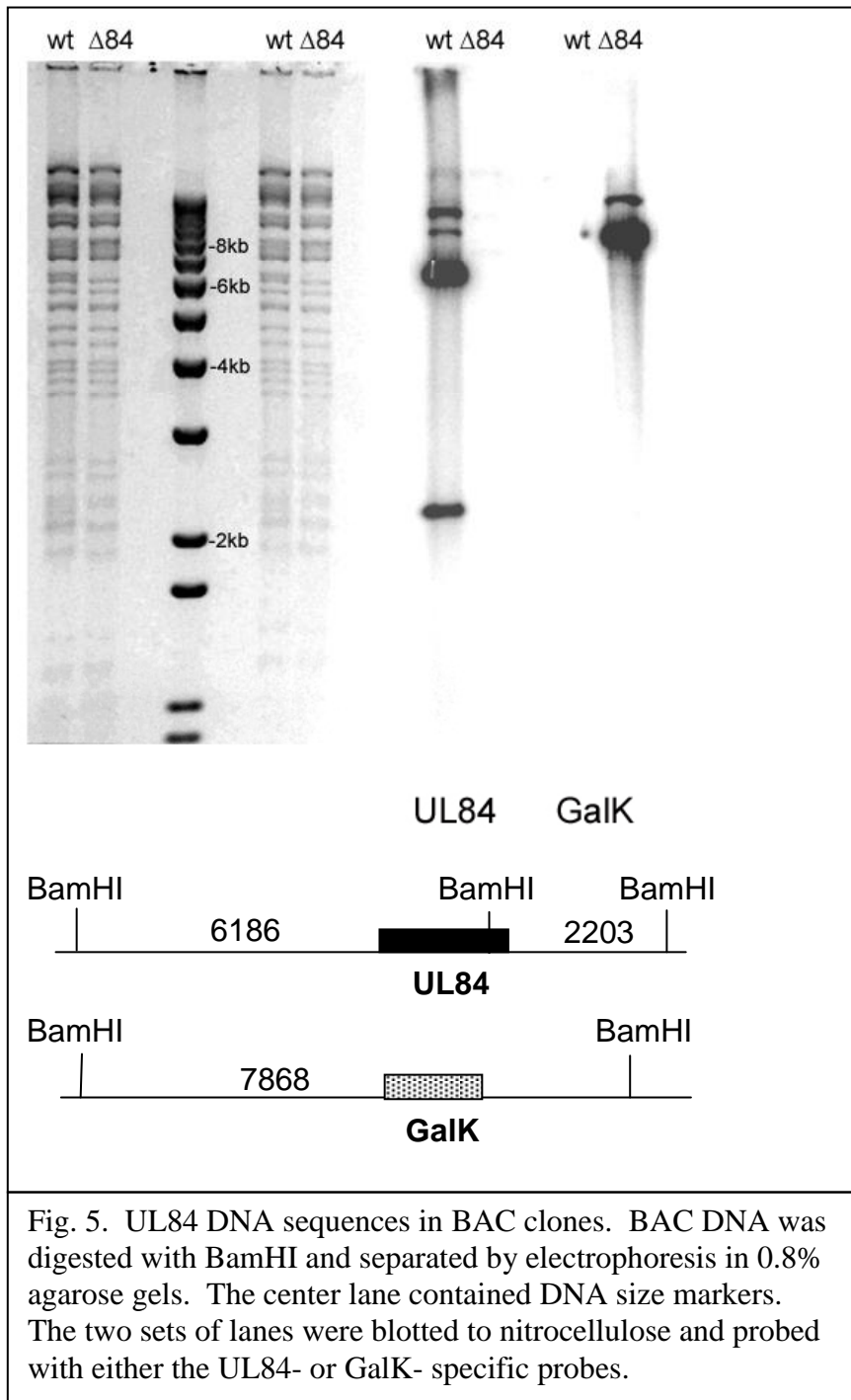


Fig. 5. UL84 DNA sequences in BAC clones. BAC DNA was digested with BamHI and separated by electrophoresis in 0.8% agarose gels. The center lane contained DNA size markers. The two sets of lanes were blotted to nitrocellulose and probed with either the UL84- or GalK- specific probes.

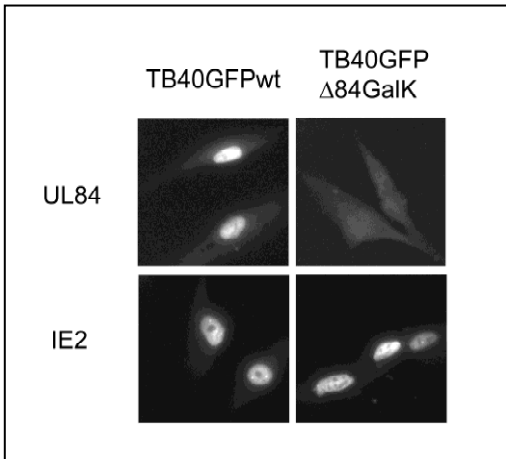


Fig. 6. Assay of UL84 expression in virus-infected cells by fluorescent antibody. MRC5 cells were infected with TB40GFPBAC (TB40) or TB40GFPBACΔ84GalK (Δ84) at a MOI of 0.1 - 0.5 and fixed at 24 hours post infection. Cells were stained with mAb 9G3 (UL84) or 3A9 (IE2) and images were captured with a 20X objective. No stained cells were observed in the samples infected with Δ84 and stained with 9G3. A representative field is shown to illustrate the background fluorescence.

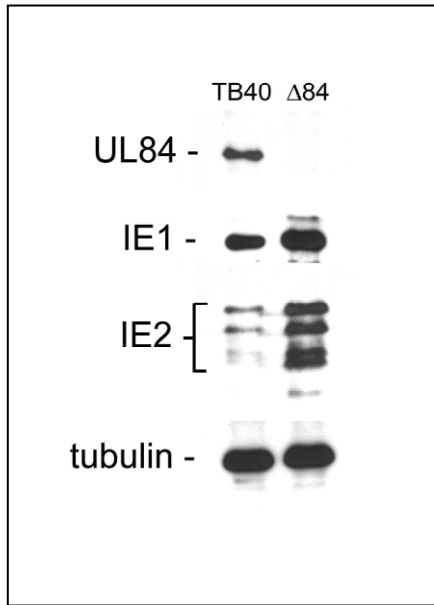


Fig. 7. Assay of protein expression in infected cells by immunoblotting. MRC5 cells were infected with TB40GFPBAC (TB40) or TB40GFPBACΔ84GalK (Δ84) at a MOI of 0.5 – 1.0, and extracts were prepared at 48 hours post infection. Blots were probed with mAb 9G3 (UL84), 3A9 (IE2), 1D12 (IE1), or anti-tubulin.

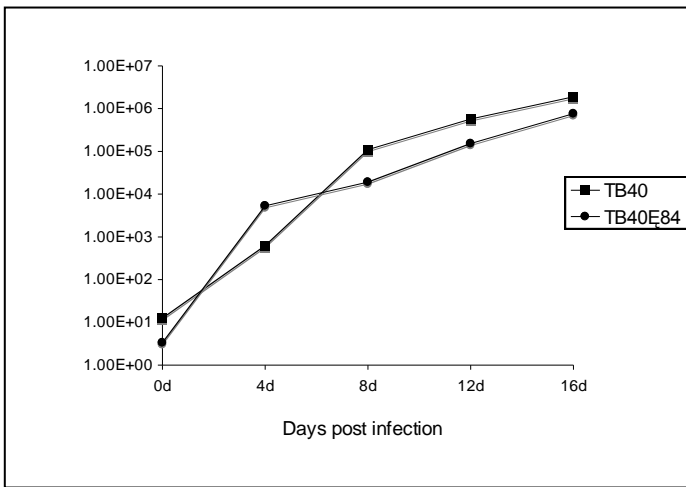


Fig. 8. Replication of a UL84-null strain of HCMV TB40. Growth curves were performed in infected MRC5 cells as described in Methods. A representative of three independent experiments is shown. TB40: TB40GFPBAC; TB40Δ84: TB40GFPBACΔ84GalK.

Research Project 32: Project Title and Purpose

Development of a Novel FdUMP Prodrug for Treatment of Breast Cancer - 5-Fluorouracil (5-FU) is one of the most active drugs in breast cancer chemotherapy. Studies have shown that the potency of 5-FU is mainly a result of the inhibitory effect by its metabolite FdUMP on the enzyme thymidylate synthase (TS). Conversion of 5-FU to FdUMP is very inefficient and requires multi-step enzymatic activation. This metabolic dependency often causes various resistance or toxicity to 5-FU and limits its clinical use. To offer more efficient and less toxic alternative of 5-FU, a novel agent FdTSP was designed to generate FdUMP in tumor cells through an enzyme-independent pathway and overcome the hydrophilicity of FdUMP that limits its entry into cells. The goal of this project is to establish the use of FdTSP as a superior alternative to 5-FU to treat breast cancer in an *in vitro* cell culture model.

Anticipated Duration of Project

11/24/2008 - 12/31/2010

Project Overview

The broad objective of this project is to investigate the potential use of a novel FdUMP prodrug, 5-fluoro-2'-deoxyuridin-5'-yl bis[2-(p-tolylsulfonyl)-1-methylethyl] phosphate (FdTSP) as a superior alternative to 5-fluorouracil (5-FU) for the treatment of breast cancer. We currently will focus on the evaluation of growth inhibitory effects of this agent in *in vitro* preclinical models. The *specific aims* of this study are, therefore: (1) to investigate the growth inhibitory effects of FdTSP in 5-FU sensitive and resistant human breast cancer MCF-7 cells; and (2) to investigate the activation of FdTSP in breast cancer cells.

Research Design and Methods:

(1) *Investigate the growth inhibitory effects of FdTSP in both 5-FU sensitive and resistant human breast cancer cells.* (a) Synthesis of FdTSP. We will synthesize FdTSP according to our published procedures which basically utilized a phosphoramidite P(III) chemistry approach. (b) Cell culture and RT-PCR. The human breast cancer MCF-7 will be used to test the growth inhibitory activity of FdTSP. 5-FU resistant cell lines will be prepared by treatment of MCF-7 cells continuously with stepwise-increasing concentrations of 5-FU every 2 weeks up to 200 µg/mL. 5-FU resistant clones will be selected and subcultured. To identify the possible mechanisms of 5-FU resistance, the expressions of genes involved in 5-FU metabolism that might be altered by exposure of the cells to 5-FU will be examined by reverse transcriptase-polymerase chain reaction (RT-PCR). (c) Growth inhibition assay. The growth inhibitory effect of FdTSP will be conducted using MTS assay and the results will be compared to that of 5-FU in 5-FU sensitive and resistant MCF-7 cells.

(2) *Investigate the activation of FdTSP in breast cancer cells.* For FdTSP to serve as a FdUMP prodrug against breast cancer, it needs to enter the tumor cells and then release FdUMP intracellularly. Therefore, we will examine the activation of FdTSP in breast cancer cells by measuring the levels of FdTSP, FdUMP and its decomposing byproduct vinylsulfone. The levels

of these compounds will be determined by HPLC and LC-MS/MS methods.

Principal Investigator

Yuan-Wan Sun, PhD
Research Associate
Penn State University College of Medicine
H171, Department of Biochemistry & Molecular Biology
500 University Drive
Hershey, PA 17033

Other Participating Researchers

Allan Lipton, MD – employed by Penn State University College of Medicine

Expected Research Outcomes and Benefits

Despite advances in chemotherapy, 5-fluorouracil (5-FU) has remained as a standard chemotherapy in the treatment of breast cancer for over four decades. The potency of 5-FU has prompted studies on the mechanism of action of this drug, which is mainly through the inhibition of thymidylate synthase (TS) by its metabolite 5-fluoro-2'-deoxyuridine-5'-monophosphate (FdUMP). The requirements for antitumor activity of 5-FU are (1) the achievement of sufficient concentrations of active metabolite FdUMP in tumor cells and (2) the maximum inhibition of TS. Attempts at improving the efficacy of 5-FU have been achieved through the combination with biochemical modulators and the development of infused 5-FU/LV regimens and oral prodrugs of 5-FU [e.g., capecitabine (Xeloda®)] to increase the bioavailability of 5-FU. However, use of 5-FU is still limited by its toxicity and resistance, which can be mainly attributed to dependency or aberrations in its metabolism.

Direct administration of FdUMP may offer therapeutic advantages over 5-FU or its oral prodrugs with respect to bypassing the multi-step enzymatic activation and possible toxic side effects caused by the incorporation of 5-FU into DNA or RNA. However, due to the presence of phosphate group in the structure, FdUMP does not enter the cells efficiently and is susceptible to be degraded extracellularly by phosphohydrolase, hampering its clinical use. The emergence of resistance to 5-FU, likely as a result of reduced metabolic activation to FdUMP in tumor cells, has prompted efforts to develop prodrug that release FdUMP intracellularly and bypass the requirement for metabolic activation. FdTSP has recently been developed by our group as a potential tumor-selective FdUMP prodrug. We expect that FdTSP will be effective against breast cancer and will be superior to 5-FU. Results of this study are requisite in providing a basis for further investigation of this drug in an *in vivo* preclinical study. Successful completion of this project may facilitate this class of anticancer agents to reach clinical application and provide more effective chemotherapeutics.

Summary of Research Completed

The major work completed in this period of time includes (1) development of 5-FU resistant human breast cancer MCF-7 cells (Aim 1b); (2) comparison of inhibitory activity of FdTSP (5-fluoro-2'-deoxyuridin-5'-yl bis[2-(p-tolylsulfonyl)-1-methylethyl] phosphate) and 5-FU against MCF-7 and 5-FU resistant MCF-7 cell lines (Aim 1c). The detailed methods and results are described as followed.

(1) Development of 5-FU resistant MCF-7 cell lines. Human breast cancer MCF-7 cell line was chosen because this cell line has been extensively studied and has shown sensitivity to 5-FU treatment. MCF-7 cell line was obtained from American Type Culture Collection (Rockville, MD) and maintained in IMDM media (Gibco-Invitrogen, Grand Island, NY) supplemented with 50 units/mL penicillin, 50 units/mL streptomycin and 10% (v/v) heat-inactivated fetal bovine serum (Gemini Bio-Products, Woodland, CA) at 37°C in a humidified atmosphere of 95% air and 5% CO₂. Confluent dishes of cells were treated with 0.05% trypsin (Gibco-Invitrogen) and counted by trypan blue dye exclusion method using a Bright-line Haemocytometer.

5-FU resistant MCF-7 cells were prepared by continuously treating cells with stepwise-increasing concentrations of 5-FU (Sigma-Aldrich, St. Louis, MO) every 2 weeks. We initiated the treatment with 0.2 µM of 5-FU dissolved in dimethyl sulfoxide (DMSO) followed by 0.5, 1, 1.5, 2, 2.5, 5, 7.5, 10, and 12.5 µM of the drug. 5-FU resistant clones were selected and subcultured. Cells were allowed to seed for at least 24 h before the next treatment. Cells exposed to 1.5, 2.5 and 12.5 µM of 5-FU were harvested and stored at liquid nitrogen in culture media containing 5% DMSO. These 5-FU resistant cell lines were assigned as MCF-7/FU1.5, MCF-7/FU2.5 and MCF-7/FU12.5, respectively.

(2) Comparison of inhibitory activity against MCF-7 and 5-FU resistant MCF-7 cell lines between FdTSP and 5-FU. Methods. A Sulforhodamine B (SRB) assay was performed to determine the growth inhibition activity of drugs. Cells were harvested and resuspended in culture media. Six thousand cells per well of a 96-well plate were seeded in culture media (100 µL) in a CO₂ incubator and incubated for at least 24 h before treatment. Cells were treated continuously with various concentrations of FdTSP or 5-FU for the indicated time in a total volume of 200 µL. Cells treated with DMSO were used as control. At the end of the incubation, cells in each well were fixed with 50 µL of 50% cold trichloroacetic acid and incubated at 4°C for 1 hour. The plates were washed five times with water and then air-dried. The fixed cells were then stained for 30 minutes with 100 µL of 0.4% sulforhodamine B solution in 1% acetic acid followed by washing with 1% acetic acid (5×) to remove unbound dye. The bound dye was dissolved with 10 mM Tris buffer and the absorbance of the resulting solution was measured at 570 nm. All treatments were performed at least in triplicate and at least three times.

Data analysis. For each experiment, the plot of percentage of cell survival vs. log concentration of drug was constructed. The drug concentration that produces a 50% reduction (IC₅₀) in cell survival was determined using a linear regression curve of the plot. From the resulting linear regression curve, the *x*-intercept (logIC₅₀) was calculated for each drug. In some experiments, selected data points were used to obtain a minimum Pearson correlation coefficient (*r*) value of 0.90.

Results. The growth inhibitory activity of FdTSP and 5-FU against MCF-7 and 5-FU resistant MCF-7 cell lines MCF-7/FU1.5, MCF-7/FU2.5 and MCF-7/FU12.5 were determined using sulforhodamine B assay. Initial studies were conducted to examine the time-dependent growth inhibitory effect of FdTSP in MCF-7 cells (Figure 1). Significant growth inhibition was observed after 4 days exposure to 0.01 μM of FdTSP. Based on our observations, we chose to determine the growth inhibition activity of FdTSP after 5 days of continuous drug exposure in all of the cell lines. Parallel experiments using 5-FU were performed for comparison.

A representative plot of cell survival vs. log concentration of drug was demonstrated in Figure 2. Our results showed that in all of the cell lines, FdTSP exerted more potent activity than 5-FU particularly at a concentration lower than IC_{50} (curves shift to right in 5FU treatments). As expected, all the 5-FU resistant cell lines were less sensitive to FdTSP treatments than MCF-7 cells; in addition, MCF-7/FU1.5 cells were more sensitive to FdTSP treatment than MCF-7/FU2.5 and MCF-7/FU12.5 cells. We also observed that MCF-7/FU12.5 and MCF-7/FU2.5 cells exhibited similar sensitivity to both FdTSP and 5-FU treatments despite a much higher concentration of 5-FU used in MCF-7/FU12.5 cell line to induce resistance. Although the characteristics of these cell lines remain to be determined (Aim 1b), it is speculated that 5-FU-induced elevation of target enzyme thymidylate synthase (TS) may reach a status of saturation.

It is also noted that the dose-response curves induced by FdTSP and 5-FU were different in all cell lines used in this study, indicating that different mechanisms of action or targets exist between these two drugs. Studies have shown that in addition to TS inhibition, incorporation of 5-FU into DNA/RNA contributes to the cytotoxicity of 5-FU. Since FdTSP is a specific inhibitor of TS, the dose-response curve induced by FdTSP may represent the growth inhibition effect induced by TS inhibition. Based on the values of IC_{50} determined in this study, FdTSP was more potent than 5-FU in all of the cell lines; FdTSP was about 200 \times more potent than 5-FU in MCF-7 cells, 76 \times more potent in MCF-7/FU/1.5, 3 \times more potent in MCF-7/FU/2.5 and 2.2 \times more potent in MCF-7/FU12.5 cells.

Figure 1. The time-dependent effect of FdTSP in MCF-7 cells

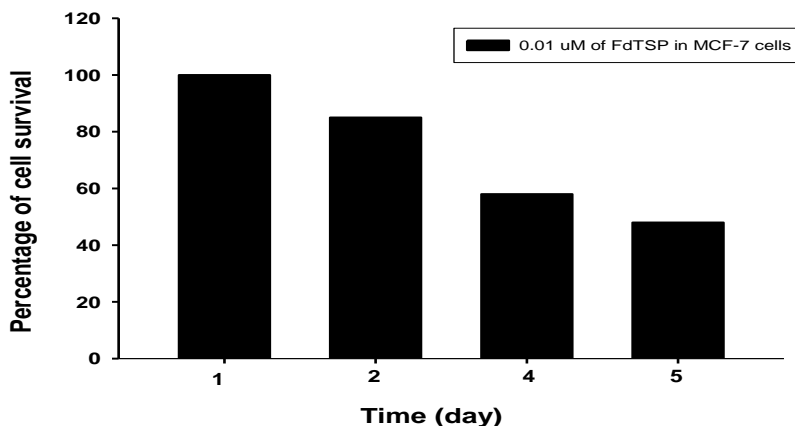


Figure 2. A representative plot of cell survival vs. log concentration of drug

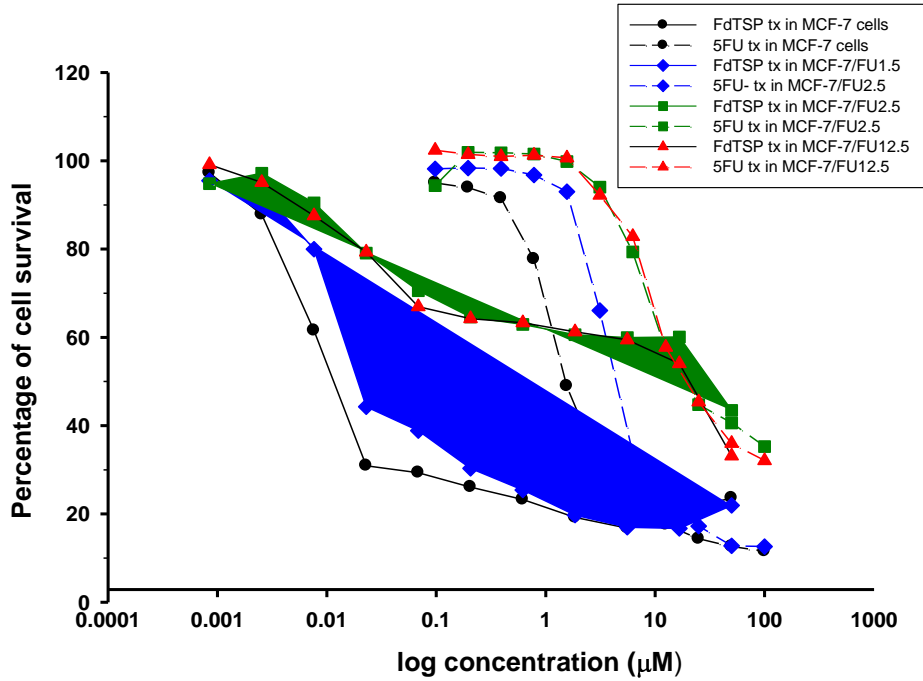


Table 1. IC₅₀ of FdTSP and 5FU in MCF-7 and 5FU resistant MCF-7 cells

Cell lines	IC ₅₀ (μM)	
	FdTSP	5-FU
MCF-7	0.016 ± 0.005	3.14 ± 0.09
MCF-7/FU1.5	0.11 ± 0.02	8.37 ± 0.37
MCF-7/FU2.5	11.13 ± 1.5	31.42 ± 3.58
MCF-7/FU12.5	12.95 ± 2.18	29.08 ± 5.01

*Results were quantitated from three independent experiments, and growth inhibition was determined by the SRB assay. Data are presented as means ± S.D.

Research Project 33: Project Title and Purpose

Antihypertensive Effects of Tetanic Baroreceptor Stimulation - The purpose of this project is to investigate the effect of brief high frequency carotid sinus baroreceptor stimulation on chronic blood pressure reduction in dogs.

Anticipated Duration of Project

11/24/2008 – 6/30/2011

Project Overview

Fifty million Americans suffer from hypertension, of which 66% are not adequately controlled and at least 10% are multi-drug resistant. Stimulation of pressure sensors in blood vessels, the baroreceptors, decreases blood pressure (BP); implantable electrical stimulators have been used to provide continuous baroreceptor activation. These devices effectively lower basal BP, but because constant stimulation disables endogenous mechanisms of BP regulation, subjects using these devices suffer compromised responses to orthostatic and other daily cardiovascular challenges. The continuous stimulation may also damage tissues. The objective of this project is to test an alternative strategy: long-term potentiation of the endogenous baroreflex mechanisms by occasional, brief high frequency (tetanic) stimulation of the baroafferent nerves.

The aortic depressor (ADN) and carotid sinus (CSN) nerves are the major baroafferent inputs carrying pressure signals from the baroreceptors to the brain. In the brainstem, the nucleus of solitary tract (NTS) is the first relay of the ADN and CSN signals. Recently, using a rat model, we showed that a brief tetanic stimulation of the ADN increased the size of subsequent ADN evoked responses in the NTS for 10-15 hours, which implies that following strong activation of the ADN, baroreflex depressor responses are enhanced; thus, brief baroreceptor nerve stimulation might ameliorate hypertension for many hours. In this project, we will systematically investigate the effects of CSN tetanus on basal BP in normotensive (Specific Aim 1) and obesity-induced hypertensive (Specific Aim 2) dogs. Four dogs will be used. In Aim 1, the protocol consists of 3 phases: Baseline (7 days), Tetanus (7 days), and Recovery (7 days). The tetanus phase consists of one daily bout of tetanus. In Aim 2, obesity hypertension will be induced over several weeks by a high fat diet; and then the protocol of Aim 1 will be repeated. We hypothesize that the seven successive daily tetanus applications will produce increasing basal BP reductions.

Principal Investigator

Xiaorui Tang, PhD
Assistant Professor
Penn State College of Medicine
Neural and Behavioral Sciences, Rm C1720
500 University Drive
Hershey, PA 17033

Other Participating Researchers

David Campbell, MD, Elizabeth Carney, DVM, Barry Dworkin, PhD, Alan Snyder, PhD - employed by Penn State College of Medicine

Expected Research Outcomes and Benefits

Expected Research Outcomes: We expect that one daily bout of high frequency (tetanic) carotid sinus baroreceptor afferent stimulation will produce increasing basal blood pressure reductions over the 7 experimental days.

Benefits: Occasional brief tetanic stimulation offers a new and effective clinical method for controlling hypertension, especially multi-drug resistant forms. In contrast to continuous stimulation, the method proposed would produce less tissue damage, and enhance, rather than diminish normal moment-to-moment baroreflex control of blood pressure, and better preserve the normal orthostatic and exercise regulation of blood pressure. The proposed method naturally lends itself to an extremely compact, electrically passive (no battery), implantable baroafferent nerve stimulator, and the project's long-range goal is to develop such a device.

Summary of Research Completed

We have reached several milestones in the project development during the past 12 month. By working together with the comparative medicine department at the Penn State College of Medicine, we have overcome initial obstacles for setting up the dog experiment, and actually performed one dog surgery on June 2nd (Fig. 1). During the surgery, we were able to successfully record the blood pressure signal, and deliver current pulse to stimulate the vagus nerve (see Fig. 2).

In order to effectively and chronically stimulate the carotid sinus baroreceptors, we have thoroughly investigated stimulation electrodes used in clinical settings, and came up with several of our own designs of the electrodes (see Fig 3 below). Fig 3 B&C are the new stimulation electrodes we designed and fabricated during the last 12 month period. The goal of these electrode designs is for the success of the main theme of this current project, i.e., to investigate the effect of brief high frequency carotid sinus baroreceptor stimulation on chronic blood pressure reduction in dogs.

Nevertheless, despite the substantial effort our research team had invested, and the substantial progress we made during the past 12 months, we have not completely mastered the preparation. We have already arranged a second surgery on June 29th. We will continue to make progress during the next 12 months, and aim to successfully complete the project by June 30th, 2011.



(A)



(B)

Fig. 1 (A) Surgical preparation (B) Carotid sinus stimulation tests

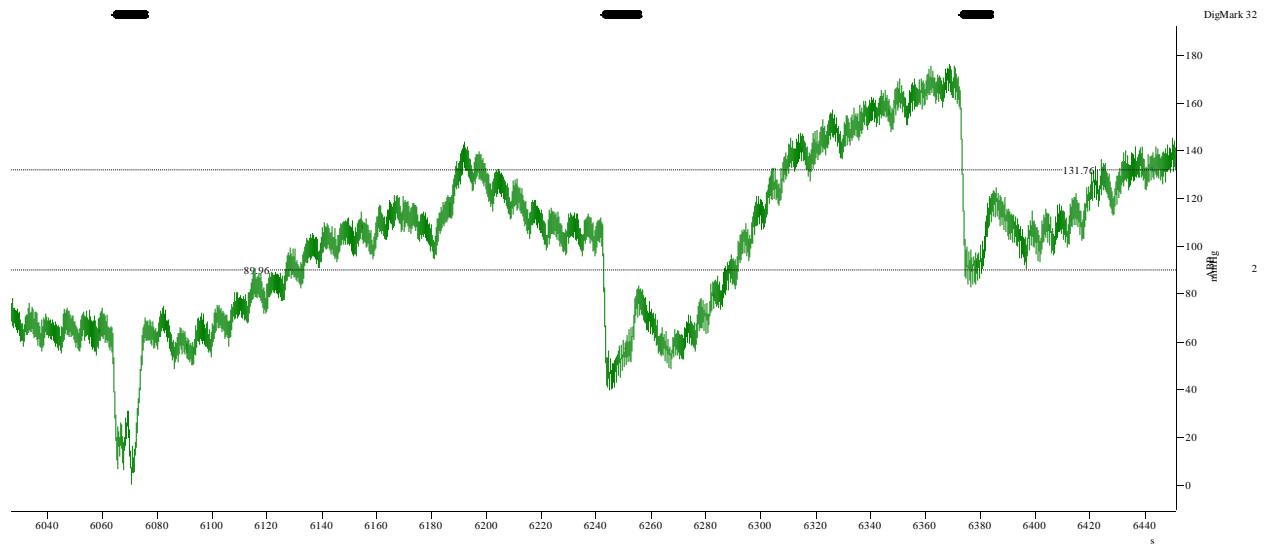


Fig. 2 Blood pressure responses to electrical stimulation of the vagus nerve in dogs. ABP: arterial blood pressure. The black bars above indicate the stimulation onset period. Electrical stimulation of the vagus nerve elicited a substantial blood pressure reduction.

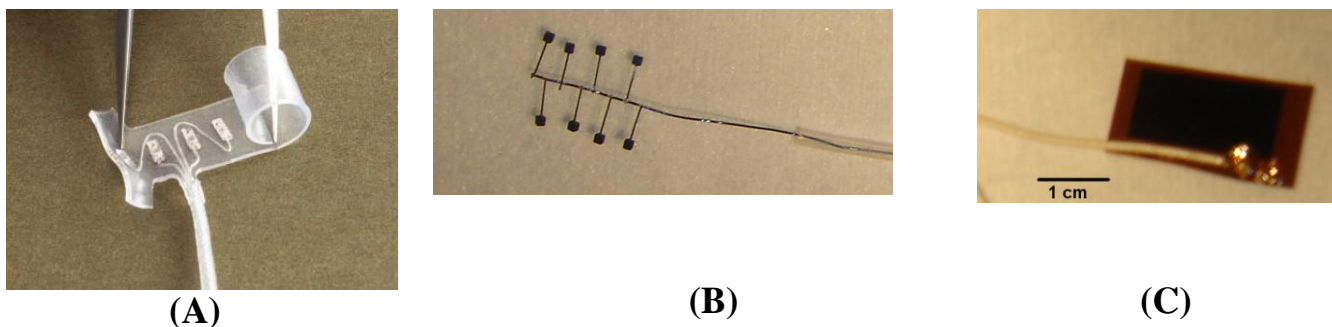


Fig. 3 (A) A commercially available spiral electrode (Ardiem Medical, Inc) we used to stimulate the vagus nerve and elicit blood pressure responses in Fig. 2. (B) A new TaTa₂O₅ electrode array we designed and fabricated during the past 12 month for the carotid sinus stimulation in dogs. (C) A TaTa₂O₅ thin film electrode we designed and fabricated during the last 12 month for the carotid sinus stimulation in dogs.

Research Project 34: Project Title and Purpose

The Role of STAT1 Inactivation in the Development of Inflammatory Bowel Disease - The overall goal of this project is to elucidate the role of STAT1 and STAT3 signaling in inflammatory bowel disease (IBD) development. Our specific hypothesis for this project is that neutralization of interferon-gamma in a STAT3 deficient IBD model will reduce STAT1 activation and prevent IBD development. Our STAT3KO and STAT1/3KO double deficient model will provide a unique system to explore the downstream target genes for future exploration as novel therapeutics.

Duration of Project

7/1/2009 - 6/30/2010

Project Overview

Crohn's disease (CD), one of the inflammatory bowel diseases (IBD), is an immune-mediated inflammatory disease of the intestinal tract. IBD affects approximately 5 per 100,000 people in the United States with a peak onset between 15-30 years of age, and the etiology(s) are unknown. Currently, there is no known cure or method by which to prevent the development of CD. Interferon gamma (IFN γ) has been shown to be increased in the intestinal tissue in patients with CD and has been targeted with some success for therapeutic intervention with Fontolizumab, a humanized monoclonal antibody to IFN γ . Experimental IBD phenotypes are also significantly inhibited in IFN γ deficient mice suggesting a role for IFN γ in the pathogenesis of IBD. In addition, many IFN γ inducible genes, such as CXCR3 in CD4⁺ T cells and CXCL11 in monocytes, may play essential roles in IBD pathogenesis. Most of the genes induced by IFN γ are transcriptionally regulated by the signal transducers and activators of the transcription (STAT) gene family, specifically STAT1 and STAT3 are the major signaling mediators for IFN γ signaling. Our previous study indicated that specific STAT3 deletion in bone marrow cells in mice (STAT3KO) caused a CD-like pathogenesis in both the small and large intestine, and an over-production of pro-inflammatory cytokines IFN γ and tumor necrosis factor alpha (TNF α). Our recent study shows that additional inactivation of STAT1 by gene targeting deficiency in the

STAT3 deficient mouse (STAT1/3KO) prevented the CD-like phenotype, indicating that a balance of STAT1 and 3 is sufficient for IBD pathogenesis. Therefore, our overall hypothesis for this project is that neutralization of interferon-gamma in the STAT3 deficient IBD model will reduce STAT1 activation and prevent IBD development. Our STAT1/3KO double deficient model will provide a unique system to explore the downstream target genes for future exploration as novel therapeutics.

Two specific aims are proposed in this study. 1) To demonstrate the efficacy of IFN γ neutralization in preventing Crohn's disease-like phenotype in the hematopoietic specific STAT3 deficient mice; and 2) To identify the downstream targets of STAT1 in T lymphocytes and macrophages by inactivation of STAT1 signaling in hematopoietic specific STAT3 deficient mice. The innovation of this project is that it uses a spontaneous mouse model of CD that clinically resembles the disease in human patients. The results will become the part of the preliminary data for an external grant application. Furthermore, inhibition of STAT1 could become a new target for treatment of IBD.

Principal Investigator

Samuel Shao-Min Zhang, MD, PhD
Assistant Professor
Penn State University Hershey
500 University Drive, H109
Hershey, PA 17033

Other Participating Researchers

Lisa S. Poritz, MD – employed by Penn State University Hershey

Expected Research Outcomes and Benefits

We envision the following subsequent experiments based on the results of our current project:

1. Bone marrow transplantation from STAT3KO into irradiated wild type mice and the converse (bone marrow transplantation from wild type mice into irradiated STAT3KO mice). This will help delineate which cell population (lymphoid vs. epithelial) plays the most important role in the development of intestinal inflammation in the STAT3KO mouse.
2. Development and use of specific STAT1 inhibitors to prevent the development of the intestinal inflammation in the STAT3KO mouse.

If a specific STAT1 inhibitor is discovered in the mouse system we will study in this project, we believe it will provide a new therapeutical target of IBD and eventually for treatment of Crohn's disease in humans.

Summary of Research Completed

1. Generation of hematopoietic specific STAT3 deficient animals:

Our lab has generated a tissue specific STAT3 deficient mouse model, where STAT3 has been deleted within bone marrow hematopoietic stem cells using Cre-Lox recombination. Exons 18-20 encode the Src homology 2 (SH2) domain of STAT3 and are responsible for the protein's function. Flanking the SH2 domain, exons 18-20, with a loxP (locus of x over P1) recognition signal targets the molecules for deletion through recombination of the DNA which is catalyzed by the Cre (cyclization recombination) protein. As a result of breeding a bone marrow (B)-TIE2 promoter driven Cre recombinase gene targeted mouse with a STAT3 lox-P (F/F) mouse we created a conditional (specific to hematopoietic stem cells) STAT3 deficiency (Fig. 1). This animal model is referred to as a STAT3 CFF mouse because contains a homozygous allelic deletion of the SH2 domain (STAT3-loxPF/F) and a heterozygous C allele (Cre+/- gene, Fig. 2). This STAT3 CFF mouse is good for in vivo studies because it exhibits a spontaneous Crohn's-like pathogenesis. The Cre expression is regulated under a tissue specific Tie2-promotor which is a cell surface tyrosine kinase-like receptor expressed during hematopoiesis.

2. Analysis of Crohn's disease-like phenotypes in BALB/c background STAT3 deficient mice:

Gross observations of the BALB/cTie2Cre⁺STAT3FF (STAT3CFF) mice demonstrated a significant reduction in length, body and carcass weights when compared to wild type and to STAT1^(-/-) mice (Fig. 3). The mice became lethargic and showed clinical signs of illness. Some mice were withdrawn from their littermates within the cage and hypoactive. They appeared unkempt with scruffy fur and slight porphyrin staining around their eyes and nostrils. At approximately eight weeks of age, once the spontaneous colitis was severe, the posture of the mice became hunched and their anogenital areas were soiled and some presented with rectal prolapse.

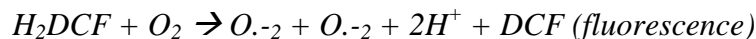
Although it was apparent that the upper GI (stomach and small intestine) were reduced in the STAT3CFF mice, the most drastic developmental differences were demonstrated in the cecum (Fig. 4). The cecum was stunted within the STAT3CFF mice and slightly elongated in the STAT1^(-/-) mice. The colon of the STAT3CFF mice was also shorter and thicker in comparison with the wild type mice. The formation of fecal pellets was reduced in STAT3CFF mice; instead the colon was more gaseous. An increase in circulating granulocytes was present within the peripheral blood of STAT3CFF mice, namely circulating monocytes and eosinophils (Fig. 5).

3. Analysis of macrophage functions under STAT1 and STAT3 deficient conditions:

Macrophage Isolation and Purification: Resident peritoneal macrophages were collected from mouse peritoneal exudates. Once euthanized with CO₂ asphyxiation the mice were sterilized with 70% ethanol and injected with ~10mL of cold, sterile phosphate buffer solution (PBS). After a 10 second gentle shaking, the peritoneal exudate was collected in a clean, sterile 5mL syringe and stored in a 15mL tube held on ice until use. Macrophages for functional assays were washed with chilled sterile 1xPBS and used immediately. The cells were plated at 1x10⁶ cell/ml and allowed to adhere. Once adherent the cells were washed with sterile 1XPBS and grown in macrophage culture medium [RPMI 1640 media supplemented with 2mM glutamine, 20mM HEPES, 10% heat-inactivated FCS, 50IU penicillin, 50ug streptomycin (MP Biomedicals, 200x Penicillin-Streptomycin), gentamicin and amphotericin B]. The adherent cells constituted 90-

95% of F480⁺CD11b⁺ macrophages. The peritoneal exudates macrophages (PEMs) were trypsinized, washed and subsequently analyzed by flow cytometry for characterization (Fig. 6).

FcγR-Mediated Phagocytosis – FcOxyBURST® Assay: FcγR-mediated phagocytosis was measured by the internalization of immune complexes prior to an oxidative burst in the phagosomal vacuole of freshly collected peritoneal macrophage exudates. The immune complexes were probes with the FcOxyBURST® assay from the company Molecular Probes. The reagent consists of insoluble BSA-anti-BSA immune complexes that are covalently labeled with dichlorodihydrofluorescein (H₂DCF). Once ingested the oxidation of the H₂DCF to DCF in the phagosomal vesicle produces a green fluorescence that can be monitored by flow cytometry.



Fresh PEMs were isolated and resuspended in glucose-PBS in preparation for the assay. Kreb's Ringer's PBS (KRP buffer: 1.0mM Ca²⁺, 1.5mM Mg²⁺ and 5.5mM glucose) was prewarmed to 37°C and used to resuspend the PEMs 30mins prior to flow analysis. Baseline measurements were taken and then the immune complexes were added. Fluorescence related to the oxidation of the FcOxyBURST was assayed by flow cytometry using a FACSCalibur every 30sec for 2mins. The cell suspension was then incubated for 30mins and reread. STAT3CFF mice show a reduction in the FcγR-mediated phagocytosis (Fig. 7).

Fluid Phase Endocytosis – FITC-Dextran Suspension Assay: Pooled peritoneal macrophages were incubated with FITC-Dextran (M.W. 40kDa; Sigma) for 30 minutes at 37°C or at 4°C. The cells were then washed with PBS three times and either plated at 1.2 x 10⁵ cells/well in 96 well plates or prepared for analysis on the FACSCalibur. The concentration of FITC-Dextran ingested was determined and analyzed using a fluorescent microplate reader (Bio-Rad, Model 680XR) with 490 nm excitation and 520 nm emission. Serially diluted samples of the marker were used as a standard. Fluid phase endocytosis is significantly reduced in STAT3CFF macrophages (Fig. 8)

Generation of Reactive Oxidative Species – Nitroblue Tetrazolium Reduction Assay: This assay measures the metabolic activity of phagocytes through a non-specific response to nitroblue tetrazolium (NBT); its focus is on the ability to produce oxygen radicals (O⁻² and OH⁻) and the reduction of tetrazolium dye to an insoluble formazan. NAD(P)H, ROIs and reactive oxidative species production are reduced in STAT3CFF macrophages (Fig. 9).

4. Analysis of Th1 and Th2 cytokines in STAT1 and STAT3 deficient animals:

Cytokines are small signaling molecules that allow cells within the immune system to communicate and respond to specific stimuli. Regulating cytokine signaling pathways plays a critical role in the pathogenesis of inflammatory bowel disease. Signal transducers and activators of transcription (STAT) proteins that respond to cytokine signaling, phosphorylate, dimerize and translocate into the nucleus from their latent cytoplasmic location to induce gene transcription of additional cytokines and chemokines. The Bio-plex® Bio-Rad cytokine assay utilizes the luminex system to analyze 25 cytokines and chemokines simultaneously.

For systemic cytokine analysis terminal blood punctures collected approximately ~700ul of blood per animal. Peritoneal exudates macrophages were collected and cultured in RPMI 1640 until adherent. The supernatant was collected for analysis of cytokines produced by macrophages (Fig. 10).

Regulation of hematopoiesis and T cell proliferation (IL-1 α and IL-1 β) is considerably normal in Btie2Cre⁺STAT3FF when compared to wild type. Meanwhile significantly reduced systemic IL-2 suggests that the development and regulation of T cells is hindered in Btie2Cre⁺STAT3FF. Systemic increase in IL-23, IL-9 and IL-6 indicate that Btie2Cre⁺STAT3FF mice produce a Th17 polarized immune response. There is a decrease in production of IL-12p40 and IL-12p70 that contribute to a Th1 response. There is also a systemic decrease in IL-4 and IL-5 which are classical Th2 cytokines. Increased IL-23 and IL-9 are indicators of a Th17 polarized response.

Systemic elevations of GM-CSF, TNF α , and the chemokine KC (CXCL1) demonstrate an increase in granulocyte proliferation and recruitment. Serum levels of Btie2Cre⁺STAT3FF mice show that the chemokines responsible for granulocyte recruitment are elevated. Chemotactic cytokines (chemokines) are responsible for stimulating the migration and adherence of circulating leukocytes to the vascular endothelium. Systemic decreases of MCP-3 and IL-10 indicate that macrophage function is dysregulated.

Activation of hematopoietic stem cells and progenitors by IL-3 is not affected in macrophages, but the production of GM-CSF is significantly reduced. This indicates that the stimulation of progenitors to differentiate is normal but that the regulation and function of macrophages is defective. Production of IL-5 which stimulates eosinophil proliferation and basophil degranulation is elevated in Btie2Cre⁺STAT3FF macrophages. These granulocytes have vesicles full of cytokines and chemokines, and an increase in circulating eosinophils was previously demonstrated. This indicates that an increase in IL-5 contributes to the eosinophil accumulation.

Decreased macrophage production of IL-6 and IL-1 β demonstrate a dysregulation of the acute phase response. While an increase in MIP-1 α indicates that the defective granulocytes are being activated and contributing to neutrophilic inflammation. Decreased cytotoxic TNF α production in STAT3CFF macrophages suggests defective autocrine induced apoptosis.

5. Efficacy of IFN γ in involving in Crohn's disease-like phenotypes of STAT3 deficient animals:
In our pilot experiments, STAT3 deficient animals in C57BL/6 background showed a short lifetime (about or less than 4 weeks) due to a significant reduction of body weight and cachexia. Under this condition, we cannot perform a treatment of anti-IFN-gamma antibody for a sufficient time period. In the meantime, we have generated a STAT3 deficient strain in a BALB/c background and it had a longer lifetime of about 8-10 weeks with similar IBD-like phenotypes. Because of the animal breeding situation, we did not get enough numbers of STAT3 deficient animals for the experiments by the end of June 2010. We plan to continue our experiments on the effects of IFN γ on the STAT3 deficient animals with BALB/c background. This work may continue to the end of this year or into early next year depending on the numbers of STAT3 deficient animals we can generate using my other private funding.

Figure 1.

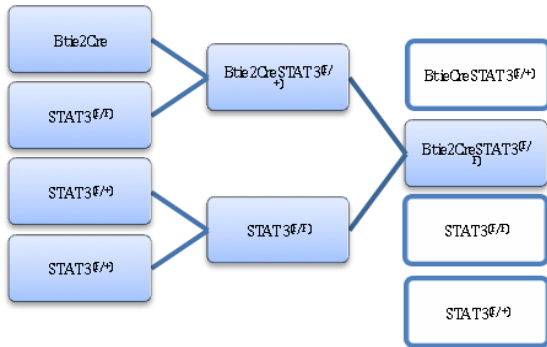


Figure 2.

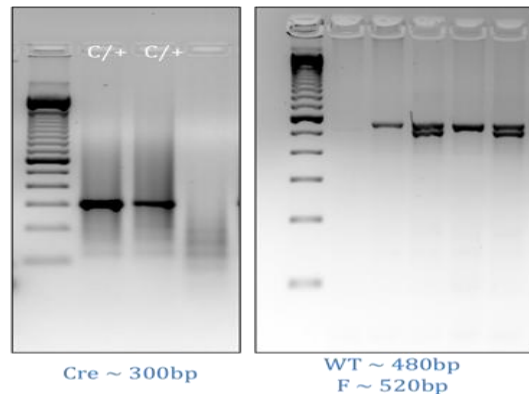


Figure 3.

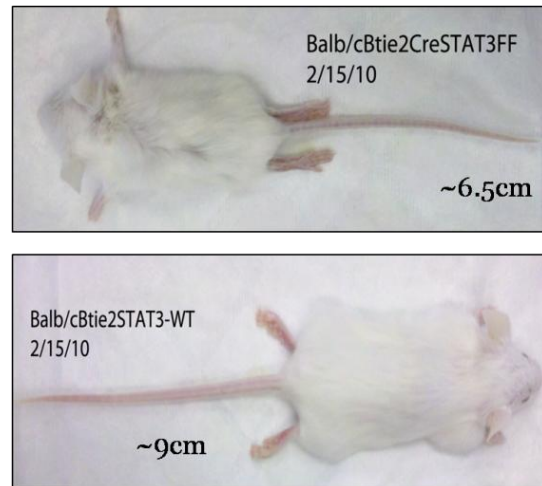
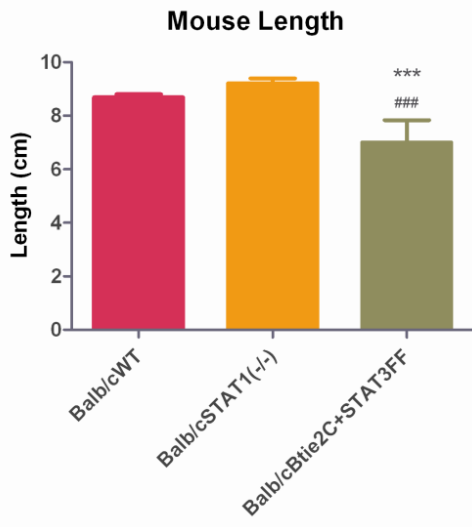


Figure 4.

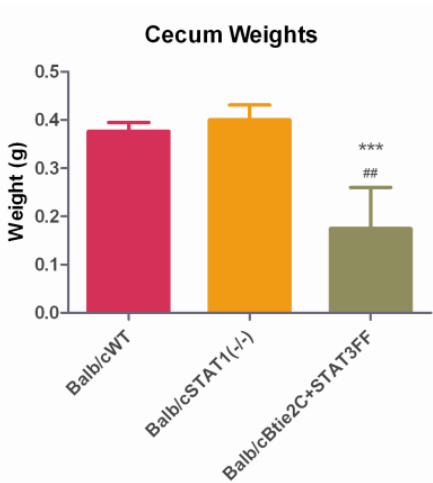


Figure 5.

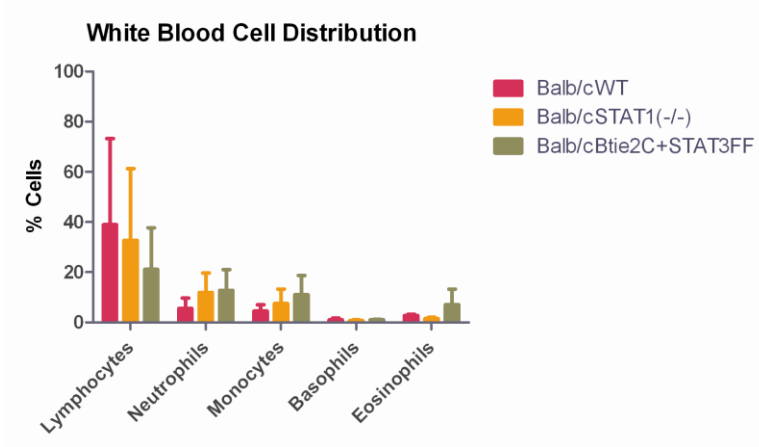


Figure 6.

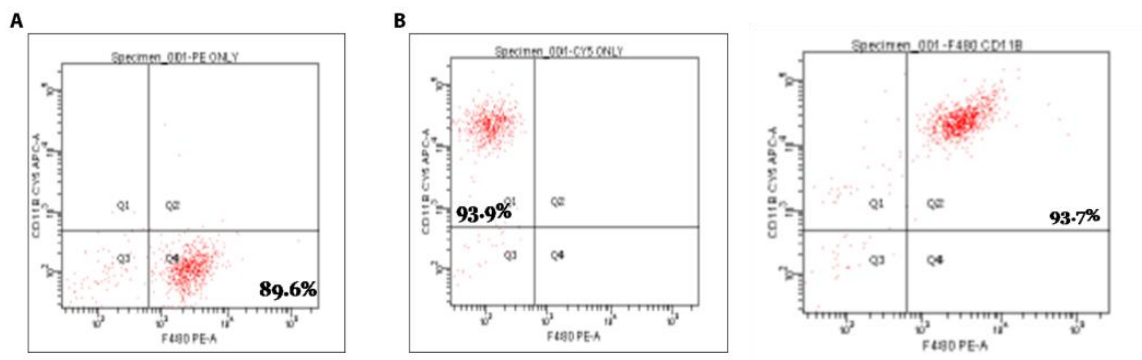


Figure 7.

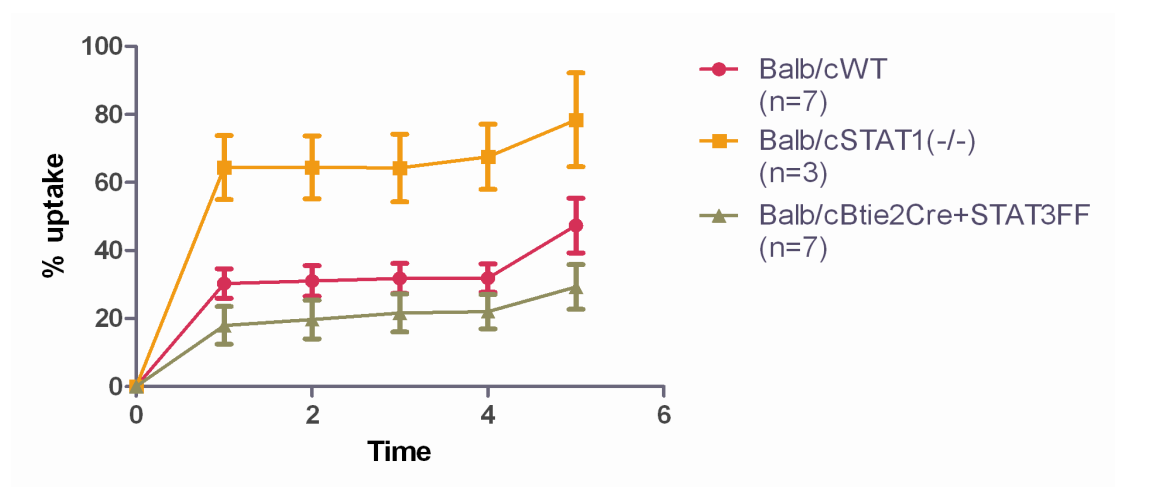


Figure 8.

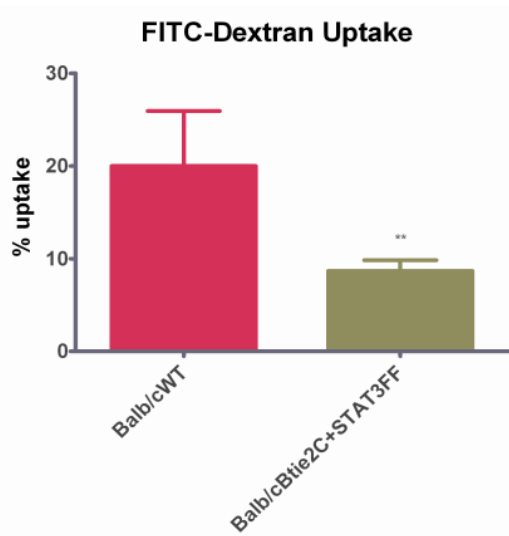


Figure 9.

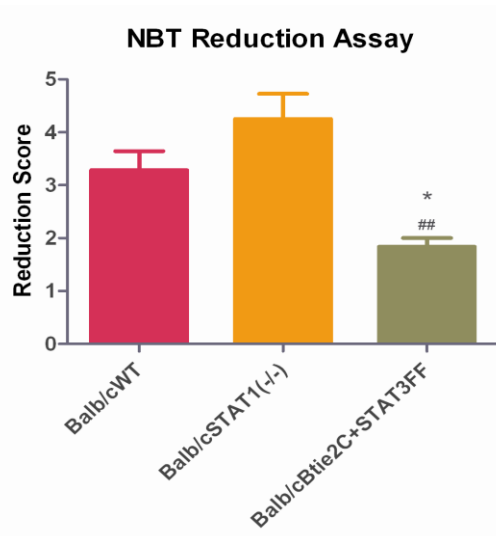
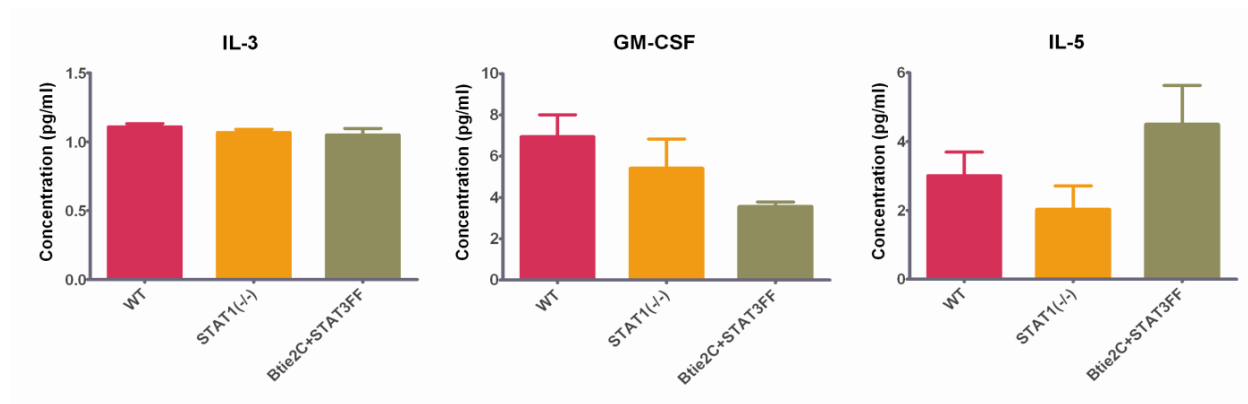


Figure 10.



Research Project 35: Project Title and Purpose

Effects of Early Diabetes on the Microvasculature: A Link between the Eye, Brain, and Heart?

The purpose of this project is to examine the relationship between blood vessel responses from the eye, brain, and heart to stimuli, which cause the vessel to get bigger (i.e., dilate) or smaller (i.e., constrict) in individuals with pre-diabetes and diabetes. Dysfunction of the eye's retinal blood vessels to dilate or constrict may prove to be a valid surrogate marker of stroke and heart disease. This project will use non-invasive Ultrasound Doppler to examine heart and brain blood flow and will use a novel tool known as the Dynamic Vessel Analyzer that allows direct visualization of the retinal blood vessels in healthy individuals and individuals with pre-diabetes and diabetes.

Anticipated Duration of Project

1/1/2009 - 6/30/2011

Project Overview

Diabetes causes functional impairment and structural damage of large and small vessels in multiple organ systems leading to vision loss, stroke, and myocardial infarction. Chronic hyperglycemia is associated with macrovascular dysfunction, but it is less well understood how the spectrum of glucose intolerance affects microvascular function of the eye, brain, and heart. Previous studies suggest that pre-diabetics may be at risk for vascular dysfunction, but this has not been well examined. It is also unclear whether or not the opposite spectrum of disease, diabetics with vascular complications, will result in a more severe vascular impairment. Therefore, the purpose of the study is to examine the relationship between changes in retinal, cerebral, and coronary vasoreactivity in patients with pre-diabetes and diabetes with and without vascular complications compared to age- and gender-matched healthy controls.

Specific Aim. To characterize microcirculatory vascular function (i.e., vasoconstriction and vasodilation) non-invasively in the cerebral, retinal, and coronary vascular beds along the spectrum of glucose dysregulation (healthy controls, impaired fasting glucose (IFG), type 2 diabetics without vascular complications, and type 2 diabetics with vascular complications) before and after hypocapnia and hypercapnia and flicker-light induced retinal vasodilation. We hypothesize that cerebral, coronary, and retinal vasoconstrictor and vasodilator responses during hypocapnia and hypercapnia, and flicker-induced retinal vasodilation will be attenuated in both pre-diabetic and diabetic groups compared to controls and that the degree of dysautoregulation worsens with disease progression.

Secondary Aim. It has been suggested that retinal blood vessels may be an index to the cerebral and coronary beds; however, examination of all three vascular beds simultaneously in the same subjects has not been explored. Thus, we seek to compare the degree of vascular regulation between these critical vascular beds for IFG and type 2 diabetics. We hypothesize that the degree of reactivity will be similar between the three vascular beds and between the groups, and the impairment of retinal vasoreactivity can predict the degree of vascular function of the brain and heart. We will use Doppler Ultrasound, and the Dynamic Vessel Analyzer (DVA), which is a relatively new diagnostic tool that allows direct visualization of the microcirculation of the retina. Retinal microvascular dysfunction may prove to be a valid surrogate marker of cerebrovascular and cardiovascular disease in chronic hyperglycemia, and could be a valuable tool to estimate the risk of stroke and myocardial infarction in this population.

Principal Investigators

Kerstin Bettermann, MD, PhD
Assistant Professor
Penn State Hershey Medical Center
Department of Neurology H037,
500 University Drive

Hershey, PA 17033

Mary Lott, PhD, MSN
Assistant Professor
Penn State Hershey Medical Center
Heart and Vascular Institute
500 University Drive
Hershey, PA 17033

Other Participating Researchers

Robert Gabbay, MD, Thomas Gardner, MD – employed by Penn State Hershey Medical Center

Expected Research Outcomes and Benefits

Individuals with diabetes are at an increased risk of stroke and developing heart and vascular disease. Chronic hyperglycemia (i.e., high glucose) is associated with vascular dysfunction and is suggested to be an early event in the atherosclerotic process. It is not clear when during the spectrum of glucose impairments the brain, eye, and heart vascular beds (i.e., cerebral, retinal, and coronary) become impaired and whether or not these changes are reversible by early treatment. Our expected outcomes are that blood vessel responses to dilator and constrictor stimuli will be impaired in early diabetic and diabetic individuals and that the degree of impairment will worsen with disease progression. This information is important to study so that interventions may be started early to delay or prevent strokes and heart attacks. Thus, the benefits of this study include providing: 1) non-invasive insight into retinal, cerebral, and coronary vascular function and their relationship to each other; and 2) potential valuable information regarding health and further advance our understanding of the impact of the spectrum of early diabetes on vascular reactivity in critical human blood vessels.

Summary of Research Completed

Methods

The studies are conducted in the General Clinical Research Center at Penn State College of Medicine. The methods of recruitment and informed consent procedures, and study group assignments have been reported in the previous progress report.

Measurements performed in this study have been previously described in detail.

Additionally the following *laboratory measurements* are obtained in all study participants: Total cholesterol, HDL, LDL, HDL/LDL ratio, Triglycerides, fasting Glucose, fasting Insulin, HbA_{1c}, hsCRP.

Experimental interventions and study protocols have been described in detail in our previous progress report:

The hypercapnia trials have been modified, now utilizing a clinically routinely used gas mixture of 5% CO₂, 95% room air instead of 5% CO₂ 95%O₂ resulting in more reproducible changes in

cerebral blood flow. We administer hypercapnic gas (5% CO₂) for 5 minutes. To minimize the risks of hypercapnia, oxygen saturation is continuously monitored and is not allowed to drop below 85% (normal is around 95%).

Milestones/Results

Continuing the project since January 2009 we have completed the following research using the Dynamic Retinal Vessel Analyzer: Thus far we have enrolled and completed measurements in 33 subjects. Nine additional subjects had to be excluded during the secondary study to meeting exclusion criteria. An in-service, additional staff training and data quality review by the manufacturer (Imedos, Jena, Germany) was performed in March 2010.

We have continued to examine the relationship between changes in retinal, cerebral, and coronary vasoreactivity in patients with pre-diabetes and type 2 diabetes with and without vascular complications compared to age and gender matched healthy controls (see Table 1 for subject demographics consisting of 9 controls, 2 prediabetics, 18 diabetics without complications and 4 diabetics with vascular complications).

1. Retinal Vessel Measurements

Results of retinal vasoreactivity measurements for each study group are summarized in figures 1-3. Early trend analysis indicates that the retinal artery responses to 100% oxygen may be attenuated in diabetics compared to healthy controls. There is also suggestion for an attenuated response in retinal arterial and venous vasoreactivity to light-flicker stimulation and hypercapnia indicating endothelial dysfunction in diabetics. Data using hyperventilation/breath hold as a stimulus for retinal vasoreactivity changes are currently being analyzed. There are too few data currently to allow further subgroup data analysis and we continue study subject enrollment. Additionally we are in process to analyze static retinal images for Arterial/Venous Ratios as an indicator of vascular risk.

2. Coronary and Cerebral Blood Flow Data

Our coronary and cerebral data is currently being examined. Thus far 10 subjects have completed data analysis of their coronary blood flow data with an additional 10 subjects currently being added. Statistical analysis is currently pending.

Preliminary analysis of a subset of our cerebral blood flow data (based on 21 individuals) suggests that diabetics may have a trend towards decreased cerebral vasoreactivity following hyperventilation/breathhold stimulation compared to controls (see figure 4). As the sample size is currently small, tests for significance are of very limited value.

As may be expected, duration and poor disease control seem to be associated with a greater degree of impairment in cerebral vasoreactivity (see figures 5 and 6), but a larger sample size will be required to confirm a potential association. The relation between cerebral and retinal blood vessel reactivity and cerebral vasoreactivity following hypercapnia, hyperoxia as well as additional ultrasound parameters will be explored as more data become available.

Publications and Presentations until June 2010

Lott MEJ, Bettermann K, Slocomb J, Smith J, Gabbay R, Gardner T. Retinal Reactivity in Type 2 Diabetes. Penn State Institute of Diabetes and Obesity, Wine and Cheese Forum, November 11, 2009.

Lott MEJ, Bettermann, K, Slocomb J, Smith J, Gabbay R, Gardner T. Retinal Reactivity in Type 2 Diabetes. Penn State Institute of Diabetes and Obesity, 2nd Annual Meeting, April 19, 2010.

Lott MEJ, Bettermann K, Slocomb J, Smith J, Gabbay R, Gardner T. Retinal Reactivity in Type 2 Diabetes. Experimental Biology, Anaheim, CA, April 24-28, Poster Presentation, 2010.

Bettermann K, Lott MEJ, Slocomb J, Patel S, Smith J, Gabbay R, Gardner T. Dynamic Retinal Vessel Analysis in Diabetes. Mid-Atlantic Ophthalmic Imaging Update, Penn State College of Medicine, March 27, 2010.

Bettermann K, Lott MEJ, Slocomb J, Patel S, Smith J, Gabbay R, Gardner T. Retinal Dynamic Vessel Analysis in Diabetes and Vascular Disease Frontiers in Eye and Vision Research Lecture, April 22nd 2010.

Table 1: Subject Demographics

Subjects	Number	Age	BMI	SBP	DBP	IOP
Healthy Controls	9	58 ± 12	28.8 ± 4.3	122 ± 12	76 ± 7	14 ± 3
Pre-Diabetic	2	58 ± 12	25.2 ± 5.0	133 ± 1	82 ± 4	13.5 ± 1
Type 2 Diabetic	18	56 ± 8	31.3 ± 5.5	132 ± 18	76 ± 10	17 ± 2
Type 2 Diabetic with Complications	4	67 ± 2	28.2 ± 2.0	123 ± 7	66 ± 4	14 ± 2

SD = Standard deviation

Complications = history of angina, myocardial infarction, or stroke

NOTE: Not included in the above numbers are 9 withdrawals due to either blood sugar, resting blood pressure, cholesterol, or IOP too high or inability to fixate using the eye device.

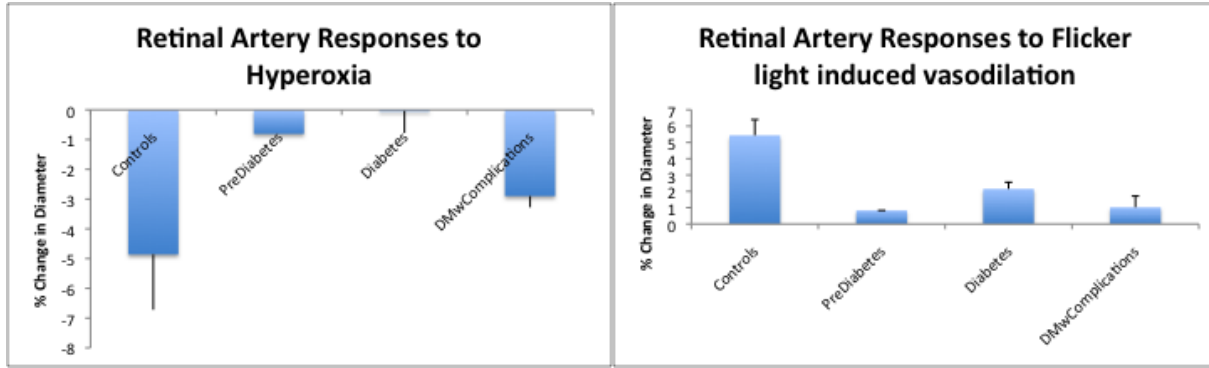


Figure 1. Retinal artery (left) and vein (right) responses to hyperoxia (100% oxygen) in healthy controls (n=9), prediabetics (n=1), type 2 diabetics without complications (n=16), and type 2 diabetics with complications. (n=4).

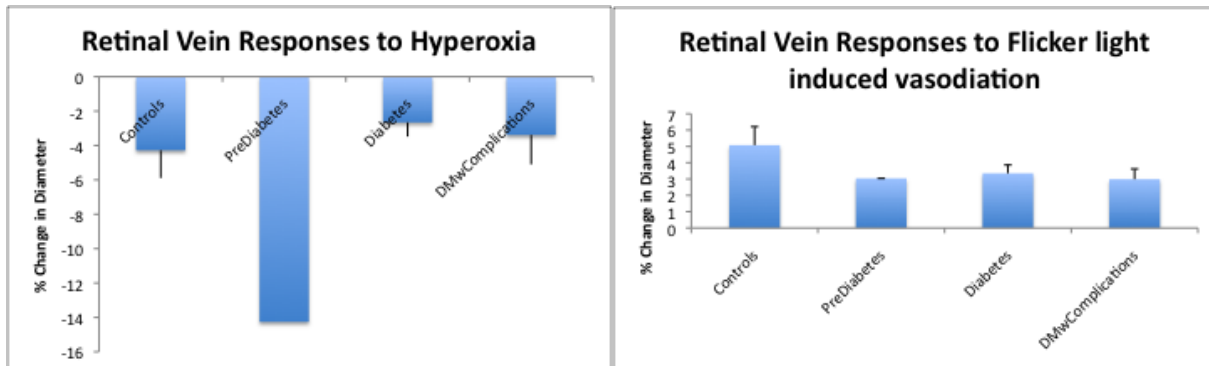


Figure 2. Retinal artery (left) and vein (right) responses to flicker light induced vasodilation in healthy controls (n=9), prediabetics (n=1), type 2 diabetics without complications (n=18), and type 2 diabetics with complications (n=4).

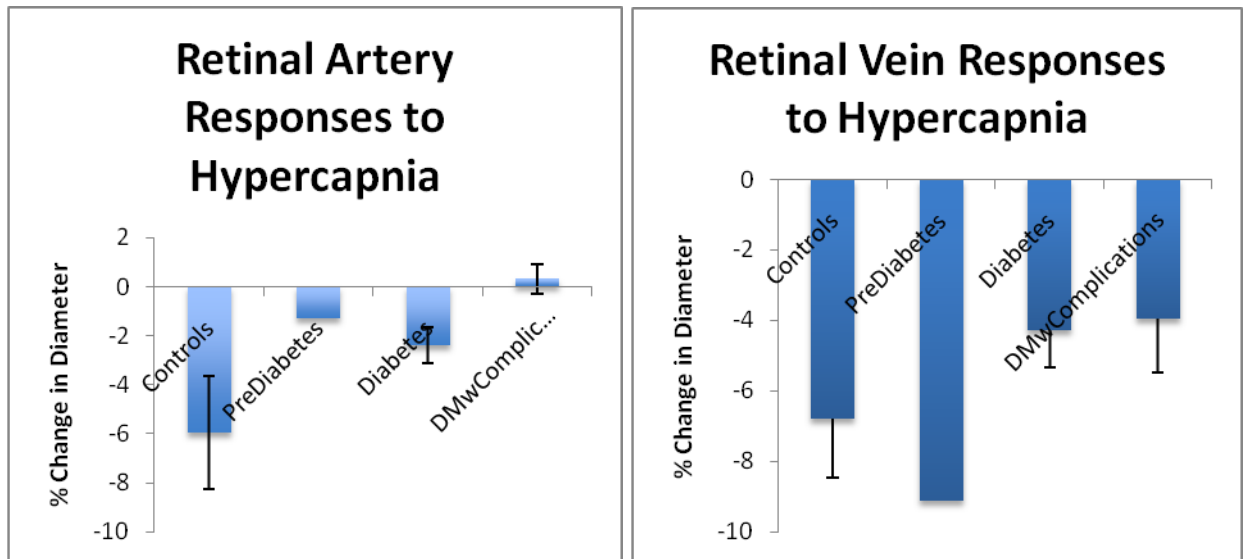


Figure 3. Retinal artery (left) and vein (right) responses to hypercapnia (5% CO₂, 95% O₂) in healthy controls (n=9), prediabetics (n=1), type 2 diabetics without complications (n=18), and type 2 diabetics with complications (n=4).

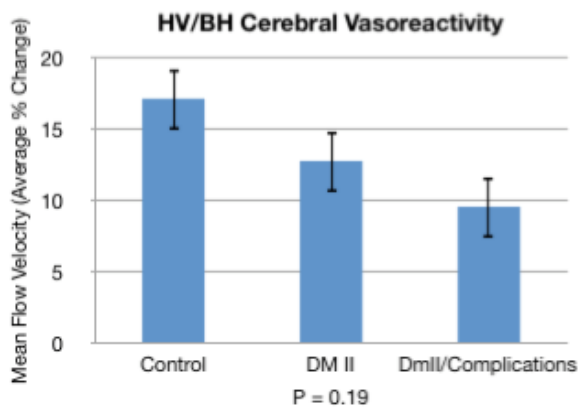


Figure 4: Cerebral vasoreactivity following hyperventilation/breathhold stimulation in healthy controls (6), type 2 diabetics without complications (11) and type 2 diabetics with vascular complications (4). Tamax=Maximal change in mean cerebral blood flow velocity of the middle cerebral artery (in%) following stimulation compared to baseline.

Diabetes Control (HbA1c Values) and Cerebral Vasoreactivity

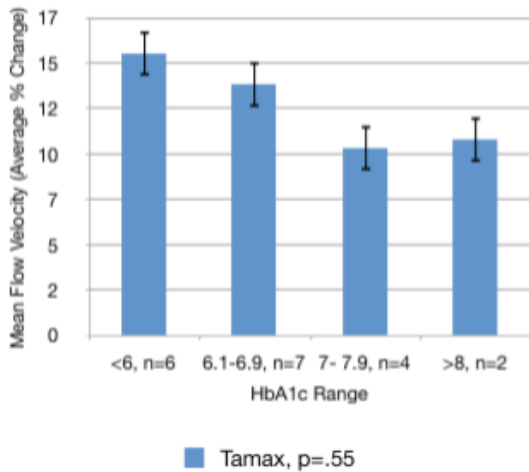


Figure 5: Cerebral vasoreactivity following hyperventilation/breathhold stimulation in healthy controls (6), and type 2 diabetics with various degrees of diabetes control measured by HbA_{1c} (13). Tamax=Maximal change in mean cerebral blood flow velocity of the middle cerebral artery (in %) following stimulation compared to baseline. In diabetics there may be an association between diabetes control and degree of cerebral vasoreactivity impairment.

Diabetes Duration and Cerebral Vasoreactivity

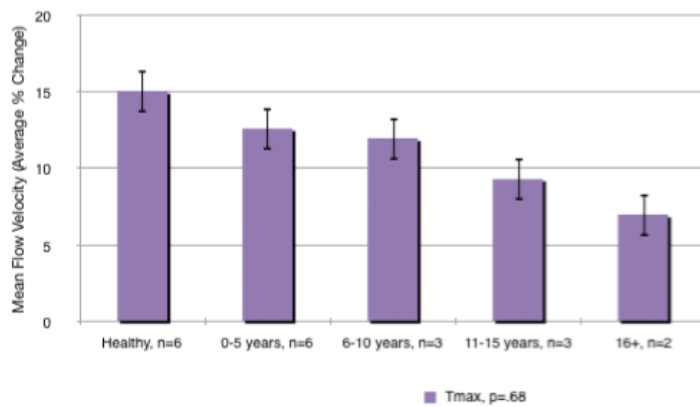


Figure 6: Cerebral vasoreactivity following hyperventilation/breathhold stimulation in healthy controls (6), and diabetics with various disease durations (14). Tamax=Maximal change in mean cerebral blood flow velocity of the middle cerebral artery (in %) following stimulation compared to baseline. In diabetics there may be a linear association between disease duration and the degree of cerebral vasoreactivity impairment.

Research Project 36: Project Title and Purpose

Adapting an RNA Sensor Platform to Protein Detection Using Aptamers - We are developing a chip-based RNA sensor, with the initial application for detection of circulating tumor cells (CTCs) in the blood of patients. This device utilizes antisense oligonucleotides (ASOs) targeted

to selected cancer-related RNA molecules. Nanowires (NWs) are functionalized with an ASO, and the selected marker RNAs are hybridized to the functionalized NWs. A second ASO, targeted to another site on the marker, is attached to Au particles, and in turn hybridized to the marker RNA bound to the NWs, forming a “hybridization sandwich”. This binding causes a shift in the resonance frequency of the NWs, which can easily be detected. We have shown that derivatized NWs remain functional throughout conditions necessary for “bottom-up” assembly, allowing multiplexing for many different markers. While this platform is being developed, we have initiated a Clinical Trial with melanoma patients, where CTCs are harvested; melanoma marker RNAs are initially being detected using real-time PCR, and the balance of the samples are being banked for subsequent detection when the chip-based RNA sensor is ready.

Anticipated Duration of Project

11/24/2008 - 12/31/2010

Project Overview

The broad objective of this project is to extend the functionality of our sensor to the detection of proteins. We propose to: 1) use our Sequential Evolution of Ligands by Exponential Enrichment (SELEX)-based library selection technology to identify aptamers (short 30-mer DNA oligonucleotides) which bind with high affinity to melanoma protein markers circulating in blood; 2) characterize the binding of these aptamers and identify the best pair which bind the melanoma markers in the “sandwich” format; and 3) use these aptamers to quantify levels of melanoma markers in serum from melanoma patients, and relate marker levels to levels of CTCs in our ongoing Clinical Trial. As with the RNA-based studies, we propose initially to quantify the melanoma protein markers using conventional ELISA, as well as with optical (fluorescence-based) methods off-chip using spotted arrays (the same coupling chemistry as with NWs is used), while banking the plasma specimens for later benchmarking with the chip-based sensor.

Research Design and Methods. This work will utilize blood from melanoma patients being collected in a Clinical Trial. In that trial, blood is fractionated using “OncoQuick” porous barrier gradient centrifugation tubes. The CTCs are collected from the interface of the buffer above the porous membrane. The liquid fraction above the interface is plasma, which we will also collect, and we will determine if removal of albumin and immunoglobulins adds sensitivity. The melanoma marker to be interrogated is S100B, which has been selected based on literature review. S100B will be expressed from recombinant DNA clones, and our novel primer-free library selection technology will be used to identify high affinity aptamers from a random 30-mer DNA library. These will be tested in pair-wise fashion to identify the best pair of aptamers which both recognize the same molecule, and serum levels of S100B will be quantified using labeled aptamers and spotted arrays, analogously to ongoing studies on melanoma RNAs. Sensitivity and specificity of S100B will be compared with that of CTCs. When the sensor platform is operational (we anticipate within 4 years, depending upon funding levels), we will functionalize NWs with a selected aptamer, and detect S100B with a sandwich assay using a second aptamer derivatized onto 50-nm Au particles, detecting resonance frequency shifts of the NWs.

Our initial results with the RNA-based sensor have indicated that the resonance frequency shifts induced with NWs by the sandwich hybridization assay are such that single-molecule detection is feasible, and these considerations are directly applicable to the use of aptamers here. This device would serve as an exquisitely sensitive screening tool for multiple types of cancer. The data generated here will also furnish a direct comparison of sensitivities of circulating protein markers vs. CTCs in melanoma patients.

Principal Investigator

Gary A. Clawson, MD, PhD
Professor of Pathology
Penn State University
500 University Drive; H059
Hershey, PA 17033

Other Participating Researchers

Rustom B. Bhiladvala, PhD, Christine D. Keating, PhD, Theresa S. Mayer, PhD, Wei-Hua Pan, MS, Kevin Staveley-O'Carroll, MD, Diane M. Thiboutot, MD – employed by Penn State University

Expected Research Outcomes and Benefits

Although major advances have occurred in understanding molecular events in various cancers, their translation into therapies has been limited, and early detection remains the cornerstone of successful treatment. Consequently, there is a great deal of interest in identifying sensitive and specific markers for individual cancers, particularly in blood. One burgeoning field involves detection of CTCs, and there are now many reports documenting the diagnostic and prognostic significance of CTC levels. To that end, we are developing a chip-based RNA sensor platform for detection of cancer-related RNAs in CTCs harvested from blood.

We have assembled a cross-campus, multi-disciplinary team for the purpose of developing a novel nanotechnology-based RNA sensor for detection of CTCs, with the goal of producing a simple screening device for early detection of many “popular” types of cancer. This project specifically seeks to establish the feasibility of extending the utility of this sensor platform to aptamers (high-affinity DNA binding ligands), so that cancer marker proteins circulating in blood can also be detected with extremely high sensitivity and specificity. Through numerous collaborations, we are establishing a novel paradigm for translational research at Penn State, in which basic science development of the platform is coupled with Clinical Trials, each of which asks/answers specific questions with regard to this particular project, and all of which provide clinical samples for subsequent benchmarking/validation of the sensor platform when it is ready for testing. This particular project builds on the expertise of various disease groups (specifically melanoma, breast, and liver/pancreas) and establishes straightforward collaborations. We have had a GCRC-funded Clinical Trial for melanoma, in which CTCs are being evaluated using state-of-the-art QPCR for marker melanoma RNAs, and the majority of the RNA samples will be stored for subsequent interrogation with the RNA sensor platform.

Summary of Research Completed

We made significant progress on our stated goals. We have continued collecting blood samples from melanoma patients under the auspices of our IRB protocol, and now have ~ 50 samples (stages T1is, T1a, T1b, and 4).

We are switching detection technologies so we are obtaining particle counts (FE-SEM) but not resonance frequency shifts. We are beginning work on direct electrical detection. In the coming year, we will complete the analogous work (described below) for melanoma-inhibitory activity (MIA).

Specifically, S100B and MIA were cloned into and expressed using the Qiagen Tagzyme system. This system employs an N-terminal 6-His tag, and we added a GGGGG-C to the carboxy-terminus. The protein was expressed, and purified using the 6-His tag and Ni-NTA columns. The 6-His tag is then removed enzymatically using enzymes (DAPase, Qcyclase) which contain C-terminal His tags. The digest is then passed over the Ni-NTA column. The enzymes are retained and the purified protein flows through.

We then coupled S100B protein to glass slides using thiol chemistry, and used the slides as a substrate for aptamer (AP) selection. A number of APs for S100B with good binding affinities were obtained, and binding assays showed K_d 's in the 10^{-7} - 10^{-8} M range. We tested the APs for additive binding, and then tested them in the sandwich binding format.

Next, we identified a pair of APs for S100B that performed excellently in the sandwich binding format (Figure 1). AP1 was coupled to the array, S100B protein was bound to AP1, and then fluorescently-labeled AP2 was added. The results show that this AP pair (showing additive binding in K_d studies) produced a robust signal, whereas other pairs (not showing additive binding) produced essentially no fluorescent signal. We then derivatized gold nanowires (NWs) with AP1, and derivatized 50 nm Au Nanoparticles (AuNPs) with AP2. We performed the sandwich format assay and got excellent binding with S100B protein with little or no binding using an irrelevant protein (HtrA1) in the sandwich format, indicating excellent specificity (Figure 2).

We are now performing testing to see approximately where our sensitivity detection range is (previous results indicated that even one binding sandwich produces an easily detectable resonance frequency shift). We will not be performing resonance frequency measurements, in part because of resource considerations but more importantly because we are now working on direct electrical readout technologies. Budgetary considerations precluded any development of novel direct electrical read-out strategies. We have completed our particle-count studies and are now ready to submit a manuscript describing our data, which indicate excellent specificity and sensitivity. Available resources will be used to develop a sandwich assay format for melanoma inhibitory activity (MIA) and macrophage migration inhibitory factor (MIF): Our clinical melanoma studies have indicated that MIF is an excellent early target for detection of early stage melanomas.

We are also testing clinical samples for S100b levels using an ELISA assay. Thus far, its performance has not reached the expected pg/ml sensitivity reported (its ~100X less sensitive), but the studies are ongoing and the aliquots have been saved and will be available for testing with our device and if the commercial ELISA assays are unsuitable, we will perform clinical laboratory studies using the Clinical Pathology Laboratory here at Hershey.

Finally, we have also initiated clinical trials for CTC detection in colon cancer patients, as well as pancreatic cancer patients, with the aim of monitoring effects of therapy (chemo/radiation therapy for pancreatic cancer, and hepatic resection of solitary metastases for colon cancer). These studies will be continued.

Figure 1. S100B Sandwich Assay with fluorescently-labeled AP2.

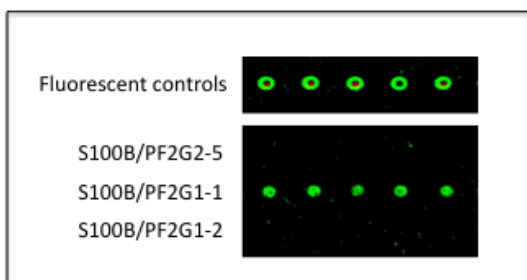
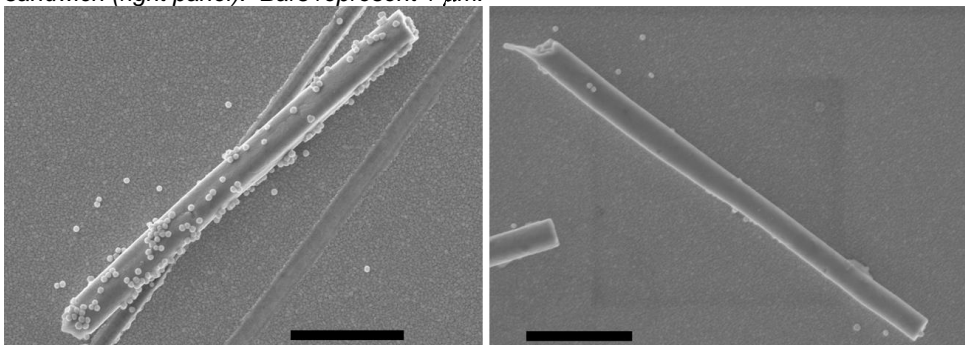


Figure 2. FE-SEM of S100B aptamer sandwich (left) and irrelevant protein (HtrA1) sandwich (right panel). Bars represent 1 μ m.



Research Project 37: Project Title and Purpose

Development of Novel Molecular Subtyping Methods for Identifying Pathways of Transmission of MRSA - This project will build on existing, unique research expertise at both University of Pennsylvania (UP) and Hershey Medical Center (HMC) to create a critical mass focused on preventing the transmission of methicillin-resistant *Staphylococcus aureus* (MRSA) in Pennsylvania communities and healthcare settings. It will translate basic scientific advancements in the fields of genomics, epidemiology, molecular epidemiology, infectious diseases, pathology and clinical medicine to prevent the transmission of MRSA to susceptible hosts. Combining these novel molecular subtyping methods with conventional epidemiologic analysis will allow us to determine the pathways by which specific endemic and epidemic clones are being transmitted in both Pennsylvania communities and at HMC. Once these pathways have been identified then targeted intervention strategies can be implemented to prevent MRSA transmission.

Duration of Project

11/24/2008 - 12/31/2009

Project Overview

Objective. To identify the pathways by which endemic and epidemic clones of MRSA are transmitted in Pennsylvania communities and at the Milton S. Hershey Medical Center (HMC)

Specific Aim 1. To develop novel molecular subtyping methods that can rapidly and accurately identify endemic and epidemic clones of MRSA

Specific Aim 2. To determine the pathways of endemic and epidemic MRSA transmission in Pennsylvania communities and at HMC

Research design and methods for achieving the objectives and aims:

Specific Aim 1. A novel multiplex PCR (MP-PCR) assay and novel multi-virulence-locus sequence typing (MVLST) and other SNP-based methods will be developed to rapidly and accurately identify endemic and epidemic clones of community-associated and healthcare-associated MRSA.

Specific Aim 2. MRSA isolates from the Pennsylvania Department of Health and HMC will be analyzed by the above methods and combined with corresponding epidemiologic data to determine the pathways by which endemic and epidemic clones of MRSA are being transmitted in Pennsylvania communities and at HMC.

Principal Investigator

Stephen J. Knabel, PhD
Professor of Food Science
Penn State University
437 Food Science Building
University Park, PA 16802

Other Participating Researchers

Cynthia J. Whitener, MD, Edward G. Dudley, PhD, Bhushan M. Jayarao, PhD, Wallace H. Green, PhD, Kathleen G. Julian, MD, B. Verghese, PhD – employed by Penn State University

Expected Research Outcomes and Benefits

First, we will expand and complement past expertise and unique capabilities at PSU in genomics and molecular epidemiology to develop new molecular subtyping tools that can rapidly and accurately identify those endemic and epidemic clones of MRSA that are causing significant morbidity and mortality. Combining these novel molecular subtyping methods with conventional epidemiologic analysis will allow us to determine the pathways by which specific endemic and epidemic clones are being transmitted in both Pennsylvania communities and at HMC. Once these pathways have been identified, targeted intervention strategies can be implemented to prevent MRSA transmission. Another important outcome of this project will be the development of preliminary data that can be used to develop a NIH Clinical and Translational Science Award proposal focused on preventing community-associated and healthcare-associated MRSA infections. The ultimate goal of this HMC-UP collaboration is the development of a model science-based infection-control system that has the potential to dramatically reduce the transmission of MRSA and other community-associated and healthcare-associated pathogens, and thus enhance public health throughout Pennsylvania, the U.S. and the world.

Summary of Research Completed

Specific Aim 1. To develop novel molecular subtyping methods that can rapidly and accurately identify endemic and epidemic clones of MRSA.

Methods

Bacterial isolates and DNA extraction.

A total of 128 isolates of methicillin-resistant *S. aureus* (MRSA) were investigated, of which 73 were from nasal swabs collected at the time of admission to the ICU at the Milton S. Hershey Medical Center, PA (HMC) (over a period of 2008-2009) and the remaining 55 isolates were from a state prison in Pennsylvania (collected January-July, 2006). Reference strains of MRSA were obtained from both CDC and NARSA. Nasal swabs were streaked on Columbia blood agar plates (Columbia Blood Agar Base (Sigma, St. Louis, MO)) containing 4 mg/l methicillin (MRSA Selective Supplement (Fluka, St. Louis, MO)) and grown at 37°C overnight. Single colonies were then grown in Tryptic soy broth (Difco, MD) overnight at 37°C. Genomic DNA

was extracted from the bacterial isolates using an UltraClean microbial DNA extraction kit (Mo Bio Laboratories, Solana Beach, CA).

Multiplex PCR

SCC*mec* typing was performed on all isolates using modified *mecA* primers. Clonal complex (CC) M-PCR primers including the *mecA* primers were designed using NCBI PrimerBLAST (<http://www.ncbi.nlm.nih.gov/tools/primer-blast/index.cgi>) and were synthesized at the Pennsylvania State University Genomics Core Facility. Amplified products were separated by agarose gel electrophoresis (2% UltraClean Agarose [MoBio Laboratories, Carlsbad, CA]) in 0.5x Tris-borate-EDTA buffer at 105 volts for 1 hour then subsequently stained in ethidium bromide.

Method Comparison. Simpson's index of diversity was used to quantify the discriminatory power of the SCC*mec*, MLST, and CC M-PCR typing methods. A strain was defined as an isolate or group of isolates that exhibited a distinctive combination of results for SCC*mec* typing, MLST and CC M-PCR. Non-typable strains were not used in the calculation of discriminatory power.

Multi-Virulence Locus Sequence Typing (MVLST)

Six virulence gene loci (*essC*, *etaA*, *htrA*, *alt*, *geh*, *hlgA*) and *cinA* were selected on the basis of an insilco comparison of sequence variations within these genes in the 11 published whole-genome sequences of *S. aureus*. Later we added virulence gene *sdrC* since this gene was able to give better resolution in typing MRSA especially between USA 800 and USA200.

Sequence Analysis

Each locus was sequenced in both directions and sequence alignments were performed using Molecular Evolutionary Genetic Analysis Software (MEGA version 4.0). An arbitrary number was assigned for each allele that was different. A unique arrangement of seven locus allele numbers (allelic profile) for each isolate defines its sequence type (ST). MEGA 4.0 was used to construct a midpoint rooted neighbor-joining tree with 1,000 bootstrap replications. An allelic profile tree was also constructed using the PubMLST website (<http://pubmlst.org/analysis>). Estimates of parameters for DNA divergence, gene diversity, nucleotide diversity, and a test for neutrality based on Tajima's D were performed using DnaSP version 4.00. Recombination analysis was carried out using RDP3 software to verify whether there was significant intragenic recombination. Multilocus linkage disequilibrium was calculated using the index of association (I_A) using MLST database (www.mlst.net/) and r_D using the program MULTILOCUS version 1.2.2.

Multi-Locus Sequence Typing (MLST)

Seven MLST housekeeping genes were amplified and sequenced as previously described (Enright et al., 2000). Each gene was compared against the alleles in the MLST database at <http://saureus.mlst.net>, and assigned an allelic number, and an allelic profile was constructed for each strain and sequence types (STs) were determined according to these allelic profiles.

Discriminatory Power

Discriminatory power of MLST and MVLST were estimated from the Index of discrimination (ID). Index of discrimination (ID) is the likelihood that two unrelated isolates drawn at random from a certain population will be placed as two different STs. The value of ID ranges from 0-1, where a value 1 would indicate that the typing method was able to distinguish every single isolate and was able to type them as separate STs. The index of discrimination was calculated using the Discriminatory Power Calculator (http://biophp.org/stats/discriminatory_power/demo.php).

Results

SCCmec typing.

SCCmec types for 66 of 82 isolates/reference strains could be determined. SCCmec type II was the most common SCCmec type, being found in 43 (67%) of the isolates/reference strains. The other SCCmec types found were type IVa (8 isolates and 5 reference strains), type III (2 isolates and 1 reference strain), type I (2 reference strains), type IVc (2 isolates), type IVd (1 isolate and 1 reference strain), and type IVb (1 isolate). Of the 13 HMC isolates and 3 reference strains for which a SCCmec type could not be determined, 7 HMC isolates and 1 reference strain lacked the *mecA* gene, while 6 HMC isolates and 2 reference strains contained the *mecA* gene but were non-typable by the SCCmec typing method used in the present study. The discriminatory power of SCCmec typing was 0.787.

MLST.

Multilocus sequence types could be determined for 77 of 82 isolates/reference strains. The remaining 5 HMC isolates were not typeable using the *S. aureus* MLST genetic markers described above. These isolates were later found not to contain the *clfB* genetic marker confirming they were not *S. aureus*. eBURST analysis determined the presence of 7 clonal complexes. The discriminatory power of MLST was 0.938.

Novel CC M-PCR.

The results of the CC M-PCR for the MRSA reference strains and an *S. epidermidis* strain isolated from an HMC nasal swab identified in the present study are shown in Figure 1. The combination of genetic markers present in each reference strain was defined as the multiplex type (MT) for that strain. Each MT was associated with the clonal complex of the reference strain determined by the MLST eBURST analysis. Isolates which shared major identifying genetic markers with a reference strain were grouped in the same clonal complex as the reference strain. Each MT is designated by the number of the clonal complex to which the reference strain belongs, and an arbitrary lowercase letter to denote different CC M-PCR genetic marker combinations within a clonal complex. The discriminatory power of CC M-PCR was 0.943.

Multi-Virulence-Locus Sequence Typing (MVLST)

MVLST-defined Genetic diversity

Nine virulence genes fragments were sequenced from 13 *S. aureus* strains obtained from NARSA and CDC. Of the nine, seven gene fragments that gave the highest number of alleles were chosen for MVLST scheme. These six virulence genes (*htrA*, *etaA*, *hlgA*, *alt*, *essC*, *geh*) and *cinA* were then sequenced for the 69 isolates of HMC. All sets of primers successfully recovered seven MVLST loci from all 141 isolates included in this study. Neither insertions nor

deletions were found within the sequences of any of the loci, and therefore sequences could be unambiguously aligned. The mean nucleotide sequence divergence was 0.55 %, where *etaA* and *alt* genes revealed a maximum (0.96%) and minimum (0.17%) sequence divergence, respectively. A total of 33 V-STs (“V” indicating MVLST scheme to avoid confusion with MLST “ST”) were recovered from 141 isolates. The total number of observed polymorphic sites was lowest (12) and highest (54) in *hlgA* and *htrA*, respectively. The average gene diversity (H) over seven loci was 0.598.

Discriminatory ability of MVLST compared to MLST.

The Simpson’s index of diversity (*D*) was determined to compare the discriminatory powers of MLST and MVLST with the set of 47 isolates that was typed by both the methods. MVLST identified 21 different genotypes whereas MLST identified only 14 genotypes. The ability of MVLST to differentiate clones was better than MLST with *D* value 0.8903 and 0.7798, respectively. However, this data set was heavily biased since most of the isolates come from a common source so it has a high number of identical strains. However, when only reference strains were used to interpret the diversity index, the MVLST scheme was still better than MLST and the *D* value were 0.9842 and 0.9242, respectively. The genes, *essC* and *cinA* revealed the highest 0.8974 and the lowest 0.6923, respectively. However the addition of *sdrC* discriminatory index was 1 for reference strains.

Relatedness of *S. aureus* isolates

Among all tested isolates, our analysis yielded 33 distinct allelic profiles from 66 isolates which included both reference strains and patient isolates from HMC. However, all the prison isolates belonged to a single allelic profile and were all MLST ST8 and were typed as V-ST18 by MVLST. The MVLST scheme could unambiguously identify them as USA300 isolates from USA500 clone (data not shown on figure) as against MLST which grouped both USA300 clones and USA500 clones into a single ST (ST8). The MVLST scheme with the reference strains included was able to differentiate all reference strains, except for USA100 and USA800 with distinct allelic profiles, however introduction of *sdrC* gene into the MVLST scheme helped to differentiate between the two PFGE types (Fig.4). Four distinct MRSA lineages were identified by cluster analysis (Fig.2). The types most represented STs were V-ST4 (34 isolates of which 19 was HMC), V-ST18 (9 isolates, 6 from HMC) V-ST1 (5 from HMC), V-ST15 (5 isolates 3 from HMC), V-ST6 (2 isolates from HMC). The MLST analysis identified 14 different allelic profiles. MLST also identified four lineages but ST diversity was low. Lineage I was represented by just two STs (ST5 and ST105), lineage II and III represented by one, ST 1 and ST8 respectively, whereas lineage III showed the same ST diversity as the MVLST scheme (ST30, ST535 and ST36). Forty two of these isolates correspond to pandemic clonal complexes CC1, CC5, CC8, CC30, and CC45. The most common types of MRSA isolated from nasal swabs were MLST types ST5, ST105, ST8, and ST1, respectively. Among the ST’s recovered from HMC isolates, ST87 was represented only twice in the entire MLST database; one from San Francisco, USA and the other from Western Australia. While ST133 an ungulate animal-specific genotype with no human association reported (Smyth et al. 2009) was also recovered from the HMC nasal swab isolates.

The MVLST sequence analysis based on HMC isolates can alone identify 7 distinct STs within lineage I. With the exception of one isolate, which had SCC *mec* IV (USA800), the remaining

isolates all belonged to HA-MRSA with *SCCmecII*. Lineage II showed very low genetic divergence, represented by just two allelic profiles, belonging to CA-MRSA (*SCCmecIV*). The MVLST scheme grouped lineage II isolates with USA400 isolate thereby was able to distinguish MRSA from methicillin susceptible *S.aureus* (MSSA). Lineage III for HMC isolates was represented by a unique subcluster A, (Fig.2) and showed little or no diversity suggesting its recent introduction. Further analysis indicated that they all were CA-MRSA, PFGE type USA300 sequence and *SCCmec IV*. However, the MLST and MVLST scheme identified 3 unique STs for lineage IV. Among the HMC patients, lineage I was the predominant isolates accounting for 61.5% of the MRSA carriers followed by lineage II, III and IV by 7.7%, 15% and 5.8%, respectively for all the MRSA carriers admitted to HMC. Both eBURST and minimum spanning tree resolved the 33 V-STs into 4 major clonal complexes (CCs) and 2 minor complexes and 8 singletons. The three major V-STs were designated as V-CC4 (19 isolates), V-CC12 (6 isolates), V-CC21 (6 isolates) and V-CC26 (5 isolates). The HMC isolates also identified four clonal clusters but only one founder ST could be assigned (V-CC4). Consistent with the phylogenetic analysis the minimum spanning tree of the HMC isolates have also revealed 4 distinct lineages (Fig.3).

Effect of recombination on the population structure of *S.aureus*

All of the five methods (RDP, GENECONV, Max Chi-square, Chimaera, and SiScan) included in RDP3 failed to detect intragenic (within-locus) recombination event within the seven MVLST genes. 'Standardised' Index of Association (I_A^S) was calculated using the MVLST allelic profile. Significant linkage disequilibrium was observed when only 35 unique STs was analyzed ($I_A^S=0.4674$, $V_d=3.9363$ and $V_e=1.0150$) also suggests that the genes are at linkage disequilibrium and mutations are responsible for genetic variation in MRSA genetic divergence.

Specific Aim 2. To determine the pathways of endemic and epidemic MRSA transmission in Pennsylvania communities and at HMC

Will be addressed in future.

Presentations and Publications

Schwalm, N., B.Vergheese and S.J. Knabel. Development of novel clonal complex multiplex PCR for detection of major clonal complexes of methicillin-resistant *Staphylococcus aureus*. to J.Clinical Microbiol (Submitted).

Vergheese, B., E.G. Dudley, and S. J. Knabel. Molecular subtyping utility of virulence genes for detecting the clonality of methicillin-resistant *Staphylococcus aureus* (MRSA). J.Clinical Microbiol (In preparation).

Vergheese, B., E.G. Dudley, and S. J. Knabel. Evidence of natural selection in the evolution of virulence-related prophage genes of methicillin-resistant *Staphylococcus aureus* (MRSA). Evol. Biol. (In preparation).

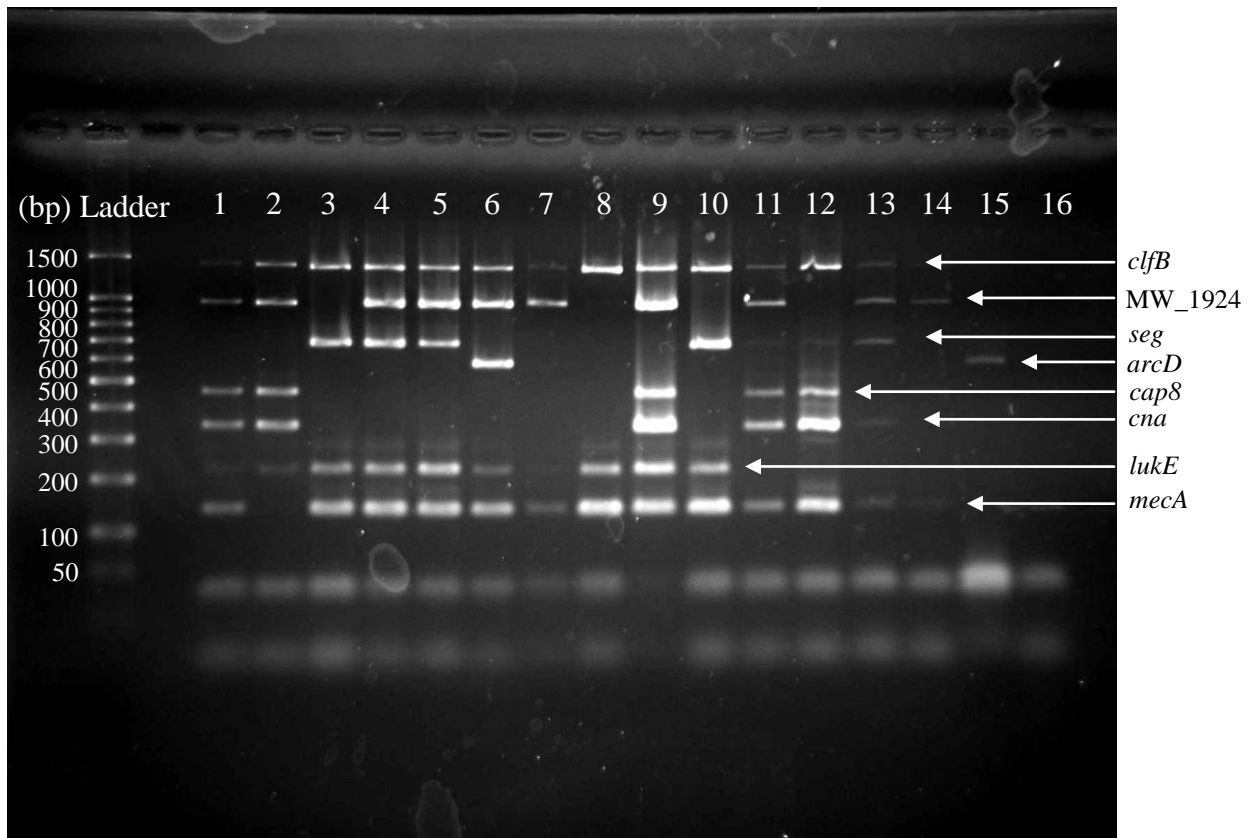


FIG 1. Multiplex PCR assay results for the *S. aureus* reference strains analyzed in the present study. Lanes 1-16 *S. aureus* reference strains 1- CDC USA400, 2- NRS72 (MSSA476), 3- CDC SCCmec I, 4- NRS70 (N315), 5- NRS387 (USA800), 6- NRS384 (USA300), 7- NRS385 (USA500), 8- NRS100 (COL), 9- CDC SCCmec III, 10- NRS386 (USA700), 11- NRS383 (USA200), 12- NRS484 (USA1100), 13- NRS22 (USA600), 14- NRS483 (USA1000), 15- *S. epidermidis* and 16- H₂O negative control.

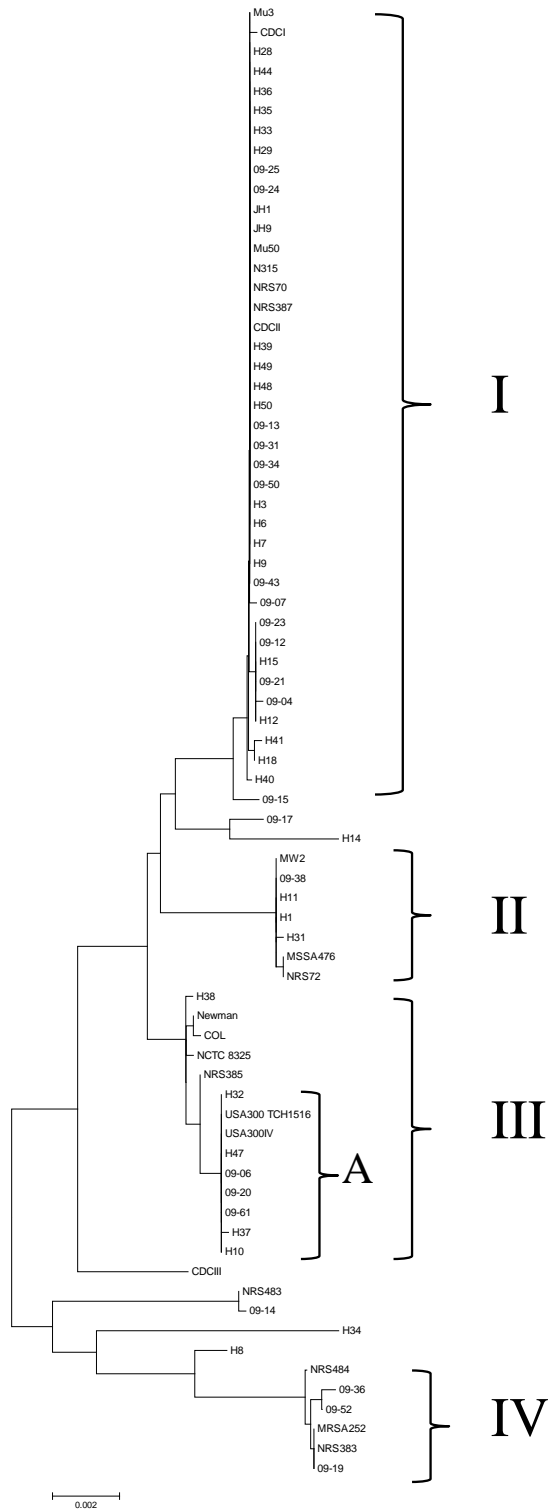


Fig 2 Inferred Neighbor-joining tree based on concatenated coding nucleotide sequences of virulence genes (*hlgA*, *alt*, *etaA*, *essC*, *htrA*, *geh* and *cinA*) showing four distinct lineages of MRSA. Reference strains are marked with asterisk. The scale at the lower left shows the substitutions/site.

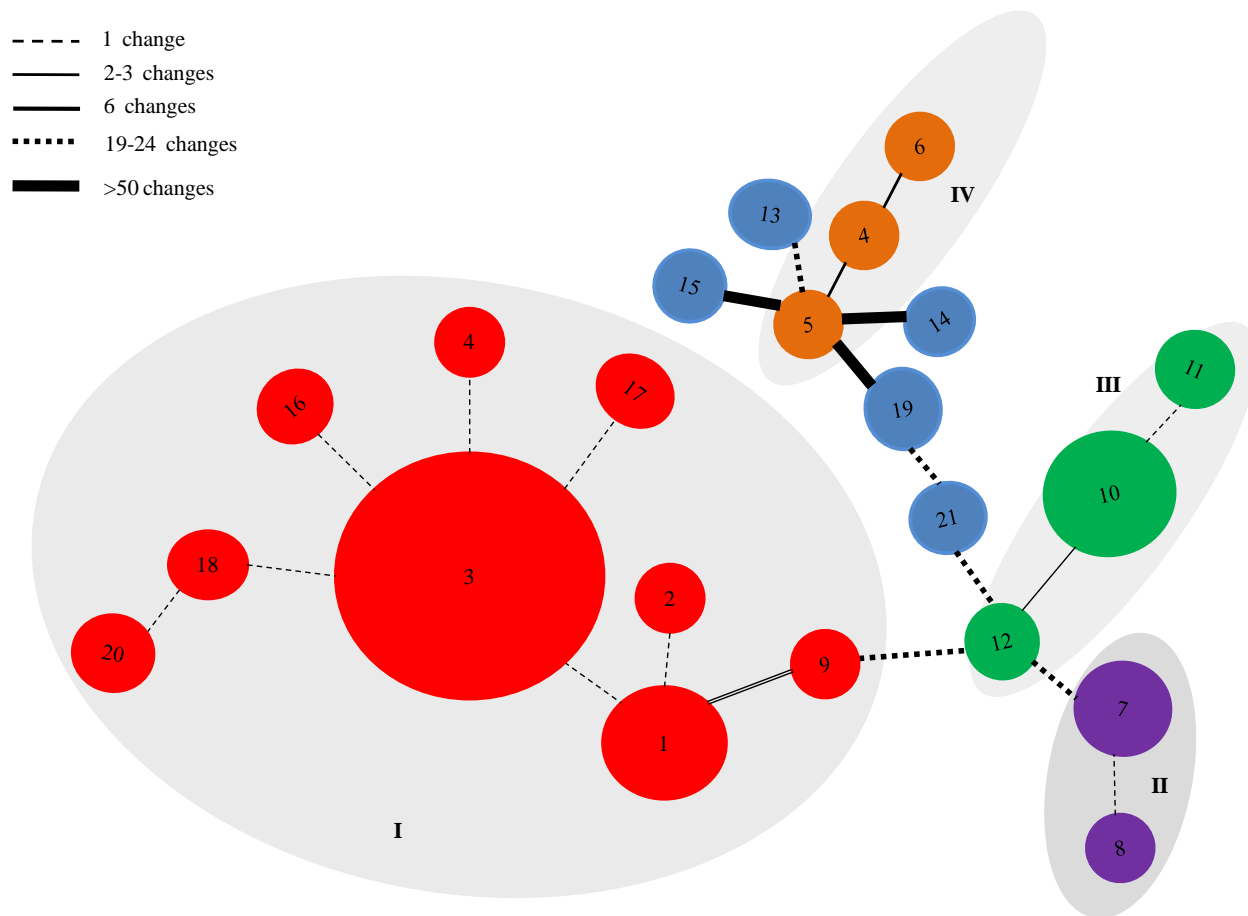


Fig.3 Minimum spanning tree depicting the genealogical relationships among different isolates of nasal carriage MRSA collected at the HMC. Each circle represents unique sequence. The size of the circle is proportional to the number of identical sequence. Connections between two consecutive circles represent the number of mutational steps (nucleotide change). The four distinct lineages (I-IV) identified by the network are shaded grey.

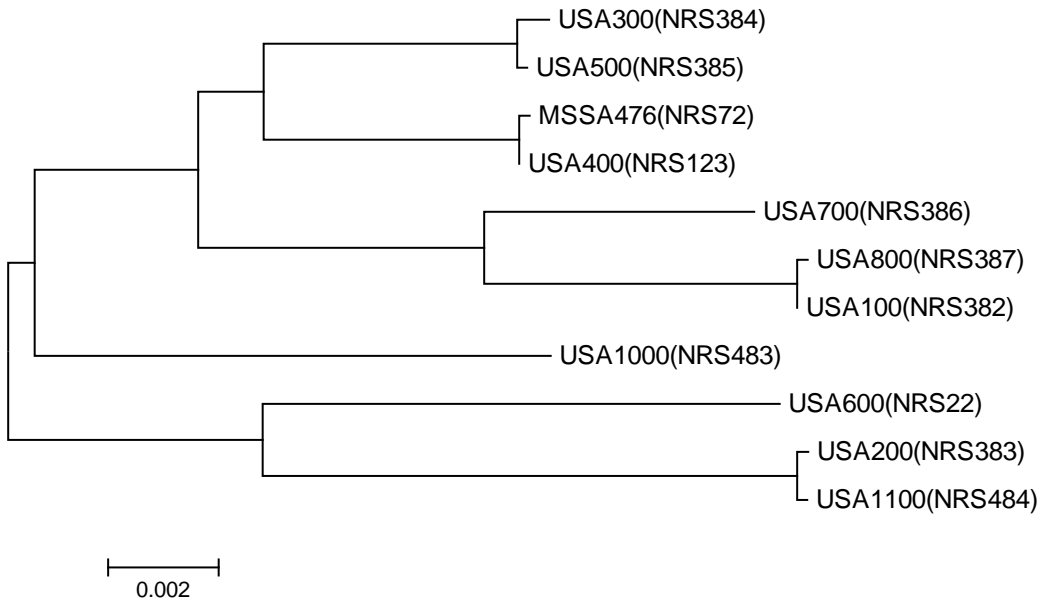


Fig.4. Cluster diagram based on MVLST analysis of all reference strains

Research Project 38: Project Title and Purpose

Sequencing of LGL Leukemia Retrovirus Genome - The broad long-term objective of this project is to understand the etiology of large granular lymphocyte (LGL) leukemia and related autoimmune diseases, including rheumatoid arthritis (RA). Preliminary serologic and molecular data indicate a high likelihood that patients are infected with a novel retrovirus with similarities to both human T-cell leukemia viruses (HTLV) and human immunodeficiency viruses (HIV). In particular, we have demonstrated transmission of an infectious retrovirus from LGL leukemia cells to co-cultured HOS target cells. Evidence for retroviral infection in this LGL-HOS cell line includes morphologic signs of retroviral infection such as formation of syncytia and other cytopathic effects, demonstration of high levels of reverse transcriptase activity, and detection of 100nm retroviral-like particles of type C morphology using electron microscopy. So far, however, we have been unsuccessful in characterizing this virus at the genomic level. Recent advances in sequencing technology and bioinformatics capability pioneered by investigators at Huck Institute have led to characterization of ancient and environmental genomes. This project represents, then, a cross-campus collaboration aimed at characterizing the LGL virus. Specifically, we plan to determine the retroviral genome of the LGL virus utilizing pyrosequencing of LGL-HOS mRNA.

Anticipated Duration of Project

11/24/2008 - 11/24/2010

Project Overview

Broad Objectives and Specific Aim: The broad long-term objective of this project is to understand the etiology of large granular lymphocyte (LGL) leukemia and related autoimmune diseases, including rheumatoid arthritis. LGL leukemia patients have high titer antibodies cross reactive to common structural regions (gag and env) of HTLV and HIV, as demonstrated using a functional peptide array. We have shown transmission of a cytopathic infectious retrovirus from LGL cell lines to target cells. Microarray characterization using a custom-designed chip containing 14,000 oligonucleotide sequences from all known plant, animal, and human retroviruses detected several “hits” which corresponded closely to regions of serologic reactivity. Taken together, these results show that patients with LGL leukemia most likely are infected with a new retrovirus with some homology to both HTLV and HIV. The specific aim of this project is to characterize the LGL leukemia retrovirus.

Research Design: We plan on using a metagenomics approach pioneered by the Schuster laboratory to identify the retroviral genome. Samples from LGL leukemia cell lines or co-cultured cell lines will be subjected to large scale sequencing using the 454 platform. The Metagenomics Analyzer (MEGAN) bioinformatics program will be utilized to identify the low frequency viral sequences. We have validated this approach by demonstrating detection of retroviral sequences in samples obtained from feline lymph nodes.

Principal Investigator

Thomas P. Loughran, MD
Director of the Penn State Cancer Institute
Penn State University
500 University Drive; H072
Hershey, PA 17033

Other Participating Researchers

Stephan Schuster, PhD, Susan Nyland, PhD, Mary Poss, DVM, PhD, Nicola Wittekindt, PhD – employed by Eberly/Huck Institute, Penn State University

Expected Research Outcomes and Benefits

Discovery of a new retrovirus associated with human disease has obvious health implications. The practical need for retroviral screening assays to prevent transmission by blood transfusion has been well established over the past 25 years. Characterization of a new virus will allow us to determine if the new virus is linked to disease causation in both LGL leukemia and rheumatoid arthritis. New retroviral therapeutics as well as preventive vaccines for such diseases could result from such work.

Summary of Research Completed

Three milestones were proposed for this period:

Milestone 1: (07/01/2009-09/30/2009) Complete Pyrosequencing Experiments:

This milestone is still in progress.

Pyrosequencing was completed on a set of LGL leukemia specimens. We used the alternate subtractive method as proposed. In addition, we performed additional experiments on quiescent versus activated specimens from leukemia patients and normal donors. We are currently analyzing the pyrosequencing data and also running the Illumina sequencing on these specimens. Therefore, this milestone is still in progress.

Milestone 2: (10/01/2009-03/31/2010) Perform Primary Validation Experiments:

This milestone is not completed due to the ongoing progress of Milestone 1.

Milestone 3: (04/01/2010-06/30/2010) Validation of Data:

This milestone cannot be performed until the Milestone 1 has been completed.

Work Performed:

PBMC Isolation – As mentioned, additional cell culture work was performed. Peripheral blood mononuclear cells (PBMCs) were collected from leukemia patients and from normal healthy donors. PBMCs were extracted over a Ficoll gradient and then were immediately cultured.

Cell cultures: Cells were cultured in different groups:

1. “Quiescent Cells”: After the initial isolation, cells were incubated in RPMI medium with fetal bovine serum (FBS) for 48 hours. Cells were checked for growth and were harvested for RNA extraction.
2. “Activated Cells”: After the initial isolation, cells were incubated in RPMI with FBS plus PHA and human IL-2 for 48 hours. Cells were checked for growth and harvested for RNA extraction during log phase growth.
3. “Enriched Normal Cells”: Magnetic beads were used to enrich the normal PBMC population for LGL cells. The outcome of this procedure was a final percent of LGL cells similar to that found in LGL leukemia (approximately 90% T LGL cells). Enriched normal donor cells were then incubated as quiescent or as activated cells.

RNA Extraction – RNA was extracted from cell cultures using Trizol. RNA was then reverse-transcribed to make cDNA for emulsion PCR.

Results and Conclusions

The accomplishments planned for this period were completion of the pyrosequencing, initiation of analyses, and initiation of validation experiments. Our results and conclusions are focused on this aspect of our proposed work. Specifically:

The 454 sequencing data was compared against BLASTx-nr and the resulting data analyzed with the software MEGAN.

We performed multiple experiments to increase the sensitivity of the reads, but still missed some expected viral sequences. Despite this, we found sequences with matches to a portion of the

HERV HCML-ARV envelope gene, with 70% to 86% sequence homology. Some HCML-ARV sequences were also found in the normal donor specimens, but were from different parts of this HERV and were better matches to the known genomes of HCML-ARV.

The metatranscriptomics profiles are depicted in Figure 1

Interestingly, more sequences were expressed in the normal samples after they were activated, but there was only one additional sequence expressed in LGL leukemia after activation. This observation is provocative because:

1. The sequences identified as HCML-ARV were different for LGL leukemia versus normal. Using BLAST, the only two sequences shared by the leukemia and normal group had matches that were characterized by numerous deletions and inversions.
2. Normal cells were more sensitive to activation in terms of HCML-ARV sequence expression. The different effect of activation on LGL leukemia versus normal specimens could be the result of a very specific immune response against a novel retrovirus sequence. In this case the sequence would be very similar to, but not exactly the same as, typical HCML-ARV sequences. This is what was observed when the sequences from the normal data were compared to the sequences from the LGL leukemia data.

Therefore it is possible that we have detected a novel viral sequence with similarities to HCML-ARV subtypes, which is somehow chronically induced in LGL leukemia, but not in normal health conditions. If this can be validated, then the preliminary results of the pyrosequencing experiments suggest that the LGL leukemia virus (LGLV) might be an uncharacterized endogenous retrovirus. This will be determined by completion of the ongoing sequence analysis. If an uncharacterized HERV was inappropriately expressed in the leukemia patients, then different validation methods are needed to confirm this finding.

We found a large number of uncharacterized (not assigned) reads. These represent reads for which there is no known match in the general NCBI database. Because uncharacterized sequences could contain very novel or unique retrovirus sequences, the uncharacterized reads are currently being analyzed specifically against the NCBI viral genome database.

On the chance that this HCML-ARV-like sequence is not the LGLV sequence, we are still performing the Illumina GAIIx ultra-deep sequencing platform. We are also still analyzing the 454 data, as proposed.

To this end, four more DNA samples are currently being prepared - The libraries have been sheared to 200-300 bp and they are being amplified on the Illumina clusterstation.

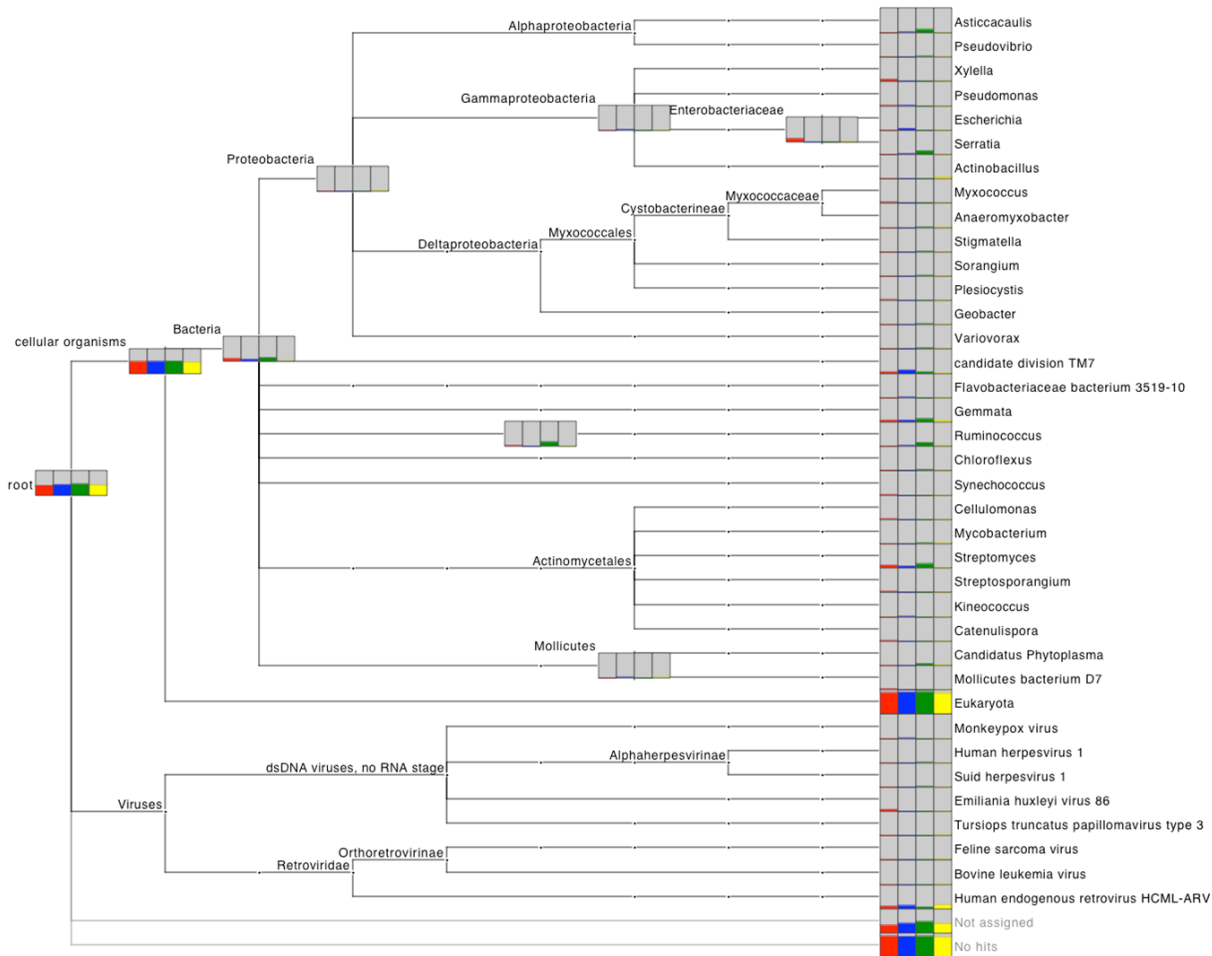


Figure 1. Initial Metatranscriptomic Profile of LGL Leukemia and Normal Donor cDNA, with and without cell activation. Red: LGL cells, not activated. Blue: LGL cells, activated. Green: Normal cells, not activated. Yellow: Normal cells, activated. Specimens were collected and processed as described above. The profile is from the first set of analyses performed. Please note that although all specimen groups have hits for the HERV HCML-ARV, the sequences are different. Also note that there was a greater increase in the number of HCML-ARV- like sequences found after activation in the normal group (from 2 to 6), but only a single increase in sequence number in the LGL leukemia group (from 3 to 4). BLAST analysis of the HCML-ARV sequences showed that each group expressed different sequences.

Research Project 39: Project Title and Purpose

Mechanisms of Unexpected Drug Side Effects Related to Obesity and Diabetes - The long-term goals of the project are to elucidate the mechanisms underlying drug side effects related to obesity and diabetes. We believe that investigating the mechanisms underlying unexplained drug side effects is an innovative approach that may reveal new targets for the treatment of obesity and diabetes. Alternatively, it may yield new drugs with fewer side effects. Obesity and diabetes are epidemics facing our state and country. Understandably, our institution has

committed to this as one of the research focus areas, along with cardiovascular disease and cancer.

Duration of Project

11/24/2008 - 12/31/2009

Project Overview

The objectives of this project are based on preliminary data from our rodent model of olanzapine-induced obesity. The primary objective is to conduct a clinical study in healthy volunteers, similar to our rodent experiments, in order to confirm the presence of acute metabolic changes in human subjects. Notably during our animal studies sexually dimorphic results were obtained. In each case the metabolic changes could bring about adiposity, but by distinct mechanisms. We hope to address the following questions. *Does the sexual dimorphism we observed in animals with regard to this side effect exist in humans or is only one type of mechanism observed? Whereas all of the animals tested exhibit either the male or female pattern of acute changes, do only a subset of humans respond?* The central hypothesis is that acute metabolic and hormonal changes apparent in the plasma occur with acute olanzapine administration and these changes precede and drive long-term metabolic changes leading to insulin resistance and obesity. The rationale for the proposed research is that once the above questions are answered in humans, it will (1) allow us to better focus our mechanistic scientific inquiries in animals and (2) identify whether or not changes are considerable enough within an individual to warrant a follow-up prospective study to examine the possibility of developing an inexpensive and rapid screening test for weight gain susceptibility in individuals being considered for olanzapine therapy and to investigate the genetic basis of this susceptibility. To accomplish this we propose one specific aim:

Aim 1 To conduct a clinical research study of the acute effects of olanzapine on plasma leptin, oral glucose tolerance, and appetite in healthy volunteers. We will test the hypotheses, that olanzapine (1) rapidly attenuates plasma leptin and (2) rapidly alters glucose tolerance in humans, by conducting oral glucose tolerance tests in healthy subjects after acute olanzapine exposure. To control for non-responders and genetic variability, respectively, we will use a standardized hunger questionnaire and perform double-blinded tests with and without drug treatment (crossover design).

Principal Investigator

Christopher J. Lynch, PhD
Professor
Penn State University
500 University Dr, H166
Hershey, PA 17033

Other Participating Researchers

Ravi Singareddy, MD, Vance L. Albaugh, BS, David Mauger, PhD – employed by Penn State University

Expected Research Outcomes and Benefits

There are several important outcomes that make this study desirable from both clinical and basic research perspectives. Notably, in contrast to the animal model, only about a third of human subjects are severely affected by this side effect, suggesting a genetic propensity. One outcome of this study may be the development of a screen that could identify individuals at risk for this side effect of olanzapine. Secondly, this study will have a significant impact on the basic science investigation of the mechanism of this side effect. It will help us select an appropriate model (male or female rats). Moreover, this study is designed to detect any potential sexual dimorphism in humans, if one exists, further clarifying the clinical effects of olanzapine and potentially other antipsychotics. Finally, the results of this pilot study will be used to determine the design of a much larger, prospective clinical study examining these effects in patients undergoing treatment with olanzapine and other antipsychotic drugs with these side effects. It will also provide our group with the translational experience to conduct other human studies on drug side effects in the future.

Summary of Research Completed

The goal of these studies is to identify mechanisms of body weight and metabolic side effects of atypical antipsychotics. In an animal model of these side effects we had observed rapid metabolic changes preceding adiposity. However it was unclear to us whether these reflected changes in humans. All of the data in humans had been from chronic studies where adiposity might be the underlying cause of a metabolic change. So we decided to look at the responses in humans through this grant mechanism.

A challenge to doing studies in humans is their variability in plasma metabolites and responses to glucose challenge. So we opted for a longitudinal placebo controlled design in which subjects would be tested in response to placebo and olanzapine. The study design is outlined in the original Strategic plan.

As mentioned in the report last year, we felt obliged to discontinue our clinical trial based on negative comments from NIH reviewers for a proposal to continue this trial. The reviewers felt that we had not controlled for factors including the possibility that the participants were consuming recreational drugs that could affect the outcome of the studies. In addition some felt that metabolic effects seemed likely, although no literature was cited to support this. We had also developed concerns that there should be three glucose tolerance tests (GTTs) in order to examine the variability of the control responses within an individual based on literature suggesting that GTTs were inherently variable. Since it was evident that no NIH funding was forthcoming we stopped the study. However this year we analyzed the data we had collected and this proved to be interesting. Nevertheless we did complete studies on 15 patients and used the

remainder of the funds for this project to pay for some of the analyses on the plasma samples collected.

In our recent paper we noted that fatty acid oxidation was accelerated and lipolysis impaired after olanzapine treatment and that this resulted in lower circulating free fatty acids (FFAs) (1). Lower FFAs have also been observed after chronic treatment of humans with olanzapine. Consistently we did observe reduced FFAs in our human subjects (Fig 1). Median FFAs were decreased by ~36% ($p = 0.017$). This suggests that our efforts to investigate the mechanism of the FFA lowering in rats would be relevant to humans.

In several animal models we have also observed ~50% reductions in plasma leptin after acute olanzapine administration (1; 2). However in our human subjects leptin actually increased modestly, but significantly ($p = 0.02$), by about 20%. This suggests that our efforts to investigate the mechanism of leptin lowering in humans, while of interest from a basic science perspective, might not be relevant to humans. Thus leptin lowering probably does not underlie the increased hunger observed in patients taking olanzapine.

Consistent with previous reports from chronic studies in humans, acute olanzapine also caused a significant rise in triglycerides (TG, Fig 3). Median triglycerides rose 19% ($p = 0.017$). This effect is not well modeled by most rodent animal models. Total cholesterol was not significantly affected nor was LDL levels. However there was a statistically significant drop in HDL (~12%, $p = 0.018$). Together these changes translated into a ~14% increase in the TG:HDL ratio, a sensitive marker of insulin resistance ($p = 0.010$).

Chronic olanzapine treatment increases the risk for diabetes in human subjects and chronic exposure leads to worsening glucose infusion rates during euglycemic hyperinsulinemic clamps. Acute olanzapine treatment in humans caused no significant change in fasting plasma glucose concentrations, in contrast to the animal model (1; 2). However, GTT-AUCs (areas under the curve) were significantly elevated by 40% in human subjects treated acutely with olanzapine, in agreement with acute elevations in the rat model (1; 2). Also consistent with significant rises in the animal model, there was a trend for elevated plasma insulin concentrations in humans following acute exposure, compared to placebo in the same subjects. Consistently there was a statistical trend for worsening of the Masuda Insulin Sensitivity Index (SI, $p = 0.08$).

In conclusion our data indicate that olanzapine does cause acute changes in metabolic endpoints that may precede the development of obesity and diabetes. These studies were useful to determine which of the acute changes we have observed in the rodent model are relevant to humans and therefore should be prioritized for further study. Our studies also indicate that these metabolic changes precede the development of adiposity, as is the case in the animal model. Further studies are needed to understand whether these are diagnostic of subjects more prone or susceptible to experience these metabolic side effects.

REFERENCES

1. Albaugh VL, Vary TC, Ilkayeva O, Wenner BR, Maresca KP, Joyal JL, Breazeale S, Elich TD, Lang CH, Lynch CJ: Atypical Antipsychotics Rapidly and Inappropriately Switch

Peripheral Fuel Utilization to Lipids, Impairing Metabolic Flexibility in Rodents. *Schizophr Bull*, 2010

2. Albaugh VL, Judson JG, She P, Lang CH, Maresca KP, Joyal JL, Lynch CJ: Olanzapine promotes fat accumulation in male rats by decreasing physical activity, repartitioning energy and increasing adipose tissue lipogenesis while impairing lipolysis. *Molecular Psychiatry* In press, 2010

FIGURES

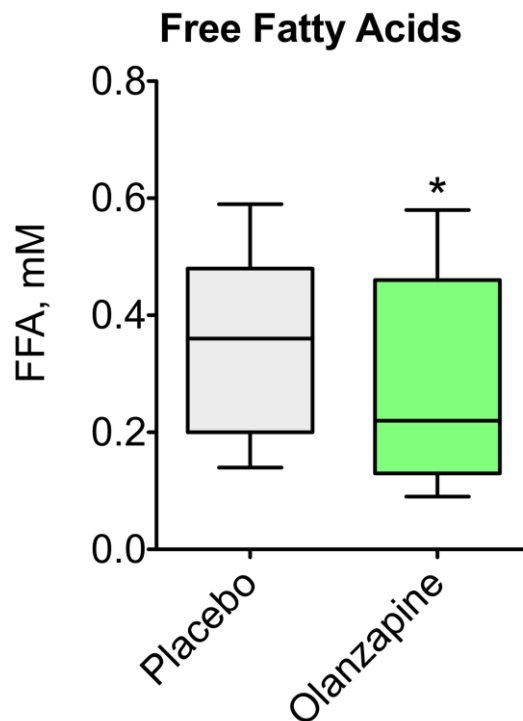


Fig 1. Effects of acute olanzapine on FFA in human subjects. Fourteen male and female subjects received either placebo or olanzapine for three days followed by an intervening washout period of several weeks wherein they were again challenged with either placebo or olanzapine for three days. Figure is a box and whiskers plot of FFA results obtained from overnight fasting plasma. Asterisk (*) indicates significant difference ($P= 0.0166$) on a Wilcoxon matched-pairs signed rank test

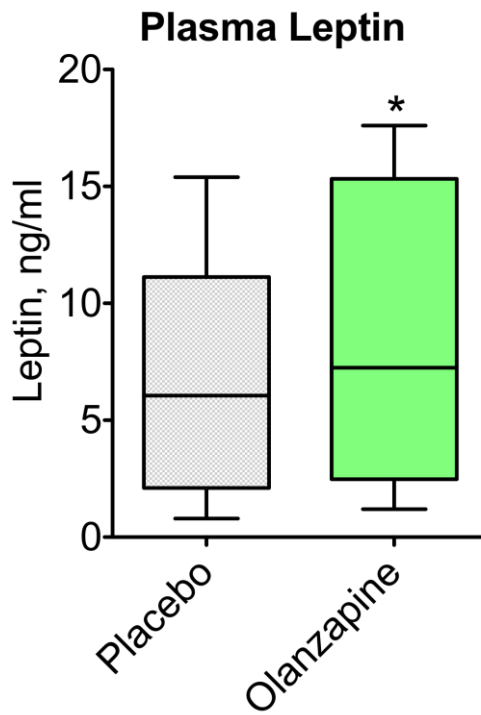


Fig 2. Effects of acute olanzapine on plasma leptin in human subjects. Figure is a box and whiskers plot of leptin results obtained from overnight fasting plasma. Asterisk (*) indicates significant difference (P= 0.02) on a Wilcoxon matched-pairs signed rank test

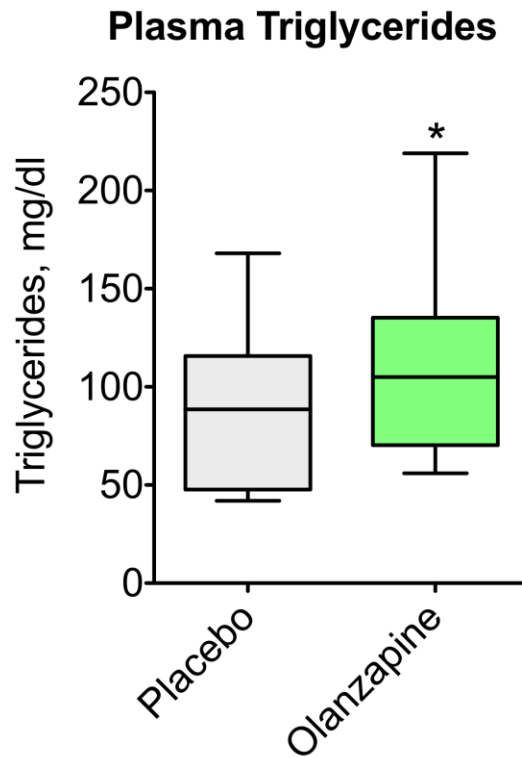


Fig 3. Effects of acute olanzapine on plasma triglycerides in human subjects. Figure is a box and whiskers plot of leptin results obtained from overnight fasting plasma. Asterisk (*) indicates significant difference (P= 0.017) on a Wilcoxon matched-pairs signed rank test

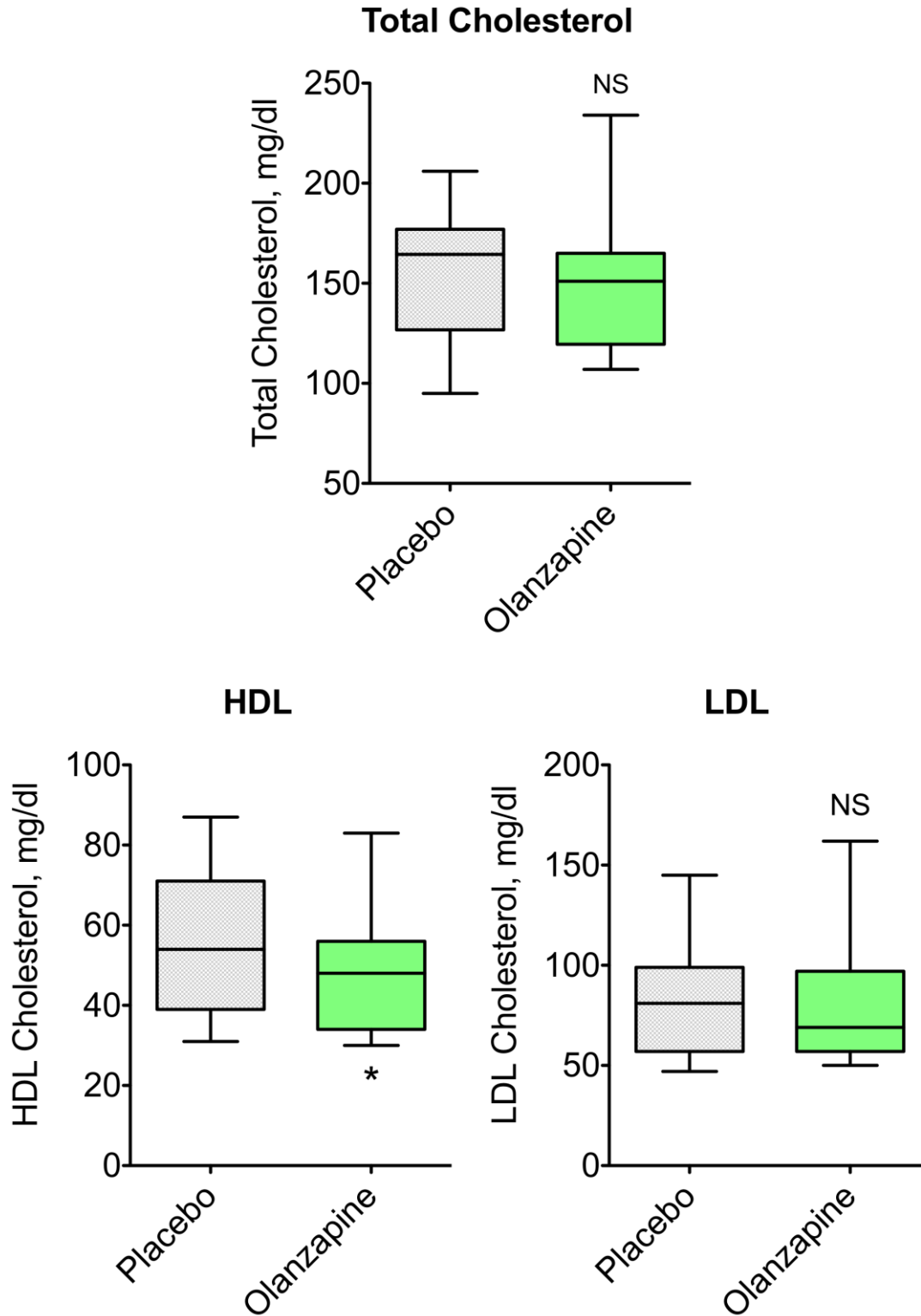


Fig 4. Effects of acute olanzapine on total, HDL and LDL cholesterol in human subjects. Asterisk (*) indicates significant difference (P= 0.0184) on a Wilcoxon matched-pairs signed rank test.

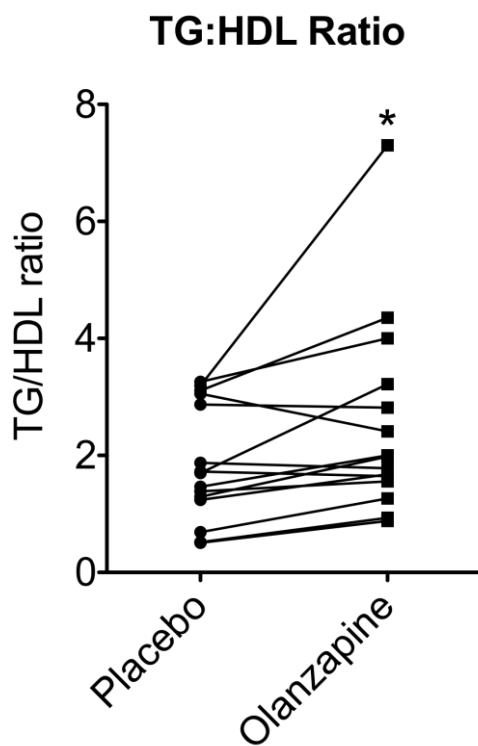


Fig 5. Effects of acute olanzapine on Triglyceride to HDL cholesterol ratio in human subjects. Asterisk (*) indicates significant difference (P= 0.010) on Wilcoxon matched-pairs signed rank test.

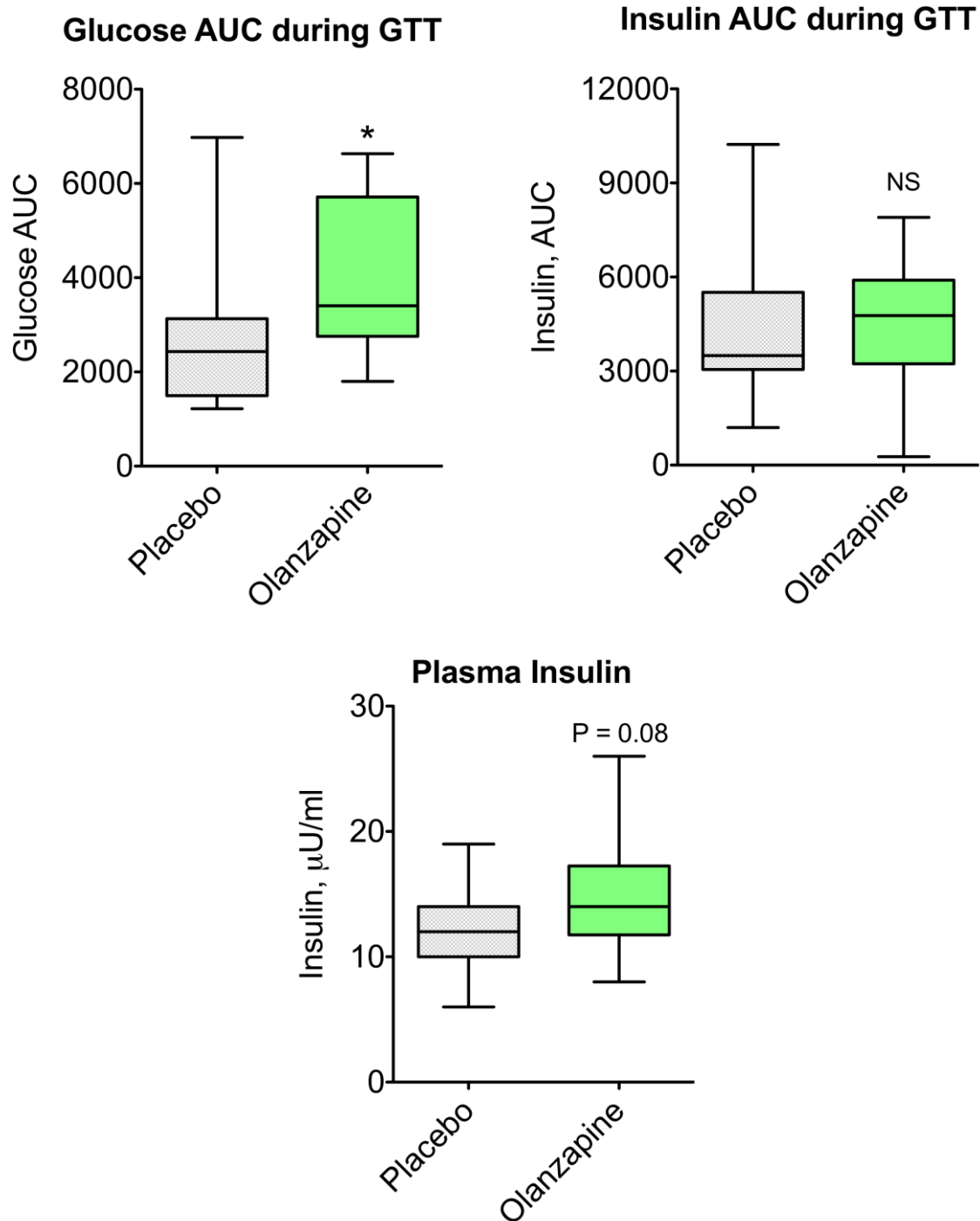


Fig 6. Effects of acute olanzapine on glucose and insulin AUCs during a GTT and fasting plasma insulin. Asterisk (*) indicates significant difference ($P= 0.011$, for glucose AUC) on Wilcoxon matched-pairs signed rank test.

Research Project 40: Project Title and Purpose

Dissecting the Interaction between Radiofrequency Ablation and Tumor Antigen-Specific Immune Response in Hepatocellular Cancer: A Murine Model and a Human Protocol -

Hepatocellular cancer can be a difficult disease to treat, with radiofrequency ablation (RFA) being a critical component of treatment for patients with inoperable cancer. The risk of recurrence associated with RFA makes it imperative that we understand the precise mechanism of RFA and methods to increase its efficacy. The proposed murine and human studies will help us understand the anti-tumor immune responses to RFA. We hope to build a foundation with our basic science findings and implement this foundation in clinical practice. The insights gained in our research and clinical practice will be used to raise new questions and guide further research. Our experimental endeavors strive to combine surgical modalities with potential immunotherapy that will enable us to harness one's own immune system to fight the cancer.

Anticipated Duration of Project

11/24/2008 - 6/30/2011

Project Overview

Hepatocellular carcinoma (HCC) is the most common primary liver cancer. It has a worldwide distribution with the highest prevalence in Africa and Southeast Asia and a rising incidence in last two decades in Europe and the United States due to a wide exposure to hepatitis C virus (HCV) in the 1960s and 1970s. Therefore, occurrence of HCC may still continue to rise for a long time because of the large pool of subjects infected by HCV. Current treatment modalities, including surgery and liver transplantation, offer limited survival benefits, with the number of deaths from the disease in the U.S. (16,780) nearly equaling the number of newly diagnosed cases (19,160). New therapies are desperately needed.

Radio frequency ablation (RFA) creates a local necrosis destroying tumoral tissues and this is followed by a marked inflammatory response with dense T-cell infiltrate. Recent studies suggest a significant increase in both the tumor specific T-cell response and memory T-cell responses after RFA treatment. We hypothesize that the RFA-induced necrotic cell death enhances antigen presentation and T cell activation inducing HCC-specific T cell responses. In this pilot study we will evaluate the immunologic effects following RFA in a murine model of HCC and simultaneously determine if RFA will induce T cell responses specific for HCC-associated antigens in humans. The overall goal of this project is to build on this data, gaining new understanding of the effects of RFA on tumor growth and tumor antigen-presentation in HCC.

Specific Aim 1: To study if RFA reverses antigen-specific CD8⁺ T-cell tolerance in a murine model of HCC and demonstrate the possible changes in the function and phenotype of the infiltrating T cells.

Specific Aim 2: To study the T cell responses specific for HCC-associated antigens following RFA in HCC patients.

Principal Investigator

Kevin F. Staveley-O'Carroll, MD, PhD
Associate Professor of Surgery
Penn State University
Department of Surgery, H070
500 University Drive, P.O. Box 850
Hershey, PA 17033

Other Participating Researchers

Serene Shereef, MD, Hephzibah Tagaram, PhD, Diego Avella, MD, Eric Kimchi, MD, Niraj J. Gusani, MD, Peter Waybill, MD, Todd Schell, PhD, Harriet Isom, PhD, Yixing Jiang, MD, PhD – employed by Penn State University

Expected Research Outcomes and Benefits

Radio frequency ablation (RFA) is a critical component of treatment for patients with inoperable HCC. Unfortunately, the recurrence rates are high and there is much that remains a mystery regarding the mechanism of RFA. Therefore, the proposed studies are unique and critically needed to expand our understanding of potential anti-tumor immune responses generated by RFA. The results gathered from the project will lead to novel clinical applications improving the efficacy of RFA and further expand our knowledge leading to unique therapeutic approaches by combining RFA and immunotherapy for treatment of patients with HCC.

Summary of Research Completed

A. Collection of blood samples from 8 control group patients without HCC from Blood bank used for standardization of the techniques before the collection of the blood samples from the pre and post RFA samples from the HCC patients.

a. Standardized the isolation of PBMC's on ficoll gradient to enrich the monocytes.

b. Synthesis of the Peptides: Peptides corresponding to defined CD8+ T cell-recognized epitopes from known HCC antigens are synthesized in the Macromolecular Core Facility of the M. S. Hershey Medical Center.

c. Generation of human Dendritic Cells (DCs) from Peripheral Blood Mononuclear Cells (PBMCs) : We were able to standardize the isolation of DC's needed for the antigen presentation of the proposed HCC antigen epitopes using blood drawn from the control individuals collected from the Penn State Blood bank at Hope Drive. Briefly, the isolated PBMCs were seeded at (1×10^7 cells/2ml) of DC media without Granulocyte Macrophage Colony Stimulating Factor (GMCSF) and Interleukin-4 (IL-4) and incubate at 37° C for 90-120 min. This allows the cells to get attached to the plate. The adherent cells were fed with 3ml of DC media supplemented with (GMCSF-1000U/ml) and IL-4 (50ng/ml, R&D Systems) and incubated at 37° C in 5% CO₂ for the generation of immature DCs. On day 3, we fed the cells by adding 0.5ml/well of fresh media with GMCSF and IL-4. On day 5, the cells were harvested, and DCs were frozen in aliquots of 5-6x10⁶ cells/vial. The cells were frozen at this point in the liquid N₂. These cells will be used to stimulate the HCC antigen peptide when the patient

samples are ready. For maturation of DCs, 10ng/ml of TNF- α , 10ng/ml of IL-1 β , 10ng/ml of IL-6 (R&D) and 1ug/ml of PGE2 (Sigma) are added. The cells are incubated at 37° C for 48 hours to obtain mature DCs.

B. Collection of blood samples from the HCC patients after radiofrequency ablation:

To date we have collected 3 pre and post RFA samples from HCC patients. The PBMCs were isolated on a density gradient centrifugation. Immature DCs were grown and frozen for further use.

C. Determining the percentage of subset of DCs in the whole blood :

Two subsets of DCs were originally identified in the peripheral blood- myeloid DCs and plasmacytoid DCs. They differ widely in many aspects like cytokine production, response to microbial action, capacity to migrate and induction of immune responses. We utilized a technique in which 300 ul of blood was used to determine the number of DC subsets in the whole blood of the patient. This technique is based on the dendritic cell-specific surface antigens: CD303 (BDCA-2), CD141 (BDCA-3), and CD1c (BDCA-1). The markers allow easy identification of three distinct dendritic cell subsets in blood: plasmacytoid dendritic cells (PDCs) are identified by *CD303 (BDCA-2)*, type-1 myeloid dendritic cells (MDC1s) are identified by *CD1c (BDCA-1)*, and type-2 myeloid dendritic cells (MDC2s) are identified by *CD141 (BDCA-3)* expression. The distinct dendritic cell subsets are analyzed within one sample by three-color (PDCs and MDC1s) or four-color (PDCs, MDC1s and MDC2s) flow cytometry. Dendritic cell subset frequency will be determined before and after the radio frequency ablation to determine if RFA plays a role in alteration of the DC subset.

D. Standardization of the technique:

Standardization of the technique to utilize the frozen control samples from the blood bank to derive the Interferon-g CD8+ CTL's against common antigens EBV and FLU peptide with the mature DC from the previous section A. The same technique will be utilized for generation of CD8+ CTL's with the HCC patient blood sample for the production of Interferon-g.

E. An enzyme-linked immunospot (ELISPOT) assay for the quantitation of single cells releasing human interferon gamma:

This will be performed in the next year.

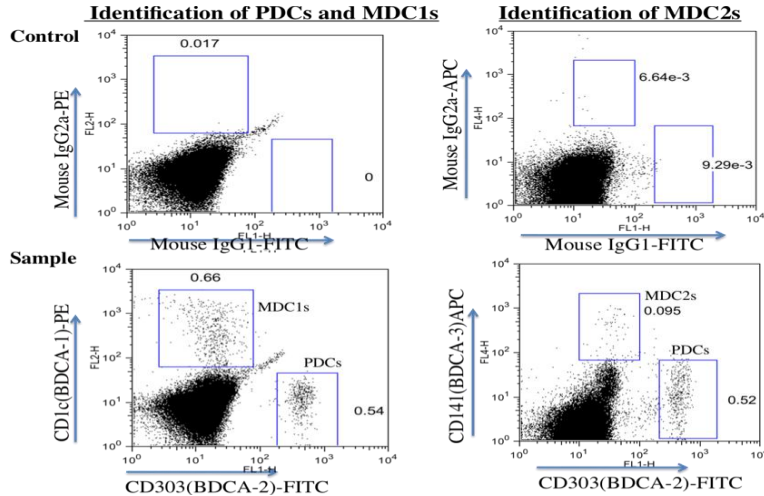


Figure 1: Determination of the subset of DC in the whole blood from the blood bank donor. The assay was performed on the whole blood. For one test, two samples of 300ul of whole blood were used. One sample was used as a test sample to detect the PDC (plasmacytoid stained for CD303-FITC), MDC1 (myeloid1 stained for CD1c-PE) and MDC2 (myeloid 2 stained for CD141-APC). The other sample was used for an isotype control. Gated cells determine the number of MDC1, and PDC's in the first graph and the MDC2 and same PDC's in the second graph.

IFN-g production by CD8+ CTL's against EBV and FLU peptide pulsed DC

IFN-g

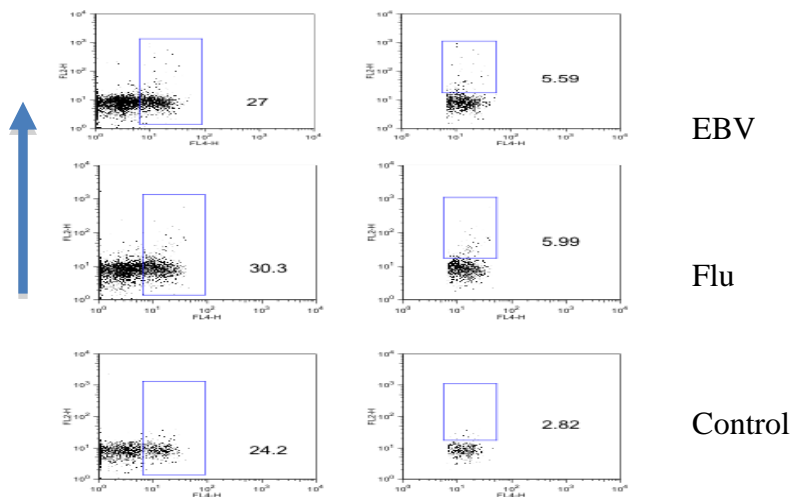


Figure 2: Activated T cells from the donor blood showing the production of interferon-g (IFN-g) against the common antigens EBV and FLU. The mature DC's are pulsed with EBV and FLU peptides with PBMC's from the same individuals. Approximately 5.59% of the CD8+T cells are producing IFN-g with EBV peptide and 5.99% with FLU peptide.

Research Project 41: Project Title and Purpose

Central Pennsylvania Women's Health Study (CePAWHS): Extending the Strong Healthy Women Behavioral Change Intervention to Urban Areas - This project builds on the highly effective *Strong Healthy Women* intervention, developed as part of the Central PA Women's Health Study (CePAWHS). This intervention was designed to modify risk factors for chronic conditions associated with adverse pregnancy outcomes such as hypertension, diabetes, and obesity by changing behaviors related to physical activity level, nutritional intake, stress reduction, and tobacco and alcohol use; it is currently being tested in low-income rural communities in Central PA. The focus of the proposed research is to modify the *Strong Healthy Women* intervention to include racially and ethnically diverse urban women in Harrisburg, Lancaster, and York. We hope that this will lead to a reduction in risks of adverse pregnancy outcomes, and to the elimination of disparities in these outcomes across geographic and race/ethnic groups.

Anticipated Duration of Project

11/24/2008 - 12/31/2010

Project Overview

The project builds on initial findings of the effectiveness of the *Strong Healthy Women* intervention, developed at Penn State as part of the CePAWHS. The intervention was designed in a 6-session, small-group format, targeting risk-related attitudes, knowledge, and behavior through a mix of presentations, discussion, incremental goal setting, and group- and home-based assignments related to nutrition, physical activity, alcohol/drug/tobacco use, stress management, and prevention of gynecologic infections. Our team conducted a preliminary test of *Strong Healthy Women* in a randomized trial involving 692 pre- and interconceptional women, ages 18-35, living in low-income rural communities in Central PA. There was significant improvement in risk factors for adverse pregnancy outcomes including attitudes, intentions, and behaviors related to nutrition, physical activity, and stress management among intervention participants compared to controls. Our experience with a largely white, rural population revealed intervention curriculum and implementation strategies that could be adapted for a more diverse population. We expect that *Strong Healthy Women* could be more broadly disseminated if the content were adapted for urban as well as rural women and for African Americans, who have a two-fold elevated risk of adverse pregnancy outcomes compared with white women. The main objective of the proposed project is to expand the *Strong Healthy Women* intervention to optimally engage urban women. The specific aims of the research proposed here are: (1) To conduct focus groups with race/ethnically diverse pre- and interconceptional women in three urban low-income communities, to guide modifications of the *Strong Healthy Women* intervention; and (2) To pilot test the modified aspects of the *Strong Healthy Women* intervention in race/ethnically diverse groups of pre- and interconceptional women in Harrisburg, Lancaster, and York. Participants will be recruited from community settings in partnership with community organizations. Three focus groups (two composed of African American women and one of white women) will be conducted in each of the three urban areas, for a total of nine focus groups. Focus group data will be used to modify the intervention content to ensure that the content is

accessible and motivating to urban women. Once the content modifications have been made, pilot testing of the modified content will be carried out in three additional focus groups in each urban area, with participants selected from the previously conducted focus groups.

Principal Investigator

Carol S. Weisman, PhD
Distinguished Professor of Public Health Sciences, Obstetrics and Gynecology, Health Policy and Administration
Penn State College of Medicine
Public Health Sciences, A210
600 Centerview Drive
Hershey, PA 17033-0855

Other Participating Researchers

Marianne M. Hillemeier, PhD, John J. Botti, MD, Danielle Symons Downs, PhD, Mark E. Feinberg, PhD – employed by Penn State University

Expected Research Outcomes and Benefits

Recent recommendations to improve preconception health and health care in the United States have called for innovative approaches to reduce adverse pregnancy outcomes, including strategies for improving women's health *before* they become pregnant. More research studying pre-pregnancy health promotion is needed to inform both clinical and public health interventions to improve women's health and pregnancy outcomes. Interventions that contribute to a reduction in adverse pregnancy outcomes, and to the elimination of disparities in these outcomes across geographic and race/ethnic groups, are of great public health importance and will have substantial impact on the overall health status of these women, as well as their children and families.

Summary of Research Completed

Specific Aim 1: To conduct focus groups with race/ethnically diverse pre- and interconceptional women in three urban low-income communities in Central Pennsylvania (Harrisburg, Lancaster, and York) to guide modifications of the Strong Healthy Women intervention.

This specific aim was accomplished during the last reporting period.

Specific Aim 2: To pilot test the modified aspects of the Strong Healthy Women intervention in race/ethnically diverse groups of pre- and interconceptional women in Harrisburg, Lancaster, and York.

The modifications to the *Strong Healthy Women* intervention suggested by the focus group for research conducted to accomplish Specific Aim 1 were made. These modifications, though not extensive, required some new content and re-organizing some of the material in the original

protocol manual. This process took longer than planned due to the extended maternity leave of our project coordinator, Sara Baker, who gave birth to triplets in January 2009.

The main content modifications involved: (1) expanded content and skill-building exercises related to domestic violence, including an abuse screener and more information on community resources; (2) expanded content and skill-building exercises related to neighborhood safety, including a self-assessment of neighborhood safety; and (3) increased number of hands-on cooking demonstrations including recipes providing alternatives to fried foods (e.g., oven-roasted chicken). These changes required modifications to 4 of the 6 sessions of the intervention, including new instructions for the facilitators, new discussion and/or activity information, and new handouts.

To offset the additional time added to 4 of the sessions by these modifications, some previously included material was deleted. Deletions included some material on smoking (since a minority of participants smoked) and some group discussion on modifiable risk factors for general health problems. Dry-runs of the modifications are underway to pilot test the new sessions and to confirm how long each session will take.